MASS. INST. OF TECHNOLOGY
JUN 1 1964
LIBRARIES

SOUND REFLECTION FROM THE SEA FLOOR AND ITS GEOLOGICAL SIGNIFICANCE

by

LLOYD ROBERT BRESLAU

S. B., Electrical Engineering, M. I. T.
(1957)

S. B., Geology and Geophysics, M. I. T.
S. M., Geology and Geophysics, M. I. T.
(1959)

SUBMITTED IN PARTIAL FULFILLMENT
OF THE REQUIREMENTS FOR THE
DEGREE OF DOCTOR OF
PHILOSOPHY

at the

MASSACHUSETTS INSTITUTE OF
TECHNOLOGY
June 1964

Signature of Author _____
Department of Geology and Geophysics,
April 27, 1964

Certified by _____
Thesis Supervisor

Accepted by _____
Chairman, Departmental Committee
on Graduate Students

ABSTRACT

GEOLOGICAL SIGNIFICANCE OF SOUND REFLECTION FROM THE SEA FLOOR

by

Lloyd Robert Breslau

Submitted to the Department of Geology and Geophysics April 27, 1964, in partial fulfillment of the requirements for the degree of Ph. D. in Oceanography.

The objective of this investigation was to measure bottom loss in normal incident reflection of pulses of twelve kcps sound and to study its geological significance. To this end a semi-automatic instrument system was developed which is capable of making continuous measurements of the peak pressure and the time integral of the square of the pressure of the sea-floor echo, from a vessel underway.

Observations were taken in both deep and shallow water areas in the Western North Atlantic. The early cruises were conducted in deep water to investigate the range and variability of bottom loss values. Geological control consisted mainly of a precise bathymetric record. The later cruises were conducted in shallow water, in areas where the geology had been well studied previously by investigators using techniques of classical geology. In these latter cruises the acoustic measurements were correlated with a schedule of sediment dredging and underwater photography.

Thirty-one thousand acoustic measurements were made. Median bottom loss values and standard deviations were computed and the results summarized in eleven hundred sets, each set corresponding to a location at sea.

Seventy-seven sediment stations were occupied. A complete particle size analysis and a water content analysis were performed on these sediments to determine their size and mass characteristics. The size characteristics included the median grain size, the sorting coefficient, and the percentages of gravel, sand, silt, and clay. A sediment class name was determined from the gravel, sand, silt, and clay percentages according to the

Shepard system of classification. The mass characteristics included porosity, bulk density, sound velocity, acoustic impedance, Rayleigh reflection coefficient, and theoretical bottom loss.

The combined results show a good correlation between measurements of bottom loss and both mass and size characteristics of the sediment. The measured bottom loss increases as the porosity increases. The measured bottom loss also increases as the silt-clay percentage increases since the porosity of sediments generally increases as this fraction increases.

It seems that the Rayleigh reflection coefficient can be used to predict acoustic bottom loss at normal incidence. Conversely, normally-incident bottom loss can be used under the assumption of a Rayleigh reflection process to determine the nature of the bottom sediment.

The acoustical and geological results have been made available in tabulations, scatter diagrams, and as geographical plots. Except for the initial measurements, all operations, including the final displays, were accomplished through automatic digital processing machines.

Thesis Supervisor: Dr. J. B. Hersey
Senior Scientist
Woods Hole Oceanographic Institution
Woods Hole, Massachusetts

and

Professor of Oceanography
Department of Geology and Geophysics
Massachusetts Institute of Technology
Cambridge, Massachusetts

TABLE OF CONTENTS

LIST OF FIGURES

Text

Appendix A

Appendix D

LIST OF TABLES

Text

Appendix C

LIST OF COMPUTER PROGRAMS

Appendix B

CHAPTER I

INTRODUCTION

General Objectives

The primary objective of this investigation was to measure the acoustic reflectivity of the sea floor and to study its geological significance. A secondary objective was to develop a practical technique that could be used for routine acoustical surveying of sea floor sediments from a vessel underway.

In principle, acoustic echoes received from the sea floor are influenced by the geological nature of the bottom and might be used for limited identification of reflectors. However, the overwhelming complexity of the generalized reflection process, the variability in echo characteristics from echo to echo, and the sheer tedium of making the measurement and performing the geological correlation have largely defeated attempts to use acoustic reflectivity for geophysical exploration.

The general plan of this investigation was to reduce the measurement of acoustic reflectivity to its simplest form, perform the shipboard data acquisition in a semi-automated fashion, measure only easily recognizable qualities of the echo wave-train, and analyze the data by high-speed digital computer. An effort was made to create a technique that eventually could be fully automated

and could perform its task on a ship underway at cruising speed without restricting any of the ship's activities. Conventional Navy sonar equipment, instruments commonly used in hydroacoustical oceanography, and standard laboratory apparatus were employed wherever feasible, primarily because of initial convenience and, additionally, so that this surveying technique, if proven fruitful, could be readily adopted by others.

Historical Background

Because of its military application much work was done in the field of underwater acoustics by numerous investigators during World War II and was later reported in summary form. The section pertaining to sound transmission studies (Physics of Sound in the Sea, Part I Transmission, Summary Technical Report of the National Defense Research Committee; 1946) contains information relevant to the reflecting properties of the sea floor which was a by-product of horizontal sound-transmission studies. These measurements, taken at various frequencies and angles of incidence with only cursory investigation of the geological environment, nevertheless established that different geological bottom types react differently acoustically, and that rock, stone, and sand bottoms are better reflectors than sand and mud, or mud bottoms. The general relationship between acoustical and geological properties was utilized to predict the acoustical behavior of a region from available geological

information, as evidenced by sediment charts prepared for pro-submarine operations (The Application of Oceanography to Subsurface Warfare, Summary Technical Report of the National Defense Research Committee; 1946). The converse prediction is attempted in this investigation.

The work done after the war that contributed toward an understanding of the acoustic reflectivity of the sea-floor progressed along two separate lines of investigation. One line of investigation, exemplified by Liebermann (1948), Urick (1954), Urick and Saling (1962), Mackenzie (1960), McKinney and Anderson (1964), and Jones et al. (1964), was concerned mainly with sound transmission and studied sound reflected from the sea floor. The other line of investigation represented by Hamilton et al. (1956), Shumway (1960), Sarmiento and Kirby (1962), Richards (1962), and Nafe and Drake (1963) was concerned mainly with sea-floor sediments per se and studied their physical and sedimentological properties.

There have been very few attempts to use the results of the acousticians and sedimentologists in a quantitative approach toward acoustical surveying of sea-floor sediments. Semi-quantitative surveys, using tonal shading of echo-sounding records as an indicator of acoustic reflectivity, have been made by Erath (1959), Loring (1962), and Hoffman and Wilkes (1962). A crude quantitative recording of average echo strength was used for a time prior to

1950 by the geophysics group at Woods Hole (Hersey, private communication). The output signal from an echo sounder was rectified and fed to an integrating condenser with a decay constant equal to about ten or twelve ping intervals. A recording was made of the potential across the condenser. Reproducible profiles of echo strength were made in shallow water near Woods Hole, but this work was dropped then because of other pressures. Quantitative surveying, using the amplitude of the peak pressure in the bottom echo, has been performed in the Caspian Sea and Continental Shelf by Sergeev (1958).

The work described in the present paper represents an extensive field investigation of acoustic reflectivity and detailed comparison with characteristics of the sea-floor sediment, using a highly automated system of data collection and analysis. This work adds a new dimension to echo sounding by utilizing the magnitudes as well as travel times of the echoes.

CHAPTER II

THEORETICAL DEVELOPMENT

The Acoustic Measurement; Rayleigh Reflection Coefficient

The approach used in this investigation was to parameterize (determine a parameter of a simple model which is assumed to represent a complex physical process) acoustic bottom loss according to a specular-reflection model in which the sea-floor is considered to be a plane interface between two fluids. Bottom loss, according to this model, is determined by the Rayleigh Reflection Coefficient at the water-sediment interface when the sound source is sufficiently far from the interface that the impinging waves are essentially plane.

The intensity of an echo which is specularly-reflected from the sea-floor is given by

$$I_R = I_S \times K \times \frac{1}{(2D)^2} \times e^{-\alpha 2D} \qquad \text{(Eq. 1)}$$

where I_R is the intensity of the echo, I_S is the intensity of the source, K is the fractional loss of intensity at the sea-floor $\frac{1}{(2D)^2}$ is transmission loss due to spherical spreading and $e^{-\alpha 2D}$ is transmission loss due to disspative attenuation of sound in sea-water.

Since

$$I_R = \frac{P_R^2}{\rho_1 c_1} \qquad \text{(Eq. 2) and} \qquad I_S = \frac{P_S^2}{\rho_1 c_1} \qquad \text{(Eq. 3)}$$

where P_R is the pressure of the echo, P_S is the pressure of the

source, ρ_1 is the density of the water and C_1 is the sound velocity in the water, Eq. 1 becomes (P_S is the pressure estimated at $D = 1$)

$$\frac{P_R^2}{\rho_1 C_1} = \frac{P_S^2}{\rho_1 C_1} \times K \times \frac{1}{(2D)^2} \times e^{-\alpha 2D} \qquad \text{(Eq. 4)}$$

Taking the integral with respect to time of both sides of Eq. 4 gives

$$\frac{1}{\rho_1 C_1} \times \int_T^{T+\tau} P_R^2 \, dt = \frac{1}{\rho_1 C_1} \times K \times \frac{1}{(2D)^2} \times e^{-\alpha 2D} \times \int_0^{\tau} P_S^2 \, dt \qquad \text{(Eq. 5)}$$

Since the source is a sine wave of duration τ

$$\int_0^{\tau} P_S^2 \, dt = P_{S(RMS)}^2 \times \tau \qquad \text{(Eq. 6)}$$

where the root mean square of the pressure is equal to the peak pressure divided by the square root of two, Eq. 5 becomes

$$\frac{1}{\rho_1 C_1} \times \int_T^{T+\tau} P_R^2 \, dt = \frac{1}{\rho_1 C_1} \times K \times \frac{1}{(2D)^2} \times e^{-\alpha 2D} \times P_{S(RMS)}^2 \times \tau \qquad \text{(Eq. 7)}$$

It is seen that K may be defined on a peak pressure basis through Eq. 4 thusly

$$K = \frac{P_R^2}{P_S^2} \times (2D)^2 \times \frac{1}{e^{-\alpha 2D}} \qquad \text{(Eq. 8)}$$

or on an energy basis through Eq. 7 thusly

$$K = \frac{\int_T^{T+\tau} P_R^2 \, dt}{P_{S(RMS)}^2 \times \tau} \times (2D)^2 \times \frac{1}{e^{-\alpha 2D}} \qquad \text{(Eq. 9)}$$

If P_{INC} represents the pressure of the wave incident on the sea-floor and P_{REF} represents the pressure of the wave reflected from the sea-floor, the K, the fractional loss of intensity at the sea-floor

is given by

$$K = \frac{P_{REF}^2}{\rho_1 C_1} \Big/ \frac{P_{INC}^2}{\rho_1 C_1} = \left(\frac{P_{REF}}{P_{INC}}\right)^2 \qquad \text{(Eq. 10)}$$

For the above mentioned model and incident plane waves, the ratio of the pressure of the wave incident on the sea-floor to the pressure of the wave reflected from the sea-floor is given by the Rayleigh Reflection Coefficient (Rayleigh, 1945) (Officer, 1958) thusly

$$R = \frac{P_{REF}}{P_{INC}} = \frac{\frac{\rho_2}{\rho_1} - \frac{\sqrt{C_1^2/C_2^2 - \sin^2\theta}}{\sqrt{1 - \sin^2\theta}}}{\frac{\rho_2}{\rho_1} + \frac{\sqrt{C_1^2/C_2^2 - \sin^2\theta}}{\sqrt{1 - \sin^2\theta}}} \qquad \text{(Eq. 11)}$$

where θ is the angle of incidence. For normal incidence ($\theta = 0$), which was the case for the measurements made in this investigation, the expression for the Rayleigh Reflection Coefficient is simplified since Eq. 11 reduces to

$$R = \frac{\rho_2 C_2 - \rho_1 C_1}{\rho_2 C_2 + \rho_1 C_1} \qquad \text{(Eq. 12)}$$

The expression $\rho \times C$ is called the specific acoustic impedance of the medium and is designated as Z. Using this convention, Eq. 12 can be put in the following form

$$R = \frac{Z_2 - Z_1}{Z_2 + Z_1} \qquad \text{(Eq. 13)}$$

where Z_1 and Z_2 refer to the specific acoustic impedances of sea-water and sediment respectively. The Rayleigh Reflection Coefficient was derived for incident plane waves by assuming a velocity potential

and requiring continuity of pressure and normal component of particle velocity at the interface. However, it has been shown (Officer, 1958) that it is a valid approximation for the reflection of an incident spherical wave under the condition that

$$\frac{c_1}{\omega D \left[c_1^2/c_2^2 - \sin^2\theta \right]^{3/2}} \ll 1 \qquad \text{(Eq. 14)}$$

For normal incidence ($\theta = 0$) this reduces to

$$\frac{c_1}{D \times 2\pi \times c_1^2/c_2^2} \ll 1 \qquad \text{(Eq. 15)}$$

which means that the approximation is valid when the sound source is a moderate number of wavelengths away from the sea floor. This condition was always satisfied in this investigation.

The relationship between the fractional loss of intensity at the sea-floor, K, and the Rayleigh Reflection Coefficient, R, is shown by Eq. 10 and Eq. 11 to be

$$K = R^2 \qquad \text{(Eq. 16)}$$

The fractional loss of intensity, K, can be measured either by the relationship expressed in Eq. 8 or by the relationship expressed in Eq. 9; both are used in this investigation. The former is considered to be a measurement on a pressure basis and the latter on an energy basis.

It is convenient and conventional to express hydroacoustic measurements in decibel form. Taking ten times the logarithm of both sides of Eq. 8 gives

(Eq. 17)

$$10 \log K = -20 \log P_S + 20 \log P_R + 20 \log 2D + 10\alpha 2D \log e$$

which may be expressed as

$$BL = S_{PL} - E_{PL} - TL_S - TL_A \qquad \text{(Eq. 18)}$$

where BL is bottom loss in db and is equal to -10 log K, S_{PL} is the pressure level of the source in db//1 dyne/cm^2 and is equal to 20 log P_S, E_{PL} is the pressure level of the echo in db//1 dyne/cm^2 and is equal to 20 log P_R, TL_S is the spreading loss in db and is equal to 20 log 2D, TL_A is the attenuation loss in db and is equal to $10\alpha 2D \log e$ or to $a2D$ where a equals $10\alpha \log e$.

Taking ten times the logarithm of both sides of Eq. 9 gives

(Eq. 19)

$$10 \log K = -10 \log (P_{S(RMS)}^2 \times \tau) + 10 \log \int_T^{T+\tau} P_R^2 \, dt + 20 \log 2D + 10\alpha 2D \log e$$

which may be expressed as

$$BL = S_{EL} - E_{EL} - TL_S - TL_A \qquad \text{(Eq. 20)}$$

where S_{EL} is the energy level of the source in db//1 erg/cm^2 and is equal to $10 \log (P_{S(RMS)}^2 \times \tau)$ or to $10 \log (P_S^2 \times \tau/2)$ E_{EL} is the energy level of the echo in db//1 erg/cm^2 and is equal to $10 \log \int_T^{T+\tau} P_R^2 \, dt$, and BL, TL_S, and TL_A are the same as described for Eq. 18.

Taking ten times the logarithm of both sides of Eq. 14 gives

(Eq. 21)

$$10 \log K = 20 \log R$$

which may be expressed as

$$BL = 20 \log R \qquad \text{(Eq. 22)}$$

where BL is bottom loss in db and R is the Rayleigh Reflection Coefficient.

The Relationship Between Bottom Loss and Physical Properties of Sediments

The relationship between bottom loss and the Rayleigh Reflection Coefficient, given in Eq. 22, and the relationship between the Rayleigh Reflection Coefficient and the acoustic impedance contrast at the water-sediment interface, given in Eq. 13, serve to establish the relationship between bottom loss and mass characteristic of the sediment. Since the acoustic impedance of the sediment is the product of the density and compressional velocity, and since these properties can be related to the porosity of naturally occuring oceanic sediments, it is possible to establish a relationship between bottom loss and porosity. This relationship will be developed below.

A marine sediment is an aggregate of rock and mineral particles whose interstices are filled with sea-water. As such it can be thought of as a multi-component system whose bulk properties are some combination of the properties of the individual components. Fortunately, since the range of specific gravities of minerals commonly occuring in natural marine sediments is slight, and since the

compressibility of water is between one and two orders of magnitude larger than the compressibilities of mineral grains, it is possible to consider the marine sediment as a two component system with regard to these properties. For the purpose of arriving at acoustic impedance the sediment may be thought of as composed of a fraction which is sea-water and a remainder which is solid material. Porosity, which is a measure of the volume fraction of the sediment occupied by sea-water, is therefore seen to be an important parameter of marine sediments in describing the way they react acoustically.

The relationship between the density and porosity of marine sediments would be perfectly linear if the specific gravity of the solid material of all marine sediments was the same. For this case the density of the sediment would be equal to that of the solid material at zero porosity, equal to that of sea-water at one hundred percent porosity, and equal to an intermediate value determined by linear interpolation at any other value of porosity. This relationship is expressed as

$$\rho_{SED} = \rho_{WAT} \cdot \Phi + \rho_{SOL} [1 - \Phi] \qquad \text{(Eq. 23)}$$

where ρ_{SED} is the density of the sediment, ρ_{WAT} is the density of sea-water, ρ_{SOL} is the density of the solid material, and Φ is the porosity of the sediment. While the densities of the solid material of naturally occuring marine sediments do differ somewhat, their

range is sufficiently restricted that a good straight-line fit for sediment density versus porosity can be made. The degree to which a linear relationship exists has been demonstrated by Nafe and Drake (1963) in which density measurements taken from Birch (1942), Hamilton, et al. (1956), Shumway (1960), Sutton, et al. (1957) and Kershaw (unpublished) were plotted versus porosity without regard to sediment type (Figure 1, after Nafe and Drake). Richards (1962) has demonstrated a similar relationship with his data, which comprise nearly 500 oceanic samples.

The equation for compressional-wave velocity in elastic media (Ewing, Jardetsky, Press, 1957) is given by

$$C = \left[\frac{K + (4/3)\mu}{\rho}\right]^{\frac{1}{2}} \qquad \text{(Eq. 24)}$$

where ρ is the density, K is the bulk modulus, and μ is the modulus of rigidity. Where rigidity is negligible Eq. 24 reduces to

$$C = (B \cdot \rho)^{-\frac{1}{2}} \qquad \text{(Eq. 25)}$$

where B is the compressibility. Wood (1945) noted that in a suspension of solid particles in water, the bulk compressibility is equal to the sum of the individual compressibilities of the particles, weighted according to their fractional volumes in the suspension. Urick (1947) tested this experimentally and found it valid. Since the compressibility of sea water is so very much larger than the compressibilities of

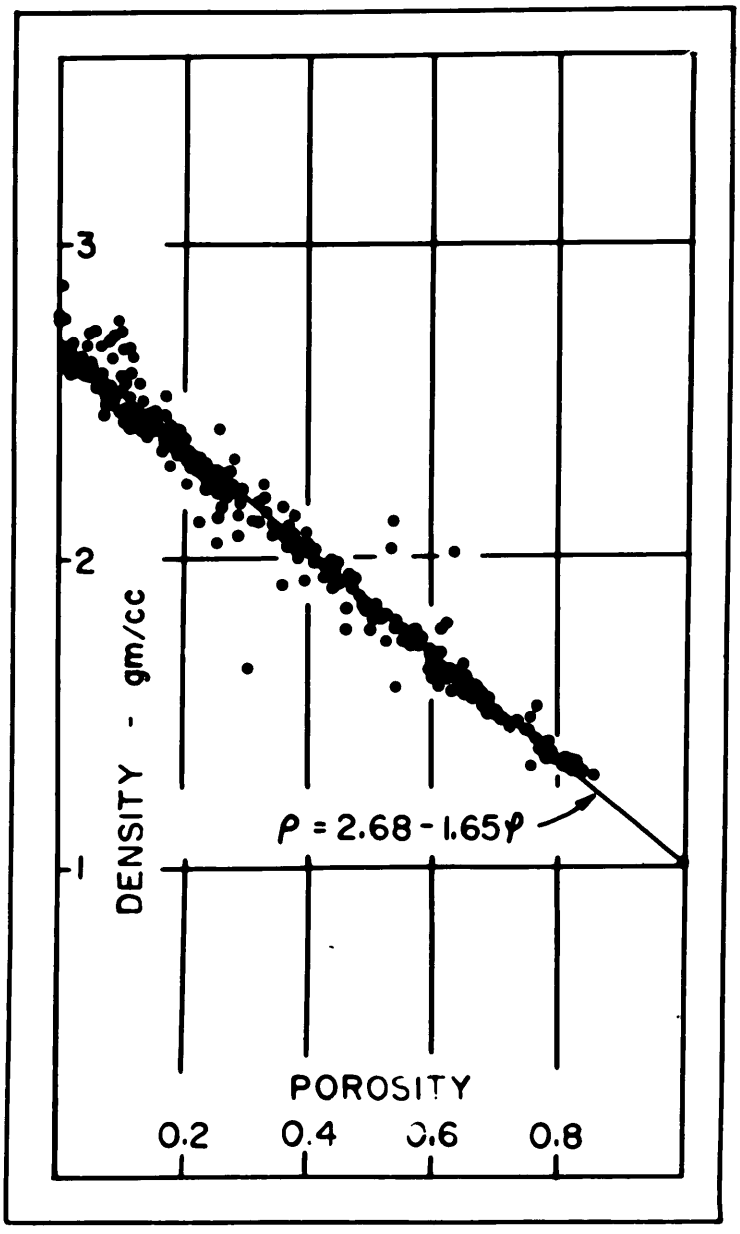

Figure 1. Experimental Values of Density Versus Porosity for Typical Oceanic Sediments (After Nafe & Drake, 1963).

mineral grains that occur in natural sediments, the volume fraction of sea-water in a natural sediment (the porosity) exerts a dominant effect on the bulk compressibility of the sediment, regardless of its mineralogical composition. This relationship is expressed as

$$\beta_{SED} = \beta_{WAT} * \Phi + \beta_{SOL}[1-\Phi] \qquad \text{(Eq. 26)}$$

where β_{SED} is the bulk compressibility of the sediment, β_{WAT} is the compressibility of sea-water, β_{SOL} is the compressibility of solid material, and Φ is the porosity of the sediment.

A natural unconsolidated sediment may be considered to resemble a suspension of solid particles in sea-water and possess a compressional-wave velocity approximating that defined by Eq. 25. The density and bulk compressibility may be approximated by Eq. 23 and Eq. 26 respectively. The compressional-wave velocity may therefore be expressed in the following form (Wood's Equation)

$$C = \left([\rho_{WAT} * \Phi + \rho_{SOL}(1-\Phi)] \times [\beta_{WAT} * \Phi + \beta_{SOL}(1-\Phi)] \right)^{-\frac{1}{2}} \qquad \text{(Eq. 27)}$$

using Eq. 23, Eq. 25, and Eq. 26. The degree to which this expression adequately describes the compressional-wave velocities of unconsolidated sediments has been demonstrated by Nafe and Drake (1963) in which measurements of compressional-wave velocity taken from Sutton (1957), Hamilton (1956), Shumway (1960), Laughton (1957) and Kershaw (unpublished) have been plotted versus porosity (Figure 2, after Nafe and Drake).

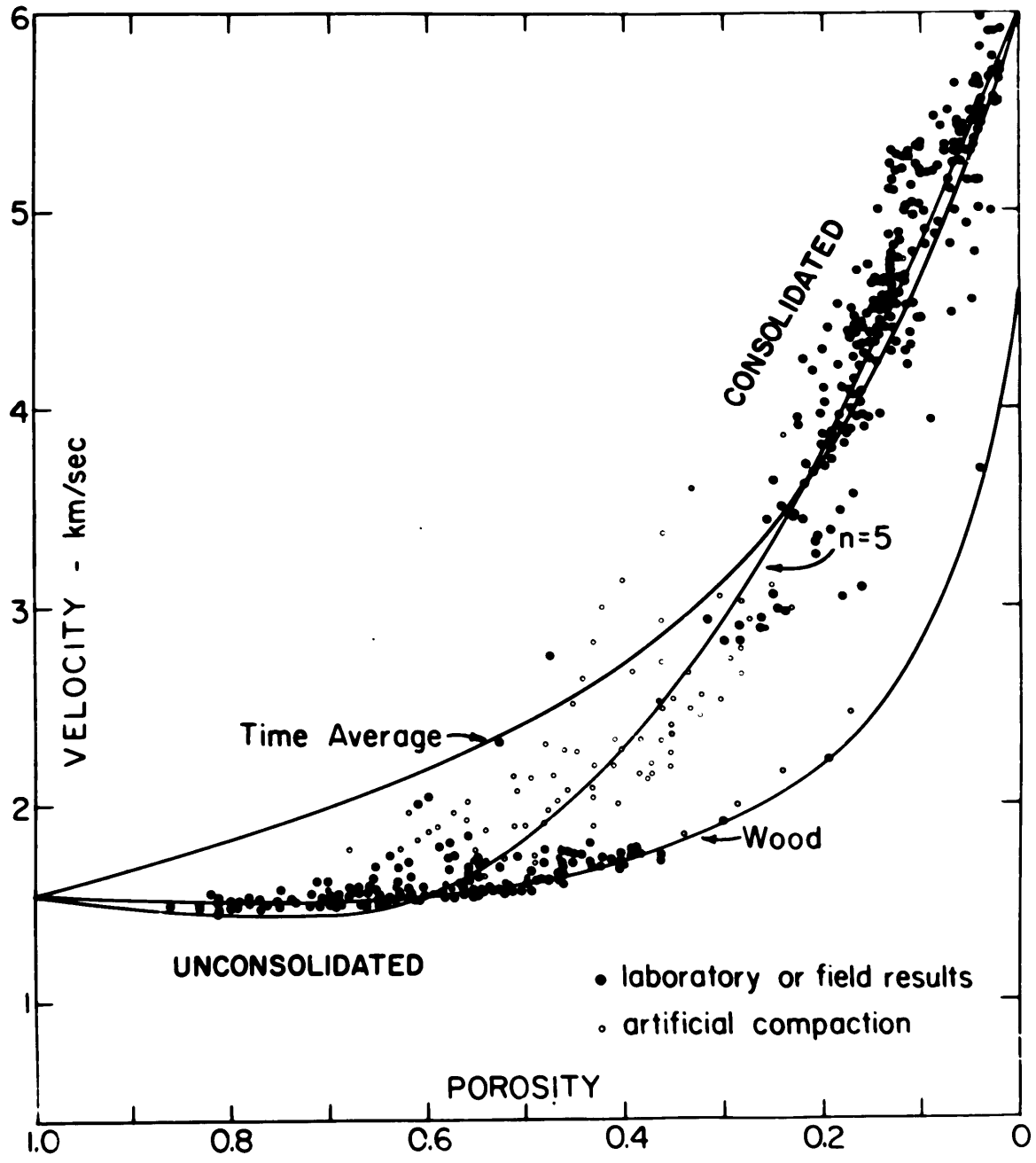

Figure 2. Experimental Values of Velocity Versus Porosity for Typical Oceanic Sediments (After Nafe & Drake, 1963).

The specific acoustic impedance of the sediment may be obtained by taking the product of the density (Eq. 23) and compressional-wave velocity (Eq. 27). This impedance, in conjunction with the specific acoustic impedance of sea-water, may be used to determine the Rayleigh Reflection Coefficient (Eq. 13). The bottom loss, in decibel form, may then be obtained through Eq. 22. A plot of density, velocity, impedance, reflection coefficient, and bottom loss versus porosity is presented in Figure 3 to portray the relationships that exist between these variables according to Eq. 13, Eq. 22, Eq. 23, Eq. 25, Eq. 26, and Eq. 27. Densities of 1.03 $g/_{cm}3$ and 2.75 $g/_{cm}3$ and compressibilities of 43×10^{-12} cm^2/dynes and 2.0×10^{-12} cm^2/dynes were assumed for sea-water and solid material, respectively. It is seen that bottom loss increases as the porosity of the sediment increases.

The Relationship Between Bottom Loss and Geological Properties of Sediments

The relationship between bottom loss and physical properties of sediments has been discussed in the previous section. In particular, bottom loss was shown to be related to the porosity of the sediment. Since the porosities of natural sediments are related, though not regorously, to the grain-size or textural characteristics of natural sediments, it is also possible to establish a general relationship between bottom loss and geological properties of sediments.

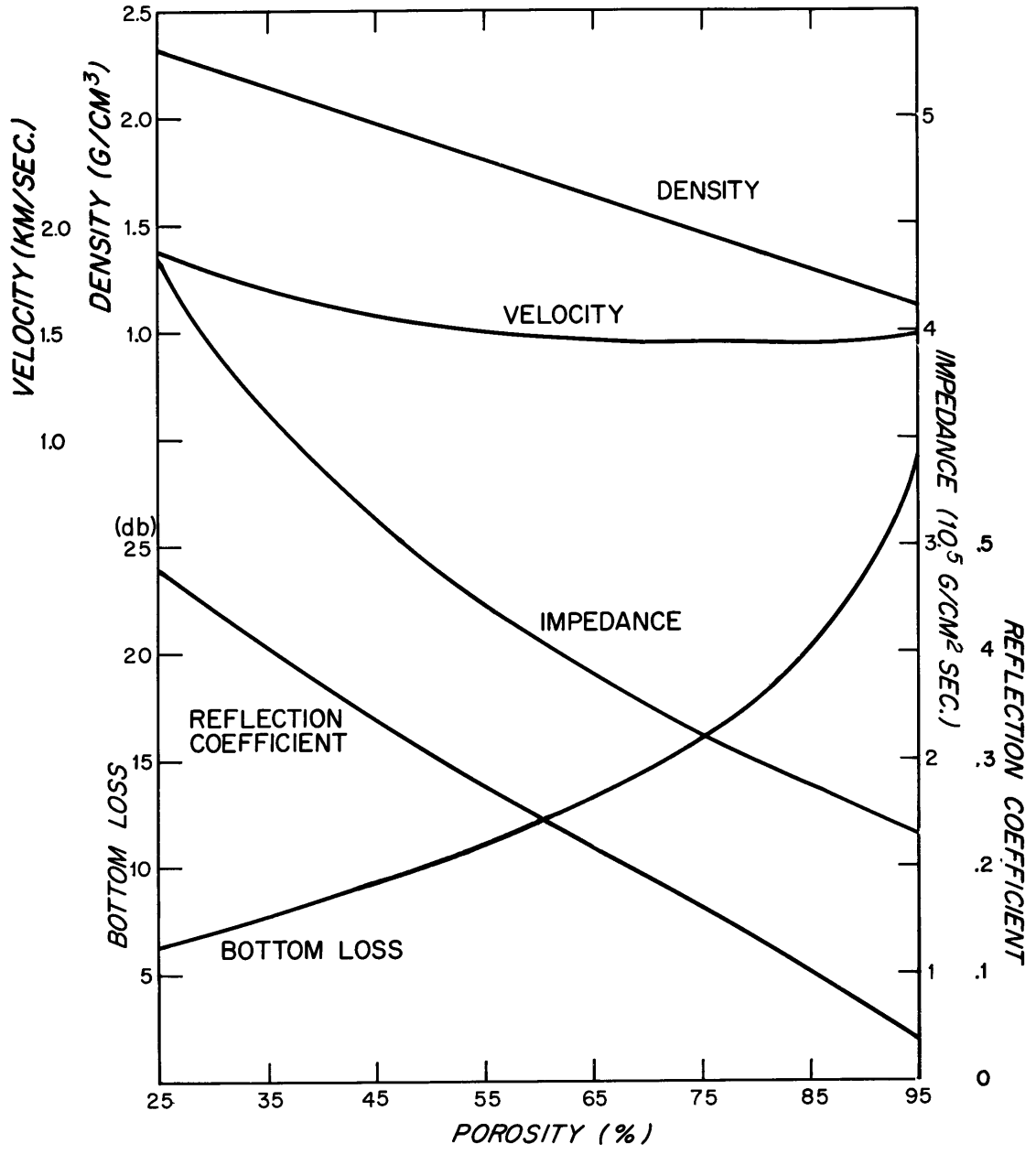

Figure 3. Theoretical Curves of Density, Velocity, Impedance, and Reflection Coefficient Versus Porosity.

Theoretically, sediments composed of spheres and possessing equal degrees of sorting would have the same porosity regardless of grain size, and a decrease in the degree of sorting would allow interstices to fill in and result in reduced porosity (Graton and Fraser, 1935). Actually, grains occuring in natural sediments are not spheres and considering them as such is oversimplifying the situation to the point that it is misleading. The porosity of a natural sediment is a function of the grain size (median grain size), distribution of grain size (sorting), shapes of the grains (roundness and sphericity), and packing or orientation (fabric). The exact form of this function is not known; the variables are usually concomitantly related in natural sediments, and it is difficult to isolate individual effects. Nevertheless, a consideration of some physical factors involved will serve to establish general relationships.

Particles in the sand and coarse silt size ranges are sufficiently large that gravity plays the major role in determining their structures in sediments. These sediments exhibit single-grained and mixed-grained structures, which are tight fabrics with attendant low porosities. Particles in the fine silt and clay size ranges are small enough to be appreciably affected by intermolecular forces. These particles tend to stick to the first grain encountered during the sedimentation process and are prone to form honeycomb and honeycomb-flocculent

structures, which are loose fabrics with attendant high porosities (Hamilton and Menard, 1956).

As the particles become smaller, the ratio of their surface area to volume increases. This results in an increase in the ratio of surface adsorbed water to particle volume with attendant increase in porosity; for small particles the surface adsorbed water may be more than that contained in the geometrical interstices of the sediment (Emery, 1960). This applies particularly to particles in the clay size range.

An increase in the angularity of the particles will generally be associated with an increase in the porosity of the sediment because the attendant increase in friction between the particles will retard the development of a tight fabric and any decrease in the sphericity or roundness will increase the surface area and therefore the volume of surface-adsorbed water. There is a general inverse relationship between angularity and particle size for natural sediments because of the platy habit of clays and the fact that smaller particles usually have experienced less rounding by natural forces (Hamilton et al., 1956).

An increase in the clay content of a sediment will increase its porosity because of the associated structural, size, and shape effects that have been previously discussed. In addition, clay particles increase the porosity of a sediment by a phenomenon known as bridging.

The clay particles with their flat sides horizontally oriented in the sediment cause a bridging effect between other grains which increases the sizes of the interstices (Terzaghi and Peck, 1948).

The degree of sorting does not seem to have a pronounced relationship to the porosity of natural sediments in contradistinction to what might be expected at first thought. It would seem that the extent to which finer grains would fill interstices between coarser grains and thus lower the porosity would be inversely related to the degree of sorting. This process is most effective for coarser sediments in which most of the water is contained in geometrical voids rather than adsorbed on grain surfaces (Fraser, 1935); it is not an important factor in finer sediments in which surface effects play a major role. Indeed, since finer sediments usually exhibit a direct relationship between degree of sorting and grain size, a decrease in sorting will be associated with an increase in porosity due to the dominant effect of grain size.

The net result of the above mentioned physical factors that influence the porosity of natural sediments is that the porosity generally increases as the grain size decreases or the percentage of silt plus clay (fine fraction of the sediment) increases; clay exerts a stronger influence on the porosity than silt. These relationships for natural sediments have been empirically established (Fraser, 1935), (Trask, 1932), (Krynine, 1947), (Birch et al., 1942), (Hamilton et al., 1956),

(Shumway, 1960), (Sutton et al., 1957), (Shumway, 1960), (Sarmiento and Kirby, 1962), (Ryan, Workum, and Hersey, 1962), and (Richards, 1962). The relationship between grain size and porosity is shown in Figure 4 (after Shumway). The relationship between the coarse fraction (the complement of the fine fraction) and porosity is shown in Figure 5 (after Shumway).

Sedimentary nomenclature is commonly based on sand-silt-clay ratios. Since clays are more porous than silts and both silts and clays are much more porous than sands, a general relationship exists between class names and porosities of natural sediments. Since each class name encompasses a range of sand-silt-clay ratios, the relationship between class name and porosity is necessarilly broad and poorly defined. Nevertheless, it is useful because many sedimentological observations are reported by class name only.

A method exists by which the median grain size of a sediment can be estimated from its sand-silt-clay percentages (Plumley and Davis, 1956) based on the assumption that sediment sizes are normally distributed. This method has been applied to the commonly used classification system of Shepard (1954) in order to establish approximately the rank and range of sizes represented by the various class names of that system. The size ranks and ranges are shown in Figure 6; because of the inverse relationship between porosity and

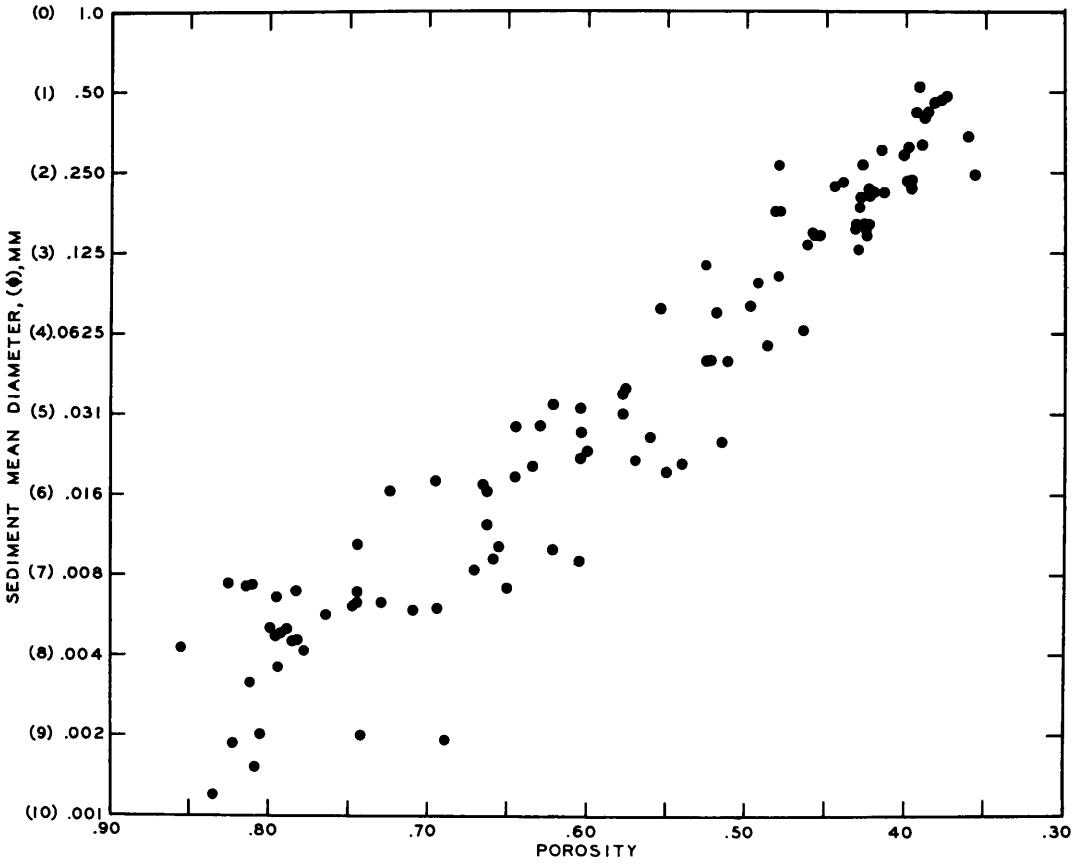

Mean diameter vs. porosity for unconsolidated marine sediments.

Figure 4. Experimental Values of Mean Diameter Versus Porosity for Typical Oceanic Sediments (After Shumway, 1960).

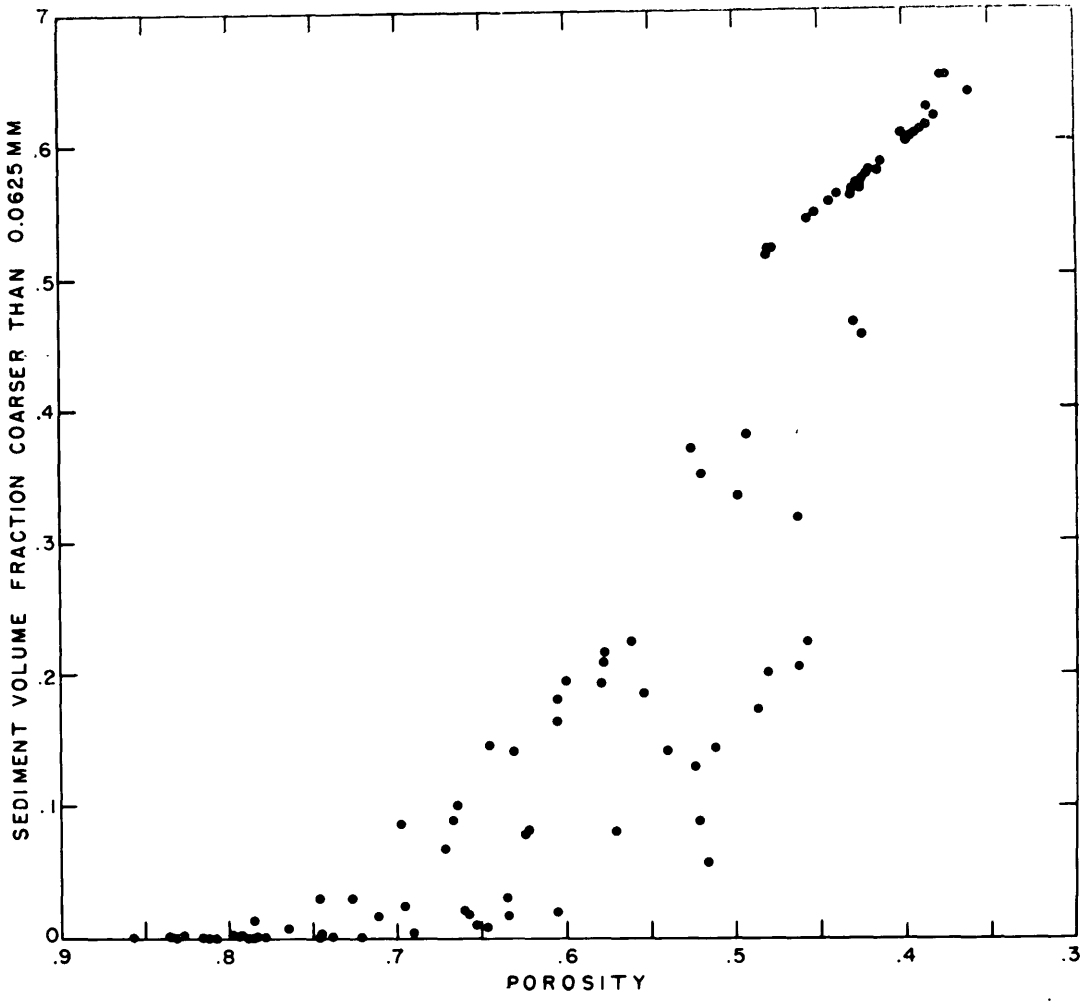

Sediment sand content vs. porosity.

Figure 5. Experimental Values of Coarse Fraction Versus Porosity for Typical Oceanic Sediments (After Shumway, 1960).

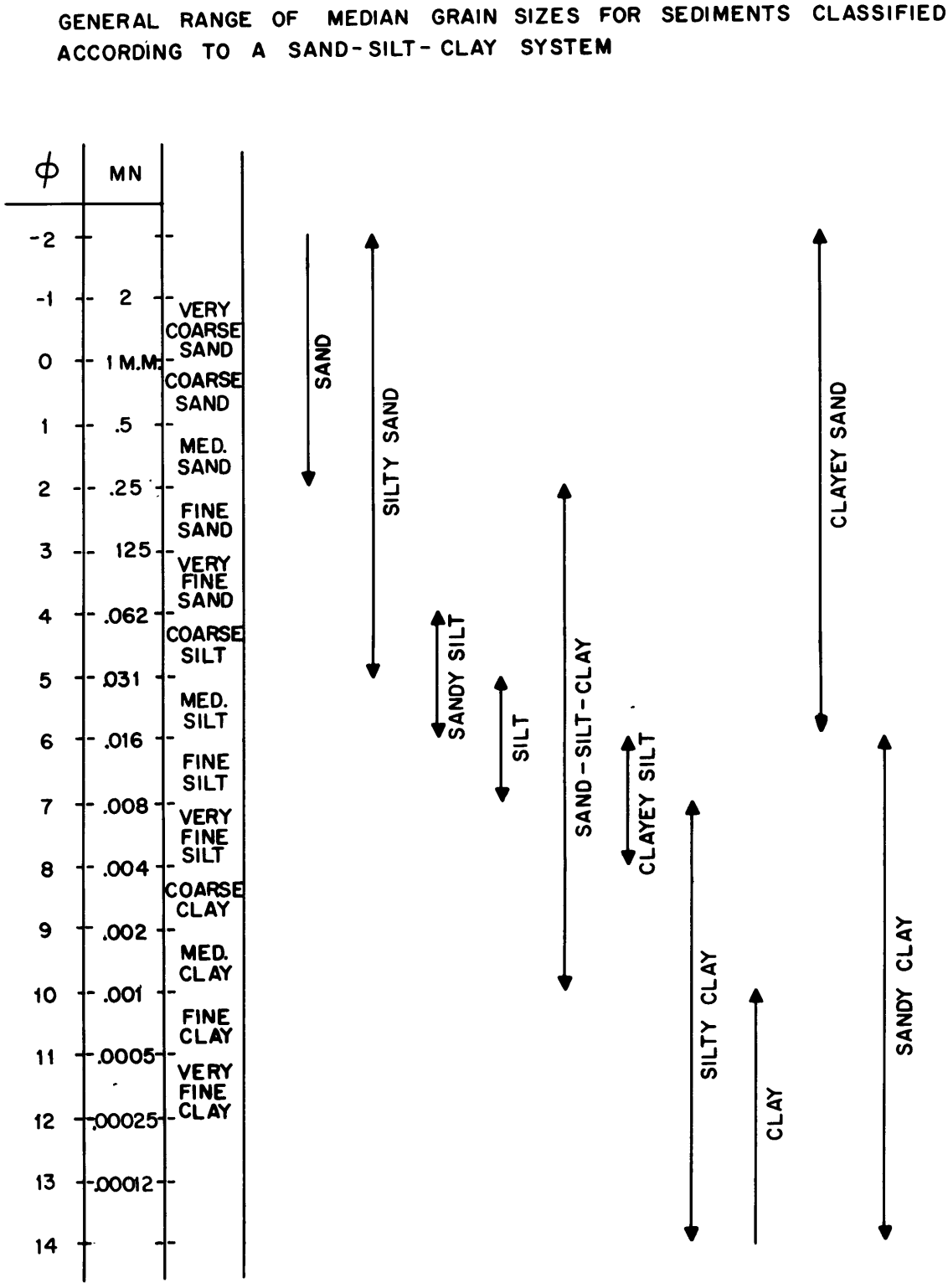

Figure 6. General Range of Median Grain Sizes for Sediments Classified According to a Sand-Silt-Clay System.

grain size, this figure also indicates the porosity ranks and ranges.

In resumé, bottom loss is inversely related to the grain size and directly related to the fine fraction for natural sediments. Where the Shepard classification system is used, bottom loss increases according to the following sequence: sand, silty sand, sandy silt, silt, sand-silt-clay, clayey silt, silty clay, and clay. The ranges of the class names overlap and silty sand, sand-silt-clay, and silty clay are the worst offenders in this respect.

CHAPTER III

METHODS

Acoustic Measurements

The acoustic-reflectivity measurements of this investigation were made only at normal incidence and only with pulses of 12-kcps sound. Normal incidence provides the largest echo return available in single-ship operation and, in fact, is the practical way to achieve a usable signal-to-noise ratio under typical field conditions. The frequency 12-kcps was used because it is a common frequency in echo sounding, and equipment employing it was available. The ping length used was 5 milliseconds in deep water and 1 or 2 milliseconds in shallow water.

The peak amplitude and total energy of an acoustic wave-train are two easily measurable qualities which characterize the observed reflection. These two qualities were used as measures of reflectivity in this research. The peak-amplitude measurement is obtained by measuring the maximum peak-to-peak excursion of the pressure wave-train. The total-energy measurement is a representation of the sum total of the energy in the echo. It is obtained by measuring the final value of the time integral of the squared pressure ($\int p^2 dt$) of the wave-train, which function is generated by an on-line analogue

computer. A time of 100 milliseconds after the first arrival of the echo was arbitrarily selected as the time at which the energy content of the echo would be considered to have reached its final value. This procedure makes the measurement not only purely objective but also amenable to machine determination, and is a compromise necessary for analyzing the large sample of data taken in this investigation.

The shipborne instrumentation system used to make the acoustic-reflectivity measurements is described in detail in Chapter IV. The acoustic-source level and echo strength were determined by electrical measurements made inside the transducer. This is inferior to an acoustic calibration, since it makes the measurement dependent on the transmitting and receiving characteristics of the transducer, but it was the only method practical during this investigation.

The transducer used as the source and receiver was the UQN-1b (Edo Corp., undated), mounted on the hull of the ship or in a towed fish (Knott and Witzell, 1961). This is a standard sonar transducer employing ammonium dihydrogen phosphate (ADP) crystals (these crystals possess piezoelectric properties; their effect in an electrical circuit is predominantly capacitative.) as the active element inside a cylindrical housing 16 inches in diameter. Included inside the transducer housing are a multi-tapped inductor and a 10-ohm resistor in series with the active element. The

multi-tapped inductor is adjusted to tune the series circuit to resonance at 12-kcps, where the transducer impedance appears real and equal to a nominal value of 200-ohms. A voltage measurement across the 10-ohm resistor, henceforth called the calibration resistor, was used as a measure of the acoustic input and output of the transducer.

Since voltages appearing anywhere in a series loop are additive, an externally generated voltage impressed upon the calibration resistor has the same effect on the circuit as a signal voltage generated by the transducer in response to an acoustic signal. The acoustic signal required to generate this signal voltage was determined by reference to the receiving sensitivity of the transducer, which is directly stipulated by the manufacturer as -73 db//1 volt for a sound field of 1 dyne/cm^2.

The voltage developed across the calibration resistor by the outgoing ping is a measure of the current passed and power dissipated by the active element of the transducer. The acoustic output was determined by reference to the relationship between the peak-to-peak source level and peak-to-peak voltage on the calibration resistor where the source level equals 79 db + 20 log (voltage). This relationship was established by measurements made on three UQN-1b transducers using a calibrated receiver (Atlantic Research Corp., 1963) and projector (Underwater Sound Reference Laboratory, 1954), (David Bogen Co., 1946). The transducers were selected at random

and were considered representative of the typical UQN-1b since their measured receiving sensitivity agreed with that specified by the manufacturer.

The discussion above pertains to the measurement of acoustic reflectivity, which comprises the major acoustic investigation. In addition, a subsidiary experiment, using a lowered pinger which is described in detail in Chapter IV, was made to study the nature of the reflection process at the sea-floor. The pinger was lowered on a wire from an oceanographic winch. At various intervals the winch was stopped and the bottom echo from the pinger was measured at the ship using the shipborne instrument system, previously mentioned.

Geologic Measurements

A grain-size analysis was performed on all the sediment samples that were obtained in parallel with measurement of acoustic-reflectivity. The gravel, sand, and both silt and clay fractions were determined by sieve, settling tube (Ziegler, Whitney, and Hayes, 1960), and pipette (Krumbein and Pettijohn, 1938) analysis, respectively.

A grab dredge, described in Chapter IV, was used to obtain the sample of the surficial sediment. These samples dried out during storage and so were allowed to soak overnight in distilled

water, with sodiumhexametaphosphate added as a dispersing agent, before being analyzed. The size analysis was then performed using only as few of the above-mentioned techniques as were necessary to obtain the twenty-five and seventy-five percent quartiles of the cumulative size distribution curve (Krumbein and Sloss, 1956) for each sample. Gravel, sand, silt, and clay percentages, using the Wentworth Particle Size Scale (Wentworth, 1922) and quartile values, were picked off the cumulative size distribution curves.

A water-content analysis was performed on a suite of sediment samples taken during a revisit to the sites of the original sediment stations. The water content of a sediment is defined in soil mechanics as the ratio of its weight of water to weight of solid matter (Taylor, 1948) and can be determined by direct measurement of its natural (net) and dried weights.

The specimen for water-content analysis was taken by pressing a tin can into an undisturbed surface section of the dredge haul and slicing the excess sediment off the top with a trowel. Water was added to fill the can when the sample was coarse grained in order to simulate the in situ conditions. The contents of the can were then placed in pre-weighed bottles in order to minimize transfer error. The bottles and contents were subsequently weighed ashore on a triple-beam balance both before and after drying in an oven at 105°C for 24 hours to obtain the wet and dry weights.

Photographs of the sea-floor to observe surface features were taken at the sites of some sediment stations. The Owen and Edgerton Cameras, described in Chapter IV, were both used at various times depending on the preference of the photographer present. Mr. David Owen accompanied some cruises and used his camera and the author used the Edgerton Camera. The resulting photographs were inspected to determine small-scale roughness of the areas investigated.

CHAPTER IV

INSTRUMENTATION

The Acoustic Reflectivity Measurement System

A semi-automated measurement system, henceforth called the Acoustic Reflectivity Measurement System, was designed and constructed to facilitate the acquisition of acoustic data on shipboard. This system is capable of automatically performing acoustic measurements repeatedly at two-second intervals after the controls involving time synchronization and dynamic range have been set manually. Data is recorded in both stored form and in real time. The pressure and the energy versus time waveforms of the echo are recorded in stored form as oscilloscope photographs. Real-time measurements of the energy in the echo are presented as digital print-out, and as a length-modulated trace on the record of the Precision Graphic Recorder.

The system, in final form, incorporates the AN/UQN-1b Sonar Sounding Set, a familiar Navy echo sounder (Edo Corp., 1954); the Precision Graphic Recorder (PGR), a correlation recorder adapted to high-resolution echo-sounding (Knott and Hersey, 1956; Knott and Witzell, 1961; Knott, 1962); the Oceanographic Computer, Model 45.001, a squaring and integrating on-line analogue computer (Baxter, 1960); the System Synchronization and Control Unit, a device made especially for this investigation which governs the

operation of the entire system; the Sweep-Synchronized Positionable Trigger, an appendage to the Precision Graphic Recorder which provides synchronization with the anticipated arrival of the echo (Witzell, in preparation); and two systems for recording the measurement: a dual-beam oscilloscope (Tektronix Inc., 1959) and camera (Fairchild Camera and Instrument Corp., 1952) and a digital voltmeter and recorder (Hewlett-Packard Co., 1961). A functional block diagram of the equipment is shown in Figure 7 and a photograph of the shipborne measurement system in Figure 8. The annotated titles in the photograph correspond to those in the block diagram.

A description of the operation of the system follows: The PGR (Figure 9) keys the echo sounder which causes a 12-kcps sonic pulse of rectangular envelope to be emitted into the water by the UQN-1b transducer. The echo from the sea floor is received back at the transducer and is amplified by the echo sounder. The amplified signal is applied to the PGR for making the usual bathymetric trace, to one channel of the dual-beam oscilloscope for display of the pressure wave train, and to the Oceanographic Computer which squares and integrates the signal and thus provides a measure of its energy content. The output of the computer is applied to the other channel of the dual-beam oscilloscope for a display of the energy contained in the wave train and also to the digital voltmeter and recorder combination which digitizes and prints the value of the

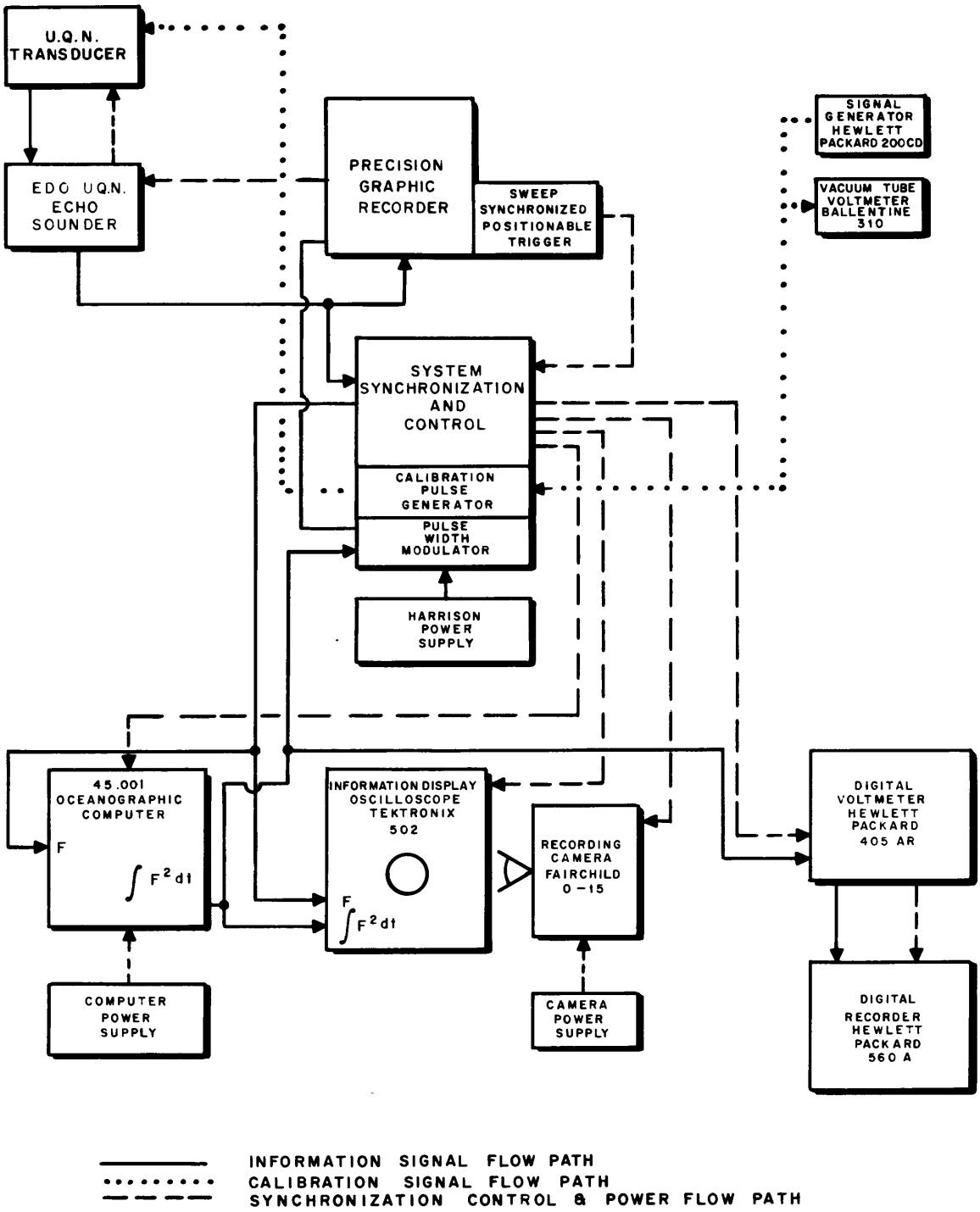

Figure 7. Block Diagram of the Acoustic Reflectivity System.

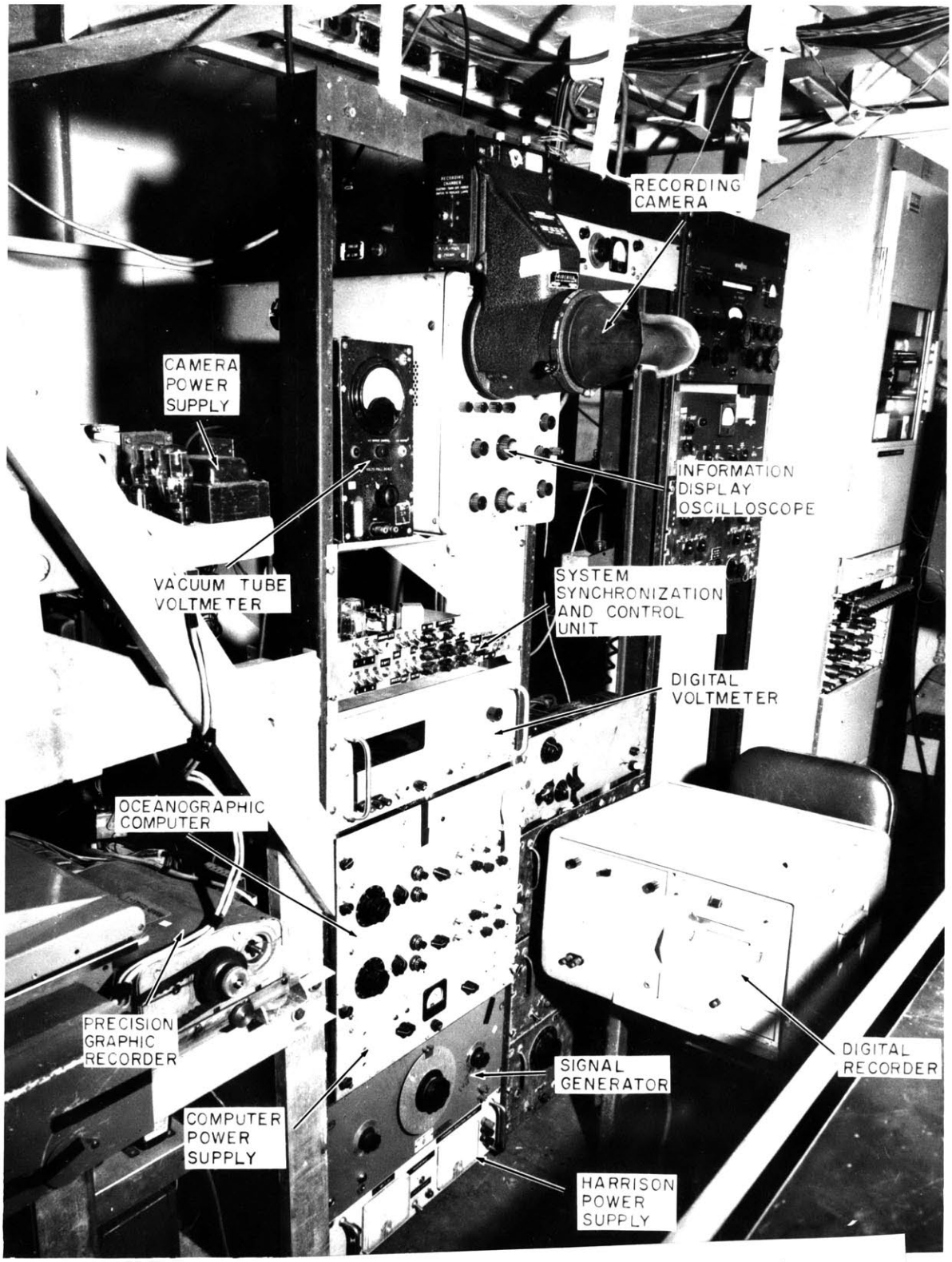

Figure 8. Photograph of the Components of the Acoustic Reflectivity System.

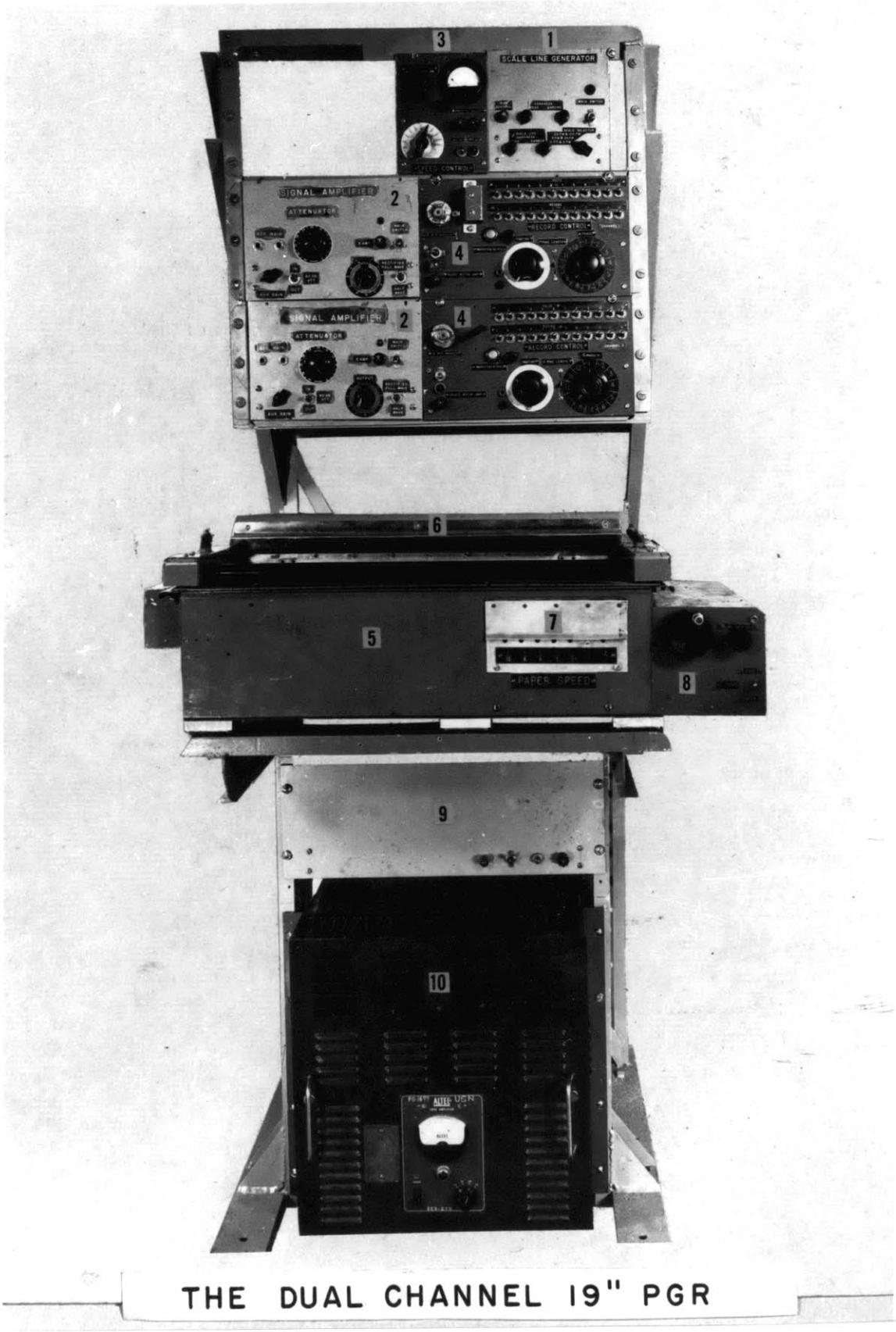

Figure 9. Photograph of the Precision Graphic Recorder (PGR) (After Knott and Witzell, 1960).

complete integral. The face of the oscilloscope is photographed by means of an automatically recording camera capable of obtaining 1600 exposures on a single hundred-foot reel of 35-mm film. In addition, a pulse-width modulator inspects the value of the complete integral and generates a pulse whose duration is equal to the analogue of the energy in the received echo. This pulse is fed to the PGR, where it appears as a mark on the record (next to the bathymetric trace) whose length is proportional to the energy contained in the reflected echo.

The system also generates a 12-kcps electrical pulse of rectangular envelope and of known voltage and duration. The pulse is automatically applied to the transducer at a time slightly earlier than that of the bottom-reflected signal. This is used in obtaining a measurement of the strength of each acoustic return as discussed in the previous chapter.

A prototype of a solid-state sonar transceiver (T. H. Gifft & Associates, undated) was designed and built by T. H. Gifft and used in place of the driver and amplifier sections of the EDO UQN-1b echo sounder, during cruises of the R/V BEAR and R/V ASTERIAS.

The transmitting and receiving directivity pattern of the transducer is circularly symmetrical and has a thirty-degree beam-width as defined by the limits where the response is 3 db down

(Figure 10). The peak of the back lobe is more than 25 db down even when mounted in a towed fish (Figure 11).

The System Synchronization and Control Unit (Figure 12) performs the entire task of synchronization between the various other units of the reflectivity measurement system. A calibration-pulse generator and the pulse-width modulator mentioned above are incorporated into this unit. The system functions that are performed by this unit are the following: 1) the zeroing of the Oceanographic Computer, 2) the injection of a calibration pulse at the transducer, 3) the opening of the shutter of the oscilloscope camera, and 4) the triggering of the information display oscilloscope, all just before the anticipated arrival on the echo, 5) the closing of the shutter of the oscilloscope camera, 6) the freezing of the output of the Oceanographic Computer, and 7) the commanding of the digital voltmeter to digitize the output of the Oceanographic Computer, all at a proper time after the arrival of the echo, 8) the generation of a calibration pulse to be injected at the transducer, and 9) the generation of a width-modulated pulse for display on the PGR. A description of the electronic circuitry of this unit is presented in Appendix A.

The Sweep-Synchronized Positionable Trigger is employed to provide synchronization of the System Synchronization and Control Unit with the anticipated arrival of the echo. This instrument uses

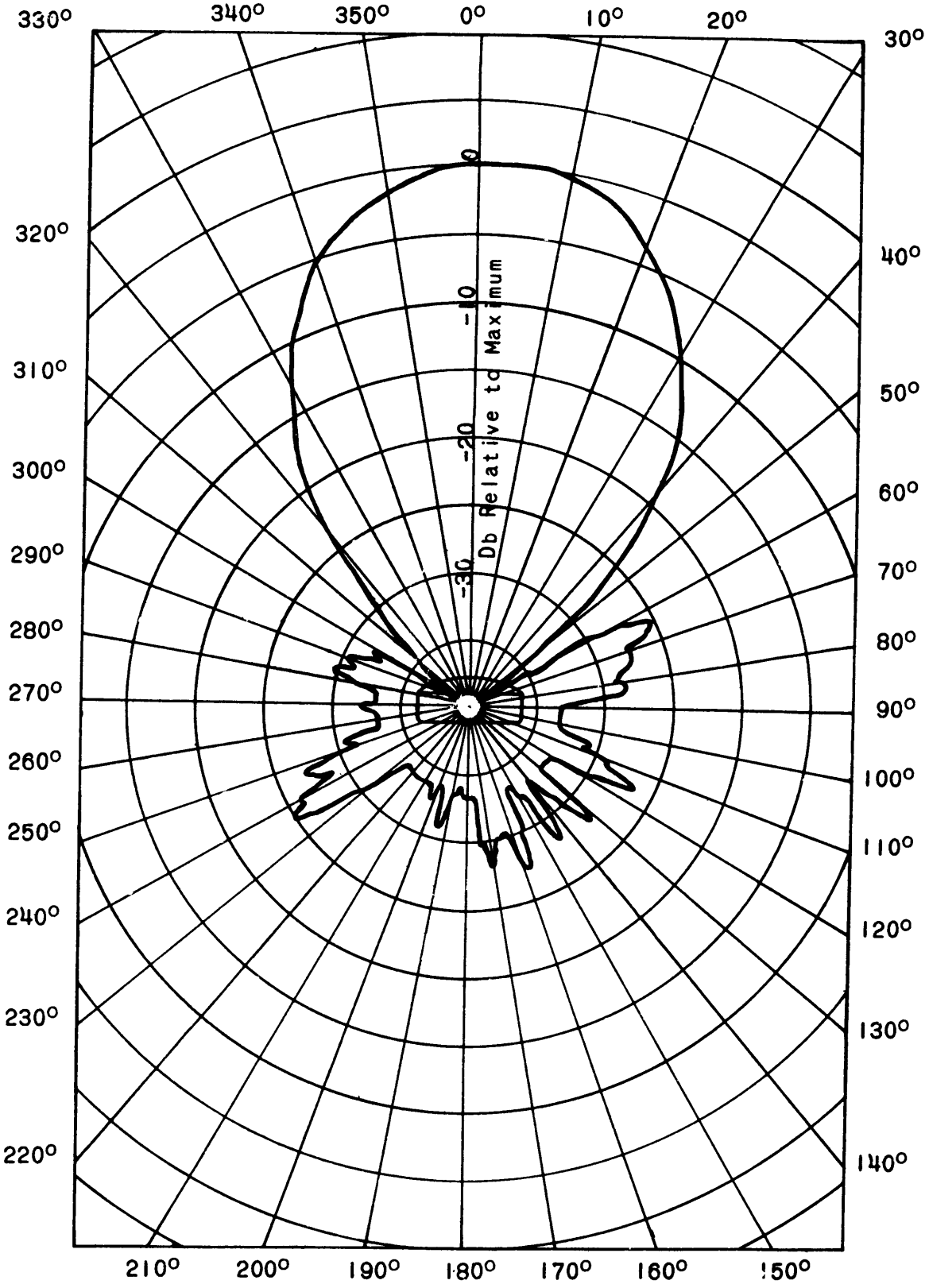

Figure 10. Transducer Directivity Pattern at 12 KC.

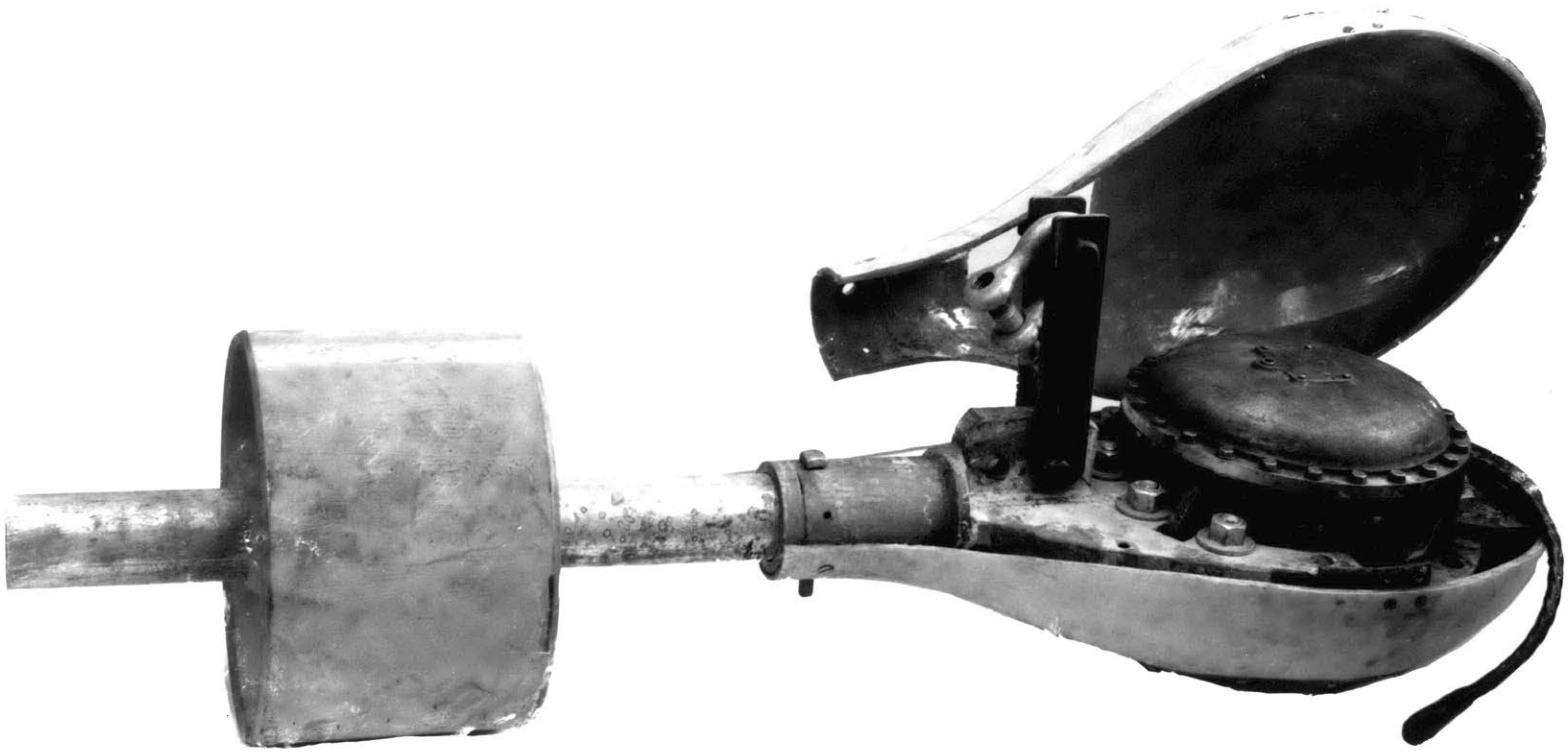

Figure 11. Photograph of the UQN-1B Transducer Mounted in a Towable "Fish" (After Knott and Witzell, 1960).

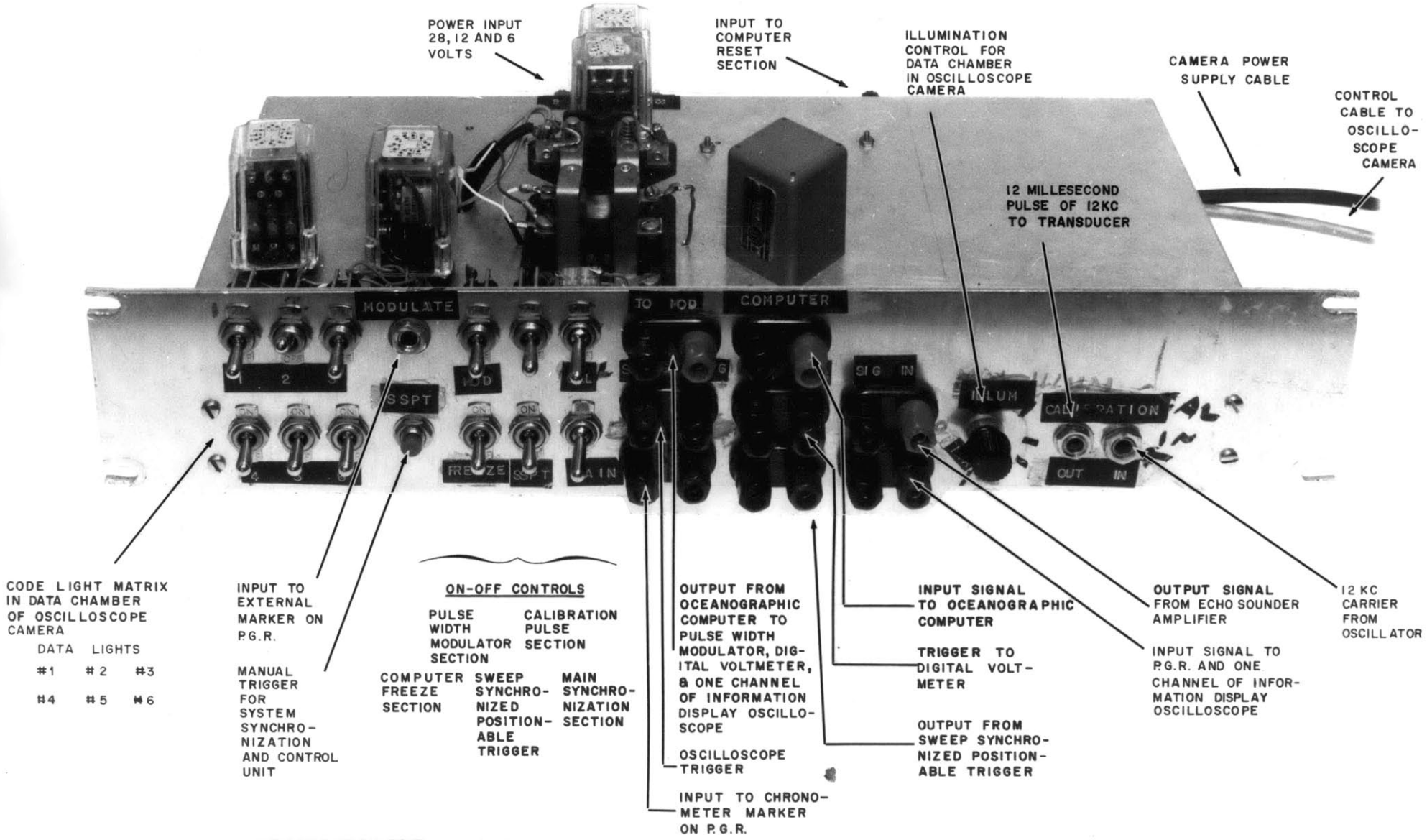

Figure 12. Photograph of the System Synchronization and Control Unit of the Acoustic Reflectivity System.

a small, permanent magnet, which is rigidly fixed to the shaft of the recording drum of the PGR, and a magnetic reed switch which may be positioned throughout 360° in a plane perpendicular to this shaft. The Sweep-Synchronized Positionable Trigger provides a trigger pulse at a manually-selectable time within a single sweep of the PGR. When used in conjunction with the recording program gate in a dual-channel PGR, it can be adjusted to feed a trigger output to the System Synchronization and Control Unit, which is synchronized to the arrival time of the echo from the sea floor. The System Synchronization and Control Unit then synchronizes and controls the remainder of the units of the reflectivity system so as to effect the automatic measurement of an echo.

Measurements are recorded as oscilloscope photographs which subsequently are treated by digital processing equipment located ashore. The oscilloscope photographs contain both the pressure versus time and energy versus time waveforms of the echo in addition to an electrical pulse injected as a calibration. A typical oscilloscope photograph is shown in Figure 13. The calibration pulse leads the echo on both traces and the trace of the pressure function is above the trace of the energy ($\int p^2 dt$) function. These photographs represent the data in its most useful though cumbersome form. This form of presentation permits culling of the data in the analysis stage to remove gross errors due to spurious

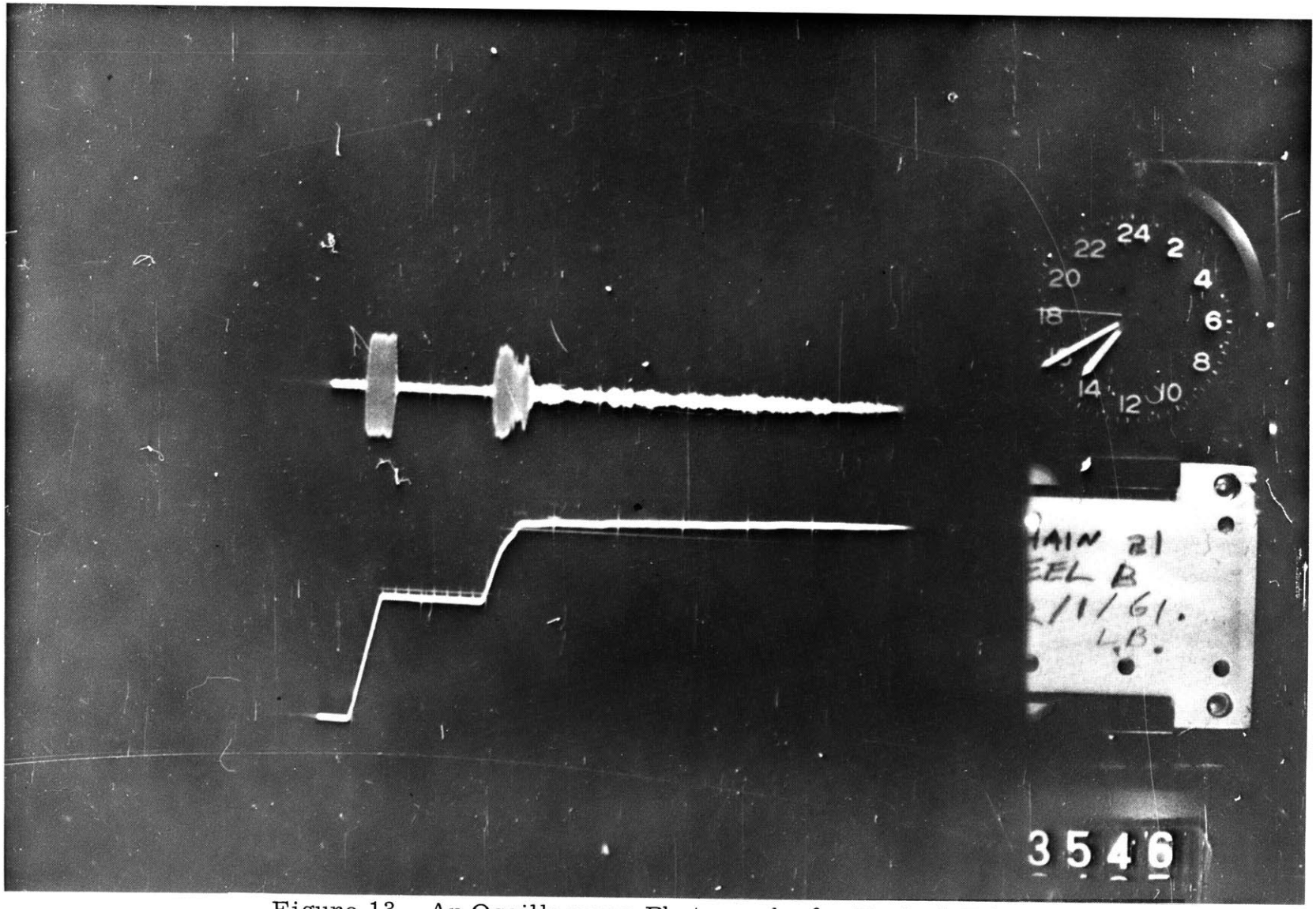

Figure 13. An Oscilloscope Photograph of a Typical Echo Received from the Sea Floor.

electrical signals, quenching (air getting under the transducer because of violent ship motion), water slap on the transducer, and excessive ship or animal noise.

Measurements of the total energy contained in the echo are also provided by both the pulse-width modulator, a subsystem of the System Synchronization and Control Unit, and the digital voltmeter and recorder combination. The output of the pulse-width modulator is presented on the PGR record as a bar graph so that the energy content of successive echoes can be correlated conveniently with the travel-time plot. The digital voltmeter and recorder combination presents the same information in the form of numbers printed on roll paper. These real-time measurements do not represent bottom loss, but rather only echo strength, since no consideration has been made of the propagation loss associated with the water depth. A real-time computer could be put on-line to correct this, but has not yet been done.

A pulse-width modulated section taken over a relatively flat sea floor is shown in Figure 14. The range of variability of the energy of the received echoes is immediately apparent as is the correspondence between the tone of the echoes in the standard bathymetric recording and the quantitative representation of their strength by the pulse-width modulator. A section of PGR record with a calibration of the pulse-width modulator on it is shown in

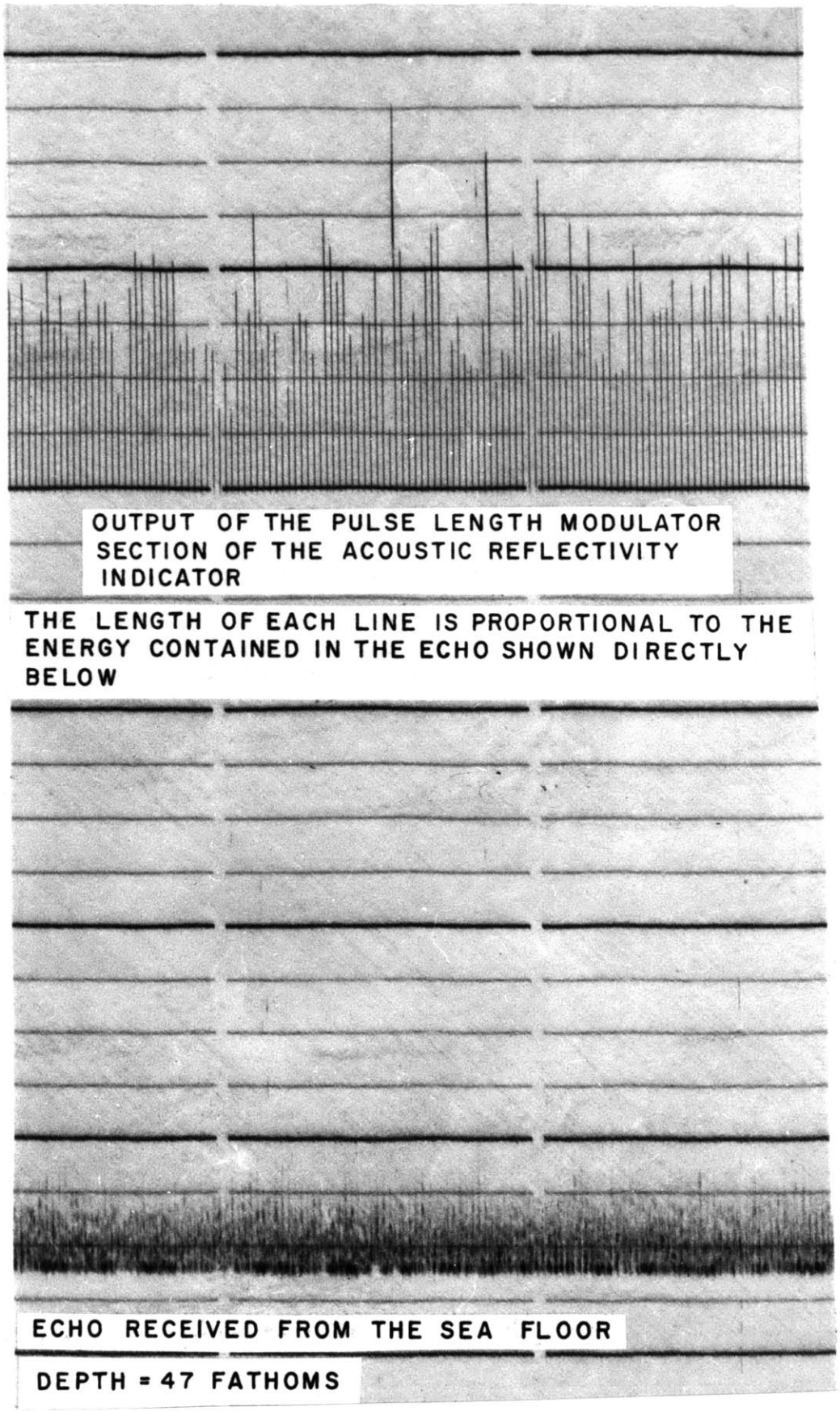

Figure 14. Section of Acoustic Reflectivity Record Obtained as an Output of the Pulse Width Modulator.

Figure 15. Note the linearity of the mark length with the modulating voltage which, in our application, is the output of the squaring and integrating on-line analogue computer.

The instrument system was developed and refined throughout this investigation. The description of the Acoustic Reflectivity Measurement System as presented above represents the final form achieved.

The Precisely Timed Submersible Pinger

A Precisely Timed Submersible Pinger (Breslau, Hersey, Edgerton and Birch, 1962) was made by including a Miniaturized Precision Time Source (Breslau, 1961) in a standard Edgerton Submersible Pinger (Edgerton and Cousteau, 1959; E. G. & G., Inc., 1961). This instrument was used in the lowered pinger experiments described previously. The pinger emits a 12-kcps pulse at precise one-second intervals and permits synchronization to be maintained between the shipboard Acoustic Reflectivity System with its associated PGR and the Precisely Timed Submersible Pinger suspended over the side. The degree of synchronization obtainable is illustrated in an annotated PGR record (Figure 16) taken during a field instrumentation test of a precisely-timed pinger and deep-sea camera combination (Figure 17). The trace of the reflected arrival is parallel to the long axis of the record when the winch is stopped, which indicates that the

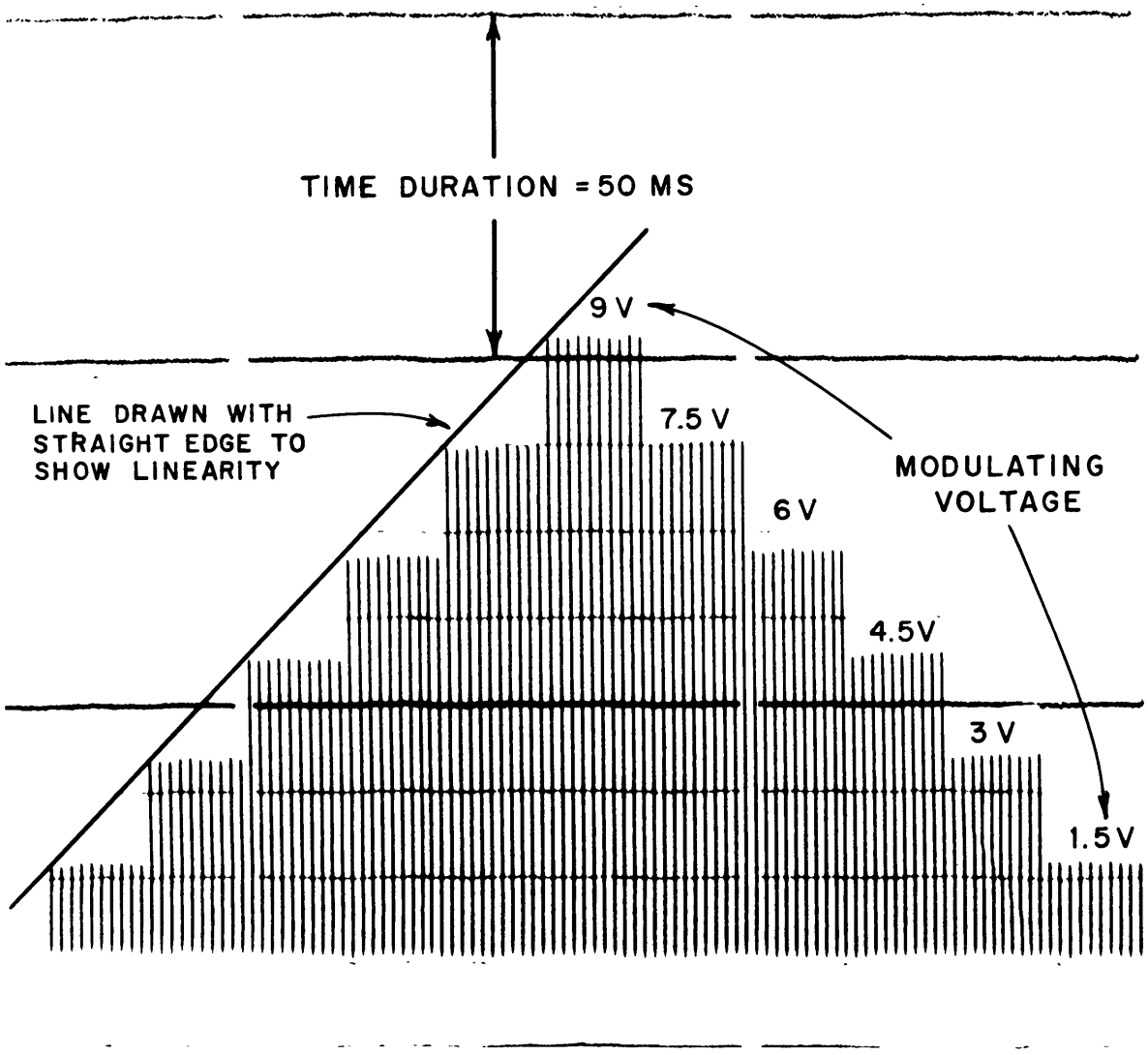

Figure 15. A Precision Graphic Recorder Record of a Calibration of the Pulse Width Modulator.

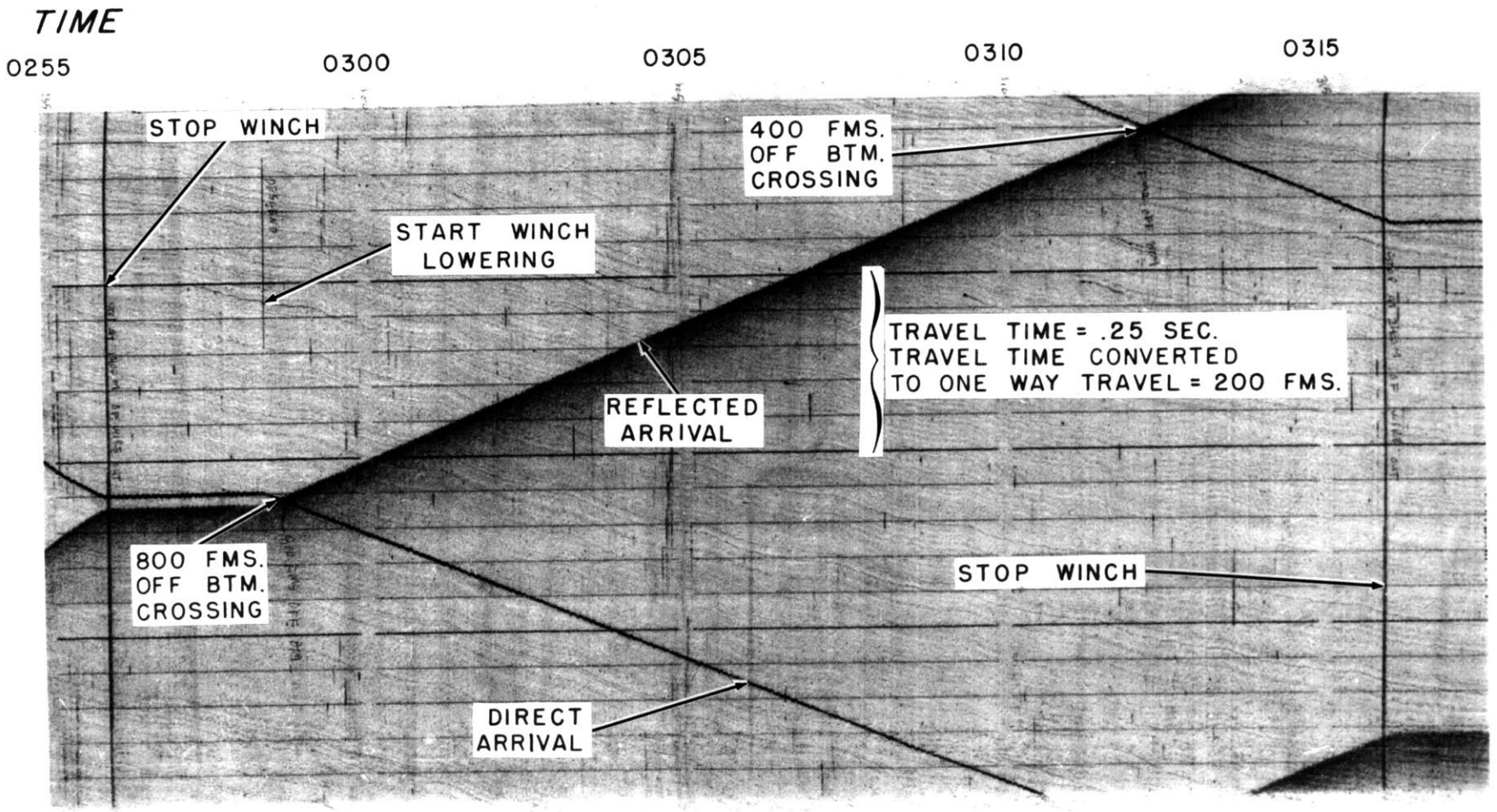

Figure 16. Section of Precision Graphic Recorder Record Obtained During a Deep Water Pinger Lowering.

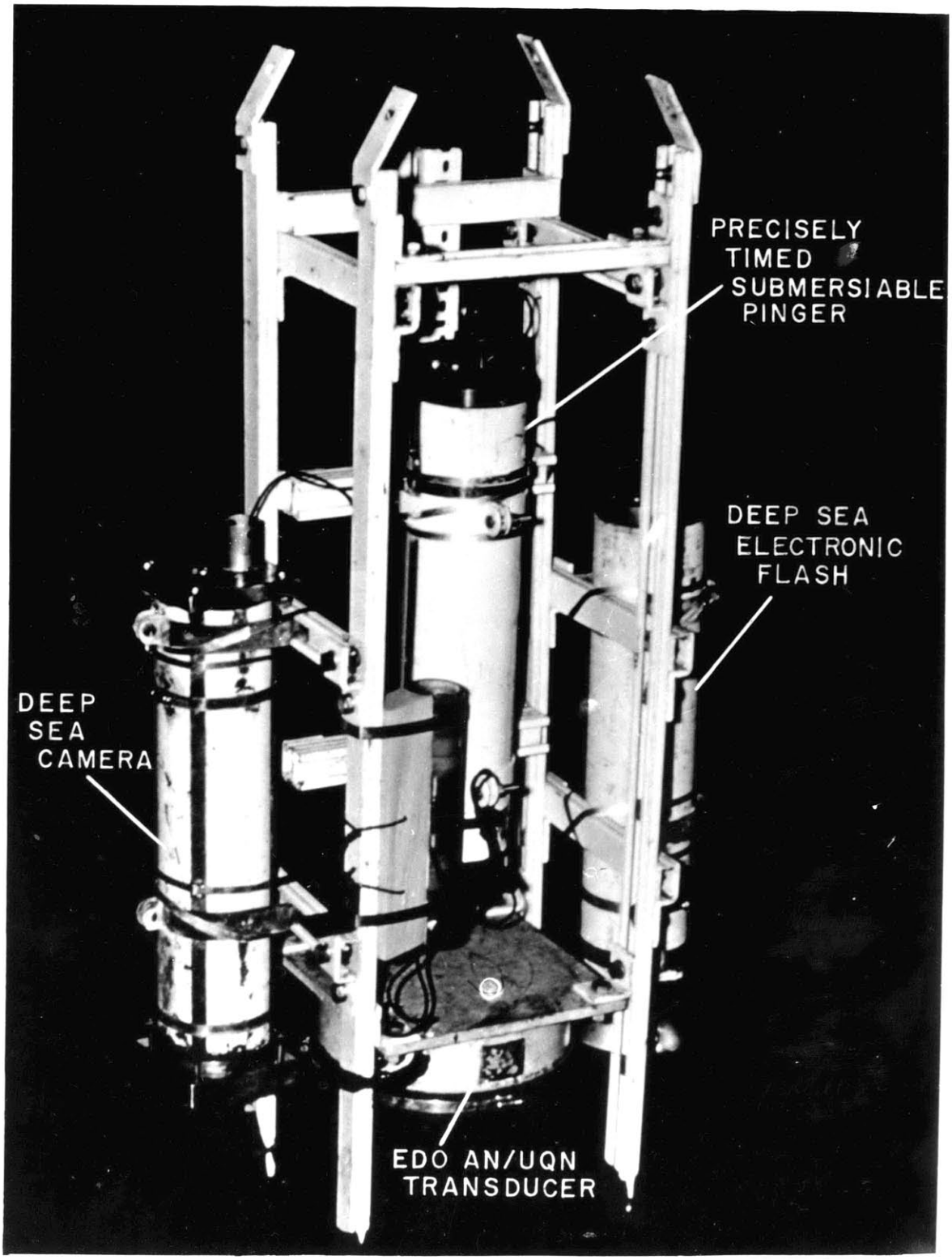

Figure 17. A Photograph of a Precisely Timed Submersible Pinger and Camera Combination.

echo consistently arrives during a particular fraction of a recording sweep of the PGR (the repetition rate of the pinger is an integral multiple of the recording-sweep rate of the PGR).

The Miniaturized Precision Time-Source (Figure 18) employs a 100-kcps crystal oscillator as its frequency standard. This frequency is counted down by five transistor decade-dividers to provide a synchronizing signal occurring at one-second intervals and at a voltage level adequate for direct application to a cold-cathode trigger-tube. The frequency stability is better than two parts per million per degree centigrade as determined by the temperature coefficient of the quartz crystal currently employed, which is operating at ambient temperature. The complete instrument, including a sealed, rechargeable, nickel-cadmium battery is capable of over five hours of operation. A description of the electronic circuitry of this unit is presented in Appendix A.

The Tape-Recording System for SCUBA Divers

A self-contained, protable tape-recording system was devised for use by SCUBA divers (Breslau, Zeigler, and Owen, 1962). The system was employed occasionally in shallow water in connection with sediment sampling. This system enables a SCUBA diver to continuously record his observations during a dive by speaking into his full-face breathing mask. It consists of a

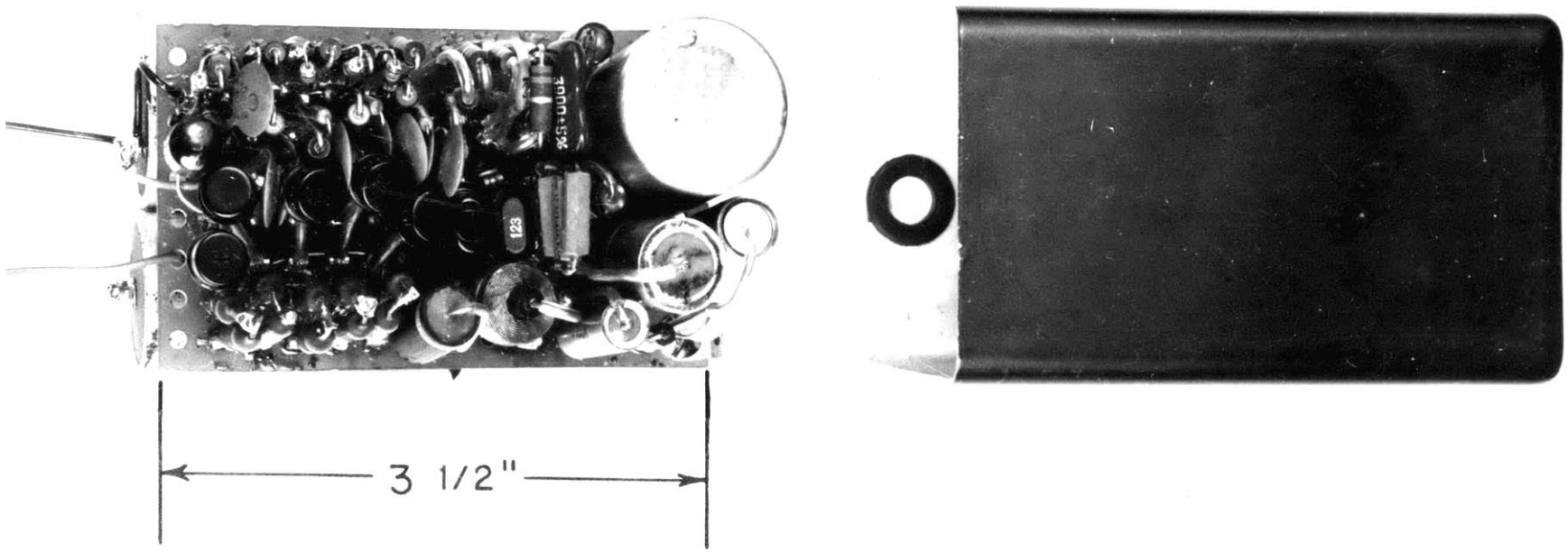

Figure 18. A Photograph of the Miniaturized Precision Time Source.

miniature ceramic hydrophone fastened inside a full-face breathing mask and a battery-operated tape-recorder enclosed in a submersible housing. Figure 19 shows this instrument being worn by a SCUBA diver.

The Sediment Dredge, Underwater Cameras, and Rapid Sediment Analyzer

A Van Veen dredge (Figure 20) (Thamdrup, 1938) was used to obtain sediment samples. This is a member of the "clamshell" group of bottomsamplers and takes a grab sample. The two heavy jaws of the "clamshell" are held open during the descent by a trigger-bar which is itself kept in position by the weight of the dredge on the taut cable. When the dredge strikes the bottom, the slackened cable releases the trigger-bar. When a strain is taken by the winch aboard ship, preparatory to the ascent, the jaws are drawn shut by their own weight, enclosing an undisturbed sediment sample covering one and one-half square feet of the water-sediment interface with a maximum vertical section of one-half foot.

An underwater stereoscopic camera designed by Dr. Harold Edgerton of M. I. T. (E. G. & G. Inc., 1960) and one designed by Mr. David Owen of WHOI (Owen, 1961) were used to obtain photographs of the sea floor. The Edgerton apparatus employs specially designed 35-mm cameras, an electronic-flash light-source, and a hydrosonic

Figure 19. Photograph of the Self-Contained Portable Tape Recording System being Worn by a SCUBA Diver.

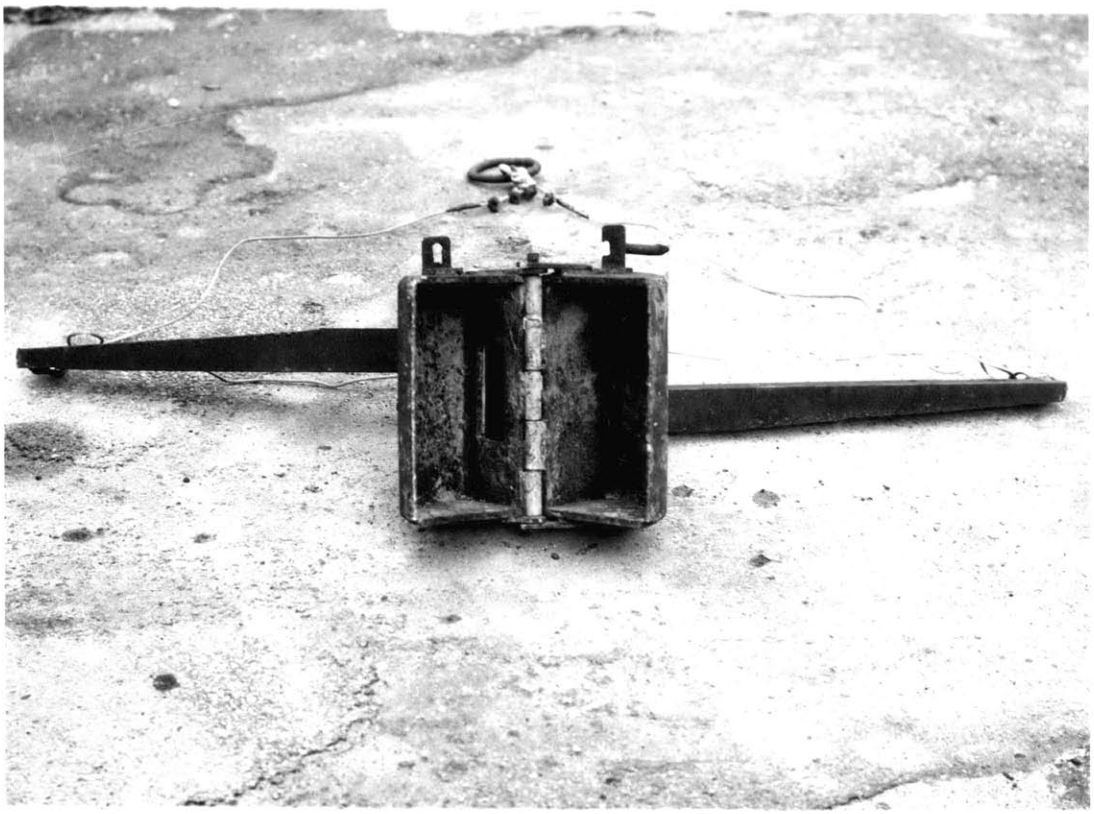

Figure 20. Photograph of a Van Veen Dredge.

positioning pinger. In operation, the apparatus is suspended above the bottom, where it automatically takes a picture every twelve seconds; its height above the bottom is monitored aboard ship with the aid of the positioning pinger. The cameras are focused at six feet and the photographs obtained at this distance cover a field about four by six feet. The Owen apparatus employs commercial, spring-driven still cameras, an electronic-flash light-source, and a bottom-sensing trigger-weight. In operation, the apparatus is raised and lowered at the bottom and takes a picture each time the suspended trigger weight contacts the bottom. The cameras are focused at two and one-half feet and the photographs obtained cover a field about one by one and one-half feet.

The Woods Hole Rapid Sediment Analyzer (Zeigler, Whitney, and Hayes, 1960) is a type of automated settling-tube which measures pressure changes induced in a column of water by sediment settling through a measured distance. The differential pressure existing between the top and bottom of a one-meter long tube is sensed by a hydrostatic bellows attached to a differential transformer and is displayed versus time on a galvanometric recorder. This device is used to obtain grain-size distributions of sediments in the silt and sand range.

CHAPTER V

DESCRIPTION OF OPERATIONS AT SEA

The specific approach utilized in this investigation made it possible to obtain the large number of measurements of acoustic reflectivity at sea needed in a study of the relationship of acoustic reflectivity to the sediment forming the actual sea floor. Observations were taken both in deep and in shallow water in the Western North Atlantic. A section of a physiographic diagram of the Atlantic Ocean (Heezen, Tharp, and Ewing, 1959) showing the location of the areas investigated is presented in Figure 21. The deep-water investigations are considered to be the ones taken over the "Bermuda" or "Puerto Rico" Profiles (these names were taken from cruise designations and are misleading), and the shallow-water ones are considered to be those taken over the Martha's Vineyard and Block Island Profiles and in Narragansett Bay.

The early cruises took place in deep water as a preliminary investigation to establish the range and variability of the acoustic reflectivity present in the natural environment. Long profiles of echo strength versus geographical location were sought. Geological control consisted mainly of continuous precise bathymetric recordings. The instrumentation system was field-tested and refined on these cruises. The better laboratory facilities and more stable

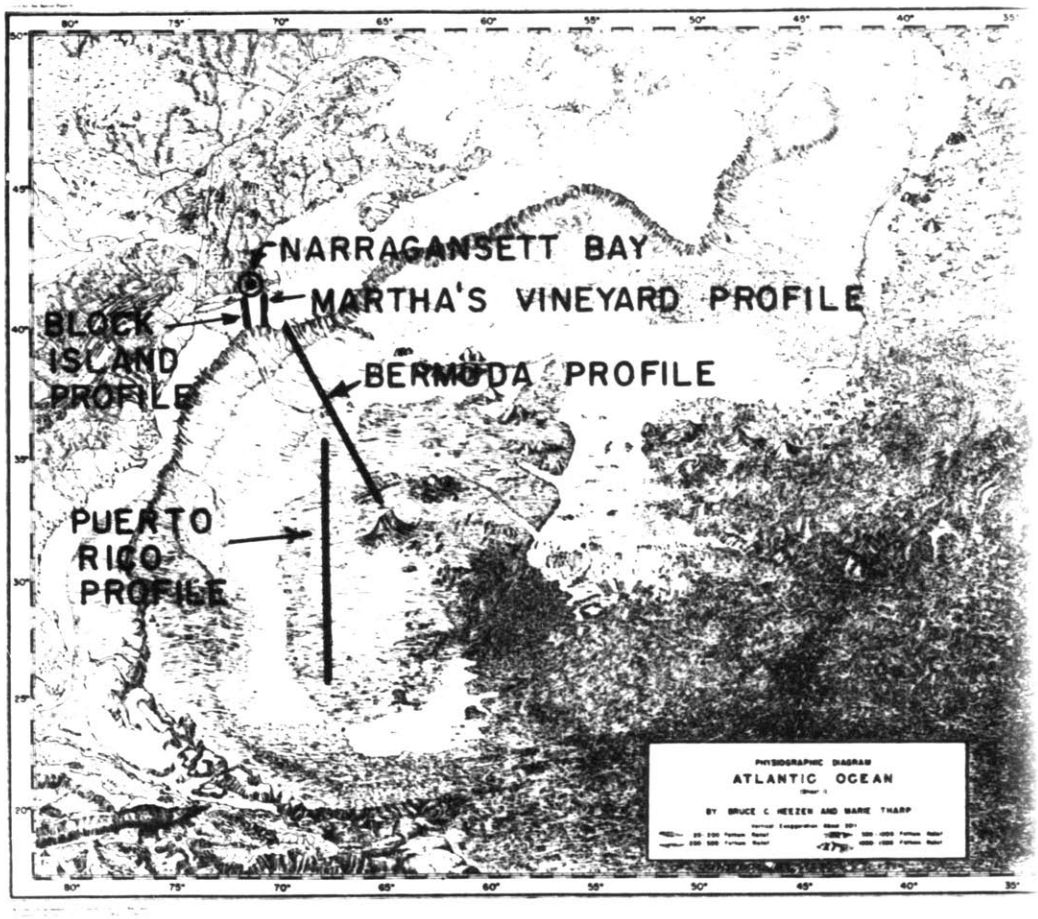

Figure 21. Physiographic Map of the Western North Atlantic (After Heezen, et al., 1959) Showing the Location of the Areas Investigated.

platform found on the large ships used for deep-water work permitted on-the-spot modifications.

The later cruises took place in shallow water where extensive efforts were made to maintain good geological control. The areas chosen for study were ones where the bottom had been thoroughly studied previously by other investigators using the techniques of classical geology. In particular, the Narragansett Bay area, studied by Dr. Robert McMaster of the Narragansett Marine Laboratories (McMaster, 1960), and profiles along the Continental Shelf south of Cape Cod, studied by the late Mr. Henry Stetson of the Woods Hole Oceanographic Institution (Stetson, 1938), were selected because of their proximity to the Woods Hole Oceanographic Institution. A moderate schedule of sediment dredging and underwater photography was undertaken by methods described previously to obtain additional geological control.

The field work can best be described in a cruise-by-cruise review. A list of the cruises performed in chronological order and a brief resume of what each attempted and accomplished with respect to this particular investigation follow:

CHAIN 19: This deep-water cruise took place from June 13 to July 7, 1961 aboard the Research Vessel CHAIN, a former T-ARS Class U. S. Navy Deep-Sea Salvage vessel 215 feet long and displacing

2000 tons. The ship made a passage from Woods Hole to the Puerto Rico Trench and back to perform various geophysical tasks. Advantage was taken of this cruise to check out the original instrumentation system, and to make echo strength profiles where opportune. The bulk of the effort expended on this cruise was directed toward working the "bugs" out of the electronics; nevertheless, approximately six-hundred echo-strength measurements were obtained at 49 locations (Figures 60 and 61) along the so-called "Puerto Rico"Profile (Figure 23), which extended from 26°05'N Lat., 67°27'W Long. to 35°54'N Lat., 67°55'W Long. The measurements were taken with a hull-mounted transducer while the ship was underway at about 10 knots. Navigation consisted of Loran-A fixes on an hourly basis. Positions were obtained by interpolation between fixes and are considered good within a three-mile radius. A continuous, precise, bathymetric recording was also obtained along the profile.

CHAIN 21: This deep-water cruise took place from November 27 to December 18, 1961 aboard the Research Vessel CHAIN. The ship made a passage from Monaco to Woods Hole via Bermuda to perform various geophysical tasks. Echo-strength measurements were taken over the Madeira Abyssal Plain but proved unusable due to improper mounting of the transducer. This situation was corrected at Bermuda by switching to a transducer mounted on a towed fish.

Approximately one-thousand echo-strength measurements were obtained at 78 locations (Figures 60 and 61) along the so-called "Bermuda Profile" (Figure 24), which extended from 34°18'N Lat., 66°05'W Long. to 39°46'N Lat., 69°57'W Long. The measurements were taken while the ship was underway at about 10 knots. Navigation consisted of Loran-A fixes on an hourly basis. Positions were obtained by interpolation between fixes and are considered good within a two-mile radius. A continuous, precise, bathymetric recording was also obtained along the profile.

CRAWFORD 73: This deep water cruise took place on February 23 and 24, 1962 aboard the Research Vessel CRAWFORD, a former Coast Guard Cutter, 125 feet long and displacing 320 tons. The ship sailed due south of Cape Cod to a 1500-fathom depth on the Continental Rise to field test the Precisely Timed Precision Pinger.

CHAIN 27: This deep-water cruise took place from June 9 to June 19, 1962 aboard the Research Vessel CHAIN. The ship made a passage from Woods Hole to the Bermuda area and back to service current metering buoys. This cruise provided an opportunity to obtain repeat measurements along the Bermuda Profile and to field test the newly developed Synchronization and Control Unit of the Acoustic Reflectivity System. This single unit replaced numerous separate units in the old system. It was developed in anticipation

of the more stringent space limitations on the smaller ships used for shallow-water work, as well as to increase overall system reliability. Approximately five-thousand echo-strength measurements were obtained at 213 locations (Figures 60 and 61). The ship pursued various courses in the immediate region north of Bermuda as it hunted drifting buoys, so that only 151 of these points actually make up the Bermuda Profile (Figure 25), which extended from 33°15'N Lat., 65°25'W Long. to 40°35'N Lat., 70°30'W Long. The measurements were taken with a hull-mounted transducer while the ship was underway at about 10 knots. Navigation consisted of Loran-A fixes on an hourly basis. Positions were obtained by interpolation between fixes and are considered good within a two-mile radius. A continuous, precise, bathymetric recording was also obtained along the profile.

ASTERIAS 1: This shallow-water cruise took place from July 11 to July 27, 1962 aboard the Motor Vessel ASTERIAS, a western dragger type of fishing boat, 40 feet long and displacing 20 tons. The cruise was made specifically to obtain echo-strength measurements under conditions of good geological control. Operations took place in Narragansett Bay and were guided by sediment charts and much advice provided by Dr. Robert McMaster of the Narragansett Marine Laboratory. The cruise demonstrated that

this acoustic technique could be successfully performed from a small ship. Approximately six-thousand echo-strength measurements were obtained at 195 locations (Figures 54 and 55). Measurements were made from a transducer mounted on a towed fish while the ship was underway at 6 knots. 13 sediment stations were occupied at which acoustic measurements were performed and sediment samples obtained by means of a Van Veen dredge. Underwater photographs were taken with the Owen Camera at the sites of 4 sediment stations where the water was not too turbid. Some direct observations of the bottom by SCUBA divers were made. A continuous, precise, bathymetric recording was taken whenever acoustic measurements were made. Position keeping was done by visual bearings on navigation marks and shore objects shown on the charts of the area, using a bearing circle mounted on a magnetic compass, and are considered good within a radius of one-twentieth of a mile.

BEAR 281: This shallow-water cruise took place from August 6 to August 15, 1962 aboard the Research Vessel BEAR, a former coastal freighter, 100 feet long and displacing 300 tons. The cruise was made specifically to obtain echo-strength measurements under conditions of good geological control on the Continental Shelf south of Cape Cod. A severe storm developed during the early part of the cruise causing conditions on the open sea to be too

hazardous to allow any work over-the-side. Therefore, the ship sought refuge in Narragansett Bay where it was able to carry on a program similar to that performed during the ASTERIAS-1 Cruise. Approximately seven-thousand echo-strength measurements were obtained at 209 locations (Figures 54 and 55). 19 sediment stations were occupied. 12 underwater photographs were taken with the Owen Camera at sites of sediment stations where water conditions permitted. When the storm abated the ship resumed its original plan and carried out investigations along the Block Island and Martha's Vineyard Profiles. Underwater photographs were obtained and pinger lowerings were performed using an Edgerton Camera and Precisely Timed Submersible Pinger Combination. Approximately ten-thousand echo-strength measurements were made at 330 locations (Figures 56 and 57) and 24 sediment stations were occupied on the Continental Shelf. Of these, approximately three and one-half thousand echo-strength measurements were made at 113 locations and 10 sediment stations were occupied along the Block Island Profile (Figure 26), which extended from 40°11'N Lat., 71°22'W Long. to 41°08'N Lat., 71°39'W Long. Approximately three and one-half thousand echo-strength measurements were made at 117 locations and 9 sediment stations were occupied along the Martha's Vineyard Profile (Figure 27), which extended from 40°15'N Lat., 70°43'W Long.

to 41°20'N Lat., 70°39'W Long. Measurements were made from a transducer mounted on a towed fish while the ship was underway at 6 knots. Navigation consisted of Loran-A fixes on an hourly basis. Positions were obtained by interpolation between fixes and are considered good within a one-mile radius. A continuous, precise, bathymetric recording was also obtained along the profile.

BEAR 285: This shallow-water cruise took place from September 7 to September 9, 1962 aboard the Research Vessel BEAR. The cruise was made specifically to field-test the newly designed pulse-width modulator, a sub-system of the System Synchronization and Control Unit of the Acoustic Reflectivity System, and to obtain measurements along the Martha's Vineyard Profile. Difficulty was experienced with the new device. This proved too severe to be corrected at sea and no data were obtained.

BEAR 290: This shallow-water cruise took place from October 1 to October 3, 1962 aboard the Research Vessel BEAR. This cruise was another attempt to achieve the objectives of BEAR 285. The cruise was successful and approximately one-thousand echo-strength measurements were obtained at 21 locations (Figures 56 and 57) along the Martha's Vineyard Profile (Figure 28). Measurements were made from a transducer mounted on a towed fish while the ship was hove-to. Sediment stations were occupied at all of the

locations and bottom photographs were obtained using the Owen Camera. A long record of the output of the pulse-width modulator was obtained and presented alongside the continuous bathymetric track on the record of the Precision Graphic Recorder. Navigation consisted of Loran-A fixes on an hourly basis. Positions were obtained by interpolation between fixes and are considered good within a one-mile radius.

ATLANTIS 293: This shallow-water cruise took place from July 1 to July 3, 1963 aboard the Research Vessel ATLANTIS, a steel ketch 140 feet long and displacing 550 tons, designed for oceanography. The purpose of this cruise was to revisit the sites of the previous sediment stations on the Continental Shelf to obtain wet-sediments samples for use in determining mass characteristics of the sediments. Loran-A was used to direct the ship to the recorded positions of the previous sediment stations.

ASTERIAS 2: This shallow-water cruise took place from July 10 to July 13, 1963 aboard the Motor Vessel ASTERIAS. The purpose of this cruise was the same as that of ATLANTIS 293 except that the area sampled was Narragansett Bay. Visual bearings on navigation marks and shore objects with a bearing circle mounted on a magnetic compass were used to direct the ship to the recorded positions of the previous sediment stations.

CHAPTER VI

DATA PROCESSING AND ANALYSIS

General Description of Techniques

The inherent variability among acoustic echoes reflected from the sea floor and measured at the ship necessitated taking a large number of measurements at each location (data point) to obtain a significant sample. The general objective and scope of this investigation required samples to be obtained at a large number of locations. A consideration of these two factors indicated that a highly automated system of data processing and analysis was imperative. This was accomplished through recourse to the Data Analysis Laboratory (Geophysics Department) and the Information Processing Center at WHOI, and the IBM Computation Center at M. I. T.

The Data Analysis Laboratory contains a Gerber Data Recording System (Gerber Scientific Instrument Co., undated), a manual analogue-to-digital converter which measures displacements on oscillograms and makes punched cards; a Printing Card Punch (International Business Machines Corp., 1959), a manual card punch which accepts information entered into a keyboard and makes punched cards; and a Dataplotter (Electronic Associates Inc., 1961), an automatic digital X-Y recorder which reads punched cards and

makes point and line plots. The first two machines were used to put raw data into machine-language form for acceptance by a digital computer and the last was used to display the computed results.

The Information Processing Center and IBM Computation Center both contain high-speed digital computers; these are the GE 225 (General Electric Co., Inc., 1963) and the IBM 7090 (International Business Machines Corp., 1961). Both computers were used, though either could have done the entire job; the IBM 7090 was available at M. I. T. before the GE 225 became available at WHOI and consequently, the earlier work was performed at M. I. T. and the later work at WHOI.

FORTRAN (McCracken, 1961) is a widely used computer compiling language which most present-day computers, including the above mentioned ones, can accept and translate into their specific instructional code. The author attended a course given by IBM in FORTRAN and subsequently wrote the computer programs needed for this investigation. Brief descriptions of what these programs do are contained in the remaining sections of this chapter. The major programs are presented in their entirety in Appendix B.

Analysis of Acoustic Data

The original data are predominantly in the form of cathode-ray oscilloscope photographs of the echo wave-train (Figure 13), displayed on 100-foot strips of 35-mm negative film. The negative

film was processed to form a continuous-strip positive print which was directly read with the Gerber Data Recording System (Figure 22). The displacements representing the peak pressure and final value of the time integral of the squared pressure, of the bottom echo and associated calibration pulse were measured and automatically recorded on punched cards. These punched cards were manually re-punched to include the water depth and geographical position of the measurement, and comprise the acoustic raw-data deck. This deck was listed by an IBM Accounting Machine, Model 407 (International Business Machines Corp., 1959), which had been especially arranged to emit titles and transpose columns, and bound in a 683 page volume which is on file at the Geophysics Department of the Woods Hole Oceanographic Institution.

This deck was processed by the ECHO-STRENGTH PROGRAM (presented in Appendix B as Computer Program I) which accepts the acoustic raw-data deck as input and produces an echo-strength deck as output. The program converts the peak-pressure and total-energy displacements of the echo and calibration pulse into values of echo strength using the method described in Chapter III. The program selects the median and maximum echo and calculates the median value of echo strength, the maximum value of echo strength, the sample size, and the standard deviation for each datum point on both

Figure 22. Photograph of the Analogue to Digital Data Reduction System being used to Digitize the Acoustic Echoes.

a peak-amplitude and total-energy basis. Each card of the echo-strength deck represents a summarized measurement corresponding to a geographical position and contains the selected information from all of the acoustic-echo samples taken at the datum point.

The echo-strength deck was processed by the Bottom-Loss Program (presented in Appendix B as Computer Program II) which accepts the echo-strength deck as input and produces a bottom-loss deck as output. The program computes the median and minimum value of bottom loss on both a peak-pressure and total-energy basis by subtracting the appropriate echo strength and propagation loss from the appropriate source level, assuming spherical spreading and an attenuation loss of 1. 2 db per kiloyard (Horton, 1959). A parameter card stipulating the source level, pulse width, and units of depth must precede the deck.

Various programs have been written to shape the results into a form acceptable for plotting on the Dataplotter. In particular, one program computes running averages of three values for profiled data and another converts latitudes into Mercator displacements for directly plotting locations on Mercator charts.

The locations of all the acoustic measurements have been automatically plotted on Mercator charts of the appropriate regions (Figures 54, 55, 56, 57, 60, and 61), and the values of bottom loss obtained at these locations have been indicated by a color code.

Curves of acoustical quantities versus distance along profiles (Figures 23-28, 62, 63, and 64) have been automatically plotted by passing the punched cards through the Dataplotter twice, once to plot the points and once to draw the lines.

Analysis of Geologic Data

Gravel, sand, silt and clay percentages and quartile values of the cumulative size distribution curves of the sediment samples were manually punched onto cards to generate the particle-size raw-data deck. This deck was processed by the Sediment Classification Program (presented in Appendix B as Computer Program III) which accepts the particle-size raw-data deck as input and produces a grain-size-characteristic deck as output. The program gives each sediment sample a class name in accordance with the commonly used three-component sand-silt-clay system (Shepard, 1954). This name is punched on the cards in Hollerith text along with a related code number for future machine analysis. The program also computes the Trask sorting-coefficient, defined as the square root of the ratio of the larger quartile to the smaller quartile (Krumbein and Sloss, 1956), and the phi median grain-size, defined as minus the log to the base two of the median grain-size in millimeters (Inman, 1952).

The wet and dry weights of the sediment samples were manually punched onto cards to generate the water-loss raw-data deck. This deck was processed by the Mass Properties Program (presented in Appendix B as Computer Program IV) which accepts the water-loss raw-data deck as input and produces a mass-characteristic deck as output. The program computes the water content, porosity, density, velocity, acoustic impedance, Rayleigh reflection coefficient, and theoretical bottom loss in db, according to the relationships developed in Chapter II.

The bottom-loss measurements taken at the sites of sediment stations were correlated with geological characteristics of the sampled sediments by use of the Correlation and Regression Program (presented in Appendix B as Computer Program V). This is a general purpose statistical program to perform a correlation and regression analysis on any two input variables and lists, as output, the correlation coefficient, the slope of the regression line, the Y intercept, the standard error of estimate, the "Z" value, and the standard deviation of "Z" (Hoel, 1962). The geological characteristics tested were the percentage of silt, clay, and fine material (silt plus clay), the median grain size, the sorting coefficient, and the porosity.

Curves of geological quantities versus distance along profiles (Figures 30-33) and scatter diagrams of acoustical versus geological quantities (Figures 42-51) have been automatically plotted. In some

cases, the name of the sediment is indicated by a particular symbol automatically selected by the Dataplotter from information on the punched cards.

CHAPTER VII

ACOUSTIC RESULTS

A tabulation of all the bottom-loss measurements obtained during the course of this investigation is presented in Table I. An explanation of the column headings follows: TAG represents the datum identification number; PEAK PRESS. MED. and PEAK PRESS. DEV. represent the median and standard deviation of bottom loss measured on a peak-pressure basis respectively; TOTAL ENG. MED. and TOTAL ENG. DEV. represent the median and standard deviation of bottom loss measured on a total energy basis respectively; AMT. is the number of echoes that were sampled to produce the datum; DEPTH is the transducer depth; and LATITUDE DG., LATITUDE MN., LONGITUDE DG., and LONGITUDE MN., are the values of latitude and longitude in degrees and minutes at the location of the acoustic measurement. The acoustic quantities are in decibels; the depth is in fathoms for measurements obtained on the CHAIN 19, CHAIN 21, and CHAIN 27 cruises and is in feet for measurements obtained on the ASTERIAS, BEAR 281, and BEAR 290 cruises.

TABLE I

MEASUREMENTS OF ACOUSTIC BOTTOM LOSS AT NORMAL INCIDENCE

TAG	PEAK PRESS. MED.	DEV.	TOTAL ENG. MED.	DEV.	AMT.	DEPTH	LATITUDE DG.	MN.	LONGITUDE DG.	MN.
MEASUREMENTS OBTAINED ON R/V CHAIN CRUISE 19										
1	22.9	2.6	19.8	1.6	17	2830	26	5.0	67	27.5
2	21.6	2.1	19.1	1.7	14	2900	26	14.0	67	28.0
3	21.8	1.7	17.9	1.2	9	2850	26	20.0	67	28.5
4	25.5	1.8	21.9	1.8	14	2820	26	20.5	67	28.5
5	21.7	3.4	18.6	1.6	16	2760	29	22.0	67	33.0
6	16.2	3.1	16.7	2.0	16	2740	29	25.0	67	33.0
7	18.9	3.5	18.5	2.1	7	2740	29	27.0	67	32.5
8	17.9	2.6	17.6	1.8	9	2740	29	28.0	67	32.5
9	18.2	3.7	15.7	1.1	10	2740	29	30.0	67	32.0
10	18.7	2.0	16.6	1.2	7	2740	29	32.0	67	32.0
11	20.3	1.6	16.4	1.1	7	2730	29	33.0	67	32.0
12	18.4	2.3	15.7	1.3	9	2730	29	35.5	67	32.5
13	20.5	2.9	18.1	2.0	8	2720	29	39.0	67	32.5
14	18.7	2.6	16.5	1.6	19	2720	29	40.0	67	33.0
15	21.5	0.5	16.3	1.2	8	2720	30	0.5	67	34.5
16	21.2	2.9	17.0	1.1	7	2710	30	4.0	67	34.5
17	22.6	1.7	18.1	1.8	8	2710	30	15.0	67	35.0
18	17.5	3.5	15.7	1.1	11	2720	30	17.5	67	35.0
19	21.6	2.0	18.5	1.1	15	2720	30	20.0	67	35.5
20	21.2	3.7	19.4	2.2	9	2720	30	30.5	67	36.0
21	23.1	2.1	16.6	1.4	18	2710	30	34.0	67	36.0
22	20.2	1.9	18.6	1.2	9	2710	30	37.0	67	36.0
23	21.2	2.8	19.2	1.9	18	2710	30	40.5	67	36.5

TABLE I

MEASUREMENTS OF ACOUSTIC BOTTOM LOSS AT NORMAL INCIDENCE

TAG	PEAK PRESS. MED.	DEV.	TOTAL ENG. MED.	DEV.	AMT.	DEPTH	LATITUDE DG. MN.	LONGITUDE DG. MN.
24	23.4	1.4	21.0	1.5	12	2690	30 41.0	67 36.5
25	23.1	2.1	20.7	1.5	19	2700	30 42.5	67 36.5
26	19.3	1.8	16.0	1.1	14	2700	30 46.0	67 37.0
27	20.5	2.4	16.6	1.0	8	2700	30 51.0	67 37.0
28	20.8	0.9	15.9	0.6	7	2710	30 55.0	67 37.0
29	23.1	2.7	19.1	1.8	7	2740	30 58.0	67 37.5
30	22.7	2.8	19.7	1.7	10	2710	31 1.0	67 38.0
31	20.8	2.8	18.6	1.8	13	2710	31 5.0	67 38.0
32	23.3	2.6	20.7	1.9	8	2660	32 58.5	67 40.0
33	19.2	2.8	15.7	2.2	21	2720	33 1.0	67 40.0
34	20.8	3.4	17.6	2.8	8	2720	33 9.0	67 40.0
35	22.4	3.9	20.7	3.9	21	2700	33 14.5	67 40.0
36	21.1	2.5	18.6	2.0	6	2720	33 21.0	67 39.5
37	19.1	2.6	17.0	2.3	14	2720	33 25.5	67 39.5
38	14.2	2.7	12.7	1.9	14	2770	35 4.5	67 49.0
39	15.5	2.3	10.6	1.8	14	2770	35 5.0	67 49.0
40	14.5	2.9	12.0	1.7	15	2750	35 5.5	67 49.0
41	8.3	2.2	5.5	1.4	15	2750	35 10.5	67 50.0
42	13.8	3.7	10.9	2.2	14	2710	35 19.0	67 51.0
43	17.7	3.9	12.5	1.8	7	2710	35 20.0	67 51.0
44	18.2	2.9	12.0	1.4	7	2710	35 21.0	67 51.5
45	16.7	3.9	12.6	1.8	14	2700	35 23.5	67 52.0
46	18.2	2.8	13.0	1.4	14	2690	35 27.0	67 52.5
47	11.7	1.5	7.1	0.7	13	2660	35 37.5	67 54.0
48	11.3	2.2	8.5	1.2	14	2650	35 50.5	67 54.5

TABLE I

MEASUREMENTS OF ACOUSTIC BOTTOM LOSS AT NORMAL INCIDENCE

TAG	PEAK PRESS. MED.	DEV.	TOTAL ENG. MED.	DEV.	AMT.	DEPTH	LATITUDE DG. MN.	LONGITUDE DG. MN.
49	11.5	3.1	9.1	1.9	19	2650	35 54.0	67 55.0
			MEASUREMENTS OBTAINED ON R/V CHAIN CRUISE 21					
1	17.7	2.7	14.9	2.9	5	2730	34 17.5	66 5.0
2	14.7	2.5	11.1	1.9	20	2730	34 18.5	66 6.5
3	15.8	1.9	12.1	2.1	20	2780	34 35.5	66 17.5
4	15.9	1.4	12.0	1.9	14	2700	34 50.0	66 27.0
5	14.4	2.7	10.4	2.5	12	2700	35 1.5	66 34.5
6	14.5	1.7	11.6	2.0	8	2700	35 6.0	66 37.5
7	15.9	2.6	12.8	2.1	16	2690	35 10.5	66 41.0
8	15.0	2.6	11.7	2.9	13	2660	35 12.5	66 42.5
9	14.9	2.4	12.4	3.4	15	2660	35 15.0	66 44.5
10	15.5	3.3	12.5	2.4	13	2630	35 17.5	66 46.5
11	16.8	2.2	15.2	2.7	11	2640	35 20.0	66 48.0
12	17.6	1.8	14.9	2.0	16	2630	35 22.0	66 50.0
13	11.6	3.9	9.8	3.3	20	2650	35 25.0	66 51.5
14	15.8	2.8	12.9	2.9	14	2650	35 28.0	66 54.0
15	17.3	1.6	13.3	2.1	5	2630	35 30.5	66 56.0
16	18.2	4.0	12.9	3.7	9	2630	35 39.0	67 1.5
17	15.0	2.6	10.5	1.3	12	2680	35 43.5	67 5.0
18	14.4	2.5	11.9	2.6	7	2680	35 49.5	67 9.5
19	11.8	2.1	8.4	1.3	12	2680	35 52.5	67 12.0
20	15.1	1.6	10.7	1.2	14	2650	35 55.0	67 13.5
21	8.2	1.8	5.2	1.2	9	2630	35 56.0	67 14.5
22	9.2	2.2	7.7	2.7	14	2620	35 58.5	67 16.0

TABLE I

MEASUREMENTS OF ACOUSTIC BOTTOM LOSS AT NORMAL INCIDENCE

TAG	PEAK PRESS. MED.	DEV.	TOTAL ENG. MED.	DEV.	AMT.	DEPTH	LATITUDE DG.	MN.	LONGITUDE DG.	MN.
23	9.7	3.4	7.0	3.1	5	2640	36	0.	67	17.5
24	9.2	2.9	6.5	2.0	11	2640	36	5.0	67	18.0
25	9.5	2.7	6.8	2.3	11	2640	36	5.5	67	21.5
26	7.0	2.3	6.5	2.2	12	2630	36	9.5	67	24.5
27	8.8	1.9	7.4	1.2	6	2610	36	12.5	67	27.0
28	13.2	1.1	8.1	1.0	7	2610	36	16.0	67	29.0
29	10.8	2.7	8.0	1.4	11	2610	36	17.5	67	30.8
30	10.5	1.8	7.6	1.2	15	2610	36	20.0	67	32.5
31	10.2	1.5	7.0	1.5	14	2610	36	22.5	67	34.0
32	10.2	1.5	8.0	1.2	8	2610	36	25.5	67	36.5
33	12.1	1.6	7.9	0.7	7	2610	36	26.5	67	37.5
34	7.9	3.5	6.5	2.3	11	2610	36	28.5	67	39.5
35	7.1	1.6	5.7	1.4	11	2610	36	32.0	67	41.5
36	5.1	2.9	4.1	2.6	8	2610	36	37.5	67	45.5
37	8.0	2.6	7.6	2.2	19	2620	36	40.0	67	47.5
38	7.5	2.1	6.3	1.5	11	2620	36	42.5	67	49.5
39	9.0	4.3	8.8	3.8	15	2620	36	45.5	67	51.0
40	7.5	2.8	7.0	2.1	14	2610	36	47.5	67	53.0
41	8.5	2.8	6.7	2.1	13	2600	36	51.5	67	56.5
42	7.3	2.3	6.4	1.7	10	2600	36	54.0	67	58.0
43	6.6	2.3	4.9	1.7	9	2600	36	56.0	67	59.0
44	7.4	1.8	5.1	1.1	16	2600	36	58.0	68	1.0
45	9.4	2.2	6.3	1.7	15	2600	37	0.5	68	2.5
46	6.9	2.4	5.2	1.8	11	2600	37	2.5	68	3.0
47	8.6	2.0	6.9	1.8	12	2590	37	5.0	68	4.5

TABLE I

MEASUREMENTS OF ACOUSTIC BOTTOM LOSS AT NORMAL INCIDENCE

TAG	PEAK PRESS. MED.	DEV.	TOTAL ENG. MED.	DEV.	AMT.	DEPTH	LATITUDE DG.	MN.	LONGITUDE DG.	MN.
48	9.2	2.2	7.2	1.4	14	2590	37	7.5	68	5.5
49	7.0	2.4	5.2	1.7	11	2580	37	10.0	68	7.0
50	12.9	2.7	9.9	1.8	11	2590	37	12.0	68	8.0
51	14.2	1.2	11.3	1.6	12	2540	37	17.0	68	10.5
52	9.3	2.6	6.8	1.4	11	2440	37	37.0	68	21.5
53	12.3	2.1	7.4	1.4	12	2380	37	48.5	68	29.0
54	10.0	2.5	6.6	1.6	13	2300	37	54.0	68	32.5
55	11.5	1.5	7.0	1.1	16	2290	37	55.0	68	34.0
56	10.5	1.6	7.1	1.4	11	2210	38	1.5	68	40.0
57	12.8	1.7	10.1	1.9	15	2160	38	5.5	68	43.5
58	11.7	2.8	8.3	1.2	6	2130	38	9.5	68	46.0
59	12.5	2.4	9.3	1.9	7	2100	38	12.0	68	48.0
60	12.4	1.7	9.1	1.6	8	2070	38	14.5	68	50.0
61	10.7	1.8	8.0	1.4	7	2050	38	17.5	68	52.0
62	15.1	1.8	12.1	1.6	13	1860	38	30.0	69	0.5
63	12.2	2.3	10.8	1.9	13	1820	38	35.0	69	3.5
64	19.1	4.2	16.4	4.0	20	1820	38	36.5	69	4.5
65	12.7	2.0	10.6	1.6	11	1740	38	44.5	69	10.5
66	9.8	2.9	7.9	2.1	12	1740	38	47.0	69	12.0
67	11.4	2.0	9.5	1.4	10	1680	38	53.5	69	17.0
68	17.6	1.2	13.5	1.6	12	1460	39	11.5	69	31.0
69	15.0	2.5	13.0	1.5	7	1360	39	17.5	69	35.0
70	14.6	3.4	12.6	2.5	11	1360	39	19.5	69	37.0
71	15.8	2.6	11.8	1.3	15	1240	39	30.5	69	45.0
72	12.0	2.0	9.2	1.7	11	1220	39	31.5	69	46.0

TABLE I

MEASUREMENTS OF ACOUSTIC BOTTOM LOSS AT NORMAL INCIDENCE

TAG	PEAK PRESS. MED.	DEV.	TOTAL ENG. MED.	DEV.	AMT.	DEPTH	LATITUDE DG. MN.	LONGITUDE DG. MN.
73	14.0	2.2	12.0	1.8	11	1220	39 32.0	69 46.5
74	17.3	1.6	14.0	1.1	14	1190	39 37.0	69 50.0
75	21.4	2.1	17.4	1.2	10	1150	39 39.0	69 51.5
76	22.2	1.5	17.8	0.6	12	1020	39 43.0	69 55.0
77	16.3	3.2	12.9	1.9	13	1000	39 44.5	69 56.0
78	19.5	2.1	15.4	1.4	16	1000	39 46.0	69 57.0
	MEASUREMENTS OBTAINED ON R/V CHAIN CRUISE 27							
1	21.3	1.6	15.6	1.7	26	2720	33 57.0	65 52.0
2	22.3	2.8	15.0	0.7	19	2610	33 55.0	65 55.5
3	16.7	2.4	14.7	1.2	23	2695	33 53.1	66 0.
4	17.0	2.3	16.4	1.8	13	2700	33 57.0	66 0.
5	17.4	3.3	16.1	1.5	16	2730	33 3.5	66 0.6
6	16.2	2.5	14.6	2.0	17	2725	34 10.0	66 1.2
7	17.1	2.4	11.8	1.0	15	2730	34 15.5	66 2.6
8	17.7	2.5	16.0	1.4	19	2745	34 21.1	66 4.0
9	15.4	2.1	12.1	1.3	19	2755	34 23.0	66 7.0
10	13.6	1.5	10.9	0.8	18	2745	34 25.0	66 11.0
11	15.9	2.3	12.5	1.7	8	2725	34 27.0	66 14.0
12	16.5	2.5	11.6	1.6	23	2720	34 28.0	66 13.0
13	18.9	3.4	12.3	1.8	21	2710	34 31.0	66 10.0
14	16.9	1.9	12.4	1.5	34	2690	34 33.0	66 6.0
15	17.0	2.3	13.0	1.4	22	2665	34 36.0	66 3.0
16	16.4	2.2	12.2	1.4	22	2670	34 36.0	66 1.0
17	17.1	2.6	12.6	2.3	21	2695	34 35.0	66 59.0

TABLE I

MEASUREMENTS OF ACOUSTIC BOTTOM LOSS AT NORMAL INCIDENCE

TAG	PEAK PRESS. MED.	DEV.	TOTAL ENG. MED.	DEV.	AMT.	DEPTH	LATITUDE DG. MN.	LONGITUDE DG. MN.
18	14.9	2.7	10.5	1.6	19	2735	34 32.0	65 58.0
19	15.0	2.7	10.7	1.6	22	2745	34 29.0	65 56.0
20	17.5	3.4	15.7	2.2	21	2545	34 23.0	65 54.0
21	17.5	1.9	12.2	1.0	24	2700	34 17.0	66 1.0
22	18.5	4.0	15.0	3.2	24	2700	34 12.0	66 4.0
23	16.5	1.8	13.1	1.7	19	2730	34 6.0	66 6.0
24	18.7	3.2	13.1	1.8	22	2725	34 1.0	66 9.0
25	14.8	2.0	13.1	1.7	16	2715	33 55.0	66 10.0
26	16.9	2.8	16.2	2.4	13	2710	33 55.0	66 11.0
27	18.7	2.7	15.0	2.3	14	2715	33 55.0	66 11.0
28	19.2	3.4	16.2	3.4	17	2720	33 55.0	66 12.0
29	17.4	2.8	15.1	1.3	13	2705	33 55.0	66 13.0
30	19.5	2.8	16.1	2.5	18	2710	33 55.0	66 18.0
31	16.1	2.7	14.2	2.0	18	2725	33 55.0	66 24.0
32	19.4	3.7	15.5	2.4	29	2735	33 55.0	66 30.0
33	18.9	3.4	17.2	2.6	26	2735	33 55.0	66 37.0
34	19.7	4.1	16.4	2.9	34	2735	33 55.0	66 37.0
35	17.6	5.1	14.4	3.8	16	2740	33 54.0	66 37.0
36	19.1	4.1	14.7	2.7	26	2735	33 54.0	66 38.0
37	19.9	4.0	15.2	2.9	14	2750	33 54.0	66 44.0
38	18.2	2.6	16.1	2.3	23	2755	33 54.0	66 50.0
39	17.8	2.2	16.1	2.7	20	2740	33 55.0	66 57.0
40	18.1	3.0	14.6	2.0	22	2740	33 55.0	67 3.0
41	18.7	2.8	16.0	2.1	30	2730	33 54.0	67 12.0
42	18.3	2.7	15.5	2.2	26	2735	33 54.0	67 21.0

TABLE I

MEASUREMENTS OF ACOUSTIC BOTTOM LOSS AT NORMAL INCIDENCE

TAG	PEAK PRESS. MED.	DEV.	TOTAL ENG. MED.	DEV.	AMT.	DEPTH	LATITUDE DG. MN.	LONGITUDE DG. MN.
43	20.6	3.3	16.4	2.0	10	2735	33 54.0	67 21.0
44	18.8	2.2	16.7	1.9	13	2735	33 54.0	67 22.0
45	19.4	4.2	16.2	3.1	12	2740	33 53.0	67 22.0
46	15.7	3.7	13.6	3.0	6	2730	33 53.0	67 22.0
47	19.7	2.3	16.2	1.8	19	2735	33 53.5	67 22.0
48	18.0	2.0	15.9	1.7	11	2735	33 44.5	67 4.0
49	16.8	3.2	13.9	2.2	23	2730	33 43.0	66 57.0
50	19.5	2.3	15.3	1.5	7	2730	33 41.5	66 51.0
51	17.4	3.5	13.4	2.4	12	2700	33 39.0	66 44.0
52	17.8	3.6	15.4	2.6	29	2730	33 36.0	66 37.0
53	18.2	2.7	16.3	2.5	28	2680	33 30.0	66 22.0
54	15.8	1.9	11.1	1.0	17	2650	33 21.0	65 59.0
55	17.4	3.0	15.2	1.9	13	2420	33 18.0	65 50.0
56	13.0	3.8	11.2	1.9	18	2605	33 15.0	65 42.0
57	16.9	3.2	13.3	2.5	12	2600	33 14.0	65 40.0
58	17.6	2.9	14.8	3.0	75	2550	33 7.0	65 19.0
59	15.2	2.6	11.3	1.9	52	2515	33 0.	65 1.0
60	11.1	2.3	9.3	1.4	24	2550	33 7.0	65 10.0
61	11.3	8.4	9.1	2.0	47	2565	33 9.0	65 11.0
62	18.3	2.8	15.5	3.2	13	2570	33 11.0	65 13.0
63	17.2	3.2	15.1	3.3	67	2560	33 13.0	65 14.0
64	16.1	2.0	14.3	1.5	42	2555	33 13.0	65 14.0
65	15.3	1.9	13.5	1.4	17	2560	33 14.0	65 12.0
66	16.9	1.7	12.7	1.4	7	2600	33 18.0	65 17.0
67	19.5	3.0	16.5	2.4	15	2565	33 22.0	65 23.0

TABLE I

MEASUREMENTS OF ACOUSTIC BOTTOM LOSS AT NORMAL INCIDENCE

TAG	PEAK PRESS. MED.	DEV.	TOTAL ENG. MED.	DEV.	AMT.	DEPTH	LATITUDE DG. MN.	LONGITUDE DG. MN.
43	20.6	3.3	16.4	2.0	10	2735	33 54.0	67 21.0
44	18.8	2.2	16.7	1.9	13	2735	33 54.0	67 22.0
45	19.4	4.2	16.2	3.1	12	2740	33 53.0	67 22.0
46	15.7	3.7	13.6	3.0	6	2730	33 53.0	67 22.0
47	19.7	2.3	16.2	1.8	19	2735	33 53.5	67 22.0
48	18.0	2.0	15.9	1.7	11	2735	33 44.5	67 4.0
49	16.8	3.2	13.9	2.2	23	2730	33 43.0	66 57.0
50	19.5	2.3	15.3	1.5	7	2730	33 41.5	66 51.0
51	17.4	3.5	13.4	2.4	12	2700	33 39.0	66 44.0
52	17.8	3.6	15.4	2.6	29	2730	33 36.0	66 37.0
53	18.2	2.7	16.3	2.5	28	2680	33 30.0	66 22.0
54	15.8	1.9	11.1	1.0	17	2650	33 21.0	65 59.0
55	17.4	3.0	15.2	1.9	13	2420	33 18.0	65 50.0
56	13.0	3.8	11.2	1.9	18	2605	33 15.0	65 42.0
57	16.9	3.2	13.3	2.5	12	2600	33 14.0	65 40.0
58	17.6	2.9	14.8	3.0	75	2550	33 7.0	65 19.0
59	15.2	2.6	11.3	1.9	52	2515	33 0.	65 1.0
60	11.1	2.3	9.3	1.4	24	2550	33 7.0	65 10.0
61	11.3	8.4	9.1	2.0	47	2565	33 9.0	65 11.0
62	18.3	2.8	15.5	3.2	13	2570	33 11.0	65 13.0
63	17.2	3.2	15.1	3.3	67	2560	33 13.0	65 14.0
64	16.1	2.0	14.3	1.5	42	2555	33 13.0	65 14.0
65	15.3	1.9	13.5	1.4	17	2560	33 14.0	65 12.0
66	16.9	1.7	12.7	1.4	7	2600	33 18.0	65 17.0
67	19.5	3.0	16.5	2.4	15	2565	33 22.0	65 23.0

TABLE I

MEASUREMENTS OF ACOUSTIC BOTTOM LOSS AT NORMAL INCIDENCE

TAG	PEAK PRESS. MED.	DEV.	TOTAL ENG. MED.	DEV.	AMT.	DEPTH	LATITUDE DG. MN.	LONGITUDE DG. MN.
68	16.9	4.4	14.3	4.2	32	2620	33 27.0	65 29.0
69	16.2	3.2	13.5	2.4	30	2630	33 32.0	65 35.0
70	18.8	1.7	14.9	1.3	10	2655	33 37.0	65 41.0
71	18.0	4.1	11.5	2.0	7	2685	33 42.0	65 47.0
72	18.9	3.8	14.5	3.8	14	2690	33 46.0	65 52.0
73	18.2	1.6	16.3	1.6	18	2690	33 54.0	65 55.0
74	15.5	2.9	12.9	2.6	109	2710	34 3.0	65 57.0
75	18.3	2.5	14.0	1.6	17	2730	34 10.0	66 0.
76	17.1	3.4	11.2	1.9	32	2730	34 18.0	65 58.0
77	17.0	2.9	12.8	1.9	21	2740	34 20.0	65 50.0
78	17.0	3.0	11.1	1.9	15	2740	34 24.0	65 43.0
79	14.4	2.1	9.0	1.5	15	2740	34 27.0	65 36.0
80	17.3	2.1	11.5	1.3	15	2655	34 40.0	65 29.0
81	19.6	1.5	13.1	1.1	26	2625	34 46.0	65 24.0
82	22.7	2.3	14.9	1.3	24	2580	34 56.0	65 19.0
83	18.7	2.6	14.4	1.8	36	2550	35 4.0	65 18.0
84	19.0	1.5	13.6	1.4	21	2555	35 7.0	65 17.0
85	16.8	2.5	12.2	1.9	18	2570	35 13.0	65 8.0
86	17.7	2.0	12.6	1.4	24	2475	35 20.0	64 59.0
87	19.6	3.2	14.3	3.7	37	2580	35 20.0	64 59.0
88	17.3	2.1	12.8	1.8	18	2580	35 24.0	65 3.0
89	20.1	2.5	15.7	3.5	12	2580	35 17.0	65 9.0
90	17.2	2.9	12.5	2.1	23	2560	35 14.0	65 12.0
91	18.7	2.2	13.6	2.0	17	2590	35 6.0	65 24.0
92	17.1	3.0	12.5	1.9	15	2610	35 1.0	65 30.0

TABLE I

MEASUREMENTS OF ACOUSTIC BOTTOM LOSS AT NORMAL INCIDENCE

TAG	PEAK PRESS. MED.	DEV.	TOTAL ENG. MED.	DEV.	AMT.	DEPTH	LATITUDE DG. MN.	LONGITUDE DG. MN.
93	19.8	2.2	13.7	1.3	13	2615	34 56.0	65 35.0
94	17.6	2.4	12.8	1.6	9	2640	34 51.0	65 30.0
95	19.9	1.5	12.6	1.5	6	2680	34 47.0	65 49.0
96	17.3	1.6	11.7	1.1	11	2675	34 44.0	65 54.0
97	17.3	2.7	13.3	2.3	14	2705	34 4.0	65 53.0
98	19.4	2.2	13.7	1.5	9	2735	34 37.0	66 3.0
99	17.0	1.3	12.3	1.0	6	2740	34 35.0	66 7.0
100	19.2	3.2	13.1	2.0	10	2735	34 36.0	66 12.0
101	16.1	2.9	10.4	2.6	13	2740	34 37.0	66 18.0
102	16.2	3.4	11.8	2.3	11	2730	34 37.0	66 24.0
103	17.4	2.5	12.3	2.3	6	2750	34 37.0	66 30.0
104	16.0	2.5	11.4	2.1	52	2750	34 37.0	66 30.0
105	15.1	2.4	9.4	2.1	16	2750	34 34.0	66 31.5
106	16.3	2.2	10.6	2.1	8	2765	34 32.0	66 32.5
107	15.5	3.6	11.8	2.8	7	2765	34 31.0	66 33.0
108	15.4	1.0	10.9	1.4	12	2760	34 33.0	66 27.0
109	17.1	3.0	11.0	2.2	18	2740	34 45.0	66 22.0
110	15.9	1.8	10.3	1.1	12	2745	34 40.0	66 16.0
111	15.5	2.0	10.4	1.8	13	2720	34 45.0	66 11.0
112	17.2	2.5	11.9	2.0	18	2680	34 47.0	66 1.0
113	17.2	1.7	11.2	1.1	25	2675	34 49.0	65 52.0
114	18.5	2.0	12.6	1.2	9	2655	34 49.0	65 51.0
115	20.5	1.9	13.2	1.5	7	2630	34 49.0	65 50.0
116	18.5	2.0	12.8	1.5	25	2615	34 53.0	65 51.0
117	17.8	2.3	12.1	1.8	97	2615	34 53.0	65 52.0

TABLE I

MEASUREMENTS OF ACOUSTIC BOTTOM LOSS AT NORMAL INCIDENCE

TAG	PEAK PRESS. MED.	DEV.	TOTAL ENG. MED.	DEV.	AMT.	DEPTH	LATITUDE DG.	MN.	LONGITUDE DG.	MN.
118	17.5	2.1	12.5	1.3	12	2630	35	2.0	65	52.0
119	16.7	3.0	11.1	3.0	16	2625	35	1.0	65	58.0
120	17.7	2.4	13.7	2.1	26	2760	35	21.0	66	48.0
121	18.4	3.2	15.5	2.9	26	2640	35	26.0	66	53.0
122	12.2	2.3	9.3	1.6	19	2675	35	39.0	67	5.0
123	13.5	3.4	8.0	2.3	19	2690	35	45.0	67	9.0
124	10.2	3.8	4.9	1.5	18	2675	35	51.0	67	13.0
125	12.7	2.8	8.7	1.5	17	2640	35	57.0	67	17.0
126	11.2	3.0	7.5	1.5	53	2640	36	3.0	67	21.0
127	11.4	2.6	7.4	2.4	27	2635	36	21.0	67	23.0
128	11.5	3.2	6.7	2.7	32	2635	36	24.0	67	23.0
129	11.9	3.1	9.1	2.6	35	2640	36	27.0	67	24.0
130	9.2	3.4	6.9	2.1	39	2645	36	30.0	67	25.0
131	9.9	3.2	7.7	2.0	36	2645	36	33.0	67	26.0
132	9.8	2.3	6.4	1.5	32	2645	36	35.0	67	26.0
133	8.8	2.8	6.2	2.1	45	2640	36	38.0	67	27.0
134	7.9	2.7	5.7	1.7	37	2635	36	41.0	67	33.0
135	7.8	2.6	5.4	1.8	42	2635	36	43.0	67	37.0
136	6.2	2.7	4.3	1.8	37	2630	36	45.0	67	40.0
137	7.5	2.6	5.1	1.9	38	2630	36	48.0	67	40.0
138	6.9	2.7	6.0	2.1	33	2630	36	51.0	67	40.0
139	8.8	3.2	6.5	3.4	36	2630	36	54.0	67	41.0
140	9.1	3.5	6.5	2.1	26	2625	36	57.0	67	41.0
141	10.4	2.3	7.1	1.9	29	2625	36	59.0	67	44.0
142	8.3	3.7	6.5	2.5	38	2620	37	0.	67	47.0

TABLE I

MEASUREMENTS OF ACOUSTIC BOTTOM LOSS AT NORMAL INCIDENCE

TAG	PEAK PRESS. MED.	DEV.	TOTAL ENG. MED.	DEV.	AMT.	DEPTH	LATITUDE DG.	MN.	LONGITUDE DG.	MN.
143	9.8	2.9	8.3	2.5	26	2615	37	1.0	67	50.0
144	10.0	3.2	8.3	2.6	34	2620	37	1.0	67	45.0
145	8.5	2.5	6.5	2.2	30	2625	37	4.0	67	40.0
146	11.0	3.0	7.2	2.4	23	2620	37	5.0	67	45.0
147	7.6	2.3	6.2	1.0	24	2615	37	3.0	67	53.0
148	7.9	1.8	5.8	0.5	19	2610	36	58.0	67	58.0
149	7.8	3.5	6.6	1.6	22	2615	36	56.0	67	51.0
150	9.1	2.9	6.6	0.9	19	2615	37	0.	67	48.0
151	7.7	2.8	6.0	1.4	20	2620	37	6.0	67	41.0
152	6.9	3.5	5.1	3.2	18	2620	37	2.0	67	50.0
153	5.6	2.8	4.0	2.6	21	2610	37	6.0	67	51.0
154	14.2	3.1	6.5	1.6	12	2565	37	14.0	67	59.0
155	15.7	3.9	8.5	1.7	20	2530	37	16.0	68	2.0
156	12.4	2.1	4.7	1.1	5	2525	37	21.0	68	5.0
157	8.5	3.5	5.5	3.0	31	2490	37	31.0	68	11.0
158	8.7	3.0	5.3	2.8	26	2475	37	36.0	68	14.0
159	9.6	3.5	6.2	2.5	31	2440	37	40.0	68	18.0
160	9.1	2.4	5.9	1.6	22	2370	37	48.0	68	24.0
161	9.8	2.2	5.9	1.6	47	2320	37	53.0	68	27.0
162	9.2	2.8	6.1	1.6	21	2280	37	58.0	68	31.0
163	11.3	2.1	7.3	1.8	25	2225	38	3.0	68	34.0
164	10.5	2.9	7.5	2.0	23	2195	38	8.0	68	36.0
165	7.1	3.2	5.5	2.4	31	2150	38	14.0	68	38.0
166	8.4	2.3	6.9	2.1	20	2090	38	18.0	68	46.0
167	11.1	2.2	8.4	2.1	22	2020	38	22.0	68	55.0

TABLE I

MEASUREMENTS OF ACOUSTIC BOTTOM LOSS AT NORMAL INCIDENCE

TAG	PEAK PRESS. MED.	DEV.	TOTAL ENG. MED.	DEV.	AMT.	DEPTH	LATITUDE DG. MN.	LONGITUDE DG. MN.
168	11.1	2.5	8.5	1.5	27	1920	38 29.0	68 54.0
169	11.6	3.4	8.0	2.6	23	1790	38 41.0	68 58.0
170	14.7	2.6	10.5	2.1	31	1720	38 52.0	69 3.0
171	15.7	2.2	12.2	1.3	18	1680	38 58.0	69 5.0
172	16.6	1.8	12.0	1.3	33	1700	38 57.0	69 9.0
173	12.0	4.3	10.4	4.0	21	1680	38 56.0	69 13.0
174	23.4	2.5	18.6	4.0	39	1725	38 58.0	69 17.0
175	14.3	3.3	11.5	2.5	34	1400	39 16.0	69 28.0
176	13.9	3.6	11.1	2.4	55	1320	39 21.0	69 32.0
177	24.5	1.4	17.0	0.6	19	1285	39 31.0	69 32.0
178	24.8	1.6	17.8	1.5	71	1285	39 31.0	69 32.0
179	17.9	2.3	12.4	1.8	59	1080	39 43.0	69 41.0
180	15.3	2.9	10.7	2.6	39	1030	39 46.0	69 42.0
181	12.3	3.5	10.1	2.2	24	1100	39 42.0	69 37.0
182	21.7	1.6	16.1	1.2	17	1140	39 41.0	69 29.0
183	13.8	2.7	9.9	2.4	47	1120	39 38.0	69 31.0
184	15.8	2.9	13.5	3.3	21	1105	39 39.0	69 32.0
185	18.2	1.8	16.3	2.4	16	1110	39 41.0	69 35.0
186	17.1	1.4	13.6	2.1	21	1070	39 43.0	69 37.0
187	22.5	1.4	19.9	1.9	19	910	39 45.0	69 39.0
188	20.8	2.3	18.5	2.1	29	930	39 45.0	69 39.0
189	19.3	2.7	14.1	2.4	14	950	39 46.0	69 40.0
190	20.4	1.3	17.6	1.7	20	920	39 47.0	69 41.0
191	21.8	1.7	17.7	2.1	19	760	39 48.0	69 42.0
192	19.8	1.9	14.4	1.6	19	615	39 48.0	69 42.0

TABLE I

MEASUREMENTS OF ACOUSTIC BOTTOM LOSS AT NORMAL INCIDENCE

TAG	PEAK PRESS. MED.	DEV.	TOTAL ENG. MED.	DEV.	AMT.	DEPTH	LATITUDE DG.	MN.	LONGITUDE DG.	MN.
193	19.1	1.9	14.5	1.4	19	530	39	49.0	69	43.0
194	18.0	3.1	13.1	2.0	21	410	39	50.0	69	44.0
195	17.1	3.1	13.1	2.2	27	290	39	51.0	69	45.0
196	14.6	3.7	12.3	2.9	32	230	39	53.0	69	47.0
197	14.3	2.8	12.1	3.2	21	170	39	54.0	69	48.0
198	13.0	3.4	11.8	3.2	38	80	39	58.0	69	51.0
199	14.5	3.8	13.1	3.7	109	80	40	0.	69	53.0
200	14.6	4.2	13.1	4.0	123	75	40	4.0	69	56.0
201	12.6	3.6	11.2	3.7	40	60	40	7.0	69	59.0
202	13.7	2.2	12.1	2.2	27	55	40	10.0	70	2.0
203	12.4	1.4	11.1	1.3	14	55	40	12.0	70	4.0
204	14.4	1.8	13.7	2.2	14	50	40	15.0	70	6.0
205	15.1	2.7	13.1	3.1	19	45	40	18.0	70	8.0
206	15.5	2.1	14.8	2.3	19	45	40	20.0	70	10.0
207	16.1	2.2	14.1	2.6	19	40	40	23.0	70	13.0
208	17.2	2.0	16.2	2.5	20	35	40	25.0	70	15.0
209	14.5	1.9	13.1	1.7	18	35	40	27.0	70	17.0
210	15.3	2.3	14.2	2.1	20	30	40	29.0	70	19.0
211	14.9	1.3	13.9	1.2	19	30	40	32.0	70	21.0
212	17.1	2.3	15.5	2.2	19	30	40	34.0	70	23.0
213	14.9	2.8	13.6	2.4	18	30	40	36.0	70	25.0
MEASUREMENTS OBTAINED ON R/V ASTERIAS CRUISE										
1	15.5	3.1	15.1	3.0	20	23	41	34.4	71	23.8
2	14.8	3.1	14.8	2.7	26	26	41	34.4	71	23.3

TABLE I

MEASUREMENTS OF ACOUSTIC BOTTOM LOSS AT NORMAL INCIDENCE

TAG	PEAK PRESS. MED.	DEV.	TOTAL ENG. MED.	DEV.	AMT.	DEPTH	LATITUDE DG. MN.	LONGITUDE DG. MN.
3	15.9	3.2	16.2	2.9	21	24	41 34.4	71 23.1
4	8.4	2.2	7.1	2.5	22	21	41 34.5	71 22.4
5	13.1	2.6	13.3	2.3	24	39	41 34.5	71 21.9
6	15.1	2.3	14.2	2.4	22	30	41 34.5	71 21.0
7	15.3	2.7	14.5	2.7	23	28	41 34.5	71 20.3
8	13.5	2.8	13.7	3.0	24	33	41 34.5	71 19.7
9	9.2	3.5	9.3	3.4	22	45	41 34.5	71 19.1
10	10.0	2.3	9.1	2.7	23	35	41 34.4	71 18.5
11	10.1	2.7	10.4	3.2	23	36	41 34.7	71 18.4
12	9.4	2.7	9.0	2.8	24	75	41 34.7	71 19.0
13	10.1	2.3	9.2	2.6	22	21	41 34.5	71 19.6
14	9.8	2.3	8.4	2.8	22	10	41 34.8	71 20.0
15	11.6	3.4	11.7	3.0	38	40	41 35.2	71 20.6
16	13.6	2.7	13.6	2.4	26	28	41 35.2	71 21.2
17	10.9	3.5	11.5	3.4	25	21	41 35.2	71 21.9
19	15.0	2.9	12.8	2.2	22	23	41 35.1	71 23.1
18	15.1	3.1	12.6	2.7	25	22	41 35.1	71 22.6
20	15.6	2.8	15.8	2.3	22	26	41 35.1	71 23.8
21	15.7	2.9	15.3	2.7	24	26	41 35.6	71 23.8
22	13.6	3.7	13.2	3.9	23	24	41 35.6	71 22.8
23	15.6	2.7	14.6	2.6	25	22	41 35.6	71 22.1
24	16.6	3.3	15.4	3.1	21	23	41 35.6	71 21.5
25	13.0	3.6	12.4	3.6	25	27	41 35.6	71 20.8
26	9.9	2.4	10.1	2.2	23	34	41 35.9	71 20.5
27	12.6	2.4	12.8	2.5	21	32	41 36.2	71 20.8

TABLE I

MEASUREMENTS OF ACOUSTIC BOTTOM LOSS AT NORMAL INCIDENCE

TAG	PEAK PRESS. MED.	DEV.	TOTAL ENG. MED.	DEV.	AMT.	DEPTH	LATITUDE DG. MN.	LONGITUDE DG. MN.
28	15.9	2.4	14.4	2.9	25	26	41 36.2	71 21.2
29	15.4	3.2	14.8	2.9	25	26	41 36.1	71 21.6
30	15.6	3.3	17.1	3.2	21	35	41 36.6	71 21.5
31	16.3	3.0	15.3	2.4	24	23	41 36.6	71 20.9
32	13.1	2.3	12.9	2.7	21	27	41 36.6	71 20.2
33	16.1	3.3	15.3	2.8	26	20	41 37.2	71 20.3
34	15.2	2.2	14.6	2.4	25	21	41 37.2	71 21.0
35	17.4	2.7	16.2	2.4	22	21	41 37.1	71 21.7
36	15.6	2.5	14.7	2.1	27	20	41 37.1	71 22.5
37	16.3	2.4	15.0	2.4	22	23	41 37.1	71 23.2
38	14.6	1.9	14.0	2.1	22	19	41 37.1	71 23.8
39	13.1	3.2	13.7	3.4	25	11	41 37.4	71 23.6
40	14.7	2.9	14.6	2.8	21	21	41 37.7	71 22.8
41	16.0	1.6	15.2	2.0	14	20	41 37.5	71 22.3
42	16.5	3.1	17.2	2.8	34	20	41 37.5	71 22.3
43	17.3	3.2	16.7	2.9	23	18	41 38.0	71 22.3
44	13.0	1.9	12.6	2.5	19	15	41 38.5	71 22.4
45	14.2	3.6	14.7	3.6	51	27	41 38.8	71 22.4
46	12.6	2.2	11.2	2.3	11	14	41 34.4	71 26.1
47	14.8	3.5	14.2	2.9	18	13	41 34.4	71 25.8
48	14.2	3.9	10.9	3.8	25	14	41 34.4	71 25.5
49	13.9	2.9	11.8	2.6	26	7	41 34.4	71 25.0
50	14.7	2.8	12.8	2.8	21	19	41 34.5	71 24.7
51	13.3	3.6	11.9	3.2	26	22	41 34.5	71 24.3
52	15.0	2.7	12.8	1.8	23	25	41 34.5	71 23.6

TABLE I

MEASUREMENTS OF ACOUSTIC BOTTOM LOSS AT NORMAL INCIDENCE

TAG	PEAK PRESS. MED.	DEV.	TOTAL ENG. MED.	DEV.	AMT.	DEPTH	LATITUDE DG. MN.	LONGITUDE DG. MN.
53	14.9	3.2	13.9	3.1	22	25	41 34.5	71 23.3
54	16.0	2.6	15.8	2.4	27	24	41 34.6	71 23.0
55	14.3	2.8	14.0	2.6	27	22	41 34.6	71 22.7
56	13.3	1.9	12.6	1.7	12	35	41 34.6	71 22.2
57	13.2	3.6	12.7	3.4	23	27	41 34.6	71 21.7
58	14.0	3.0	13.5	2.8	21	28	41 34.6	71 21.4
59	14.9	1.8	13.4	1.7	21	28	41 34.6	71 21.0
60	14.4	2.9	14.0	2.8	28	30	41 34.6	71 20.7
61	9.2	2.7	8.7	2.6	21	29	41 34.6	71 20.0
62	9.1	2.5	8.7	2.7	21	28	41 34.5	71 19.6
63	9.0	3.0	7.5	3.5	22	50	41 34.4	71 19.2
64	7.2	2.6	7.1	2.6	25	63	41 34.4	71 18.7
65	11.9	3.4	12.5	3.5	34	23	41 34.3	71 18.3
66	15.9	2.8	14.5	2.5	20	24	41 34.1	71 18.3
67	11.6	2.1	9.9	1.5	20	55	41 33.9	71 18.5
68	11.9	2.6	10.9	2.4	23	57	41 33.9	71 18.8
69	11.1	3.4	10.1	3.0	22	80	41 33.9	71 19.2
70	10.7	2.9	10.9	2.5	30	55	41 34.0	71 19.5
71	10.5	3.5	9.7	3.2	22	27	41 34.0	71 19.9
72	14.2	2.3	13.7	2.1	25	30	41 34.0	71 20.3
73	13.7	2.6	11.9	2.7	24	32	41 34.1	71 20.7
74	10.4	1.8	9.4	1.5	27	43	41 34.1	71 21.1
75	11.8	2.6	10.8	2.3	22	42	41 33.8	71 21.4
76	11.9	2.8	11.4	2.2	32	39	41 33.8	71 21.0
77	13.0	2.8	12.2	2.1	23	36	41 33.8	71 20.7

TABLE I

MEASUREMENTS OF ACOUSTIC BOTTOM LOSS AT NORMAL INCIDENCE

TAG	PEAK PRESS. MED.	DEV.	TOTAL ENG. MED.	DEV.	AMT.	DEPTH	LATITUDE DG. MN.	LONGITUDE DG. MN.
78	15.2	1.9	14.2	1.7	17	34	41 33.7	71 20.3
79	12.5	3.6	12.6	4.0	21	24	41 33.7	71 20.0
80	14.9	2.2	14.9	2.3	106	51	41 33.3	71 19.5
81	13.8	2.3	12.8	2.5	23	75	41 33.3	71 19.1
82	13.5	2.8	12.9	2.4	29	45	41 33.3	71 18.8
83	14.4	1.8	14.0	2.0	25	45	41 33.1	71 19.0
84	13.6	2.3	13.2	2.2	24	50	41 32.8	71 20.0
85	12.8	2.3	11.4	2.2	25	60	41 32.5	71 19.6
86	13.3	2.4	11.7	2.3	23	60	41 32.5	71 20.1
87	9.1	2.6	9.0	2.2	32	60	41 32.4	71 21.2
88	11.0	2.7	10.6	2.7	24	48	41 32.4	71 21.6
89	10.0	2.3	9.3	2.1	24	55	41 32.1	71 21.6
90	7.8	2.7	8.0	3.0	22	52	41 31.7	71 21.6
91	9.4	3.3	8.7	2.9	36	76	41 31.4	71 21.2
92	8.4	2.8	8.1	2.2	25	97	41 31.4	71 20.5
93	10.7	2.4	9.1	2.0	11	105	41 31.4	71 20.1
94	13.9	4.0	14.2	4.4	9	49	41 30.7	71 20.1
95	9.4	2.9	9.0	2.6	77	83	41 30.5	71 21.2
96	8.6	2.8	8.2	2.3	22	117	41 30.7	71 21.1
97	7.9	2.2	7.8	1.8	34	101	41 31.1	71 20.8
98	11.8	3.1	11.0	2.8	52	95	41 31.5	71 20.5
99	10.5	3.5	9.7	3.3	30	120	41 31.7	71 20.4
100	11.0	2.2	9.9	2.1	23	95	41 32.0	71 20.1
101	11.9	2.9	10.1	2.7	36	72	41 32.4	71 19.9
102	12.2	2.7	11.4	2.5	39	71	41 32.7	71 19.7

TABLE I

MEASUREMENTS OF ACOUSTIC BOTTOM LOSS AT NORMAL INCIDENCE

TAG	PEAK PRESS. MED.	DEV.	TOTAL ENG. MED.	DEV.	AMT.	DEPTH	LATITUDE DG. MN.	LONGITUDE DG. MN.
103	12.4	1.7	11.2	2.0	22	80	41 33.1	71 19.4
104	10.1	3.9	9.9	3.0	28	86	41 33.3	71 19.3
105	10.5	3.3	9.8	2.9	24	84	41 33.6	71 19.1
106	9.9	3.1	9.4	2.9	24	69	41 33.9	71 18.9
107	9.4	2.1	9.0	2.1	17	59	41 34.1	71 18.7
108	7.3	2.3	5.7	2.7	28	70	41 34.3	71 18.6
109	9.8	2.0	7.2	2.2	22	60	41 34.3	71 19.0
110	11.5	2.9	10.5	2.9	22	35	41 34.3	71 19.5
111	16.2	3.1	15.1	2.7	20	25	41 34.3	71 20.0
112	15.2	1.9	14.6	2.1	34	26	41 34.4	71 20.4
113	13.6	2.2	12.4	2.3	29	27	41 34.5	71 20.9
114	14.3	2.6	13.9	2.6	21	27	41 34.5	71 21.3
115	12.3	2.4	10.6	2.4	20	34	41 34.6	71 22.0
116	12.8	2.7	11.5	2.4	19	33	41 34.6	71 22.3
117	14.6	2.4	13.3	1.9	21	33	41 34.7	71 22.8
118	11.4	2.9	11.2	2.5	23	22	41 34.7	71 23.3
119	13.4	3.3	14.6	2.5	44	42	41 33.4	71 21.4
120	8.1	2.9	9.8	2.7	24	85	41 31.0	71 21.3
121	10.4	2.9	11.9	2.5	27	106	41 31.0	71 20.8
122	12.6	3.5	14.5	3.3	25	56	41 31.0	71 20.1
123	14.4	3.2	15.8	3.2	25	31	41 30.5	71 20.2
124	11.6	2.7	13.2	2.7	39	82	41 30.5	71 20.8
125	12.8	2.8	14.3	2.6	26	85	41 30.4	71 21.3
126	8.7	2.2	8.7	2.5	24	57	41 30.1	71 21.4
127	10.9	2.6	12.4	1.7	26	126	41 30.1	71 20.9

TABLE I

MEASUREMENTS OF ACOUSTIC BOTTOM LOSS AT NORMAL INCIDENCE

TAG	PEAK PRESS. MED.	DEV.	TOTAL ENG. MED.	DEV.	AMT.	DEPTH	LATITUDE DG.	MN.	LONGITUDE DG.	MN.
128	11.2	2.5	11.5	2.5	25	122	41	29.7	71	20.8
129	10.5	2.5	12.6	2.3	24	123	41	29.3	71	20.8
130	11.0	3.0	12.8	2.5	54	84	41	28.9	71	20.5
131	9.4	2.7	9.5	2.5	107	48	41	28.4	71	20.8
132	7.7	2.3	8.9	2.3	105	50	41	28.4	71	20.8
133	7.8	2.0	8.6	2.0	106	48	41	28.4	71	20.8
134	11.7	3.2	13.3	3.5	44	87	41	28.4	71	21.7
135	9.1	2.0	10.8	1.9	27	60	41	28.4	71	22.7
136	10.1	1.3	11.9	1.5	100	30	41	28.6	71	22.9
137	10.1	1.7	12.6	1.7	118	28	41	28.6	71	22.9
138	11.7	1.9	11.0	2.3	51	29	41	28.6	71	22.9
140	9.0	3.3	7.8	2.1	27	70	41	28.2	71	22.7
141	9.4	2.7	7.8	2.2	21	110	41	27.5	71	23.0
142	11.5	2.4	11.2	2.5	28	70	41	27.0	71	23.6
143	10.1	3.3	7.8	2.6	22	35	41	26.7	71	24.2
144	9.4	1.2	7.8	1.2	21	51	41	27.2	71	24.6
145	9.8	1.8	8.7	1.5	22	42	41	27.8	71	24.6
146	13.9	3.3	11.4	2.7	21	43	41	28.5	71	24.6
147	14.9	3.1	12.3	2.4	18	41	41	29.1	71	24.6
148	14.9	2.3	12.0	2.3	20	40	41	29.8	71	24.5
149	17.1	2.7	14.9	2.8	28	26	41	30.3	71	24.5
150	12.6	2.6	11.7	2.4	25	47	41	31.1	71	24.3
151	14.7	3.3	11.8	1.8	23	25	41	31.6	71	24.0
152	14.7	3.1	11.0	2.2	23	36	41	32.3	71	24.4
153	15.2	2.0	14.4	1.9	16	24	41	32.8	71	24.7

TABLE I

MEASUREMENTS OF ACOUSTIC BOTTOM LOSS AT NORMAL INCIDENCE

TAG	PEAK PRESS. MED.	DEV.	TOTAL ENG. MED.	DEV.	AMT.	DEPTH	LATITUDE DG. MN.	LONGITUDE DG. MN.
154	16.2	3.1	14.1	2.7	20	21	41 33.5	71 25.2
155	14.7	2.3	11.4	2.1	20	13	41 33.9	71 25.7
156	13.3	3.3	10.5	2.8	25	12	41 34.1	71 26.0
157	15.5	3.6	12.9	3.8	22	12	41 34.2	71 25.9
158	15.0	3.7	12.4	3.1	23	17	41 33.7	71 25.3
159	16.4	2.8	15.7	2.2	22	26	41 32.9	71 24.6
160	10.6	1.5	10.1	1.5	98	28	41 28.6	71 22.9
161	9.8	2.1	9.8	2.1	103	29	41 28.6	71 22.9
162	13.7	2.6	10.0	2.5	9	98	41 28.0	71 22.6
163	12.4	2.9	10.3	2.5	108	98	41 28.0	71 22.6
164	11.3	2.8	9.4	2.2	101	99	41 28.0	71 22.6
165	11.1	3.7	10.5	3.6	23	85	41 28.2	71 22.1
166	10.1	2.8	8.8	2.6	22	115	41 28.3	71 21.7
167	12.1	2.9	9.9	2.2	102	100	41 28.4	71 21.4
168	12.8	2.3	10.0	2.4	23	11	41 34.4	71 26.1
169	14.5	2.6	12.5	4.3	25	12	41 34.1	71 25.9
170	13.9	2.6	11.6	2.6	23	13	41 33.8	71 25.5
171	13.5	2.8	12.3	2.7	21	16	41 33.7	71 25.3
172	13.7	2.8	13.0	2.4	15	24	41 33.5	71 25.1
173	12.3	1.9	12.1	2.1	9	24	41 33.3	71 25.0
174	12.7	3.6	12.1	3.3	9	25	41 33.3	71 24.5
175	10.5	1.7	9.8	1.8	21	31	41 33.3	71 24.0
176	9.2	1.9	8.4	1.9	101	32	41 33.3	71 23.7
177	13.2	2.1	12.6	2.9	98	31	41 33.2	71 24.6
178	11.5	2.3	9.6	2.1	18	34	41 33.1	71 23.7

TABLE I

MEASUREMENTS OF ACOUSTIC BOTTOM LOSS AT NORMAL INCIDENCE

TAG	PEAK PRESS. MED.	DEV.	TOTAL ENG. MED.	DEV.	AMT.	DEPTH	LATITUDE DG.	MN.	LONGITUDE DG.	MN.
179	11.6	4.0	11.1	3.5	31	25	41	32.9	71	23.8
180	10.5	3.0	10.4	3.4	30	38	41	32.7	71	24.0
181	11.6	2.2	10.5	2.1	96	38	41	32.7	71	24.0
182	13.0	2.6	13.0	2.5	23	31	41	32.5	71	24.0
183	9.5	3.7	7.8	2.4	20	30	41	32.2	71	24.0
184	9.8	2.4	9.3	2.2	35	36	41	32.1	71	24.0
185	13.8	1.9	11.9	1.9	20	21	41	31.9	71	24.0
186	6.8	4.5	5.0	2.8	24	25	41	31.5	71	24.0
187	10.9	3.4	9.7	2.5	21	52	41	31.3	71	24.1
188	11.5	2.4	10.0	3.3	28	47	41	31.1	71	24.1
189	12.6	2.6	11.6	2.3	24	53	41	30.8	71	24.2
190	14.2	3.7	13.3	3.6	26	33	41	30.5	71	24.3
191	14.7	2.7	13.1	2.1	30	36	41	30.3	71	24.4
192	14.2	3.4	12.8	3.0	22	26	41	30.1	71	24.4
193	11.1	1.8	9.0	2.4	26	26	41	29.9	71	24.4
194	12.8	2.7	12.8	2.6	22	42	41	29.7	71	24.5
195	14.4	2.2	12.5	2.0	102	43	41	29.6	71	24.5

MEASUREMENTS OBTAINED ON R/V BEAR CRUISE 281

1	11.4	3.1	8.5	2.9	62	65	41	26.4	71	22.1
2	10.9	2.4	7.9	2.9	25	82	41	26.4	71	22.5
3	12.3	3.0	11.1	3.1	24	79	41	26.4	71	23.0
4	9.5	2.6	8.4	2.7	24	77	41	26.4	71	23.4
5	10.6	3.0	10.0	4.4	25	79	41	26.3	71	23.8
6	11.0	2.4	9.8	1.9	24	76	41	26.3	71	24.2

TABLE I

MEASUREMENTS OF ACOUSTIC BOTTOM LOSS AT NORMAL INCIDENCE

TAG	PEAK PRESS. MED.	DEV.	TOTAL ENG. MED.	DEV.	AMT.	DEPTH	LATITUDE DG. MN.	LONGITUDE DG. MN.
7	11.1	3.1	11.3	2.9	24	67	41 26.3	71 24.6
8	9.7	2.4	8.3	3.0	24	59	41 26.3	71 25.1
9	7.4	2.4	6.1	2.8	25	56	41 26.3	71 25.6
10	10.2	2.5	9.3	1.9	47	56	41 26.2	71 25.8
11	7.5	2.3	7.6	2.1	71	51	41 26.4	71 25.5
12	9.6	2.0	8.8	1.5	25	57	41 26.4	71 25.0
13	11.4	3.4	9.9	2.0	24	64	41 26.5	71 24.4
14	10.8	2.8	7.8	1.7	29	74	41 26.5	71 23.8
15	9.7	3.1	7.7	1.8	26	79	41 26.6	71 23.0
16	11.3	3.5	10.3	3.0	24	90	41 26.6	71 22.6
17	10.9	2.8	8.1	1.7	76	82	41 26.7	71 22.0
18	11.9	3.1	11.4	2.1	60	80	41 26.7	71 22.0
19	10.3	1.6	9.2	1.5	126	26	41 28.6	71 22.8
20	9.5	1.9	11.1	1.5	94	25	41 28.6	71 22.9
21	14.0	4.6	12.1	3.5	51	60	41 26.9	71 22.0
22	13.2	2.9	10.7	1.9	29	78	41 26.9	71 22.4
23	9.9	2.4	8.1	1.6	23	95	41 26.9	71 22.7
24	10.1	3.1	7.8	1.9	26	113	41 26.9	71 23.2
25	11.2	3.3	9.9	2.8	21	76	41 26.9	71 23.6
26	10.3	2.2	8.7	2.0	50	66	41 26.9	71 23.8
27	12.1	2.5	9.8	1.8	49	59	41 27.0	71 24.2
28	9.3	3.2	8.3	2.3	23	53	41 27.0	71 24.4
29	9.6	2.7	8.8	1.8	24	46	41 27.0	71 24.9
30	9.7	2.7	8.7	2.6	24	35	41 27.0	71 25.4
31	9.7	2.9	8.6	2.5	48	38	41 27.0	71 25.4

TABLE I

MEASUREMENTS OF ACOUSTIC BOTTOM LOSS AT NORMAL INCIDENCE

TAG	PEAK PRESS. MED.	DEV.	TOTAL ENG. MED.	DEV.	AMT.	DEPTH	LATITUDE DG.	MN.	LONGITUDE DG.	MN.
32	11.2	2.9	9.7	2.4	26	43	41	26.9	71	25.5
33	9.1	1.4	8.3	1.3	24	45	41	26.6	71	25.6
34	12.3	1.9	9.2	1.3	24	51	41	26.3	71	25.8
35	10.5	2.4	8.7	1.6	21	57	41	26.0	71	25.9
36	12.2	2.5	9.4	1.6	29	61	41	25.7	71	26.1
37	11.6	6.0	9.8	2.2	49	60	41	25.7	71	26.1
38	10.8	4.9	9.8	3.0	98	60	41	25.7	71	26.1
39	15.9	4.1	13.5	2.7	23	58	41	25.7	71	26.1
40	10.1	5.7	9.3	3.5	47	41	41	25.7	71	26.6
41	8.7	2.4	7.2	2.1	25	33	41	26.0	71	26.7
42	8.0	1.2	6.0	1.0	20	44	41	26.0	71	26.2
43	9.1	2.8	5.1	2.1	24	62	41	26.0	71	25.6
44	9.8	2.5	8.6	1.9	23	68	41	26.0	71	25.1
45	12.5	2.5	9.3	1.7	23	75	41	26.0	71	24.5
46	12.1	2.9	9.3	2.2	34	79	41	26.0	71	24.0
47	11.9	3.3	10.4	2.7	48	79	41	26.0	71	23.8
48	7.8	2.8	6.3	2.9	24	75	41	26.0	71	23.4
49	12.4	4.4	10.1	2.7	69	74	41	25.9	71	23.1
50	12.2	3.7	11.1	3.0	17	78	41	26.4	71	22.6
51	11.9	2.6	10.3	1.8	25	81	41	26.8	71	22.3
52	13.1	4.4	11.9	2.8	98	76	41	26.9	71	22.2
53	8.1	2.9	6.5	2.6	26	131	41	27.5	71	22.4
54	11.3	2.7	10.0	3.1	9	61	41	28.0	71	22.6
55	9.7	2.1	8.5	1.7	23	46	41	28.0	71	22.6
56	11.4	2.7	11.3	2.0	166	23	41	28.7	71	22.9

TABLE I

MEASUREMENTS OF ACOUSTIC BOTTOM LOSS AT NORMAL INCIDENCE

TAG	PEAK PRESS. MED.	DEV.	TOTAL ENG. MED.	DEV.	AMT.	DEPTH	LATITUDE DG. MN.	LONGITUDE DG. MN.
57	7.8	2.9	7.8	2.4	24	90	41 28.3	71 21.9
58	8.5	2.1	6.6	1.3	24	145	41 28.6	71 21.3
59	10.2	2.4	9.6	2.5	25	126	41 28.9	71 21.0
60	11.6	3.5	9.3	2.3	24	44	41 30.6	71 20.0
61	8.5	2.7	8.4	2.5	24	72	41 31.0	71 20.2
62	9.9	2.8	8.6	2.5	25	100	41 31.5	71 20.3
63	7.8	1.5	7.3	1.3	23	75	41 32.0	71 20.3
64	14.6	2.1	12.0	1.5	24	40	41 32.5	71 20.4
65	14.2	2.0	12.2	1.8	24	38	41 33.0	71 20.4
66	15.2	2.1	13.4	1.7	24	34	41 33.5	71 20.5
67	14.1	2.4	12.1	1.9	24	30	41 33.9	71 20.5
68	13.8	2.3	11.7	1.7	25	27	41 34.4	71 20.6
69	14.5	2.5	15.6	1.4	25	24	41 34.7	71 21.2
70	12.3	2.7	11.2	2.4	28	30	41 33.7	71 23.5
71	10.8	2.6	9.9	2.3	27	36	41 33.0	71 23.6
72	9.7	3.0	8.1	2.2	26	61	41 32.3	71 23.8
73	8.8	2.2	9.1	2.4	25	65	41 32.0	71 23.8
74	7.3	2.1	7.4	2.2	29	66	41 31.2	71 24.1
75	10.2	3.7	10.4	3.0	27	50	41 30.8	71 24.2
76	13.7	2.9	13.9	2.9	26	26	41 30.4	71 24.4
77	12.6	2.7	10.5	2.3	26	43	41 29.8	71 24.6
78	10.7	1.8	10.8	1.9	24	33	41 29.3	71 24.6
79	10.3	2.6	10.3	2.4	25	38	41 28.7	71 24.7
80	8.2	2.6	8.1	2.6	25	40	41 28.2	71 24.7
81	8.2	2.4	8.5	2.2	25	48	41 27.6	71 24.7

TABLE I

MEASUREMENTS OF ACOUSTIC BOTTOM LOSS AT NORMAL INCIDENCE

TAG	PEAK PRESS. MED.	DEV.	TOTAL ENG. MED.	DEV.	AMT.	DEPTH	LATITUDE DG.	MN.	LONGITUDE DG.	MN.
82	12.1	3.0	10.3	2.3	23	63	41	26.5	71	24.7
83	11.3	2.2	9.8	1.6	25	82	41	25.4	71	24.7
84	13.4	2.5	10.9	2.2	24	94	41	24.6	71	24.7
85	12.3	2.1	10.0	1.8	24	100	41	23.5	71	24.7
86	10.4	2.1	9.3	1.9	24	102	41	22.5	71	24.7
87	9.9	2.4	8.5	1.7	24	103	41	21.5	71	24.7
88	10.7	2.5	9.9	1.9	24	102	41	20.4	71	24.5
89	13.2	2.6	11.1	2.1	23	104	41	19.2	71	24.3
90	12.2	3.1	10.4	2.2	24	107	41	18.1	71	24.1
91	12.9	2.5	10.9	2.0	37	109	41	17.0	71	24.1
92	10.9	2.2	9.7	1.5	24	120	41	16.1	71	24.1
93	11.0	2.5	10.4	2.5	24	113	41	15.1	71	24.2
94	10.7	2.8	9.5	2.5	26	112	41	14.1	71	24.2
95	9.5	2.0	9.4	1.8	23	116	41	13.1	71	24.3
96	12.1	2.3	9.8	2.3	21	111	41	12.1	71	24.3
97	9.7	2.6	8.6	2.5	28	116	41	11.0	71	24.4
98	8.7	2.4	7.3	2.3	19	100	41	10.1	71	24.6
99	8.2	2.6	6.3	2.4	22	115	41	9.3	71	24.7
100	11.1	3.2	9.7	1.7	7	120	41	6.2	71	24.5
101	8.2	2.1	6.9	1.8	14	127	41	4.2	71	24.6
102	8.2	2.2	7.7	2.1	24	139	41	3.2	71	24.6
103	10.7	2.6	8.8	2.1	44	38	41	8.2	71	37.1
104	8.5	2.4	6.2	1.4	24	67	41	7.3	71	37.1
105	9.9	2.8	5.7	1.3	45	100	41	6.4	71	37.0
106	10.5	3.9	8.4	2.5	49	128	41	3.2	71	36.8

TABLE I

MEASUREMENTS OF ACOUSTIC BOTTOM LOSS AT NORMAL INCIDENCE

TAG	PEAK PRESS. MED.	DEV.	TOTAL ENG. MED.	DEV.	AMT.	DEPTH	LATITUDE DG.	MN.	LONGITUDE DG.	MN.
107	12.0	3.2	10.1	2.3	31	122	41	2.0	71	36.8
108	12.0	3.0	10.7	2.2	30	128	41	1.0	71	36.9
109	11.7	3.9	10.5	2.8	34	126	41	1.0	71	36.4
110	11.1	2.6	10.0	2.3	29	111	41	1.0	71	35.8
111	12.6	4.4	11.5	3.4	28	108	41	1.1	71	35.6
112	8.8	2.1	7.4	1.7	30	119	41	2.9	71	34.6
113	8.5	2.4	7.5	1.9	24	115	41	3.7	71	34.4
114	9.3	2.2	7.6	1.9	23	117	41	4.4	71	34.1
115	9.5	3.8	8.6	2.3	24	105	41	5.2	71	33.8
116	10.2	2.3	9.1	2.1	22	59	41	5.8	71	33.4
117	8.6	2.5	5.8	1.8	24	50	41	6.4	71	33.0
118	8.4	2.6	4.6	1.6	24	61	41	7.5	71	32.0
119	9.0	2.8	5.7	2.1	23	66	41	8.7	71	31.0
120	7.7	2.8	3.7	1.7	20	90	41	10.2	71	31.1
121	10.5	2.4	10.2	1.6	24	105	41	11.7	71	30.6
122	8.9	3.2	9.3	2.4	27	100	41	13.2	71	30.1
123	13.7	2.0	11.4	1.6	28	120	41	16.1	71	29.0
124	6.3	2.3	5.7	2.4	23	56	41	17.6	71	28.4
125	6.0	2.6	4.9	2.1	25	50	41	19.2	71	27.8
126	10.0	3.4	7.0	2.0	24	63	41	20.6	71	27.3
127	5.3	1.9	4.1	1.9	24	56	41	22.0	71	26.8
128	12.7	2.3	9.7	1.9	35	83	41	23.6	71	26.2
129	11.6	2.0	9.1	1.6	24	76	41	25.0	71	25.7
130	10.9	2.3	10.1	2.2	24	50	41	26.3	71	24.9
131	8.4	1.6	8.0	1.6	24	50	41	27.5	71	24.5

TABLE I

MEASUREMENTS OF ACOUSTIC BOTTOM LOSS AT NORMAL INCIDENCE

TAG	PEAK PRESS. MED.	DEV.	TOTAL ENG. MED.	DEV.	AMT.	DEPTH	LATITUDE DG. MN.	LONGITUDE DG. MN.
132	7.5	1.5	7.1	1.8	24	42	41 28.0	71 24.4
133	12.4	2.8	11.4	2.5	24	44	41 28.4	71 24.4
134	8.2	1.0	8.7	2.2	23	27	41 29.0	71 24.4
135	11.7	3.2	10.9	2.6	24	42	41 29.4	71 24.3
136	8.5	3.1	7.9	3.0	23	41	41 29.8	71 24.1
137	13.2	2.4	12.8	1.5	24	41	41 30.2	71 23.7
138	15.2	2.7	14.6	1.9	99	28	41 30.6	71 24.0
139	12.8	2.3	12.1	1.8	24	36	41 30.6	71 24.0
140	6.9	3.0	5.9	2.3	24	86	41 31.1	71 23.9
141	9.7	2.8	9.2	2.5	24	62	41 31.6	71 23.9
142	9.4	2.4	8.2	2.2	24	65	41 32.0	71 23.8
143	11.2	3.4	10.7	3.0	24	36	41 32.4	71 23.7
144	11.2	1.9	9.4	1.7	24	43	41 32.8	71 23.7
145	10.7	3.8	9.6	2.8	24	35	41 33.2	71 23.6
146	12.3	2.7	10.6	2.2	24	30	41 33.6	71 23.5
147	14.0	3.3	14.0	2.1	23	27	41 34.0	71 23.2
148	14.9	2.7	12.8	2.1	48	28	41 34.5	71 20.2
149	11.3	3.1	10.9	2.6	25	29	41 34.3	71 19.9
150	5.3	2.1	4.6	1.9	26	56	41 34.2	71 19.4
151	6.5	2.4	3.4	1.8	24	65	41 34.5	71 19.2
152	9.1	2.2	7.4	2.0	30	64	41 35.2	71 18.7
153	10.7	2.3	8.0	1.7	30	69	41 35.6	71 18.5
154	6.9	2.1	6.1	2.0	30	52	41 36.1	71 18.2
155	8.5	2.7	6.2	2.2	24	77	41 36.5	71 17.9
156	9.3	2.7	8.5	2.1	23	58	41 36.8	71 17.7

TABLE I

MEASUREMENTS OF ACOUSTIC BOTTOM LOSS AT NORMAL INCIDENCE

TAG	PEAK PRESS. MED.	DEV.	TOTAL ENG. MED.	DEV.	AMT.	DEPTH	LATITUDE DG. MN.	LONGITUDE DG. MN.
157	8.1	2.3	6.5	1.9	24	60	41 37.1	71 17.4
158	9.3	2.0	8.1	2.1	31	32	41 37.5	71 17.2
159	9.7	2.5	7.9	2.2	100	50	41 37.5	71 17.2
160	6.7	1.5	5.5	1.5	22	65	41 37.3	71 17.7
161	10.1	2.7	7.8	1.9	16	80	41 35.8	71 18.2
162	8.8	2.8	6.8	2.0	26	93	41 35.1	71 18.5
163	8.4	2.7	6.0	2.0	22	78	41 34.8	71 18.6
164	8.1	1.8	5.9	1.5	26	98	41 34.2	71 18.9
165	12.1	2.1	8.6	1.2	21	79	41 33.5	71 19.3
166	13.8	2.8	12.1	2.2	10	68	41 33.0	71 19.5
167	12.1	2.2	9.8	1.8	8	71	41 32.4	71 19.8
168	9.5	2.3	8.5	1.5	18	100	41 31.4	71 20.1
169	10.7	2.7	10.7	2.9	23	35	41 30.6	71 20.0
170	8.8	2.2	6.4	2.2	23	47	41 30.1	71 19.8
171	6.9	2.5	6.2	2.8	36	34	41 29.1	71 20.3
172	9.9	2.8	7.8	2.3	28	151	41 28.8	71 20.8
173	9.1	2.5	8.2	1.9	26	128	41 28.5	71 21.1
174	11.1	2.8	8.9	2.0	32	127	41 28.1	71 21.8
175	7.0	3.2	5.9	2.6	27	136	41 27.6	71 22.2
176	8.1	2.7	7.7	2.6	35	85	41 27.1	71 22.3
177	9.6	2.8	8.7	2.0	24	80	41 26.1	71 22.6
178	12.9	2.9	11.2	2.7	31	83	41 25.6	71 22.7
179	12.1	3.3	10.3	2.8	34	82	41 25.5	71 22.2
180	11.2	3.3	10.6	3.4	25	73	41 25.4	71 21.6
181	8.3	2.3	6.7	2.0	27	64	41 25.2	71 21.4

TABLE I

MEASUREMENTS OF ACOUSTIC BOTTOM LOSS AT NORMAL INCIDENCE

TAG	PEAK PRESS. MED.	DEV.	TOTAL ENG. MED.	DEV.	AMT.	DEPTH	LATITUDE DG. MN.	LONGITUDE DG. MN.
182	8.1	2.7	6.2	2.4	99	65	41 25.2	71 21.4
183	9.0	3.1	6.4	2.2	49	80	41 25.2	71 21.4
184	8.0	2.9	6.1	2.4	42	84	41 25.1	71 21.5
185	9.7	3.1	7.5	2.4	27	81	41 25.1	71 21.1
186	11.4	3.1	9.2	1.8	26	87	41 25.0	71 20.6
187	13.3	2.9	9.3	1.8	66	97	41 25.0	71 19.5
188	12.5	3.0	9.2	1.7	22	93	41 24.9	71 19.1
189	12.6	2.9	11.1	2.2	31	92	41 24.9	71 19.1
190	11.1	3.2	10.2	2.2	14	90	41 24.9	71 18.8
191	16.0	1.1	11.1	2.8	5	87	41 25.0	71 18.0
192	10.6	2.6	11.1	4.0	8	82	41 25.0	71 17.3
193	8.9	2.6	8.2	2.4	20	80	41 25.1	71 16.9
194	10.9	2.5	8.6	2.1	21	80	41 25.1	71 16.6
195	9.4	2.2	8.9	2.3	26	78	41 25.1	71 16.2
196	8.8	2.2	8.5	2.2	25	76	41 25.1	71 15.8
197	11.8	2.4	11.1	2.4	22	74	41 25.2	71 15.1
200	8.8	2.7	6.4	2.2	107	68	41 25.3	71 13.8
199	9.5	2.5	8.3	2.2	34	68	41 25.3	71 13.9
198	9.6	2.3	7.0	1.9	24	72	41 25.4	71 14.2
201	8.9	2.1	6.8	1.9	99	70	41 25.3	71 13.8
202	6.7	2.6	3.2	2.0	24	71	41 25.5	71 13.8
203	9.5	2.7	7.3	2.3	24	71	41 25.8	71 13.8
204	9.9	3.1	7.9	2.7	24	68	41 26.0	71 13.9
205	10.5	2.9	8.5	2.3	23	65	41 26.3	71 13.9
206	9.8	2.7	8.4	2.8	24	63	41 26.7	71 13.8

TABLE I

MEASUREMENTS OF ACOUSTIC BOTTOM LOSS AT NORMAL INCIDENCE

TAG	PEAK PRESS. MED.	DEV.	TOTAL ENG. MED.	DEV.	AMT.	DEPTH	LATITUDE DG. MN.	LONGITUDE DG. MN.
207	7.9	3.4	4.8	3.0	25	57	41 27.1	71 13.7
208	8.0	2.9	4.8	2.6	24	56	41 27.6	71 13.7
209	7.0	2.2	4.8	2.4	24	54	41 28.0	71 13.6
210	6.6	2.6	4.6	2.6	24	50	41 28.4	71 13.5
211	8.2	2.8	5.9	2.6	24	44	41 28.9	71 13.4
212	8.8	2.4	6.0	2.3	24	38	41 29.2	71 13.3
213	10.4	2.1	8.1	2.1	98	33	41 29.7	71 13.2
214	8.6	1.5	5.6	2.0	24	32	41 29.8	71 13.2
215	9.3	1.1	7.3	1.3	24	26	41 30.4	71 13.2
216	11.0	2.4	10.7	2.7	98	25	41 31.8	71 12.9
217	8.1	2.3	5.3	2.1	24	39	41 29.0	71 12.6
218	5.8	2.7	2.8	2.5	20	45	41 28.4	71 12.4
219	9.2	2.2	6.6	2.0	95	46	41 28.3	71 12.5
220	8.5	2.4	6.1	2.3	25	62	41 26.4	71 12.9
221	6.7	2.8	5.2	2.9	24	66	41 26.4	41 13.3
222	9.5	2.7	8.7	2.5	24	66	41 26.3	71 14.0
223	9.3	2.5	8.6	2.0	24	69	41 26.3	71 14.7
224	11.5	2.5	9.4	1.9	24	70	41 26.2	71 15.5
225	10.3	2.8	7.8	2.1	24	73	41 26.1	71 16.4
226	10.5	2.5	9.0	1.9	23	74	41 26.0	71 17.1
227	12.4	3.1	11.6	2.7	98	77	41 26.0	71 17.2
228	10.5	2.5	9.3	2.3	15	78	41 26.2	71 17.4
229	11.9	2.8	11.1	2.8	19	74	41 26.4	71 17.2
230	11.0	3.9	9.3	3.1	21	74	41 26.7	71 17.0
231	8.0	2.2	6.0	1.9	25	54	41 27.9	71 16.4

TABLE I

MEASUREMENTS OF ACOUSTIC BOTTOM LOSS AT NORMAL INCIDENCE

TAG	PEAK PRESS. MED.	DEV.	TOTAL ENG. MED.	DEV.	AMT.	DEPTH	LATITUDE DG. MN.	LONGITUDE DG. MN.
232	10.5	2.3	10.3	2.3	94	50	41 28.1	71 16.3
233	8.2	1.5	7.2	1.4	35	49	41 28.4	71 16.0
234	8.2	3.8	6.3	3.3	24	42	41 28.6	71 15.8
235	10.5	1.4	7.3	1.5	24	30	41 28.8	71 15.6
236	10.8	1.9	7.2	1.7	95	30	41 28.7	71 15.6
237	8.6	2.4	5.1	2.0	99	40	41 28.4	71 16.6
238	15.1	3.1	13.9	3.2	23	33	41 30.1	71 23.7
239	15.0	2.8	12.8	1.9	25	55	41 29.6	71 24.2
240	14.6	2.6	12.3	2.0	24	41	41 29.2	71 24.3
241	10.2	2.0	8.6	1.8	24	44	41 28.3	71 24.5
242	11.2	1.8	10.3	2.0	23	42	41 27.8	71 24.5
243	9.8	1.5	9.0	1.5	27	50	41 27.3	71 24.6
244	10.3	2.3	9.7	1.6	25	60	41 26.6	71 24.8
245	12.6	2.4	10.4	1.7	28	70	41 26.0	71 24.9
246	12.0	2.6	10.4	1.9	24	68	41 25.7	71 25.4
247	10.9	2.7	9.8	2.2	24	57	41 25.7	71 26.2
248	9.5	1.5	8.5	1.7	26	44	41 25.7	71 26.4
249	11.0	2.5	10.1	2.3	100	43	41 25.7	71 26.7
250	8.6	2.5	7.0	1.8	97	30	41 25.8	71 27.0
251	9.3	2.4	8.6	2.3	100	32	41 25.8	71 26.9
252	10.9	2.9	10.5	1.8	25	64	41 25.7	71 25.8
253	11.0	2.5	9.5	1.6	23	69	41 25.7	71 25.5
254	11.9	3.5	9.8	2.6	26	79	41 25.3	71 25.2
255	13.6	2.1	11.1	1.6	25	87	41 24.6	71 25.3
256	13.0	2.4	10.5	1.7	24	92	41 24.0	71 25.3

TABLE I

MEASUREMENTS OF ACOUSTIC BOTTOM LOSS AT NORMAL INCIDENCE

TAG	PEAK PRESS. MED.	DEV.	TOTAL ENG. MED.	DEV.	AMT.	DEPTH	LATITUDE DG. MN.	LONGITUDE DG. MN.
257	15.1	2.3	11.9	1.8	24	93	41 23.4	71 25.3
258	12.9	2.2	10.7	1.6	38	95	41 22.8	71 25.3
259	15.1	2.0	12.0	1.5	40	98	41 22.2	71 25.3
260	12.8	2.2	11.1	1.3	24	99	41 21.7	71 25.3
261	14.3	2.4	11.4	1.5	24	98	41 21.1	71 25.3
262	13.5	3.1	11.8	2.2	6	92	41 18.9	71 25.3
263	8.5	2.7	7.1	2.6	23	81	41 18.2	71 25.2
264	6.3	2.3	5.1	2.1	26	79	41 17.7	71 25.2
265	9.7	2.6	8.1	1.5	31	83	41 17.0	71 25.2
266	7.6	2.3	6.7	2.1	26	91	41 16.7	71 25.2
267	13.4	2.6	10.3	2.1	25	120	41 16.1	71 25.2
268	10.1	3.8	8.8	2.7	95	120	41 15.4	71 25.2
269	10.4	1.6	8.3	1.4	40	110	41 15.0	71 25.2
270	10.2	2.2	8.0	1.9	24	112	41 14.5	71 25.3
271	9.0	2.7	8.3	2.2	20	110	41 14.0	71 25.3
272	9.0	3.5	8.2	2.6	23	109	41 13.4	71 25.3
273	12.1	2.9	10.5	2.1	35	115	41 12.9	71 25.4
274	10.7	3.0	10.3	2.4	33	118	41 12.4	71 25.4
275	12.1	3.1	11.3	2.4	24	125	41 12.0	71 25.4
276	12.4	2.9	11.7	2.5	34	130	41 11.5	71 25.5
277	11.4	2.6	10.8	2.0	20	131	41 11.1	71 25.5
278	12.5	2.8	11.6	2.2	120	131	41 10.8	71 25.5
279	9.4	3.2	8.7	2.4	24	126	41 10.8	71 25.5
280	9.7	2.5	9.6	2.1	25	126	41 10.3	71 25.5
281	10.8	3.2	10.7	2.9	29	111	41 9.7	71 25.5

TABLE I

MEASUREMENTS OF ACOUSTIC BOTTOM LOSS AT NORMAL INCIDENCE

TAG	PEAK PRESS. MED.	DEV.	TOTAL ENG. MED.	DEV.	AMT.	DEPTH	LATITUDE DG.	MN.	LONGITUDE DG.	MN.
282	10.4	2.4	8.9	2.1	26	96	41	9.2	71	25.5
283	10.4	2.8	9.5	2.5	31	104	41	8.7	71	25.5
284	10.3	3.2	8.3	2.4	24	104	41	8.8	71	25.3
285	8.0	3.0	6.7	2.4	26	97	41	7.3	71	25.5
286	9.5	3.1	7.2	2.5	109	101	41	7.0	71	25.6
287	9.5	2.9	8.6	3.0	24	98	41	7.1	71	25.5
288	9.7	2.3	8.8	2.1	25	90	41	7.1	71	27.1
289	9.9	2.3	9.3	2.2	24	82	41	7.1	71	27.6
290	10.1	4.2	9.6	3.2	101	82	41	7.1	71	27.9
291	10.0	2.3	9.1	2.5	24	81	41	7.1	71	28.2
292	8.4	2.6	6.7	2.2	27	79	41	7.1	71	28.5
293	10.4	2.7	8.2	2.3	33	86	41	7.1	71	29.0
294	8.1	2.2	6.4	1.9	33	85	41	7.1	71	29.4
295	8.8	2.0	7.0	1.9	24	74	41	7.2	71	33.1
296	7.9	2.5	5.8	2.4	23	65	41	7.2	71	33.6
297	7.5	2.5	5.7	2.3	27	73	41	7.3	71	34.1
298	5.7	2.8	4.2	2.3	27	73	41	7.4	71	34.7
299	4.6	2.7	4.0	2.8	24	68	41	7.7	71	36.1
300	6.9	2.4	7.1	2.1	24	53	41	8.0	71	36.7
301	7.0	2.2	7.5	2.2	26	36	41	8.3	71	37.4
302	6.8	2.4	6.9	3.0	29	37	41	8.7	71	37.8
303	8.0	1.9	6.6	2.5	25	31	41	9.4	71	37.7
304	5.3	2.5	3.1	2.2	24	49	41	9.9	71	37.6
305	7.9	2.7	7.6	2.5	25	58	41	10.4	71	37.4
306	7.1	2.2	6.0	2.4	24	55	41	10.7	71	37.1

TABLE I

MEASUREMENTS OF ACOUSTIC BOTTOM LOSS AT NORMAL INCIDENCE

TAG	PEAK PRESS. MED.	DEV.	TOTAL ENG. MED.	DEV.	AMT.	DEPTH	LATITUDE DG.	MN.	LONGITUDE DG.	MN.
307	10.8	2.7	8.4	1.2	26	72	41	11.2	71	37.0
308	15.8	2.7	12.7	2.7	27	88	41	11.4	71	36.8
309	13.1	2.6	13.3	2.2	100	74	41	11.6	71	36.5
310	6.1	2.7	5.4	2.6	112	44	41	7.8	71	38.6
311	8.9	2.7	8.1	2.5	23	44	41	7.7	71	38.5
312	8.3	2.7	7.4	2.9	24	47	41	7.2	71	38.3
313	6.8	2.8	5.8	2.1	24	58	41	6.8	71	38.2
314	8.4	1.4	7.6	1.1	23	73	41	6.4	71	38.1
315	8.0	2.9	7.3	2.5	24	90	41	5.9	71	38.0
316	8.0	2.5	6.5	1.9	21	103	41	5.4	71	37.9
317	6.2	1.6	5.4	1.4	39	110	41	4.9	71	37.4
318	7.4	2.1	6.6	1.5	27	119	41	4.4	71	37.1
319	7.1	2.6	6.1	1.3	25	126	41	3.9	71	36.8
320	8.2	3.0	6.6	1.9	24	129	41	3.4	71	36.6
321	9.5	3.9	8.8	3.6	23	130	41	2.9	71	36.4
322	8.3	1.7	6.6	2.1	24	130	41	2.3	71	36.4
323	9.0	2.9	8.5	2.5	28	126	41	1.9	71	36.3
324	8.5	3.1	8.2	2.5	27	122	41	1.4	71	36.3
325	10.5	2.8	8.4	2.8	24	122	41	0.9	71	36.2
326	8.0	2.9	6.3	2.7	25	125	41	0.4	71	36.2
327	8.1	1.6	6.5	1.9	26	131	40	59.9	71	36.1
328	8.8	3.2	7.5	2.6	45	133	40	59.6	71	35.7
329	9.3	2.3	9.2	1.9	29	176	40	54.8	71	33.9
330	8.9	1.6	8.4	1.7	31	178	40	54.0	71	33.2
331	11.4	2.7	10.1	1.9	96	180	40	53.8	71	33.0

TABLE I

MEASUREMENTS OF ACOUSTIC BOTTOM LOSS AT NORMAL INCIDENCE

TAG	PEAK PRESS. MED.	DEV.	TOTAL ENG. MED.	DEV.	AMT.	DEPTH	LATITUDE DG. MN.	LONGITUDE DG. MN.
332	10.5	2.1	9.6	1.9	35	185	40 53.4	71 33.0
333	9.7	2.3	9.0	1.7	31	186	40 52.8	71 32.9
334	10.7	2.0	10.6	1.8	30	188	40 52.1	71 32.8
335	10.9	2.4	10.1	1.9	26	190	40 51.4	71 32.8
336	9.9	2.9	9.2	2.0	26	192	40 50.7	71 32.7
337	10.1	1.9	9.2	1.6	32	200	40 49.8	71 32.4
338	11.7	2.4	11.2	1.4	21	204	40 49.1	71 32.2
339	12.4	2.4	11.1	1.9	26	204	40 48.0	71 31.9
340	11.8	2.1	10.8	1.9	26	200	40 47.7	71 31.8
341	11.1	3.5	10.5	2.4	37	200	40 47.3	71 31.8
342	12.1	2.0	11.0	1.6	32	200	40 47.3	71 31.8
343	11.0	2.1	9.6	2.0	19	200	40 46.8	71 31.5
344	13.5	3.4	11.9	2.9	15	202	40 46.1	71 31.4
345	12.8	2.3	11.2	1.9	20	204	40 45.6	71 31.2
346	11.2	2.1	10.4	1.7	23	206	40 45.0	71 31.1
347	12.7	2.4	11.2	2.0	19	210	40 43.8	71 30.8
348	14.2	2.2	12.7	1.6	24	212	40 43.2	71 30.6
349	15.1	1.9	13.4	1.6	21	212	40 42.6	71 30.4
350	14.4	2.5	13.0	1.8	21	210	40 42.0	71 30.3
351	13.2	1.8	12.3	1.5	16	208	40 41.4	71 30.1
352	12.1	2.3	11.9	1.9	21	206	40 41.0	71 29.9
353	12.2	3.5	11.6	2.7	37	204	40 40.8	71 29.9
354	12.8	2.5	11.4	2.2	25	202	40 40.7	71 30.0
355	12.2	2.3	11.3	2.0	31	201	40 40.5	71 29.9
356	15.3	2.9	13.4	2.4	22	202	40 40.2	71 29.7

TABLE I

MEASUREMENTS OF ACOUSTIC BOTTOM LOSS AT NORMAL INCIDENCE

TAG	PEAK PRESS. MED.	DEV.	TOTAL ENG. MED.	DEV.	AMT.	DEPTH	LATITUDE DG. MN.	LONGITUDE DG. MN.
357	13.7	1.9	12.3	1.9	29	203	40 39.9	71 29.6
358	13.7	3.2	11.6	2.6	23	204	40 39.7	71 29.4
359	13.4	3.6	12.0	2.7	25	205	40 39.3	71 29.3
360	13.5	2.8	11.6	2.3	23	207	40 39.1	71 29.2
361	12.4	2.6	11.2	2.1	30	208	40 38.3	71 28.9
362	12.1	2.2	11.6	2.1	24	208	40 37.7	71 28.6
363	13.8	2.9	12.2	2.7	25	209	40 37.0	71 28.4
364	10.0	2.5	9.4	2.3	25	210	40 36.4	71 28.1
365	14.0	2.7	12.1	2.1	25	211	40 35.7	71 27.8
366	14.0	2.4	12.4	2.2	33	212	40 35.1	71 27.5
367	14.9	3.2	13.2	2.1	52	215	40 34.4	71 27.3
368	14.2	2.8	12.2	1.9	58	215	40 34.3	71 27.3
369	15.2	1.9	12.6	1.7	25	217	40 34.2	71 27.2
370	16.2	2.9	13.7	2.0	27	220	40 33.7	71 27.2
371	14.1	2.3	12.4	1.6	39	220	40 33.3	71 27.2
372	14.0	1.8	11.8	1.5	28	220	40 32.8	71 27.0
373	13.3	2.3	11.7	1.9	26	221	40 32.4	71 27.0
374	13.7	2.5	12.5	2.0	25	220	40 32.0	71 26.9
375	14.1	3.1	13.3	2.6	24	221	40 31.7	71 26.9
376	14.2	3.1	12.0	2.5	25	222	40 31.2	71 26.8
377	15.0	2.6	13.0	1.9	25	224	40 30.9	71 26.7
378	13.7	3.2	12.3	2.5	25	225	40 30.5	71 26.7
379	15.8	2.8	13.5	2.0	25	227	40 30.1	71 26.6
380	14.6	2.4	13.3	1.7	25	229	40 29.6	71 26.6
381	15.5	4.5	13.2	2.2	96	230	40 29.4	71 26.5

TABLE I

MEASUREMENTS OF ACOUSTIC BOTTOM LOSS AT NORMAL INCIDENCE

TAG	PEAK PRESS. MED.	DEV.	TOTAL ENG. MED.	DEV.	AMT.	DEPTH	LATITUDE DG. MN.	LONGITUDE DG. MN.
382	15.3	2.5	12.6	2.0	38	230	40 28.9	71 26.4
383	16.1	2.2	14.1	1.4	28	230	40 28.5	71 26.2
384	15.7	2.4	13.7	1.9	28	231	40 28.0	71 26.1
385	15.0	2.2	13.3	1.6	29	232	40 27.5	71 25.9
386	14.1	3.5	13.1	2.6	37	234	40 26.9	71 25.7
387	12.9	2.6	12.2	2.2	23	235	40 26.6	71 25.6
388	14.1	2.7	12.3	2.1	40	238	40 26.1	71 25.4
389	15.7	2.4	14.4	1.5	21	240	40 25.6	71 25.3
390	16.5	3.3	14.5	2.4	27	242	40 25.3	71 25.2
391	14.7	2.7	13.4	1.9	20	245	40 24.9	71 25.0
392	15.8	2.0	13.5	1.3	29	248	40 24.2	71 24.9
393	15.9	1.9	13.2	1.5	23	250	40 23.8	71 24.8
394	14.2	3.2	12.4	2.1	50	250	40 23.5	71 24.6
395	15.8	3.2	12.9	1.8	55	250	40 23.5	71 24.5
396	17.3	1.7	14.3	1.5	25	250	40 22.9	71 24.3
397	17.6	2.3	14.7	1.4	25	252	40 22.2	71 24.0
398	17.3	2.2	14.6	1.5	25	254	40 21.7	71 23.8
399	16.2	1.8	13.0	1.2	25	256	40 21.1	71 23.5
400	16.2	2.3	14.1	1.9	25	260	40 20.5	71 23.3
401	16.0	2.0	13.3	1.4	25	260	40 20.0	71 23.1
402	16.5	2.0	13.3	1.7	25	260	40 19.5	71 23.1
403	12.7	3.0	11.8	2.4	25	258	40 19.2	71 23.0
404	13.6	2.2	12.6	1.8	25	260	40 18.8	71 23.0
405	14.2	2.3	12.1	1.8	25	263	40 18.5	71 23.0
406	14.3	2.3	12.4	1.7	25	267	40 18.0	71 22.9

TABLE I

MEASUREMENTS OF ACOUSTIC BOTTOM LOSS AT NORMAL INCIDENCE

TAG	PEAK PRESS. MED.	DEV.	TOTAL ENG. MED.	DEV.	AMT.	DEPTH	LATITUDE DG. MN.	LONGITUDE DG. MN.
407	15.2	2.1	13.6	1.4	25	270	40 17.7	71 22.9
408	16.3	3.1	12.8	1.6	80	272	40 16.8	71 22.8
409	15.8	1.9	13.2	1.3	25	273	40 16.5	71 22.7
410	16.3	2.4	13.4	1.5	25	273	40 16.0	71 22.7
411	16.2	2.5	13.6	1.6	25	274	40 15.6	71 22.6
412	16.8	2.1	14.3	1.2	25	276	40 15.2	71 22.5
413	14.4	2.7	13.0	1.8	25	278	40 14.8	71 22.4
414	12.5	2.6	11.1	2.1	25	280	40 14.4	71 22.3
415	15.0	2.8	13.4	1.7	25	282	40 14.0	71 22.2
416	14.2	2.3	11.9	1.8	25	284	40 13.6	71 22.1
417	13.8	2.8	11.4	2.2	25	283	40 13.2	71 22.0
418	10.6	2.9	9.5	2.2	35	283	40 12.8	71 22.0
419	14.5	3.0	12.9	2.5	22	282	40 12.4	71 21.9
420	13.5	3.3	12.0	2.4	23	288	40 12.0	71 21.8
421	11.2	3.6	10.1	2.8	26	287	40 11.6	71 21.7
422	13.4	4.5	11.2	2.4	43	289	40 11.6	71 21.7
423	17.7	2.4	12.6	0.9	32	285	40 23.8	70 44.5
424	17.6	2.5	13.8	2.1	44	285	40 23.8	70 44.5
425	16.9	1.6	13.7	1.5	25	280	40 24.2	70 44.5
426	16.8	1.5	13.5	1.6	25	275	40 24.7	70 44.4
427	18.4	1.4	14.9	1.6	25	270	40 25.1	70 44.2
428	17.9	2.2	15.5	2.1	24	267	40 25.7	71 44.1
429	17.6	1.7	14.3	1.8	25	263	40 26.1	70 44.1
430	18.6	1.7	15.1	1.7	25	260	40 26.8	70 44.1
431	19.1	2.6	16.4	2.1	25	256	40 27.3	70 44.2

TABLE I

MEASUREMENTS OF ACOUSTIC BOTTOM LOSS AT NORMAL INCIDENCE

TAG	PEAK PRESS. MED.	DEV.	TOTAL ENG. MED.	DEV.	AMT.	DEPTH	LATITUDE DG. MN.	LONGITUDE DG. MN.
432	17.7	2.5	16.5	2.7	24	253	40 28.0	70 44.3
433	18.1	2.5	16.0	2.4	24	250	40 28.4	70 44.3
434	18.0	2.2	15.7	2.1	24	245	40 29.0	70 44.3
435	18.5	2.6	16.0	2.5	15	242	40 29.6	70 44.3
436	18.1	2.4	14.2	2.2	25	240	40 30.2	70 44.4
437	18.5	3.0	16.3	2.8	27	237	40 30.7	70 44.6
438	18.7	2.8	16.0	2.4	88	234	40 30.9	70 44.6
439	18.2	2.5	14.7	2.2	25	230	40 32.2	70 44.6
440	18.3	1.6	14.5	1.6	25	228	40 33.0	70 44.6
441	17.9	1.9	13.9	1.3	25	224	40 33.5	70 44.7
442	16.7	1.9	13.4	1.8	25	222	40 34.2	70 44.8
443	16.8	1.8	12.8	1.4	25	220	40 35.0	70 44.8
444	17.8	2.3	13.7	2.1	25	217	40 35.6	70 44.9
445	17.6	2.3	13.3	1.5	25	212	40 36.3	70 44.9
446	17.5	2.6	12.9	2.4	25	211	40 37.0	70 45.0
447	18.2	2.3	13.7	1.8	25	210	40 37.7	70 45.1
448	17.1	2.1	13.5	1.9	25	206	40 38.4	70 45.1
449	14.9	2.2	12.2	1.6	25	202	40 39.2	70 45.2
450	16.1	2.8	12.5	2.5	49	202	40 39.4	70 45.2
451	17.9	3.5	14.2	2.6	54	202	40 39.4	70 45.2
452	14.9	2.3	11.7	1.9	30	201	40 39.6	70 45.1
453	17.1	2.2	13.8	2.1	33	202	40 40.0	70 44.8
454	16.2	2.1	12.1	1.8	24	203	40 40.5	70 44.6
455	15.5	2.3	11.3	1.9	25	201	40 40.9	70 44.4
456	15.4	2.7	11.0	2.2	25	200	40 41.3	70 44.1

TABLE I

MEASUREMENTS OF ACOUSTIC BOTTOM LOSS AT NORMAL INCIDENCE

TAG	PEAK PRESS. MED.	DEV.	TOTAL ENG. MED.	DEV.	AMT.	DEPTH	LATITUDE DG. MN.	LONGITUDE DG. MN.
457	14.0	1.7	10.2	1.6	25	200	40 41.7	70 44.0
458	15.3	2.4	10.6	1.7	25	200	40 42.2	70 43.8
459	12.9	2.8	3.6	2.3	24	199	40 42.7	70 43.4
460	14.6	2.3	9.0	1.9	23	198	40 43.4	70 43.1
461	15.6	2.0	10.0	2.7	24	197	40 43.6	70 43.0
462	14.7	3.0	9.1	2.3	22	195	40 44.0	70 42.8
463	13.6	2.5	7.8	2.5	29	193	40 44.5	70 42.6
464	14.9	4.0	11.4	2.6	101	191	40 44.7	70 42.4
465	14.8	2.1	11.4	1.9	23	191	40 45.0	70 42.3
466	14.1	2.9	11.6	1.8	21	190	40 46.3	70 42.1
467	14.8	3.0	11.7	2.2	25	190	40 47.0	70 42.1
468	12.6	3.5	10.6	2.5	29	188	40 47.7	70 42.0
469	14.1	2.5	11.9	1.8	26	187	40 48.3	70 41.8
470	12.6	2.9	10.3	2.0	29	182	40 49.1	70 41.7
471	12.4	2.9	10.8	2.1	27	182	40 49.8	70 41.6
472	11.3	2.7	9.2	2.4	23	181	40 50.5	70 41.5
473	14.1	2.7	10.7	2.1	32	180	40 51.2	70 41.3
474	15.3	2.6	11.3	1.7	22	180	40 51.9	70 41.3
475	13.4	2.3	11.2	2.0	23	177	40 52.6	70 41.2
476	10.9	2.2	9.4	2.3	43	173	40 53.2	70 41.1
477	10.8	4.1	8.7	3.1	104	170	40 53.4	70 41.1
478	12.8	2.0	10.7	2.0	27	161	40 53.7	70 41.0
479	9.4	1.8	8.0	1.9	24	160	40 54.1	70 40.9
480	10.1	2.9	8.0	2.7	24	158	40 54.5	70 40.9
481	12.1	2.9	9.6	2.6	19	156	40 55.1	70 40.8

TABLE I

MEASUREMENTS OF ACOUSTIC BOTTOM LOSS AT NORMAL INCIDENCE

TAG	PEAK PRESS. MED.	DEV.	TOTAL ENG. MED.	DEV.	AMT.	DEPTH	LATITUDE DG.	MN.	LONGITUDE DG.	MN.
482	11.2	2.2	9.1	1.9	24	158	40	55.5	70	40.7
483	10.4	2.5	9.3	2.1	19	160	40	55.9	70	40.7
484	13.7	3.3	10.9	2.4	24	166	40	56.4	70	40.6
485	10.2	2.4	9.2	2.0	27	164	40	56.8	70	40.5
486	10.4	1.9	9.2	1.9	20	161	40	57.3	70	40.5
487	11.2	1.8	9.4	1.9	24	158	40	57.7	70	40.4
488	12.4	1.4	10.9	1.3	22	155	40	58.1	70	40.3
489	10.8	2.1	10.0	2.0	24	153	40	58.7	70	40.2
490	14.3	3.7	11.6	2.7	95	162	40	58.9	70	40.3
491	12.7	3.3	10.6	2.9	24	158	40	59.5	70	40.3
492	10.0	2.4	8.6	2.0	24	154	41	0.	70	40.3
493	11.2	2.9	9.5	2.3	24	151	41	0.5	70	40.3
494	10.4	2.7	9.3	2.4	24	145	41	1.0	70	40.3
495	10.2	2.7	8.5	2.6	24	146	41	1.4	70	40.3
496	11.3	1.9	10.6	1.7	24	145	41	1.9	70	40.3
497	11.0	2.8	9.7	2.8	24	146	41	2.3	70	40.4
498	11.5	2.5	9.7	2.0	24	144	41	2.8	70	40.4
499	10.2	2.3	8.9	2.4	24	142	41	3.3	70	40.4
500	10.4	2.2	8.9	2.1	23	141	41	3.7	70	40.4
501	9.7	3.0	7.5	2.8	24	140	41	4.3	70	40.4
502	12.7	6.3	10.8	3.5	91	139	41	4.6	70	40.5
503	9.8	3.0	9.7	2.9	26	140	41	4.9	70	40.5
504	11.4	2.4	11.3	2.1	17	139	41	5.2	70	40.5
505	10.1	2.7	9.1	2.7	24	139	41	5.4	70	40.7
506	10.4	3.4	9.5	3.2	25	139	41	5.6	70	40.7

TABLE I

MEASUREMENTS OF ACOUSTIC BOTTOM LOSS AT NORMAL INCIDENCE

TAG	PEAK PRESS. MED.	DEV.	TOTAL ENG. MED.	DEV.	AMT.	DEPTH	LATITUDE DG.	MN.	LONGITUDE DG.	MN.
507	10.7	3.0	9.4	3.1	24	138	41	5.9	70	40.7
508	11.2	3.5	11.1	3.2	24	137	41	6.2	70	40.7
509	9.5	3.3	9.1	3.1	26	136	41	6.5	70	40.7
510	8.5	3.8	8.0	3.4	25	136	41	6.8	70	40.7
511	12.0	3.4	11.4	3.0	25	138	41	7.0	70	40.7
512	9.8	1.7	9.3	1.9	25	134	41	7.3	70	40.8
513	10.7	1.7	9.6	2.1	22	132	41	7.5	70	40.8
514	10.3	3.9	9.2	3.4	18	128	41	7.8	70	40.8
515	12.8	4.2	11.5	3.8	66	122	41	8.0	70	40.8
516	11.0	3.0	10.9	3.0	8	117	41	8.4	70	40.9
517	9.3	2.8	9.8	2.6	9	114	41	8.9	70	40.9
518	10.2	3.1	10.4	2.9	11	112	41	9.5	70	40.9
519	9.5	3.0	8.3	2.6	22	107	41	9.9	70	41.0
520	11.6	1.8	9.8	2.0	22	101	41	10.5	70	41.1
521	10.7	2.9	9.7	2.6	20	100	41	11.0	70	41.1
522	10.9	2.2	9.3	1.8	23	92	41	11.5	70	41.2
523	8.9	2.5	8.1	2.6	25	87	41	12.1	70	41.3
524	10.5	2.2	9.8	2.1	24	87	41	12.6	70	41.2
525	10.1	3.2	9.0	3.1	27	86	41	13.1	70	41.3
526	11.4	4.2	9.7	3.0	31	87	41	13.6	70	41.4
527	11.3	3.1	9.9	2.7	27	86	41	14.1	70	41.4
528	10.0	2.7	9.6	2.6	27	84	41	14.7	70	41.5
529	12.1	4.6	10.6	3.6	100	82	41	14.9	70	41.5
530	10.5	2.4	9.3	2.4	27	83	41	15.1	70	41.4
531	9.9	3.0	8.6	2.9	27	82	41	15.5	70	41.2

TABLE I

MEASUREMENTS OF ACOUSTIC BOTTOM LOSS AT NORMAL INCIDENCE

TAG	PEAK PRESS. MED.	DEV.	TOTAL ENG. MED.	DEV.	AMT.	DEPTH	LATITUDE DG. MN.	LONGITUDE DG. MN.
532	9.3	3.1	8.3	2.8	24	80	41 16.0	70 41.1
533	9.8	3.1	8.4	2.9	33	77	41 16.4	70 40.8
534	9.9	3.5	8.1	3.1	36	72	41 16.9	70 40.8
535	8.4	3.1	6.5	3.0	24	69	41 17.4	70 40.5
536	7.2	3.1	5.6	3.2	28	66	41 17.9	70 40.4
537	9.7	2.4	8.1	2.3	28	59	41 18.4	70 40.2
538	11.0	3.0	9.2	2.8	24	49	41 18.9	70 40.0
539	11.1	2.3	11.3	2.4	27	37	41 19.3	70 39.8
	MEASUREMENTS OBTAINED ON R/V BEAR CRUISE 290							
1	10.6	2.0	9.4	2.2	46	62	41 16.5	70 39.4
2	9.5	2.2	9.0	2.1	49	72	41 13.4	70 39.6
3	10.6	2.9	10.7	3.2	49	90	41 10.2	70 39.5
4	10.4	3.1	10.2	3.1	49	114	41 7.5	70 39.0
5	10.6	3.1	10.7	2.8	50	122	41 4.0	70 39.0
6	10.1	3.1	10.2	2.9	49	132	41 0.	70 40.0
7	12.3	3.8	12.4	3.1	48	136	40 57.1	70 41.4
8	10.8	2.5	10.0	2.1	49	147	40 54.5	70 42.4
9	10.4	3.1	9.7	2.5	99	150	40 51.5	70 42.5
10	14.3	3.0	13.0	2.3	50	164	40 48.8	70 42.5
11	13.5	2.2	12.0	1.9	50	174	40 45.5	70 42.5
12	12.8	2.3	11.5	1.8	49	180	40 42.0	70 40.8
13	14.3	2.6	13.0	1.9	49	182	40 40.0	70 42.8
14	13.9	2.8	11.8	2.0	49	192	40 37.0	70 41.5
15	16.5	2.3	14.2	1.5	50	204	40 33.5	70 42.0

TABLE I

MEASUREMENTS OF ACOUSTIC BOTTOM LOSS AT NORMAL INCIDENCE

TAG	PEAK PRESS. MED.	DEV.	TOTAL ENG. MED.	DEV.	AMT.	DEPTH	LATITUDE DG. MN.	LONGITUDE DG. MN.
16	17.1	2.5	15.0	2.0	50	216	40 30.5	70 42.2
17	18.0	3.0	16.0	2.1	50	236	40 26.5	70 42.5
18	16.8	2.4	14.4	1.4	50	255	40 24.4	70 43.5
19	16.3	2.4	14.0	1.6	50	285	40 22.1	70 43.5
20	19.2	3.4	17.6	2.1	50	336	40 18.7	70 42.8
21	20.8	2.0	16.6	1.9	53	366	40 15.4	70 43.0

The median value, minimum value, and standard deviation of bottom loss on both a peak pressure and total energy basis, along with the depth, have been plotted versus distance in miles along the profiles depicted in Figure 21 of Chapter V. These acoustic measurement profiles are presented in Figures 23 to 28.

These profiles are shown here in order to present an overall picture of the range and variability of the acoustic measurements and to establish some of their general relationships; a discussion of their geological significance, which will shed additional light on them, is postponed until Chapter IX.

Certain features of the acoustic quantities are immediately apparent. The similarity of the bottom-loss values for both the BEAR 281 and BEAR 290 cruises over the Martha's Vineyard Profile and for the CHAIN 21 and CHAIN 27 cruises over the Bermuda Profile attest to the repeatability of this type of measurement. This result is particularly significant since it indicates that bottom loss at normal incidence can be used to sense some characteristic of the sea floor.

The general trend of both the median bottom-loss values measured on a peak-pressure basis and those measured on a total-energy basis are observed to be similar on all of the profiles. This outcome indicates that both types of measurement sense the

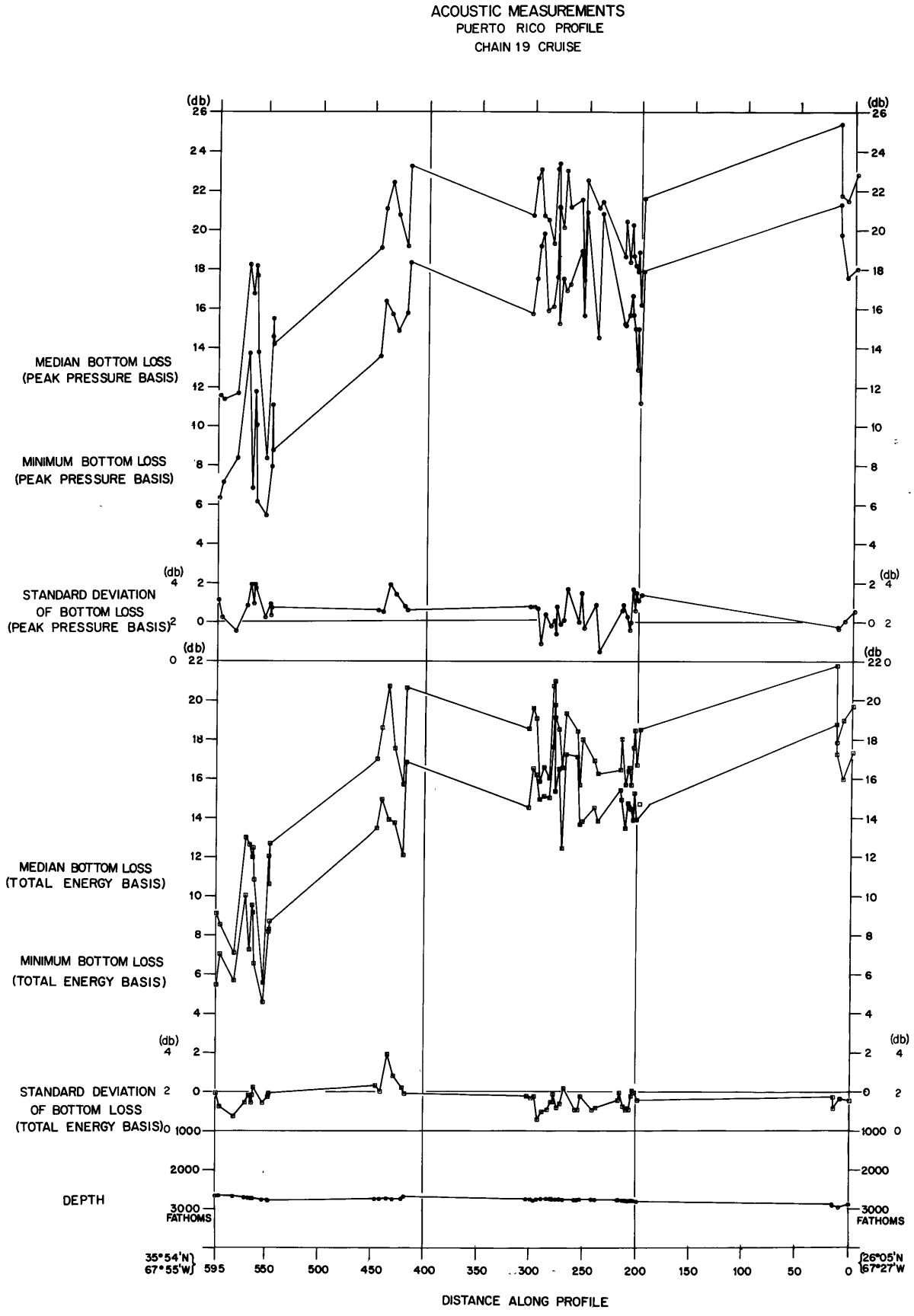

Figure 23. Bottom Loss Measurements Obtained on CHAIN 19 Cruise Along the Puerto Rico Profile.

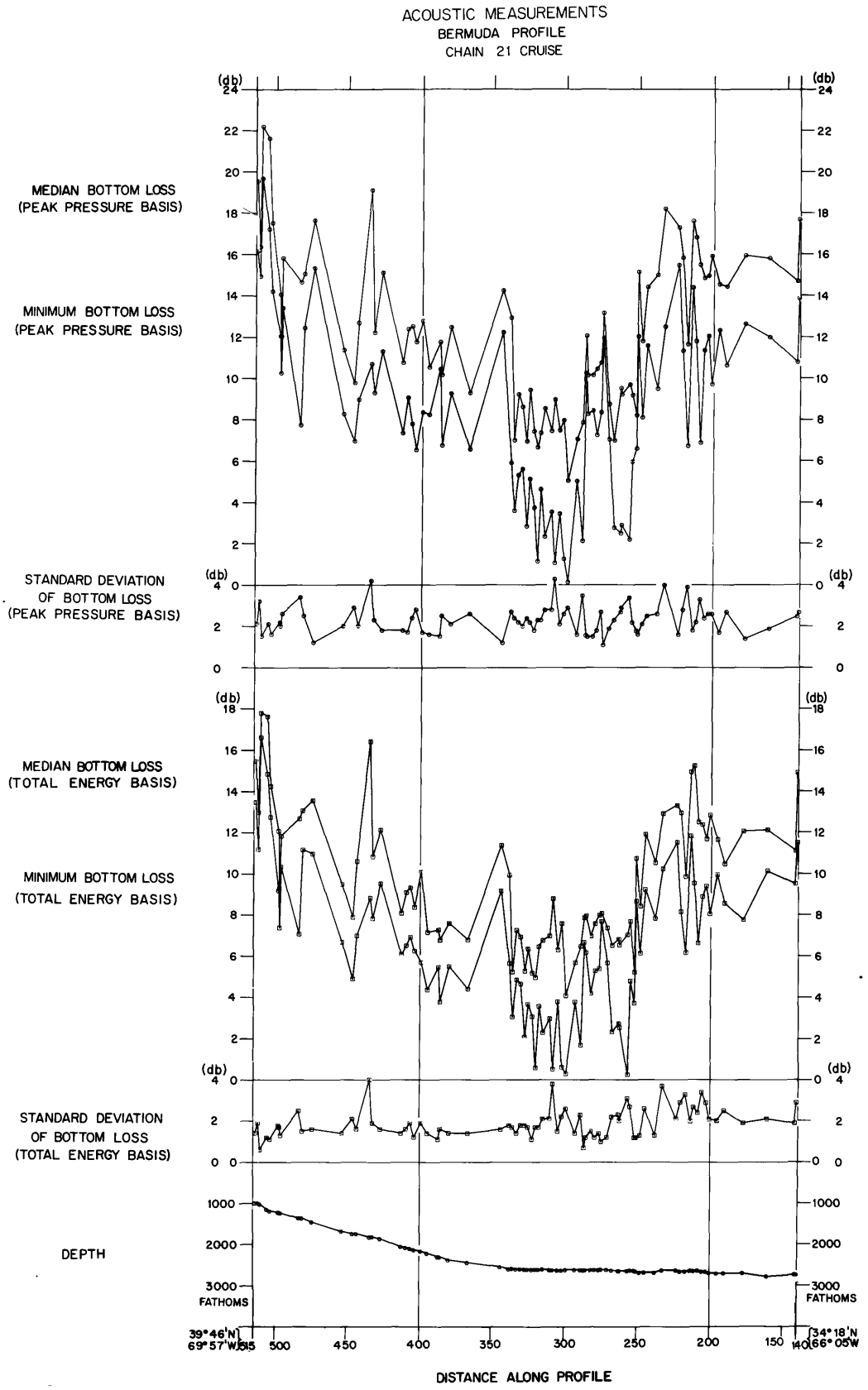

Figure 24. Bottom Loss Measurements Obtained on CHAIN 21 Cruise Plotted Versus Distance Along the Bermuda Profile.

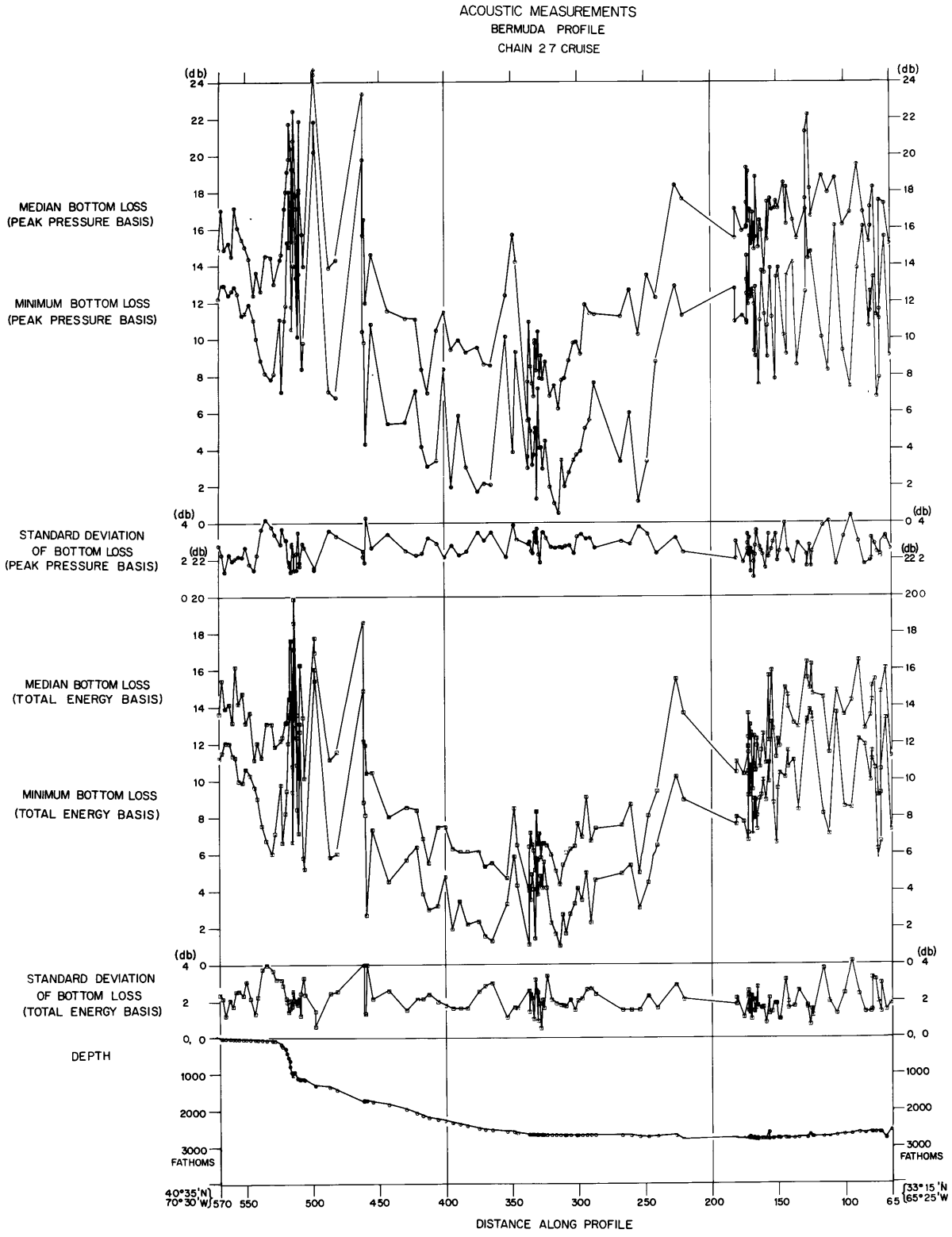

Figure 25. Bottom Loss Measurements Obtained on CHAIN 27 Cruise Plotted Versus Distance Along the Bermuda Profile.

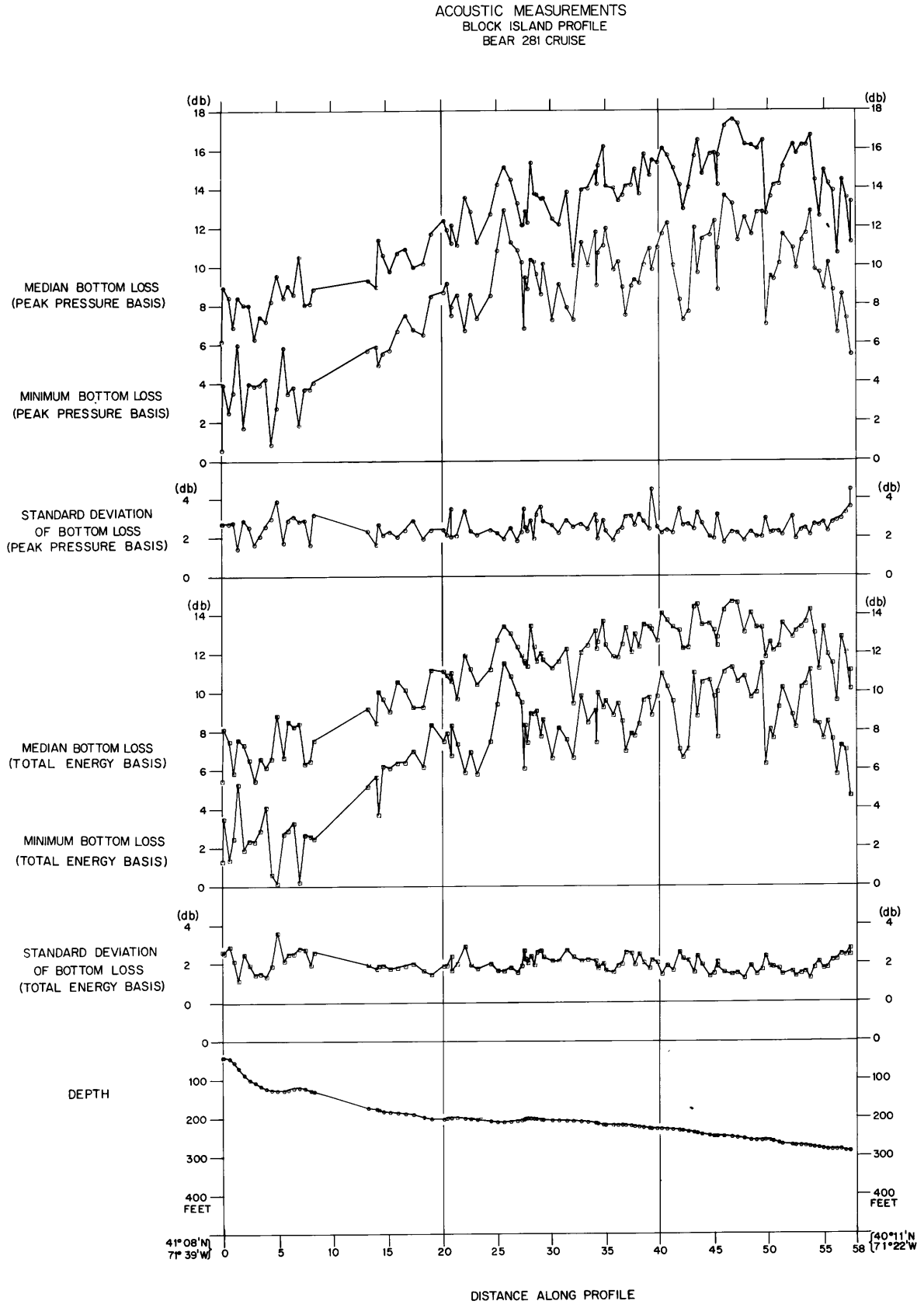

Figure 26. Bottom Loss Measurements Obtained on BEAR 281 Cruise Plotted Versus Distance Along the Block Island Profile.

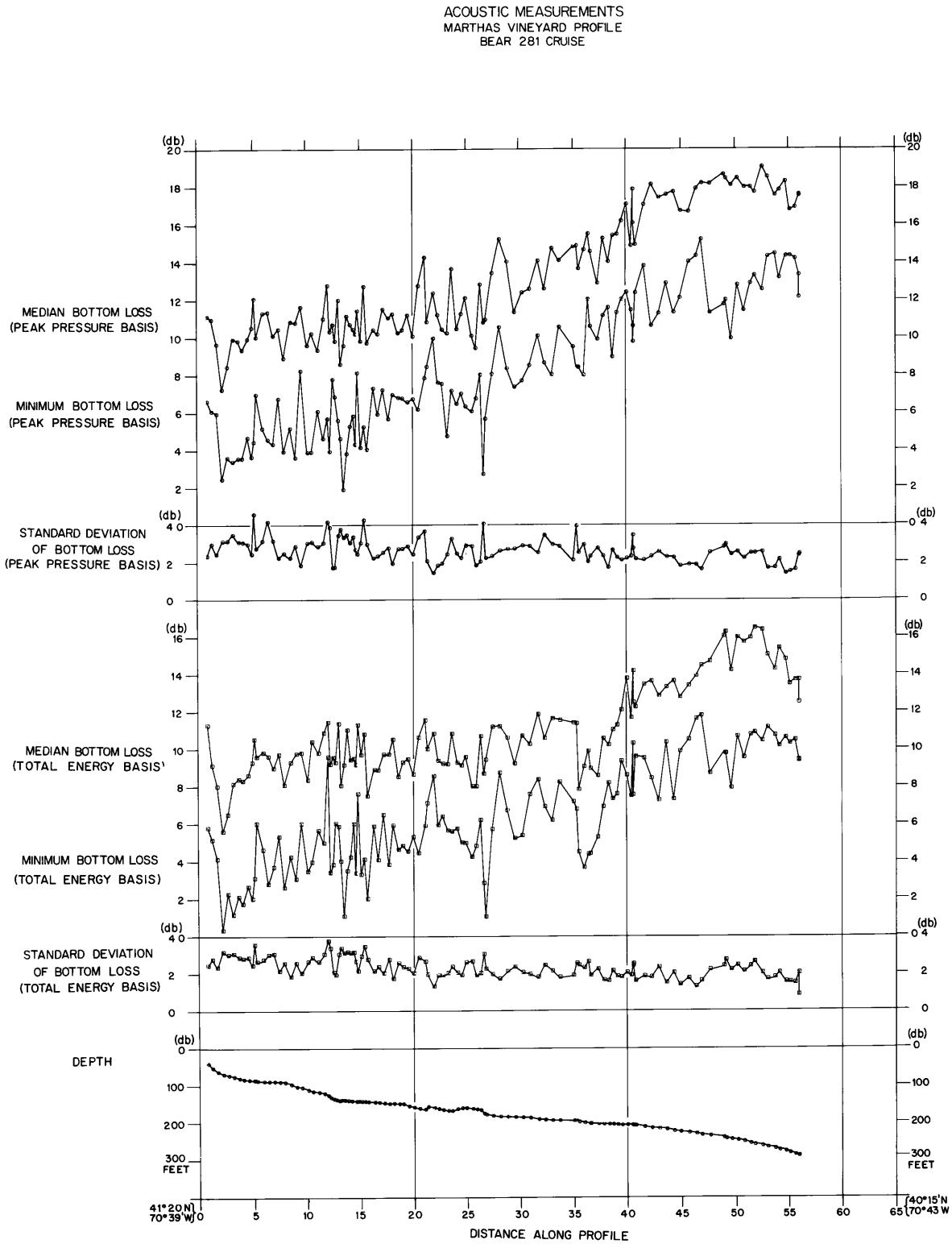

Figure 27. Bottom Loss Measurements Obtained on BEAR 281 Cruise Plotted Versus Distance Along the Martha's Vineyard Profile.

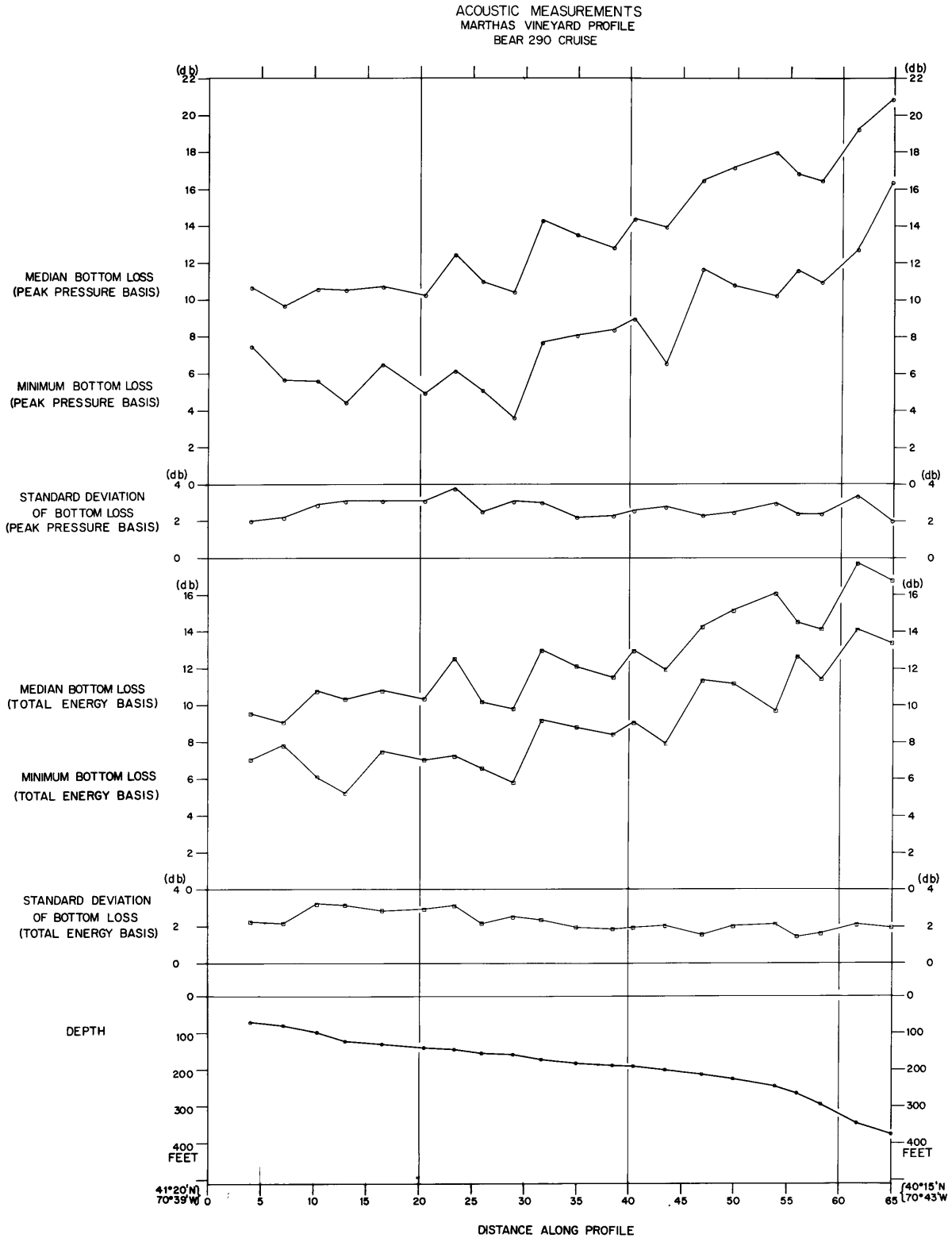

Figure 28. Bottom Loss Measurements Obtained on BEAR 290 Cruise Plotted Versus Distance Along the Martha's Vineyard Profile.

same characteristic of the sea floor. The median bottom-loss values measured on a total-energy basis do tend to be somewhat lower than those measured on a peak-pressure basis. This is ascribed to the reverberation component in the echo which is integrated along with the specular component when bottom loss is measured on a total-energy basis.

The standard deviations of the median bottom loss measured on a total-energy basis tend to be slightly smaller than those measured on a peak-pressure basis as expected. This means that fewer echoes need be sampled to obtain a given significance level for median bottom loss when measured on a total-energy basis as opposed to a peak-pressure basis.

The general trend of both the minimum bottom-loss values measured on a peak-pressure basis and those measured on a total-energy basis are observed to parallel their respective medians. Nevertheless, minimum values are not good sensors of a characteristic of the sea floor since their value has a dependence on the number of echoes measured. This is clearly shown by observing that the spread between the medians and minimums on both a peak-pressure and total-energy basis for the CHAIN 21 cruise is less than that for the CHAIN 27 cruise, which covered the same profile but sampled more echoes per measurement.

A table of all the echo-strength measurements that were used to obtain the bottom-loss measurements above is presented as Table VIII of Appendix C. An explanation of the column headings follows: TAG' represents the datum identification number; P1, P2, and P3 represent the median, standard deviation, and maximum values of echo strength respectively measured on a peak-to-peak pressure basis and expressed as db//1 dyne/cm^2; N represents the number of echoes that were sampled to produce the datum; E1, E2, and E3 represent the median, standard deviation, and maximum values of echo strength respectively, measured on a total-energy basis and expressed as db//1 erg/cm^2; DEPTH represents the transducer depth expressed in fathoms for measurements obtained on the CHAIN 19, CHAIN 21, and CHAIN 27 cruises and in feet for measurements obtained on the ASTERIAS, BEAR 281 and BEAR 290 cruises; and LAT. and LONG. are latitude and longitude with the first two digits of each representing degrees, the second two representing minutes and the last representing tenths of minutes.

A tabulation of echo-strength measurements received at the ship during the lowered-pinger experiments is presented in Table II. The column headings are self-explanatory, and the geographical location of the lowerings are given by the sites of sediment stations shown in Figures 56 and 57 of Chapter IX.

TABLE II

RELATIVE MEASUREMENTS OF ECHO STRENGTH RECEIVED FROM SUBMERSIBLE PINGER LOWERINGS

PINGER LOWERINGS	SEDIMENT STATION SITE	HEIGHT ABOVE BOTTOM (FEET)	SAMPLE SIZE	TOTAL PATH (FEET)	ECHO STRENGTH (db//1 erg/cm^2)
1	39	30	27	163	0.0
		50	24	183	-2.2
		70	14	203	-2.2
2	41	30	13	230	0.0
		60	8	260	-0.7
		90	13	290	-2.1
		120	23	320	-0.7
		150	15	350	-2.4
3	43	30	11	245	0.0
		60	15	275	0.0
		90	16	305	-1.7
		120	9	335	-1.9
		150	22	365	-1.6
4	45	30	18	280	0.0
		60	20	310	+0.1
		90	20	340	-2.2
		120	43	370	-0.9
		150	33	400	-0.6
		180	19	430	-4.0
5	47	30	39	320	0.0
		60	25	350	+1.5
		90	23	380	-1.5
		120	16	410	+0.7
		150	19	440	-1.8
6	74	30	20	315	0.0
		60	15	345	-1.3
		90	23	375	-1.3
		120	22	405	-2.7
		150	17	435	-1.3
		180	28	465	-4.6
7	67	30	23	232	0.0
		60	16	262	-2.7
		90	20	292	-0.3
		120	19	322	-1.1
		150	15	352	-3.7

TABLE II

RELATIVE MEASUREMENTS OF ECHO STRENGTH RECEIVED FROM SUBMERSIBLE PINGER LOWERINGS

PINGER LOWERINGS	SEDIMENT STATION SITE	HEIGHT ABOVE BOTTOM (FEET)	SAMPLE SIZE	TOTAL PATH (FEET)	ECHO STRENGTH (db//1 erg/cm^2)
8	60	30	28	200	0.0
		60	23	230	+0.3
		80	18	250	-0.7
		100	26	270	-0.5
		120	26	290	-1.9
9	54	30	9	169	0.0
		50	19	189	+1.1
		70	9	209	-2.5
		90	24	229	-0.5
10	49	30	23	114	0.0
		50	21	134	-1.5
		70	23	154	-1.8

The values of echo strength are relative to the value measured along the shortest total path (total path is equal to the depth of water plus the pinger height off the bottom) used in each individual lowering; absolute values are not useful since the battery charge and attendant source-level of the pinger varied from lowering to lowering.

These echo-strength measurements have been plotted versus total path in Figure 29 and a best-fitting line, determined by a least-squares analysis, has been drawn through the experimental points of each pinger lowering. The Y axis of this graph is quite expanded and the scatter of experimental points about the best-fitting line can be ascribed to experimental error. Also plotted are lines representing the theoretical relationship expected for scatterer and specular models of the reflection process and a line representing the average measured relationship for all the pinger lowerings. It seems that the experimental relationships of echo strength versus total path of the individual pinger lowerings are not significantly different from each other and that the specular reflection process is dominant.

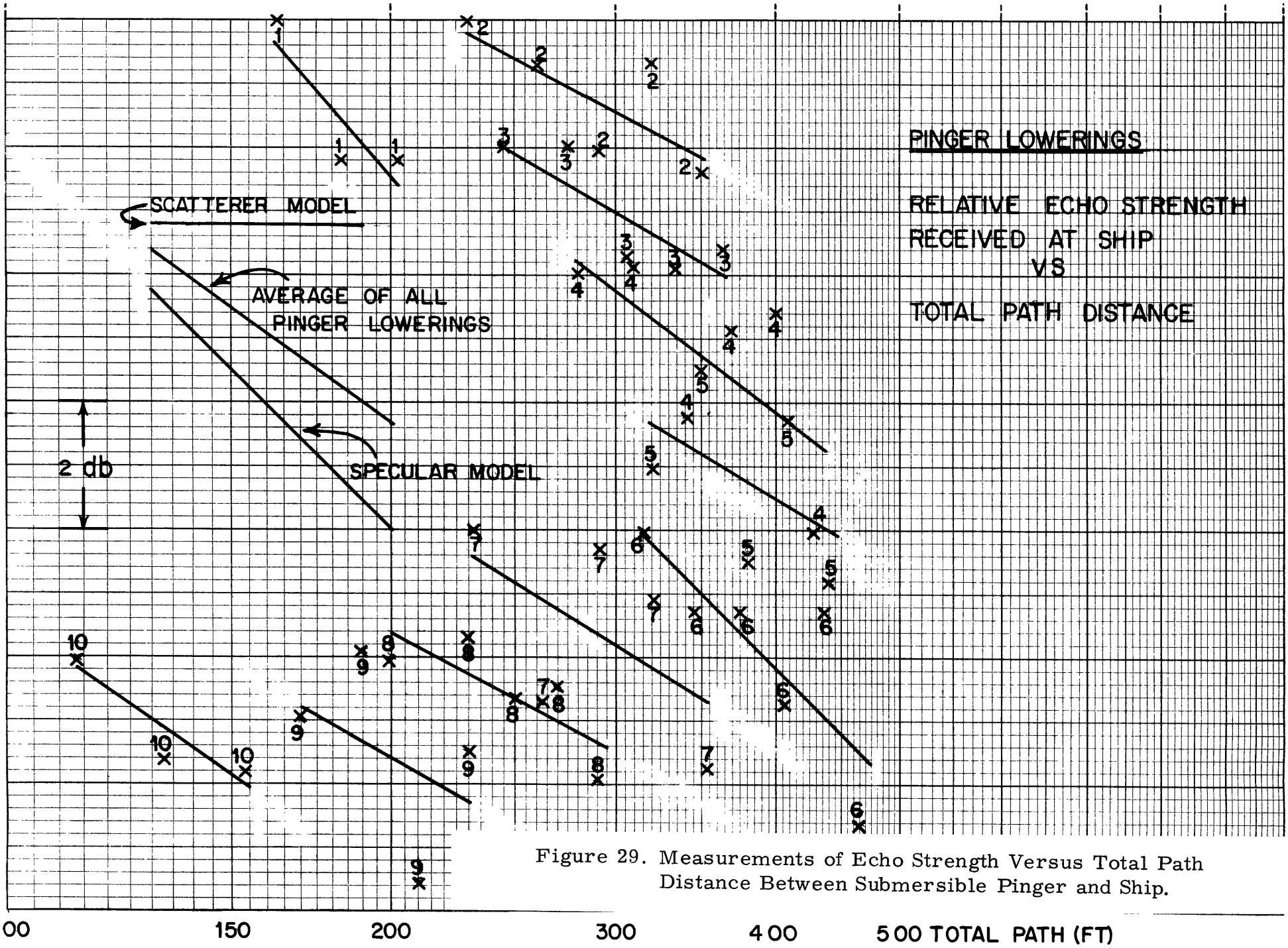

Figure 29. Measurements of Echo Strength Versus Total Path Distance Between Submersible Pinger and Ship.

CHAPTER VIII

GEOLOGIC RESULTS

The object of the geological phase of this investigation was to determine the character of the sea-floor where the acoustic measurements were made. The geologic measurements were used directly for correlation with the acoustic-reflectivity measurements and to spot-check the geologic results of other investigations which were correlated with the acoustic-reflectivity measurements. No attempt was made to study the regional geology since more extensive geological investigations have already been made in the areas involved. The correlation of acoustic and geologic results are discussed in Chapter IX; the geologic results are presented in this chapter.

A tabulation of the grain-size characteristics of all the sediment samples obtained during the course of this investigation is presented in Table III. An explanation of the column headings follows: TAG represents the identification number of the sediment station; CLASS represents the sedimentological name (Shepard, 1954); SIZE represents the phi median grain-size (Inman, 1952); SORT represents the Trask sorting-coefficient (Krumbein and Sloss, 1956); and FINE, GRAV., SAND, SILT, and CLAY, represent the percentages of material in the fine (silt + clay), gravel, sand, silt, and clay size-categories. The locations of the sites of all the sediment

TABLE III

GRAIN SIZE CHARACTERISTICS OF SEDIMENT SAMPLES

TAG	CLASS	SIZE	SORT.	FINE	GRAV.	SAND	SILT	CLAY
1	SANDY SILT	5.1	5.7	62.0	0.	38.0	46.0	16.0
2	SAN SIL CLY	5.6	4.5	69.0	0.	30.0	44.0	25.0
3	SAN SIL GRV	3.3	3.3	36.0	17.0	47.0	28.0	8.0
4	SAND	1.2	1.6	13.0	0.	87.0	13.0	0.
5	GRAV SAND	-0.3	3.8	3.0	42.0	55.0	3.0	0.
6	SANDY GRAV	-2.2	5.5	4.0	60.0	36.0	4.0	0.
7	SAND	3.3	1.2	10.0	0.	90.0	10.0	0.
8	SAND	2.8	1.3	12.0	0.	88.0	12.0	0.
9	SILTY SAND	3.4	3.6	43.0	0.	57.0	43.0	0.
10	SAND	3.2	1.4	20.0	0.	80.0	20.0	0.
11	SILTY SAND	3.3	1.7	30.0	0.	70.0	30.0	0.
12	SAND	2.4	1.6	17.0	0.	83.0	17.0	0.
13	SILTY SAND	2.3	2.5	35.0	0.	65.0	30.0	5.0
14	SAND	3.4	1.2	8.0	0.	92.0	8.0	0.
15	SAND	3.2	1.1	10.0	0.	90.0	10.0	0.
16	SILTY SAND	3.4	1.5	28.0	0.	72.0	24.0	4.0
17	SAND	3.2	1.2	10.0	0.	90.0	10.0	0.
18	SAND	2.8	1.2	1.0	0.	99.9	1.0	0.
19	SAND	1.8	1.6	5.0	0.	95.0	5.0	0.
20	SAND	3.3	1.1	4.0	0.	96.0	4.0	0.
21	SANDY SILT	6.0	2.8	79.0	0.	21.0	60.0	19.0
22	CLAYEY SILT	6.0	2.2	91.0	0.	9.0	73.0	18.0
23	SANDY SILT	5.5	2.8	76.0	0.	24.0	60.0	16.0
24	GRAV SAND	-0.5	2.3	0.	38.0	62.0	0.	0.
25	SAND	2.3	1.1	0.1	0.	99.9	0.1	0.
26	SAND	2.5	1.3	4.0	0.	96.0	4.0	0.

TABLE III

GRAIN SIZE CHARACTERISTICS OF SEDIMENT SAMPLES

TAG	CLASS	SIZE	SORT.	FINE	GRAV.	SAND	SILT	CLAY
27	SANDY SILT	5.2	3.1	71.0	0.	29.0	57.0	14.0
28	SAND	2.3	1.2	2.0	0.	98.0	2.0	0.
29	SAND	2.3	1.1	2.0	0.	98.0	2.0	0.
30	SAND	2.3	1.5	2.0	0.	98.0	2.0	0.
31	SAND	3.0	1.4	2.0	0.	98.0	2.0	0.
32	SAND	2.5	1.4	2.0	0.	98.0	2.0	0.
33	SAND	2.4	1.9	10.0	0.	90.0	10.0	0.
34	SILTY SAND	3.2	2.2	34.0	0.	66.0	26.0	8.0
35	GRAVEL	-3.4	2.8	0.	82.0	18.0	0.	0.
36	SAND	2.3	1.1	0.1	0.	99.9	0.1	0.
37	SAND	3.1	1.2	10.0	0.	90.0	7.0	3.0
38	SAND	0.1	1.3	0.	8.0	92.0	0.	0.
39	SAND	0.3	1.2	0.1	0.	99.9	0.1	0.
40	SAND	2.2	1.2	2.0	0.	98.0	2.0	0.
41	SAND	2.6	1.3	6.0	0.	94.0	6.0	0.
42	SAND	2.1	1.5	15.0	0.	85.0	15.0	0.
43	SAND	2.6	2.2	24.0	0.	76.0	17.0	7.0
44	SAND	2.2	1.5	12.0	0.	88.0	12.0	0.
45	SILTY SAND	2.1	2.6	26.0	0.	74.0	22.0	4.0
46	SILTY SAND	3.1	3.1	45.0	0.	55.0	37.0	8.0
47	SAND	1.2	1.1	2.0	0.	98.0	2.0	0.
48	SAND	2.2	1.2	4.0	0.	96.0	4.0	0.
49	SAND	0.9	1.7	0.	6.0	94.0	0.	0.
50	SAND	0.1	1.5	0.1	0.	99.9	0.1	0.
51	SAND	1.2	1.2	1.0	0.	99.0	1.0	0.
52	SAND	1.7	2.2	1.0	14.0	85.0	1.0	0.

TABLE III

GRAIN SIZE CHARACTERISTICS OF SEDIMENT SAMPLES

TAG	CLASS	SIZE	SORT.	FINE	GRAV.	SAND	SILT	CLAY
53	SAND	0.7	1.1	1.0	0.	99.0	1.0	0.
54	SAND	2.2	1.1	1.0	0.	99.0	1.0	0.
55	SAND	1.9	1.5	6.0	0.	94.0	6.0	0.
56	SAND	2.2	1.3	4.0	0.	96.0	4.0	0.
57	SAND	2.6	1.4	9.0	0.	91.0	9.0	0.
58	SAND	2.4	1.5	17.0	0.	83.0	17.0	0.
59	SAND	2.2	1.9	12.0	0.	88.0	12.0	0.
60	SAND	1.3	1.2	0.1	0.	99.9	0.1	0.
61	SAND	0.8	1.3	2.0	0.	98.0	2.0	0.
62	SILTY SAND	2.9	2.8	30.0	0.	70.0	22.0	8.0
63	SILTY SAND	3.8	2.7	46.0	0.	54.0	33.0	13.0
64	SAND	2.7	1.9	22.0	0.	78.0	18.0	4.0
65	SILTY SAND	4.0	3.4	52.0	0.	48.0	38.0	14.0
66	SILTY SAND	3.7	1.5	30.0	0.	70.0	26.0	4.0
67	SILTY SAND	3.3	2.3	36.0	0.	64.0	28.0	8.0
68	SANDY SILT	4.4	2.1	68.0	0.	32.0	54.0	14.0
69	SANDY SILT	4.8	2.4	77.0	0.	23.0	59.0	18.0
70	SANDY SILT	4.7	2.4	70.8	0.	30.0	58.8	12.0
71	SANDY SILT	4.8	2.6	78.0	0.	22.0	60.0	18.0
72	CLAYEY SILT	5.2	2.9	82.0	0.	18.0	59.0	23.0
73	CLAYEY SILT	5.0	2.4	83.0	0.	17.0	63.0	20.0
74	SANDY SILT	5.0	2.6	72.0	0.	28.0	58.0	14.0
75	SANDY SILT	4.6	2.4	70.0	0.	30.0	54.0	16.0
76	CLAYEY SILT	5.0	2.4	85.0	0.	15.0	65.0	20.0
77	CLAYEY SILT	5.1	2.5	83.0	0.	17.0	63.0	20.0

stations are shown in Figures 54, 55, 56, and 57 of Chapter IX. The numerals represent the identification numbers of the sediment stations and the arrows pin-point their geographical positions.

Grain-size characteristics obtained from the sediment samples, and those published by Stetson (1938) have been plotted versus distance in miles along both the Martha's Vineyard profile (Figure 30) and the Block Island Profile (Figure 31); the values obtained by this investigation are indicated by circles and Stetson's are indicated by squares. The median grain size expressed both in millimeters and phi units, Trask sorting coefficient, and percentages of material in the clay, silt, and sand + gravel categories, as well as the bathymetry, are presented. In addition, the class names of the sediments are indicated by symbols that are coded in accordance with the associated legend. The grain-size characteristics obtained in this investigation in general agree well with those published by Stetson as evidenced by the above-mentioned figures. The disagreement that does exist is probably in part caused by a positional error between the two investigations; modern navigational equipment was not available to Stetson.

The grain-size characteristics obtained from the sediment samples and those published by McMaster (1960) for Narragansett Bay are not amenable to a profiled display since there is no regular positional relationship between the sample sites of both investigations.

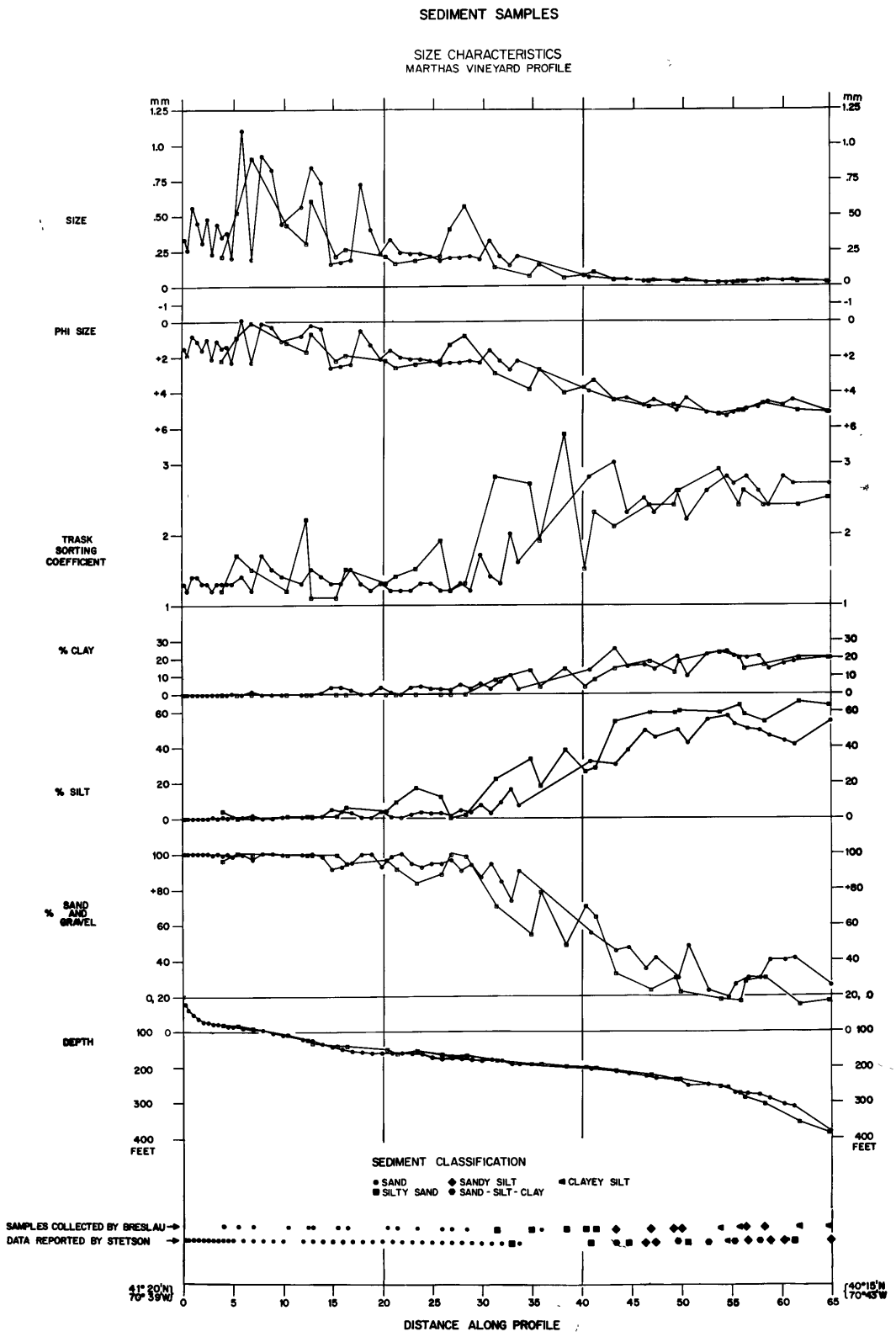

Figure 30. Size Characteristics of Sediment Samples Plotted Versus Distance Along the Martha's Vineyard Profile.

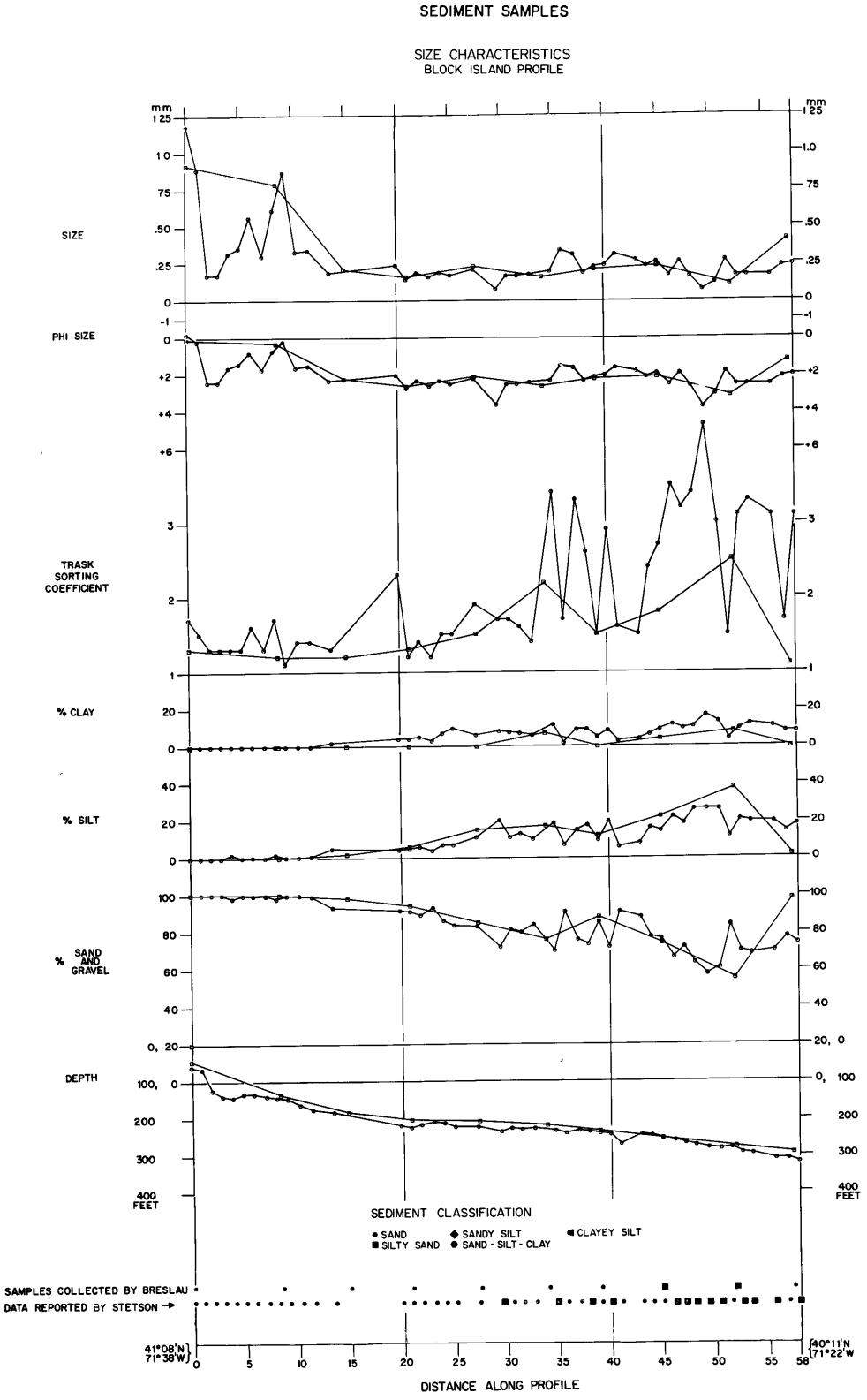

Figure 31. Size Characteristics of Sediment Samples Plotted Versus Distance Along the Block Island Profile.

They may be compared, however, by reference to the table of grain-size characteristics (Table III) and the charts of Narragansett Bay with their sedimentological overlays (Figures 54 and 55); the sedimentological overlays are taken from McMaster and indicate the class name and percentage of the sand fraction of the sediment flooring Narragansett Bay. The results of both investigations in general agree moderately well; about two-thirds of the class names of the samples of this investigation are located in regions of corresponding class name (gravel is taken as sand for classification on a three-component basis) as published by McMaster, whereas about one-third differ by one class unit and one-tenth are in complete disagreement. The disagreement between the results of both investigations is larger in Narragansett Bay than on the Continental Shelf. This is ascribed to a combination of two factors: the comparison made on sedimentological regions defined by interpolated boundaries and the extreme variability or patchiness of the sediment distribution in Narragansett Bay.

The cumulative size-distribution curves of all the sediment samples are presented in Appendix D. A tabulation of the grain-size measurements used to obtain the grain-size characteristics is presented in Table IX of Appendix C. An explanation of the column headings follows: TAG and DEPTH represent the identification number and water depth in feet of the sediment station; Q3, MEDIAN,

and Q1 respectively represent the seventy-five, fifty, and twenty-five per cent quartiles of the cumulative size-distribution curve, expressed in millimeters; and GRAV., SAND, SILT, and CLAY represent the percentages of material in the gravel, sand, silt, and clay-size categories.

A tabulation of the mass characteristics of all the sediment samples obtained during the course of this investigation is presented in Table IV. An explanation of the column headings follows: TAG represents the identification number of the sediment station; WATER represents the water content of the sediment (Taylor, 1948); and POROUS, DENSITY, VELCTY, IMPED, REF COEF, and BTMLOSS represent respectively the density, compressional velocity, acoustic impedance, Rayleigh reflection coefficient, and bottom loss calculated from the measured water content according to the relationships developed in Chapter II.

Mass characteristics obtained from the sediment samples have been plotted versus distance in miles along both the Martha's Vineyard Profile (Figure 32) and the Block Island Profile (Figure 33). The water content, porosity, impedance, reflection coefficient, bottom loss, velocity, and density, as well as the bathymetry, are presented. These quantities may be observed for the Narragansett Bay region by reference to the table of mass characteristics (Table

TABLE IV

MASS CHARACTERISTICS OF SEDIMENT SAMPLES

TAG	WATER	POROUS	DENSTY	VELCTY	IMPED	REF COEF	BTMLOSS
1	0.74	66.5	1.61	1.46	2.34	0.21	13.7
2	1.03	73.3	1.49	1.45	2.16	0.17	15.6
3	1.02	73.2	1.49	1.45	2.16	0.17	15.5
4	0.48	56.4	1.78	1.50	2.66	0.27	11.5
5	0.72	65.7	1.62	1.46	2.37	0.21	13.5
6	0.42	52.7	1.84	1.52	2.79	0.29	10.8
7	0.49	56.6	1.78	1.49	2.66	0.27	11.5
8	0.58	60.9	1.70	1.48	2.51	0.24	12.4
9	0.32	46.2	1.96	1.56	3.06	0.33	9.6
10	0.49	56.5	1.78	1.49	2.66	0.27	11.5
11	0.73	66.2	1.61	1.46	2.35	0.21	13.6
12	0.74	66.3	1.61	1.46	2.35	0.21	13.6
13	0.60	61.7	1.69	1.47	2.49	0.24	12.6
14	0.51	57.7	1.76	1.49	2.62	0.26	11.7
15	0.49	56.6	1.78	1.49	2.66	0.27	11.5
16	0.48	56.1	1.79	1.50	2.67	0.27	11.4
17	0.34	47.7	1.93	1.55	2.99	0.32	9.9
18	0.29	43.6	2.00	1.59	3.17	0.35	9.2
19	0.27	41.5	2.04	1.61	3.27	0.36	8.9
20	0.46	55.3	1.80	1.50	2.70	0.27	11.3
21	0.46	55.0	1.80	1.50	2.71	0.28	11.2
22	0.96	72.0	1.51	1.45	2.19	0.17	15.2
23	1.78	82.6	1.33	1.45	1.92	0.11	19.1
24	0.23	37.8	2.10	1.65	3.47	0.38	8.3
25	0.20	35.4	2.14	1.68	3.60	0.40	7.9
26	0.29	43.6	2.00	1.59	3.17	0.35	9.2

TABLE IV

MASS CHARACTERISTICS OF SEDIMENT SAMPLES

TAG	WATER	POROUS	DENSTY	VELCTY	IMPED	REF COEF	BTMLOSS
27	0.66	63.9	1.65	1.47	2.42	0.22	13.1
28	0.29	43.7	2.00	1.58	3.17	0.35	9.2
29	0.27	42.3	2.02	1.60	3.23	0.35	9.0
30	0.25	40.4	2.05	1.62	3.33	0.37	8.7
31	0.24	39.0	2.08	1.64	3.40	0.38	8.5
32	0.29	44.0	1.99	1.58	3.15	0.34	9.3
33	0.17	31.6	2.21	1.74	3.84	0.43	7.4
34	0.43	53.5	1.83	1.51	2.77	0.28	10.9
35	0.24	39.0	2.08	1.64	3.40	0.38	8.5
36	0.24	39.3	2.07	1.63	3.38	0.37	8.5
37	0.42	53.2	1.84	1.51	2.78	0.29	10.9
38	0.21	36.1	2.13	1.67	3.56	0.40	8.0
39	0.26	41.1	2.04	1.61	3.29	0.36	8.8
40	0.27	42.2	2.02	1.60	3.24	0.36	9.0
41	0.34	47.9	1.93	1.55	2.98	0.32	9.9
42	0.49	56.5	1.78	1.49	2.66	0.27	11.5
43	0.42	53.1	1.84	1.51	2.78	0.29	10.9
44	0.51	57.6	1.76	1.49	2.62	0.26	11.7
45	0.37	50.0	1.89	1.53	2.90	0.31	10.3
46	0.37	49.5	1.90	1.54	2.92	0.31	10.2
47	0.51	57.5	1.76	1.49	2.62	0.26	11.7
48	0.30	44.3	1.99	1.58	3.14	0.34	9.3
49	0.25	40.1	2.06	1.62	3.34	0.37	8.7
50	0.27	41.9	2.03	1.60	3.25	0.36	8.9
51	0.25	39.9	2.06	1.62	3.35	0.37	8.6
52	0.33	47.2	1.94	1.55	3.01	0.32	9.8

TABLE IV

MASS CHARACTERISTICS OF SEDIMENT SAMPLES

TAG	WATER	POROUS	DENSTY	VELCTY	IMPED	REF COEF	BTMLOSS
53	0.30	44.4	1.99	1.58	3.14	0.34	9.3
54	0.24	39.3	2.07	1.63	3.38	0.37	8.5
55	0.31	45.3	1.97	1.57	3.10	0.34	9.5
56	0.38	50.2	1.89	1.53	2.89	0.30	10.3
57	0.39	50.8	1.88	1.53	2.87	0.30	10.4
58	0.41	52.0	1.85	1.52	2.82	0.29	10.7
59	0.36	49.1	1.91	1.54	2.94	0.31	10.1
60	0.35	48.7	1.91	1.54	2.95	0.31	10.1
61	0.22	36.6	2.12	1.67	3.53	0.39	8.1
62	0.67	64.3	1.64	1.46	2.41	0.22	13.2
63	0.86	69.6	1.55	1.45	2.26	0.19	14.5
64	0.94	71.6	1.52	1.45	2.20	0.18	15.1
65	0.96	71.9	1.51	1.45	2.19	0.17	15.2
66	0.70	65.2	1.63	1.46	2.38	0.21	13.4
67	0.76	67.0	1.60	1.46	2.33	0.20	13.8
68	1.12	74.9	1.46	1.45	2.11	0.16	16.1
69	0.87	69.8	1.55	1.45	2.25	0.19	14.6
70	0.58	60.9	1.70	1.48	2.51	0.24	12.4
71	1.05	73.8	1.48	1.45	2.14	0.16	15.7
72	1.05	73.8	1.48	1.45	2.14	0.16	15.7
73	0.92	71.1	1.53	1.45	2.21	0.18	14.9
74	0.95	71.8	1.51	1.45	2.19	0.18	15.1
75	0.84	69.1	1.56	1.45	2.27	0.19	14.4
76	0.81	68.3	1.58	1.45	2.29	0.20	14.2
77	1.00	72.7	1.50	1.45	2.17	0.17	15.4

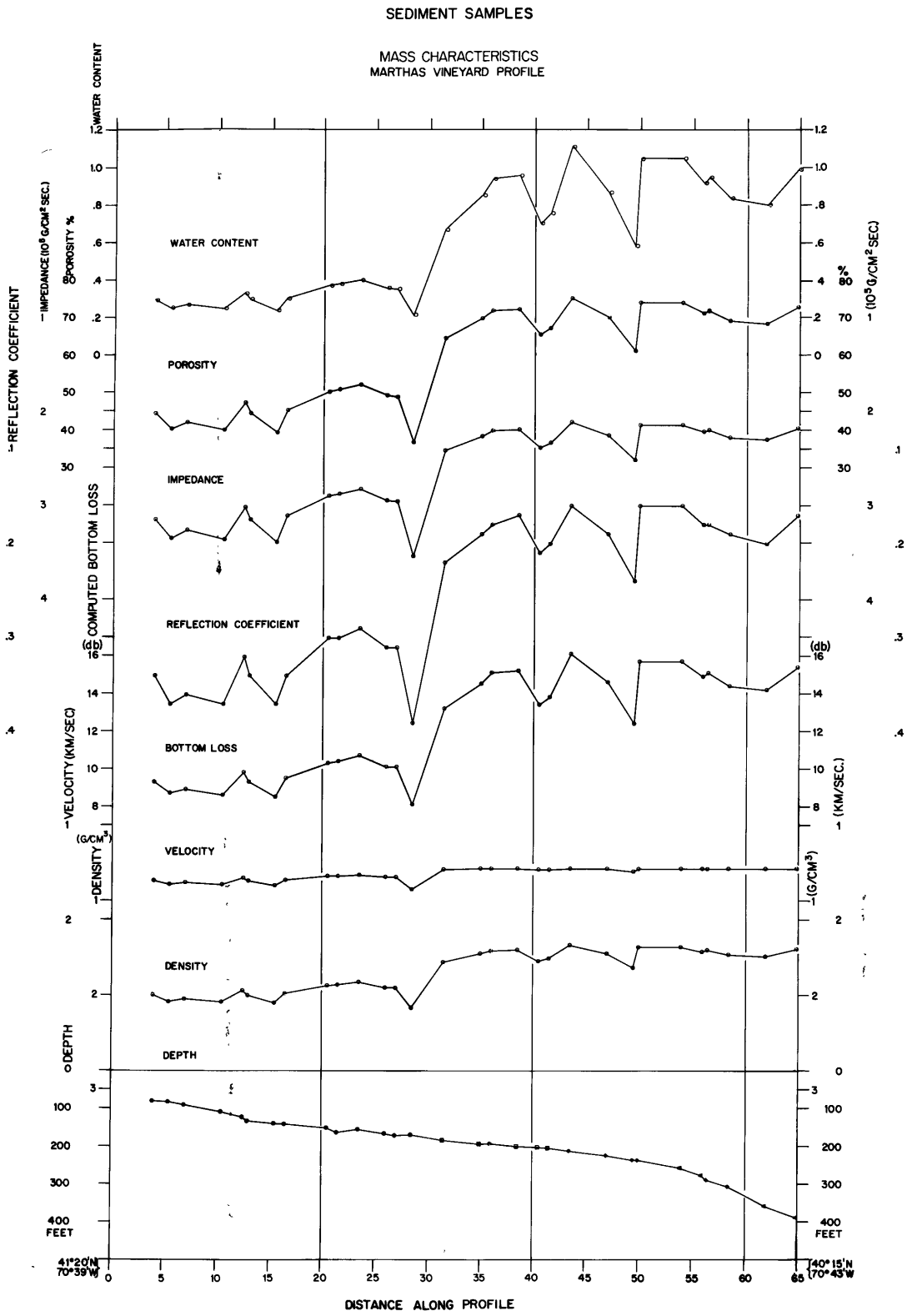

Figure 32. Mass Characteristics of Sediment Samples Plotted Versus Distance Along the Martha's Vineyard Profile.

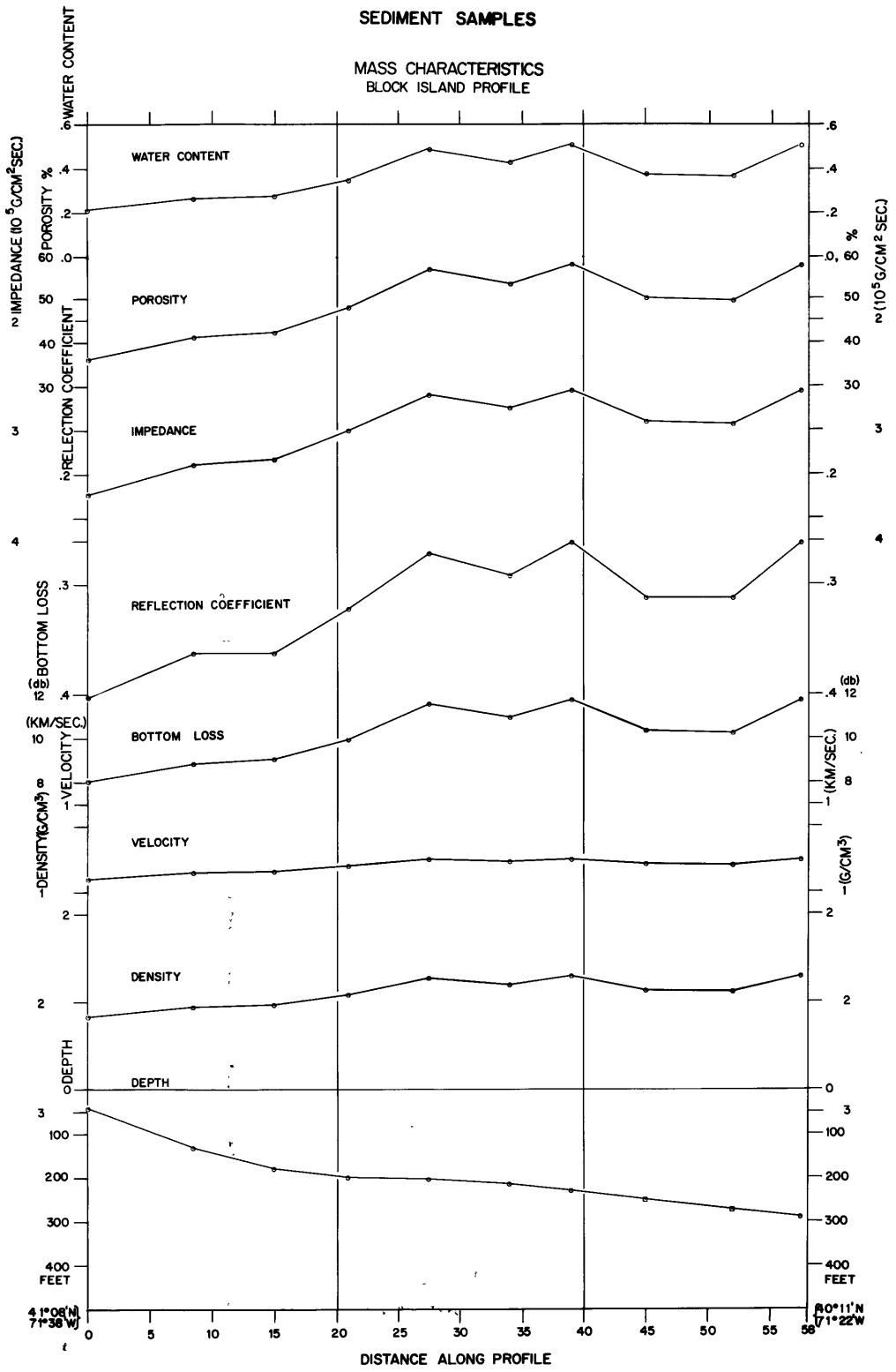

Figure 33. Mass Characteristics of Sediment Samples Plotted Versus Distance Along the Block Island Profile.

IV) and the charts of Narragansett Bay (Figures 54 and 55). No comparisons are made with the results of other investigations because there have been none.

A tabulation of the water-content measurements used to obtain the mass characteristics is presented in Table X of Appendix C. An explanation of the column headings follows: TAG represents the identification number of the sediment station; WET WEIGHT and DRY WEIGHT represent the weights, measured before and after drying, of a fixed amount of sediment.

The photographs which were obtained at the sites of the sediment stations were examined by eye to ascertain the surficial nature of the sea-floor. Some of these photographs are presented as figures 34 A, 34 B, 35 A, 35 B, 36 A, 36 B, 37 A, 37 B, 38 A, 38 B, 39 A, and 39 B, which were taken at the sites of sediment stations 41, 45, 47, 5, 18, 19, 25, 48, 55, 63, 71 and 77 respectively. The photographs of figures 34 A, 34 B, and 35 A were taken with the Edgerton Camera which was aimed perpendicular to the sea-floor; the cropped photographs that are presented cover a distance of about three feet in both their horizontal and vertical directions. The other photographs were taken with the Owen Camera (by Owen) which was aimed at an angle to the sea-floor; the photographs cover a distance of 17 inches in the horizontal direction and 16 to 17.5 inches

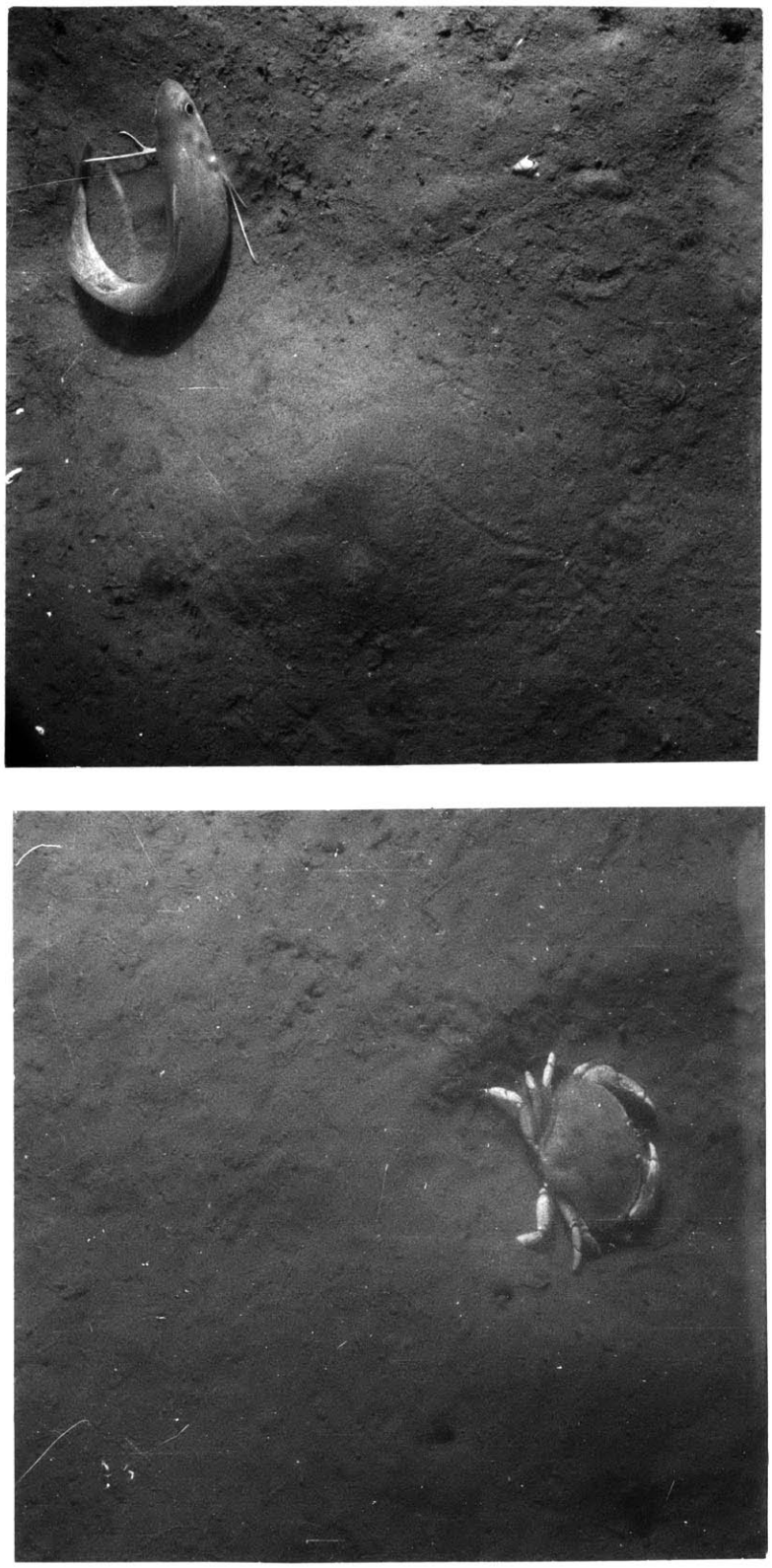

Figure 34 A, B. Photographs of the Sea-floor Taken at Sediment Station Sites 41 and 45 Respectively.

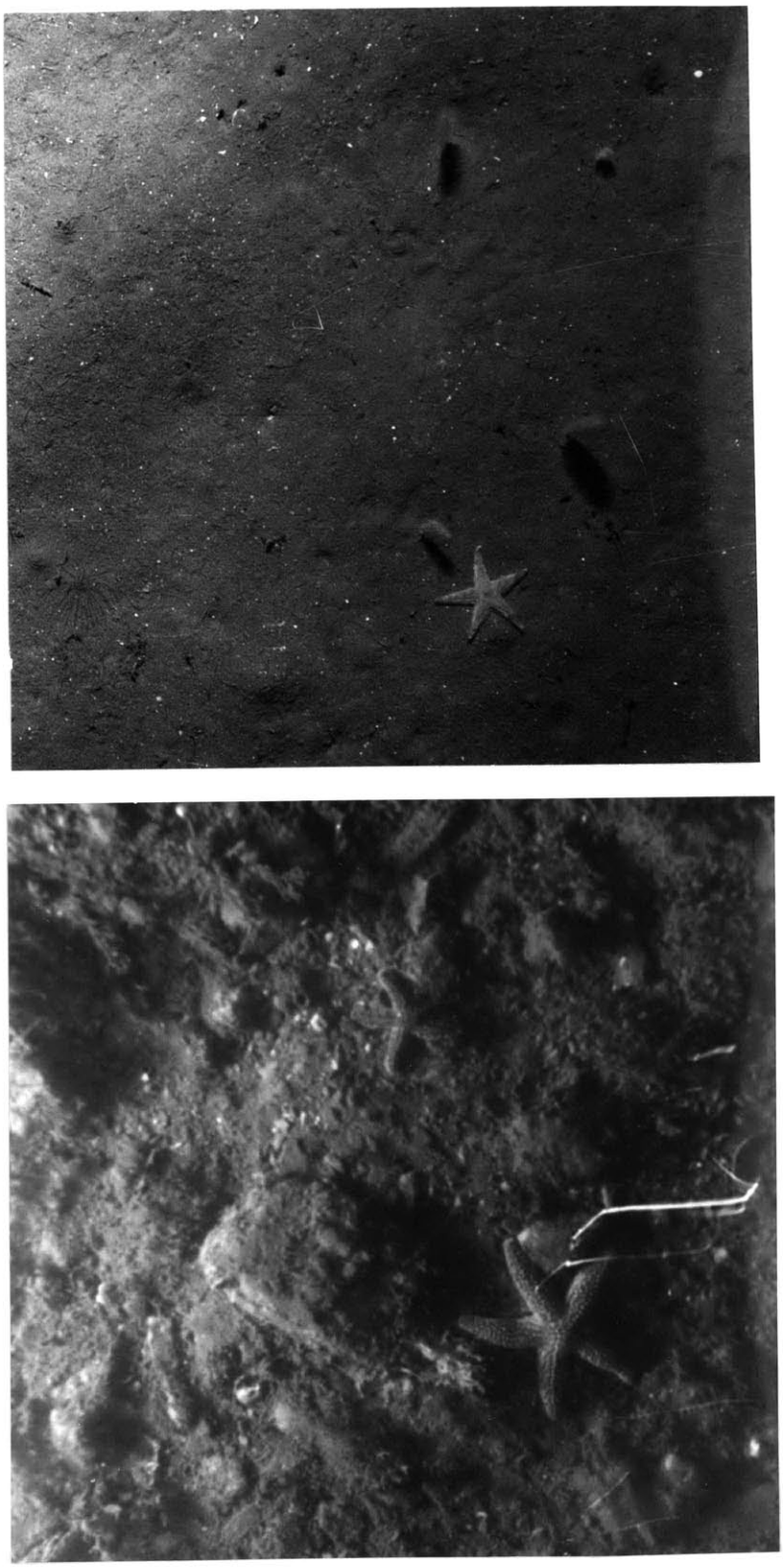

Figure 35 A, B. Photographs of the Sea-floor Taken at Sediment Station Sites 47 and 5 Respectively.

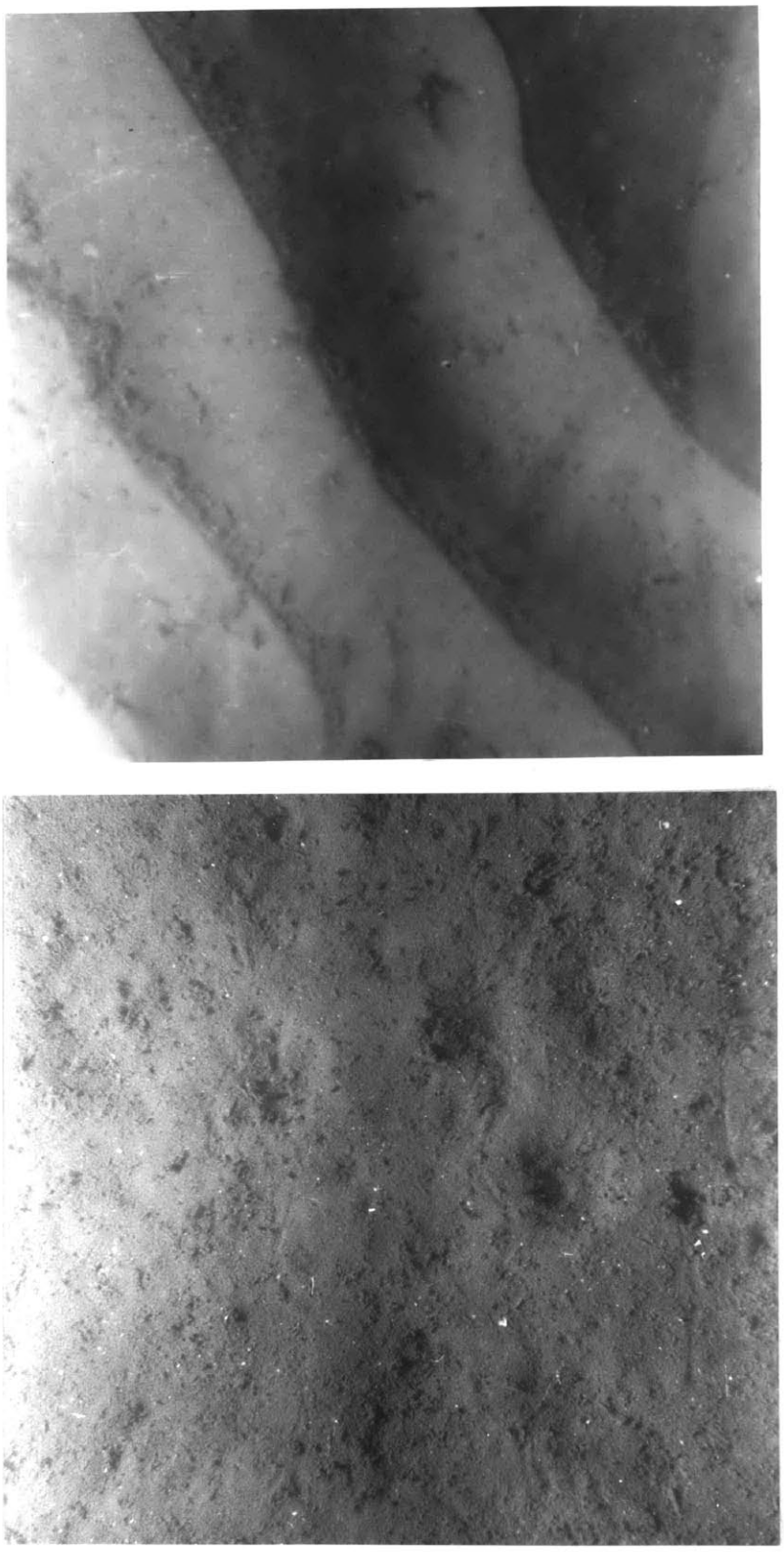

Figure 36 A, B. Photographs of the Sea-floor Taken at Sediment Station Sites 18 and 19 Respectively.

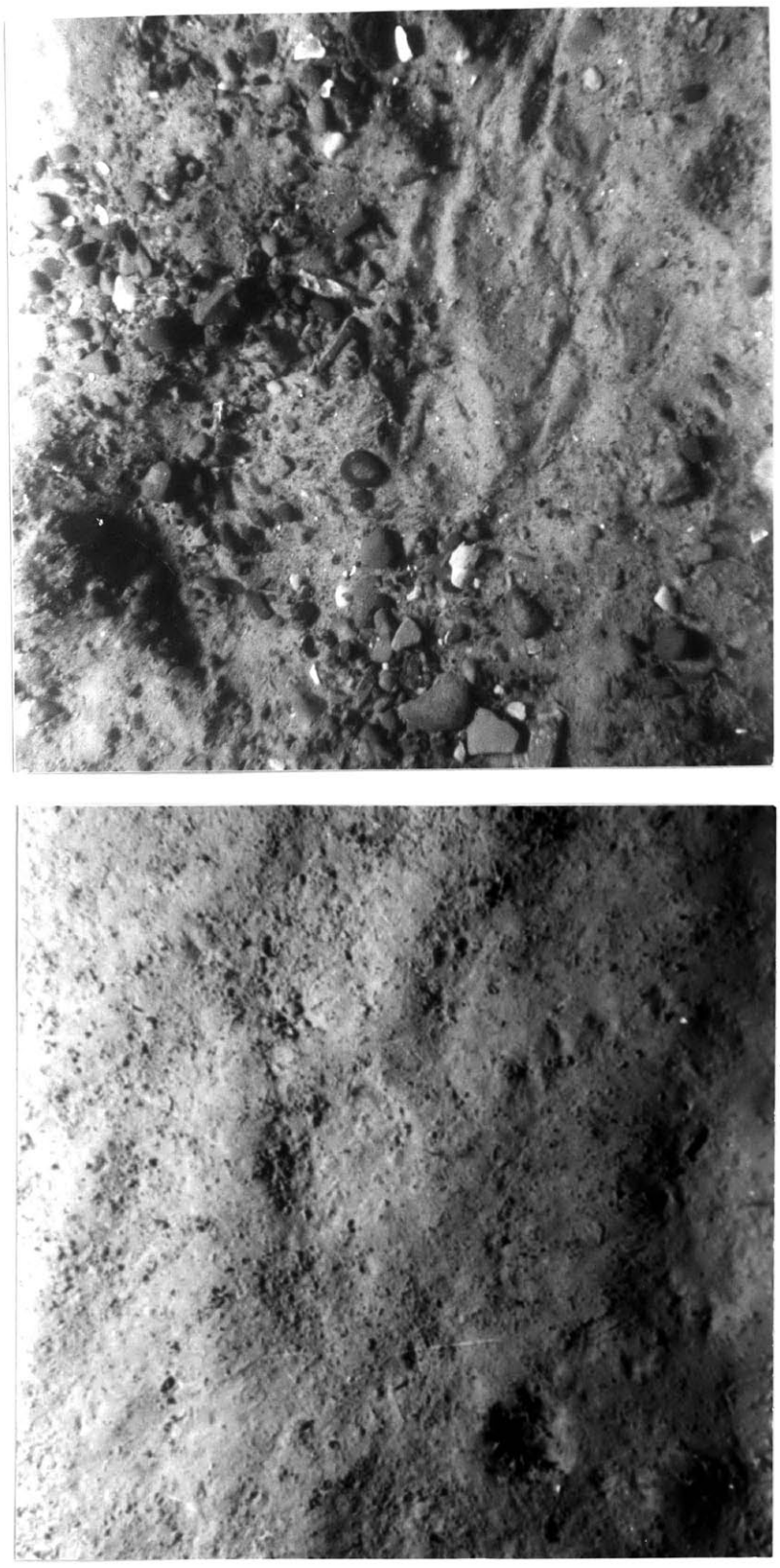

Figure 37 A, B. Photographs of the Sea-floor Taken at Sediment Station Sites 25 and 48 Respectively.

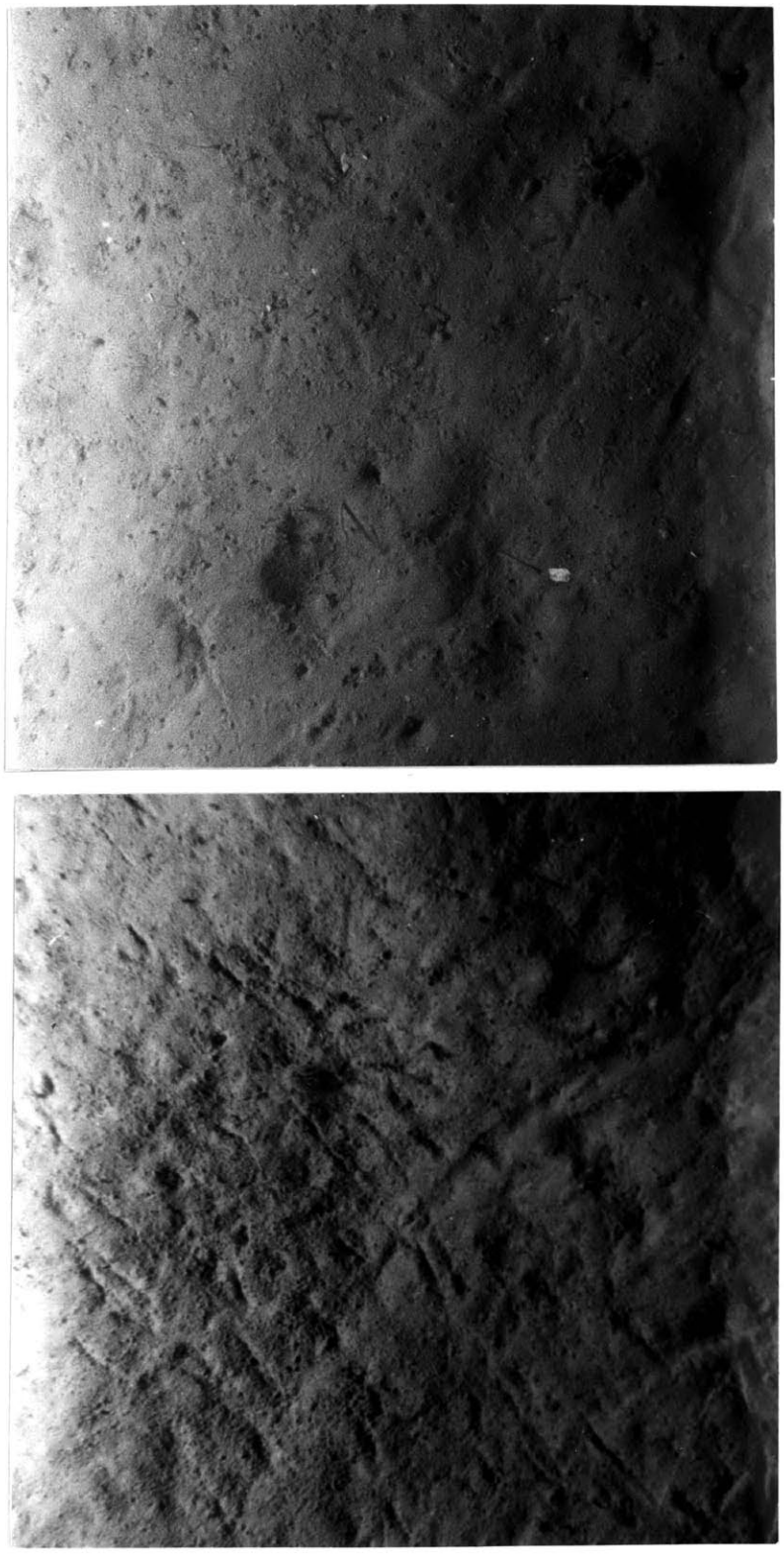

Figure 38 A, B. Photographs of the Sea-floor Taken at Sediment Station Sites 55 and 63 Respectively.

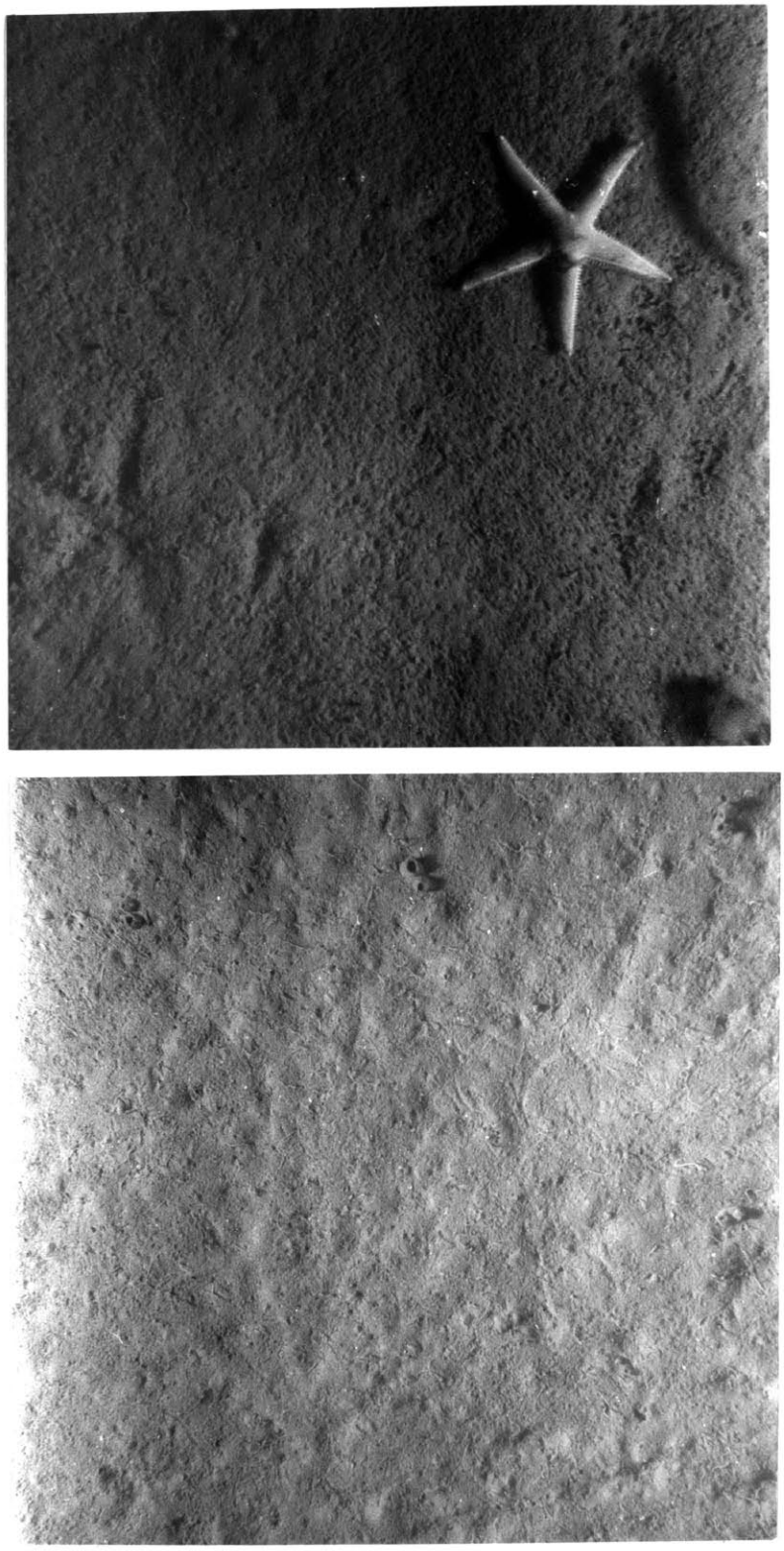

Figure 39 A, B. Photographs of the Sea-floor Taken at Sediment Station Sites 71 and 77 Respectively.

in the vertical direction (about one and one-half feet in both horizontal and vertical directions). Therefore, the photographs taken with the Edgerton Camera are presented at approximately half the magnification of those taken with the Owen Camera.

The results of all of the photographic observations are tabulated in Table V. The relief of the sea-floor is considered to be flat, moderate, or rough, respectively, depending upon whether the magnitudes of the vertical excursions of protuberances and depressions are generally smaller than one inch, between one and three inches, or larger than three inches. The bottom material is noted as coarse when a considerable amount of gravel is observed; otherwise it is noted as fine. This is a classification based on the resolution obtained in these photographs and of course is not the same as the classification used in grain size analysis (coarse is equal to gravel + sand; fine, equal to silt + clay).

TABLE V

PHOTOGRAPHIC OBSERVATIONS AT SITES OF SEDIMENT STATIONS

SEDIMENT STATION SITE	SURFICIAL CHARACTER OF THE SEA FLOOR
4	Small relief, coarse material, many mussels, few starfish
5	Moderate relief, coarse material, some rockweed, few starfish
9	Small relief, coarse material, many mussels, few starfish
10	Small relief, coarse material, many mussel shells
14	Small relief, fine material
16	Small relief, fine material
17	Small relief, some ripples < 1" high and 2"-4" apart, fine material
18	Moderate relief, some ripples 1"-2" high and 4"-5" apart, fine material
19	Small relief, fine material
20	Small relief, fine material, a starfish
24	Small relief, coarse material, rockweed
25	Small relief, coarse material
26	Small relief, fine material
28	Small relief, coarse material
29	Small relief, fine material, worm tubes
31	Small relief, coarse material
39	Small relief, fine material, sand dollar
41	Small relief, fine material, fish
43	Small relief, fine material, small dimples < 1/2" deep, starfish

TABLE V

PHOTOGRAPHIC OBSERVATIONS AT SITES OF SEDIMENT STATIONS

SEDIMENT STATION SITE	SURFICIAL CHARACTER OF THE SEA FLOOR
45	Small relief, fine material, crab
47	Small relief, fine material, few starfish, few sea pens
48	Small relief, small dimples < 1/2" deep, fine material
50	Small relief, gentle ripple mark < 1/2" high and 10" ח, fine material
51	Small relief, fine material, starfish
53	Small relief, small dimple < 1/2" deep, fine material
54	Small relief, fine material
55	Small relief, small dimples < 1/2" deep, fine material
56	Small relief, small dimples < 1/2" deep, fine material
58	Small relief, small dimples < 1/2" deep, fine material
59	Small relief, small dimples < 1/2" deep, fine material
60	Small relief, fine material, starfish
61	Small relief, fine material
62	Small relief, fine material
63	Small relief, few tracks < 1/2" deep and < 1" wide, fine material
65	Small relief, few tracks < 1/2" deep and < 1" wide, fine material
66	Small relief, few tracks < 1/2" deep and < 1" wide, fine material, starfish
67	Small relief, fine material, starfish

TABLE V

PHOTOGRAPHIC OBSERVATIONS AT SITES OF SEDIMENT STATIONS

SEDIMENT STATION SITE	SURFICIAL CHARACTER OF THE SEA FLOOR
68	Small relief, fine material, starfish
69	Small relief, fine material
71	Small relief, fine material
72	Small relief, few tracks < 1/2" deep and < 1" wide, fine material, sea pens, starfish
73	Small relief, fine material
74	Small relief, fine material, sea pens
75	Small relief, fine material, some worm tubes
76	Small relief, fine material, some worm tubes
77	Small relief, fine material, some worm tubes

CHAPTER IX

CORRELATION OF ACOUSTIC AND GEOLOGIC RESULTS

Sediment Stations

Several times, during the shallow-water cruises, the ship was hove-to and measurements of acoustic bottom loss (Table VI) and sediment samples from the sea-floor were obtained. These sediments were subjected to a grain-size analysis (Table III). At a later date, the same sites of the sediment stations were revisited and a second set of sediment samples was obtained. This second set was subjected to a water-content analysis (Table IV). The locations of these measurements are shown by the numerals and associated arrows on figures 54, 55, 56, and 57.

A correlation and regression analysis (Table VII) was performed between the acoustic measurements and the characteristics of the sediment samples. The statistical quantities obtained were the regression equation, the correlation coefficient, and the Z statistic (Hoel, 1962). Bottom loss, measured on both a peak-pressure and on a total-energy basis, was tested against porosity (Figures 40 and 41), median grain-size (Figures 42 and 43), sorting coefficient (Figures 44 and 45), percentage of fine material (silt + clay) (Figures 46 and 47), percentage of silt (Figures 48 and 49), and percentage of clay (Figures 50 and 51). The experimental

TABLE VI

ACOUSTIC MEASUREMENTS AT SITES OF SEDIMENT STATIONS

TAG	DEPTH (FEET)	LATITUDE	LONGITUDE	BOTTOM LOSS(db) (PRESSURE BASIS)	BOTTOM LOSS(db) (ENERGY BASIS)
1	20	41°37.5'	71°22.3'	16.5	17.2
2	27	41°38.8'	71°22.4'	14.2	14.7
3	51	41°33.3'	71°19.5'	14.9	14.9
4	83	41°30.5'	71°21.2'	9.4	9.0
5	84	41°28.9'	71°20.5'	11.0	12.8
6	50	41°28.4'	71°20.8'	7.7	8.9
7	30	41°28.6'	71°22.9'	10.1	11.9
8	98	41°28.0'	71°22.6'	12.4	10.3
9	100	41°28.4'	71°21.4'	12.1	9.9
10	32	41°33.3'	71°23.7'	9.2	8.4
11	31	41°33.2'	71°24.6'	13.2	12.6
12	38	41°32.7'	71°24.0'	11.6	10.5
13	43	41°29.6'	71°24.5'	14.4	12.5
14	26	41°28.6'	71°22.8'	10.3	9.2
15	25	41°28.6'	71°22.9'	9.5	11.1
16	60	41°25.7'	71°26.1'	11.6	9.8
17	41	41°25.7'	71°26.6'	10.1	9.3
18	30	41°25.8'	71°27.0'	8.6	7.0
19	74	41°25.9'	71°23.1'	12.4	10.1
20	76	41°26.9'	71°22.2'	13.1	11.9
21	23	41°28.7'	71°22.9'	11.4	11.3

TABLE VI

ACOUSTIC MEASUREMENTS AT SITES OF SEDIMENT STATIONS

TAG	DEPTH (FEET)	LATITUDE	LONGITUDE	BOTTOM LOSS(db) (PRESSURE BASIS)	BOTTOM LOSS(db) (ENERGY BASIS)
22	28	41°30.6'	71°24.0'	15.2	14.6
23	50	41°37.5'	71°17.2'	9.7	7.9
24	65	41°25.2'	71°21.4'	8.1	6.2
25	68	41°25.3'	71°13.8'	8.8	6.4
26	33	41°29.7'	71°13.2'	10.4	8.1
27	25	41°31.8'	71°12.9'	11.0	10.7
28	46	41°28.3'	71°12.5'	9.2	6.6
29	77	41°26.0'	71°17.2'	12.4	11.6
30	50	41°28.1'	71°16.3'	10.5	10.3
31	30	41°28.7'	71°15.6'	10.8	7.2
32	40	41°28.4'	71°16.6'	8.6	5.1
33	120	41°15.4'	71°25.2'	10.1	8.8
34	131	41°10.8'	71°25.5'	12.5	11.6
35	101	41°7.0'	71°25.6'	9.5	7.2
36	82	41°7.1'	71°27.9'	10.1	9.6
37	74	41°11.6'	71°36.5'	13.1	13.3
38	44	41°7.8'	71°38.6'	6.1	5.4
39	133	40°59.6'	71°35.7'	8.8	7.5
40	180	40°53.8'	71°33.0'	11.4	10.1
41	200	40°47.3'	71°31.8'	11.1	10.5
42	204	40°40.8'	71°29.9'	12.2	11.6

TABLE VI

ACOUSTIC MEASUREMENTS AT SITES OF SEDIMENT STATIONS

TAG	DEPTH (FEET)	LATITUDE	LONGITUDE	BOTTOM LOSS(db) (PRESSURE BASIS)	BOTTOM LOSS(db) (ENERGY BASIS)
43	215	40°34.4'	71°27.3'	14.9	13.2
44	230	40°29.4'	71°26.5'	15.5	13.2
45	250	40°23.5'	71°24.6'	14.2	12.4
46	272	40°16.8'	71°22.8'	16.3	12.8
47	289	40°11.6'	71°21.7'	13.4	11.2
48	62	41°16.5'	70°39.4'	10.6	9.4
49	82	41°14.9'	70°41.5'	12.1	10.6
50	72	41°13.4'	70°39.6'	9.5	9.0
51	90	41°10.2'	70°39.5'	10.6	10.7
52	122	41°80.0'	70°40.8'	12.8	11.5
53	114	41°7.5'	70°39.0'	10.4	10.2
54	139	41°4.6'	70°40.5'	12.7	10.8
55	122	41°4.0'	70°39.0'	10.6	10.7
56	132	41°0.0'	70°40.0'	10.1	10.2
57	162	40°58.9'	70°40.3'	14.3	11.6
58	136	40°57.1'	70°41.4'	12.3	12.4
59	147	40°54.5'	70°42.4'	10.8	10.0
60	170	40°53.4'	70°41.1'	10.8	8.7
61	150	40°51.5'	70°42.5'	10.4	9.7
62	164	40°48.8'	70°42.5'	14.3	13.0
63	174	40°45.5'	70°42.5'	13.5	12.0

TABLE VI

ACOUSTIC MEASUREMENTS AT SITES OF SEDIMENT STATIONS

TAG	DEPTH (FEET)	LATITUDE	LONGITUDE	BOTTOM LOSS(db) (PRESSURE BASIS)	BOTTOM LOSS(db) (ENERGY BASIS)
64	191	40°44.7'	70°42.4'	14.9	11.4
65	180	40°42.0'	70°40.8'	12.8	11.5
66	182	40°40.0'	70°42.8'	14.3	13.0
67	202	40°39.2'	70°45.2'	14.9	12.2
68	192	40°37.0'	70°41.5'	13.9	11.8
69	204	40°33.5'	70°42.0'	16.5	14.2
70	234	40°30.9'	70°44.6'	18.7	16.0
71	216	40°30.5'	70°42.2'	17.1	15.0
72	236	40°26.5'	70°42.5'	18.0	16.0
73	255	40°24.4'	70°43.5'	16.8	14.4
74	285	40°23.8'	70°44.5'	17.6	13.8
75	285	40°22.1'	70°43.5'	16.3	14.0
76	336	40°18.7'	70°42.8'	19.2	17.6
77	366	40°15.4'	70°43.0'	20.8	16.6

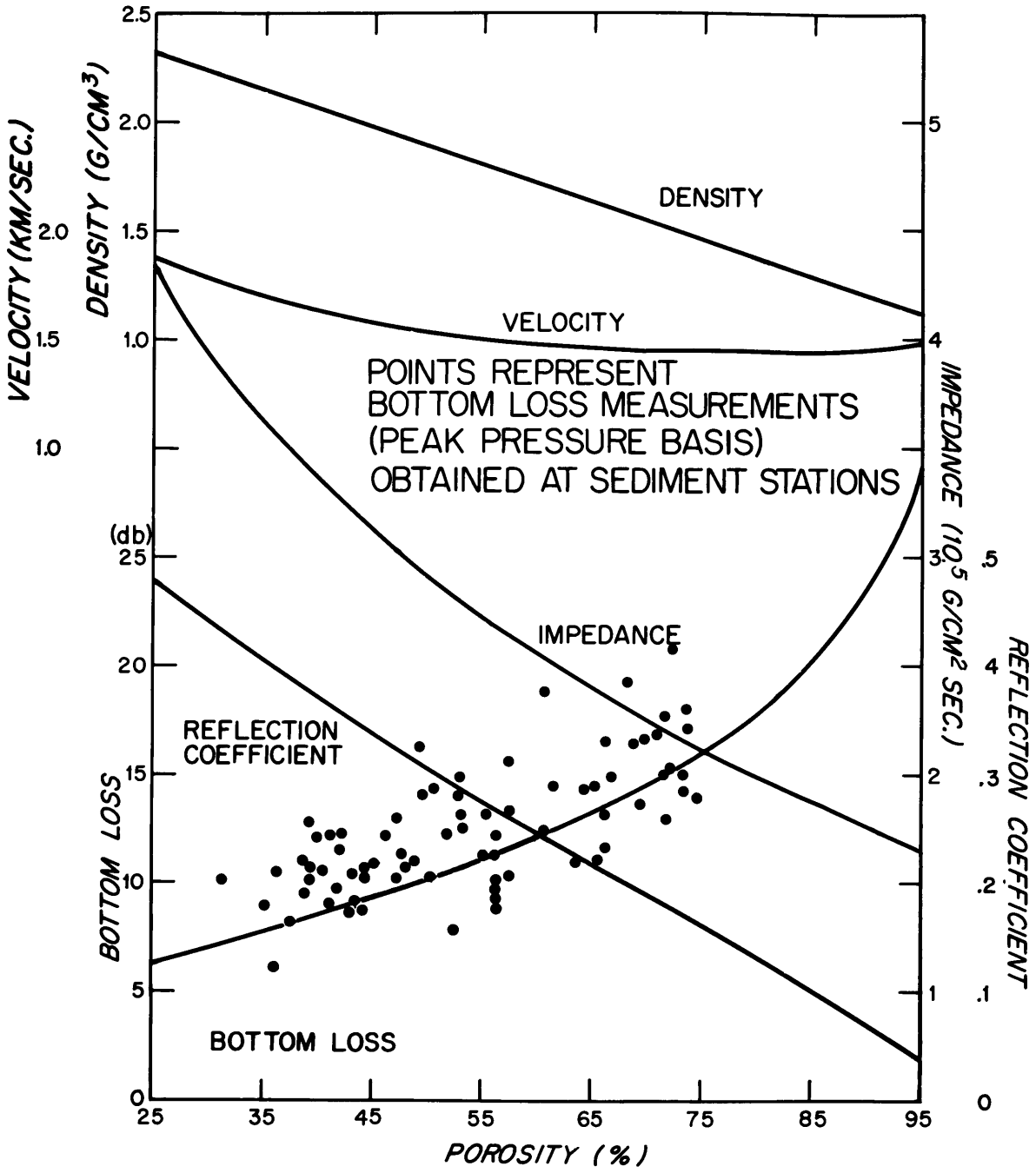

Figure 40. Bottom Loss Measurements (Peak Pressure Basis) at Sediment Stations Versus Measured Porosity of the Sediment.

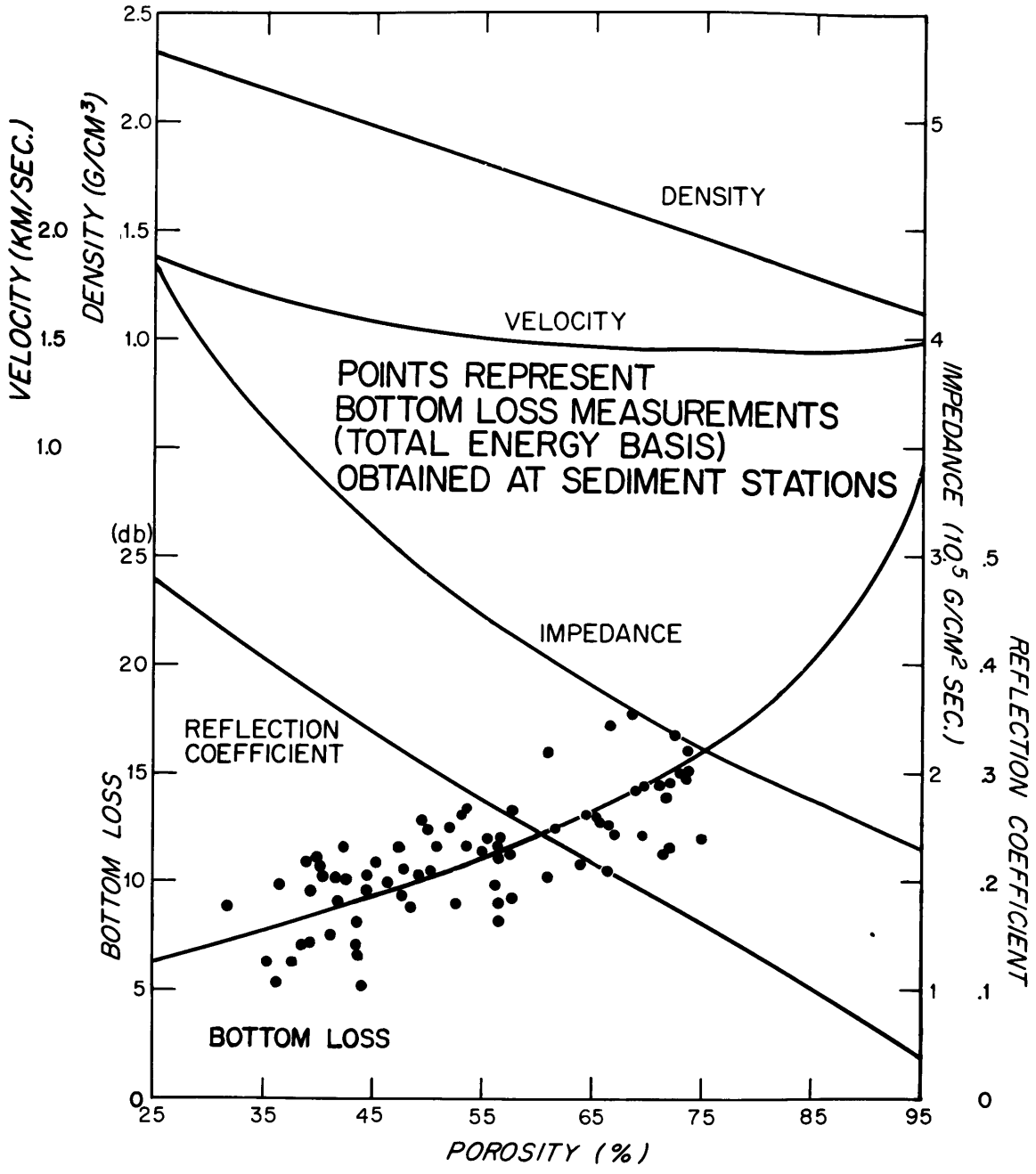

Figure 41. Bottom Loss Measurements (Total Energy Basis) at Sediment Stations Versus Measured Porosity of the Sediment.

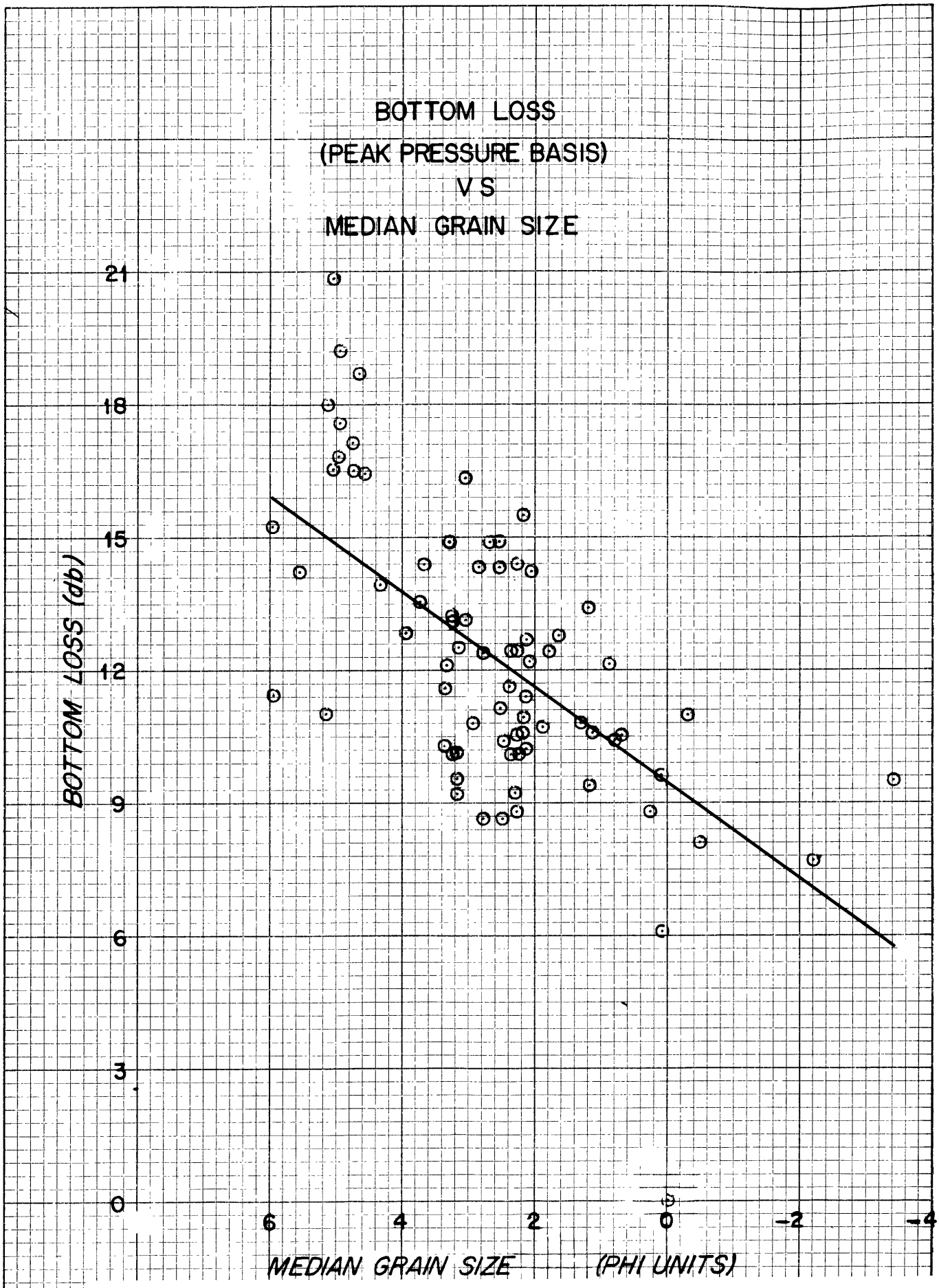

Figure 42. Scatter Diagram of Bottom Loss (Peak Pressure Basis) Versus Median Grain Size.

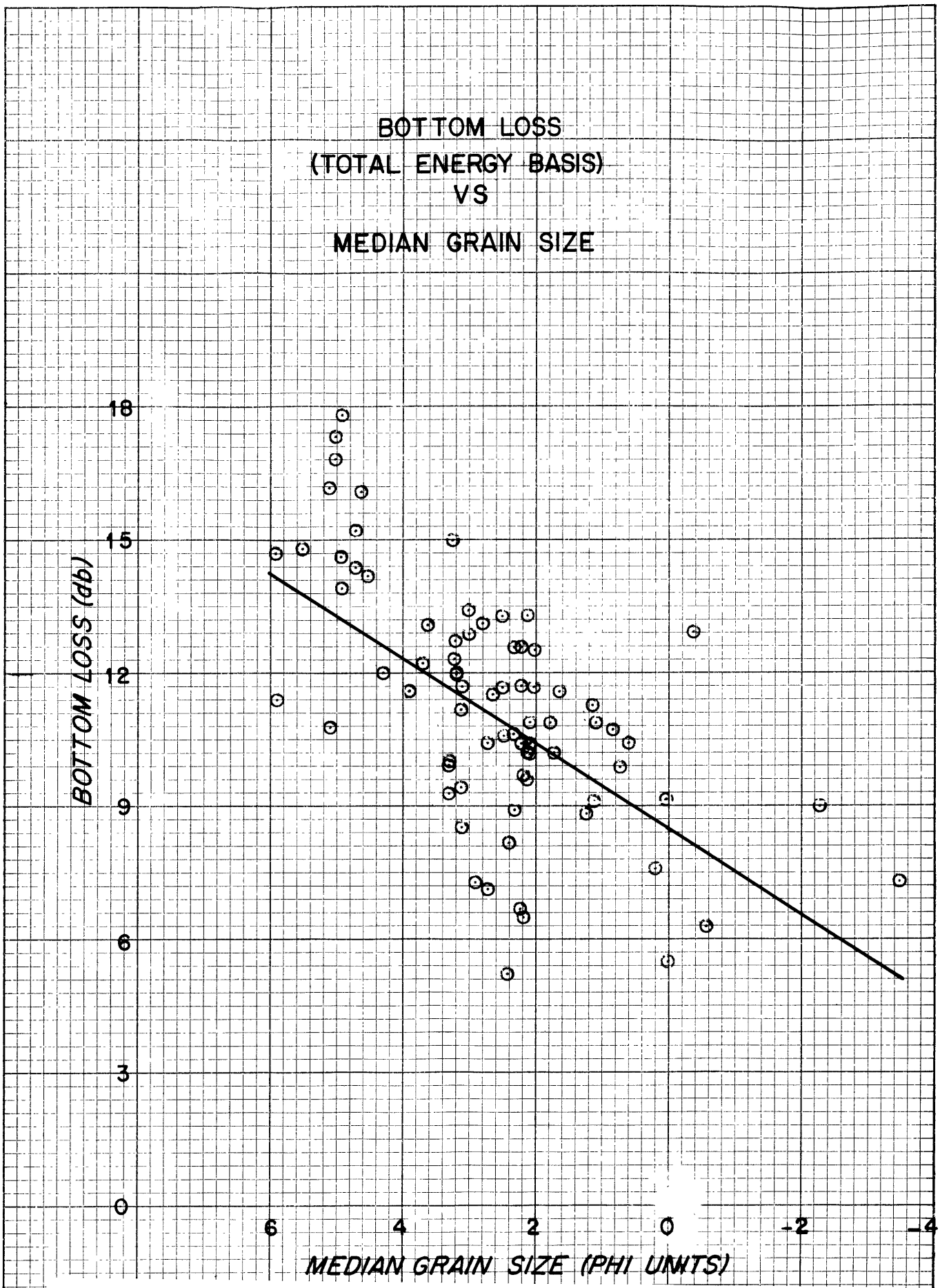

Figure 43. Scatter Diagram of Bottom Loss (Total Energy Basis) Versus Median Grain Size.

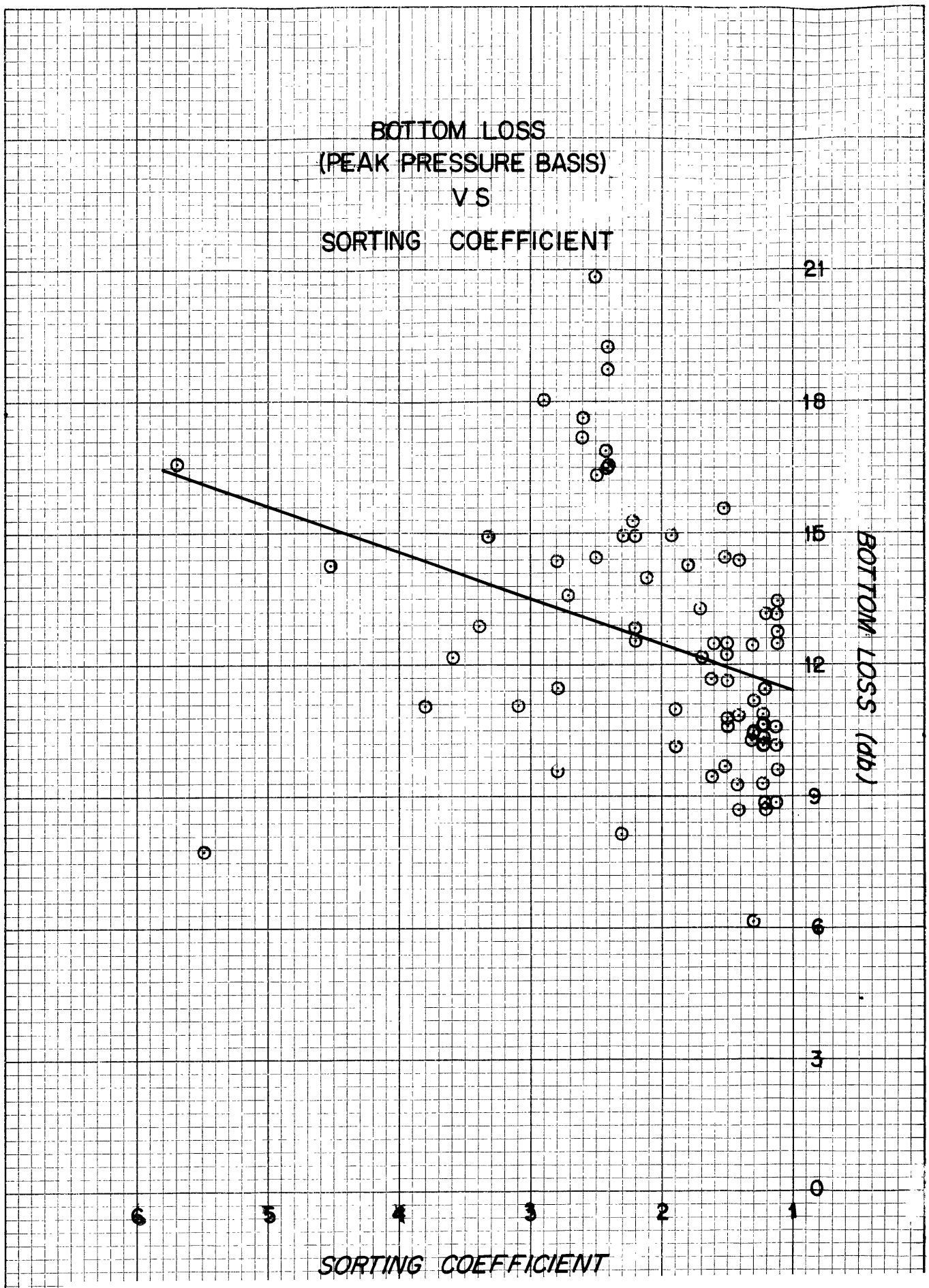

Figure 44. Scatter Diagram of Bottom Loss (Peak Pressure Basis) Versus Sorting Coefficient.

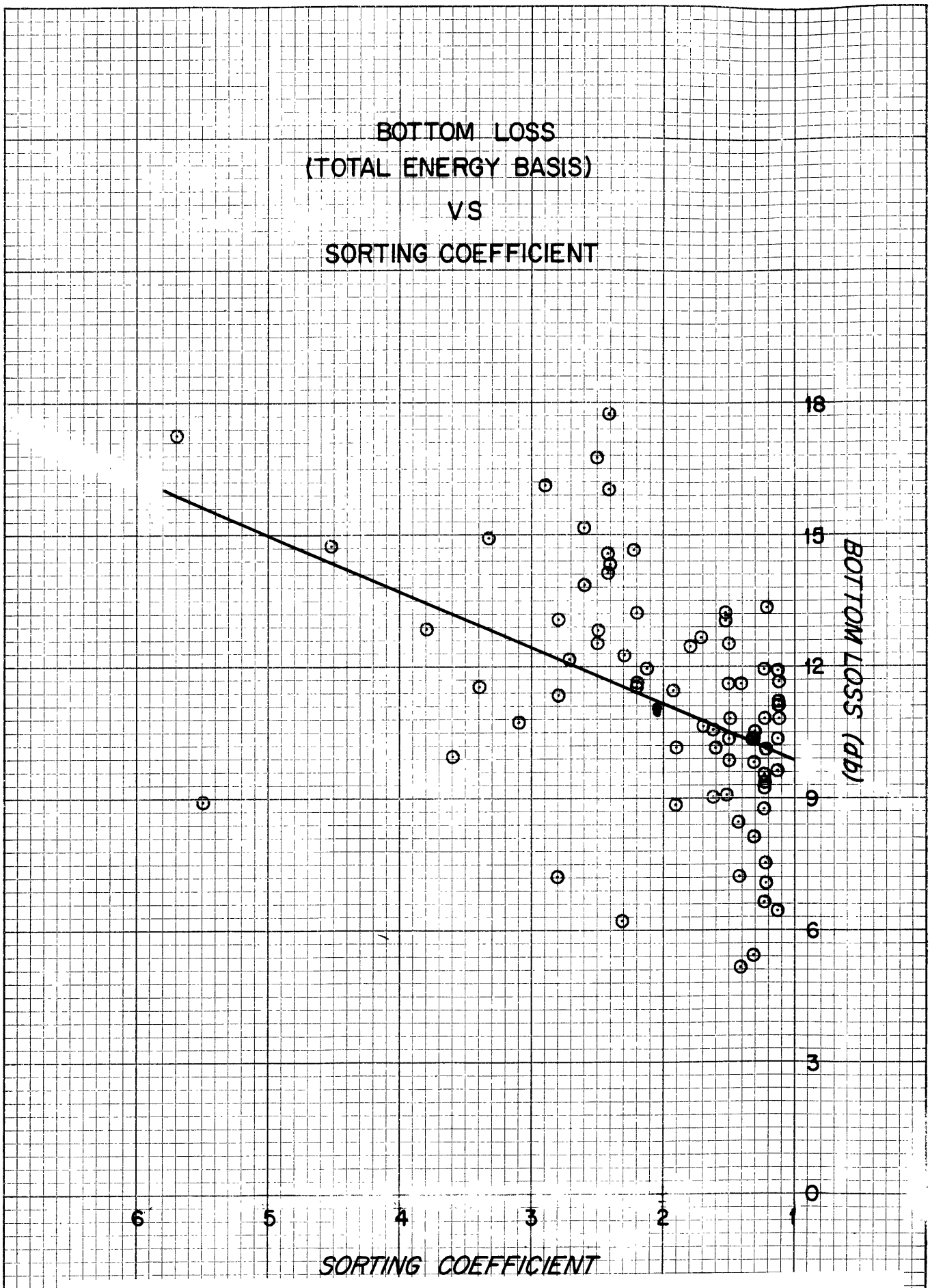

Figure 45. Scatter Diagram of Bottom Loss (Total Energy Basis) Versus Sorting Coefficient.

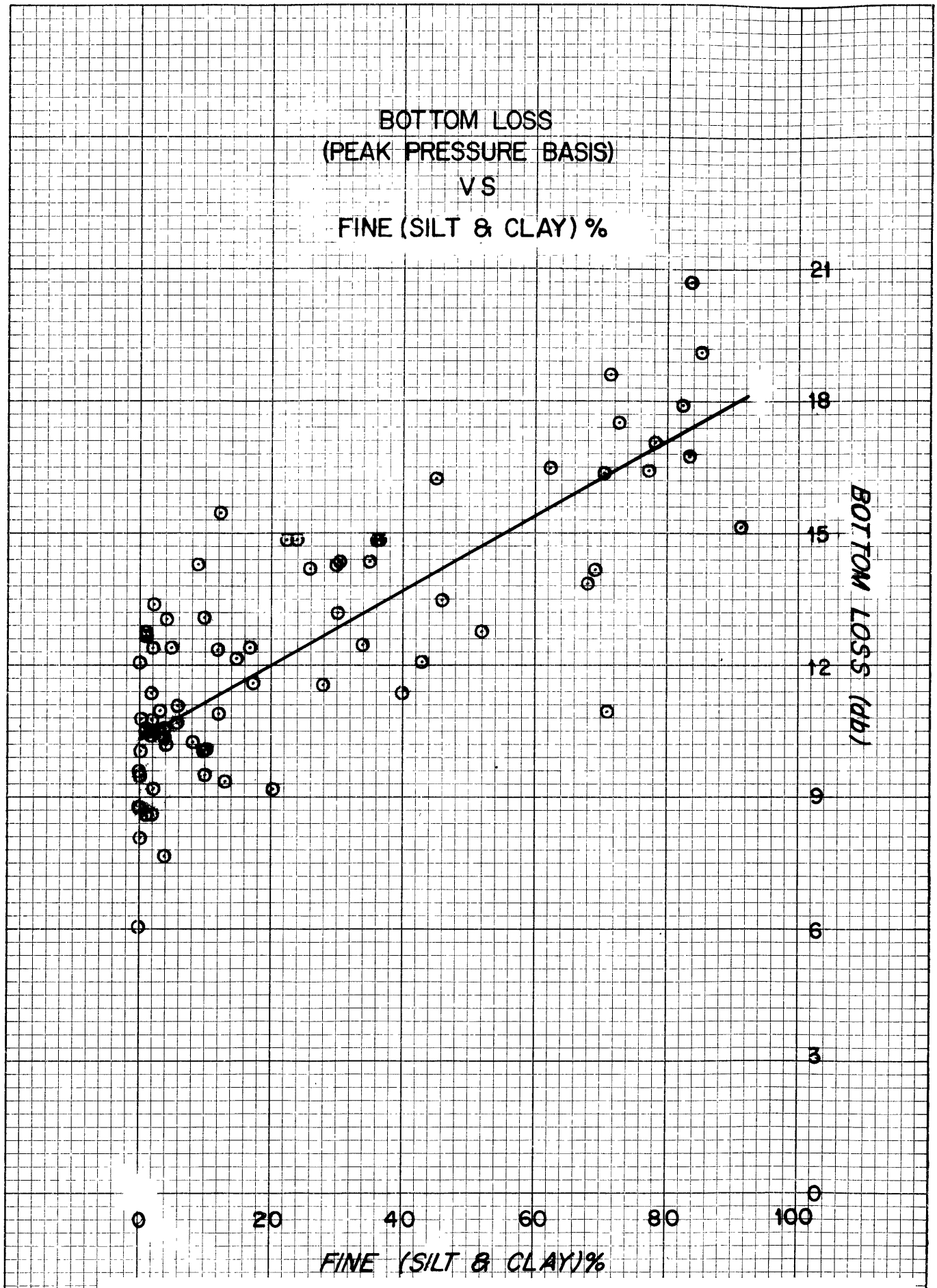

Figure 46. Scatter Diagram of Bottom Loss (Peak Pressure Basis) Versus Fine (Silt Plus Clay) Percentage.

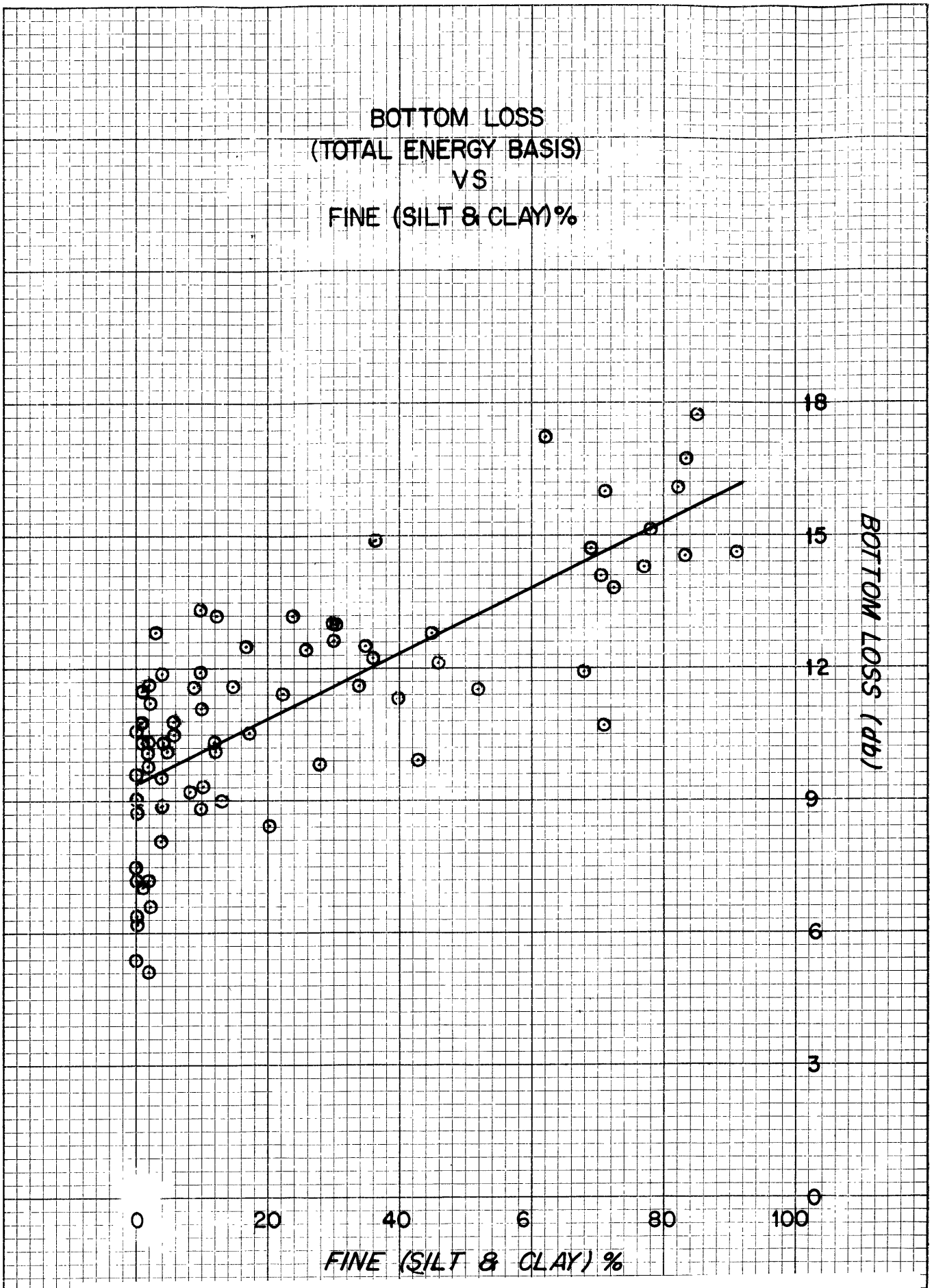

Figure 47. Scatter Diagram of Bottom Loss (Total Energy Basis) Versus Fine (Silt Plus Clay) Percentage.

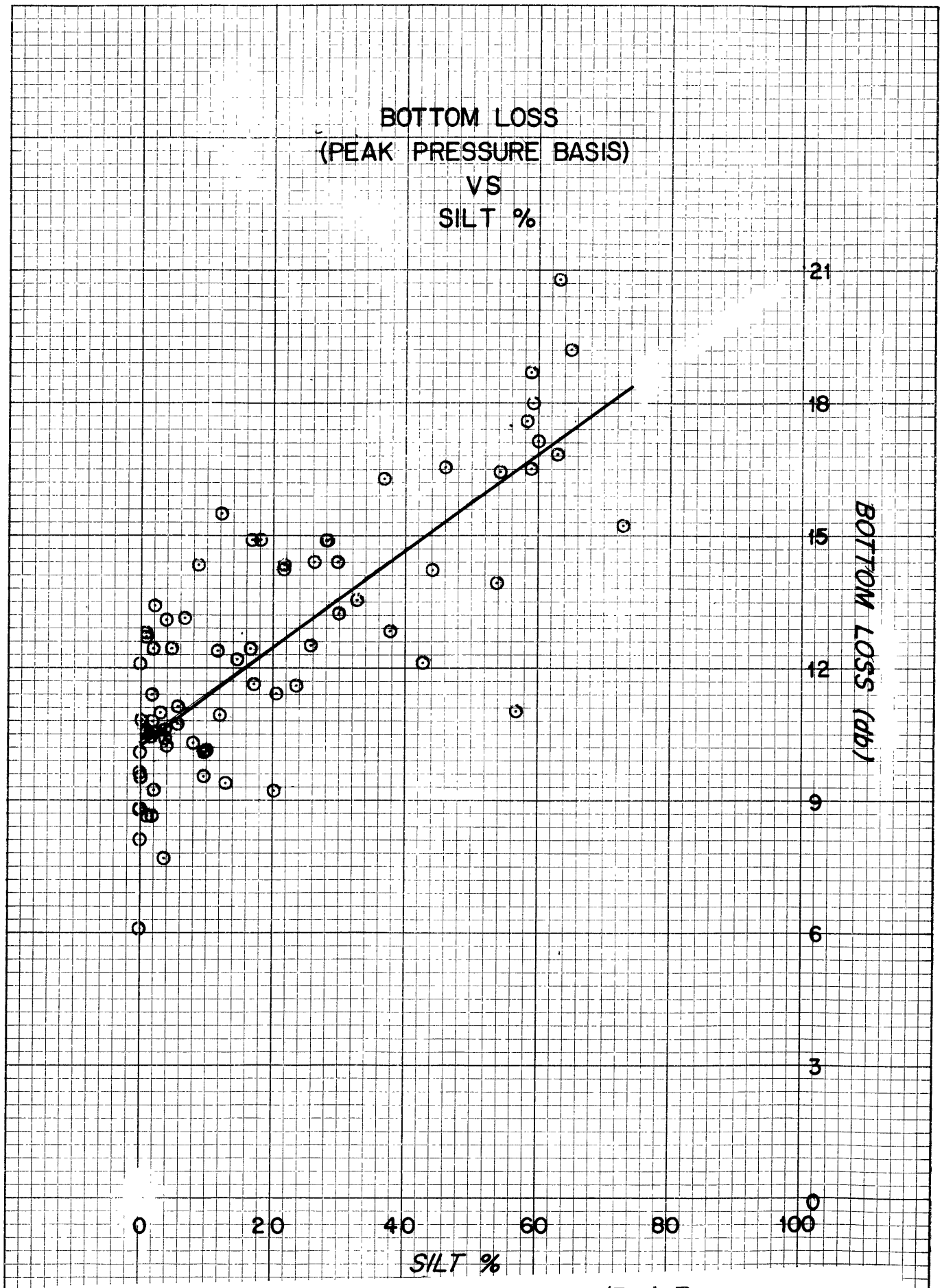

Figure 48. Scatter Diagram of Bottom Loss (Peak Pressure Basis) Versus Silt Percentage.

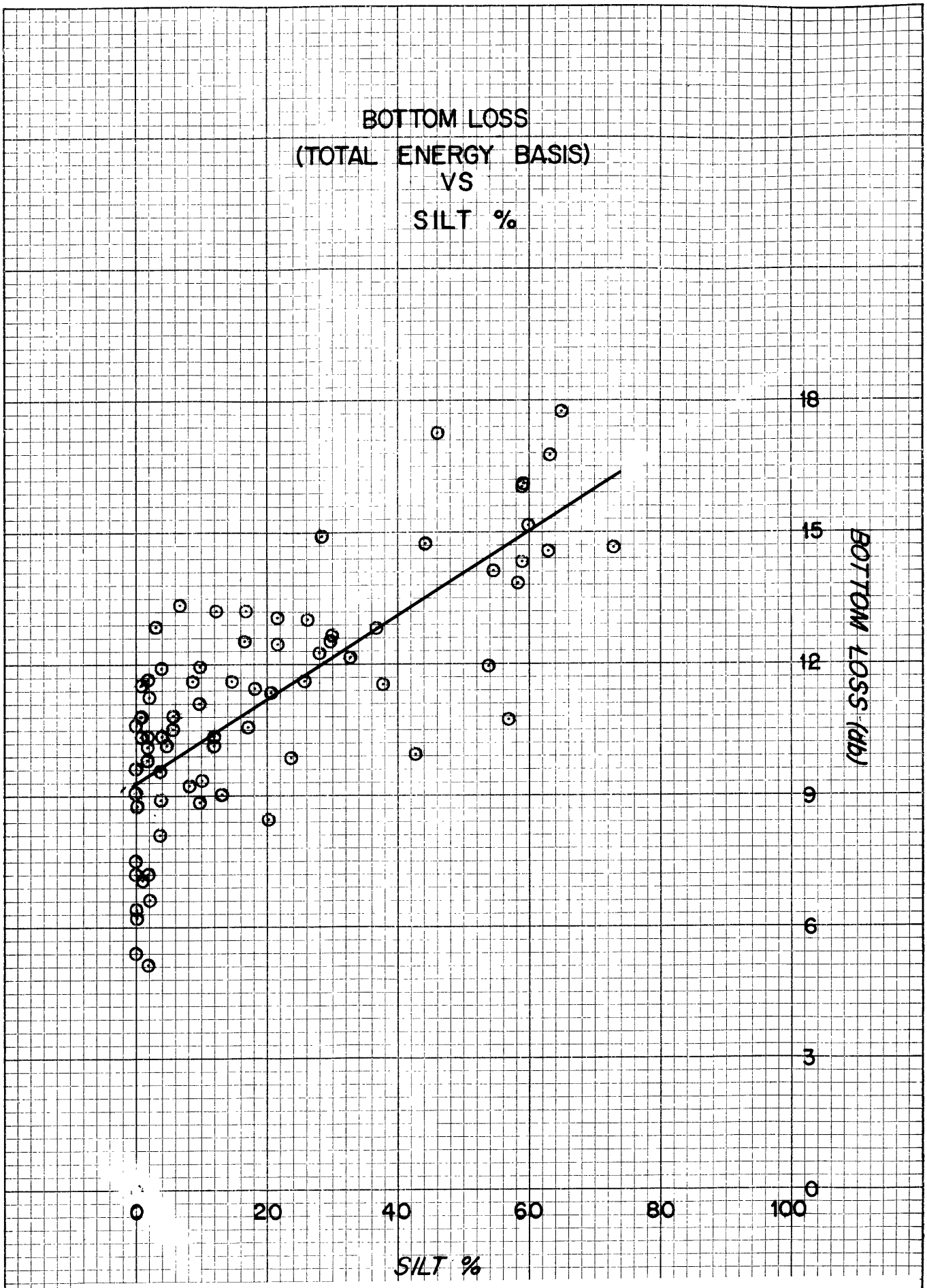

Figure 49. Scatter Diagram of Bottom Loss (Total Energy Basis) Versus Silt Percentage.

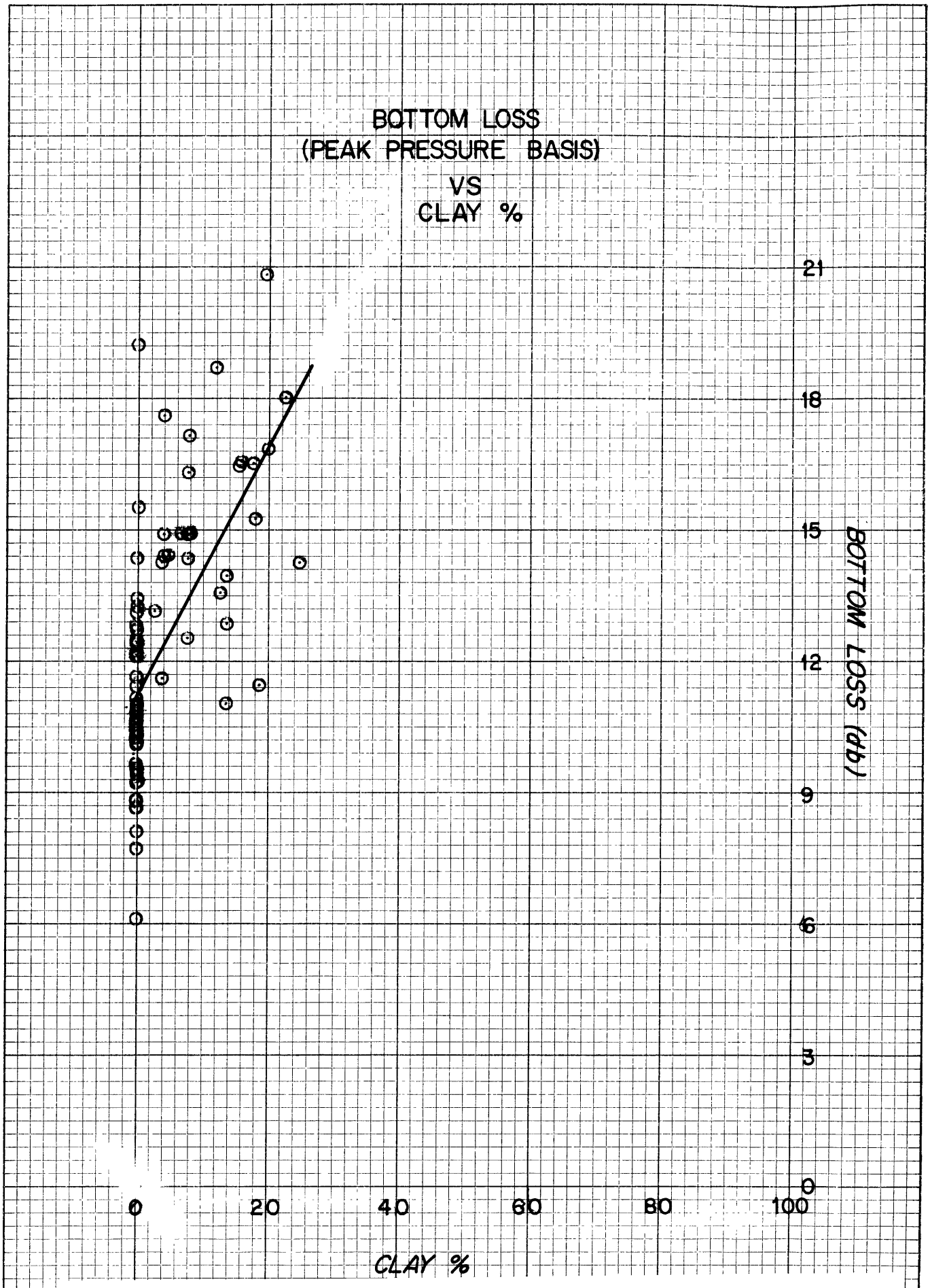

Figure 50. Scatter Diagram of Bottom Loss (Peak Pressure Basis) Versus Clay Percentage.

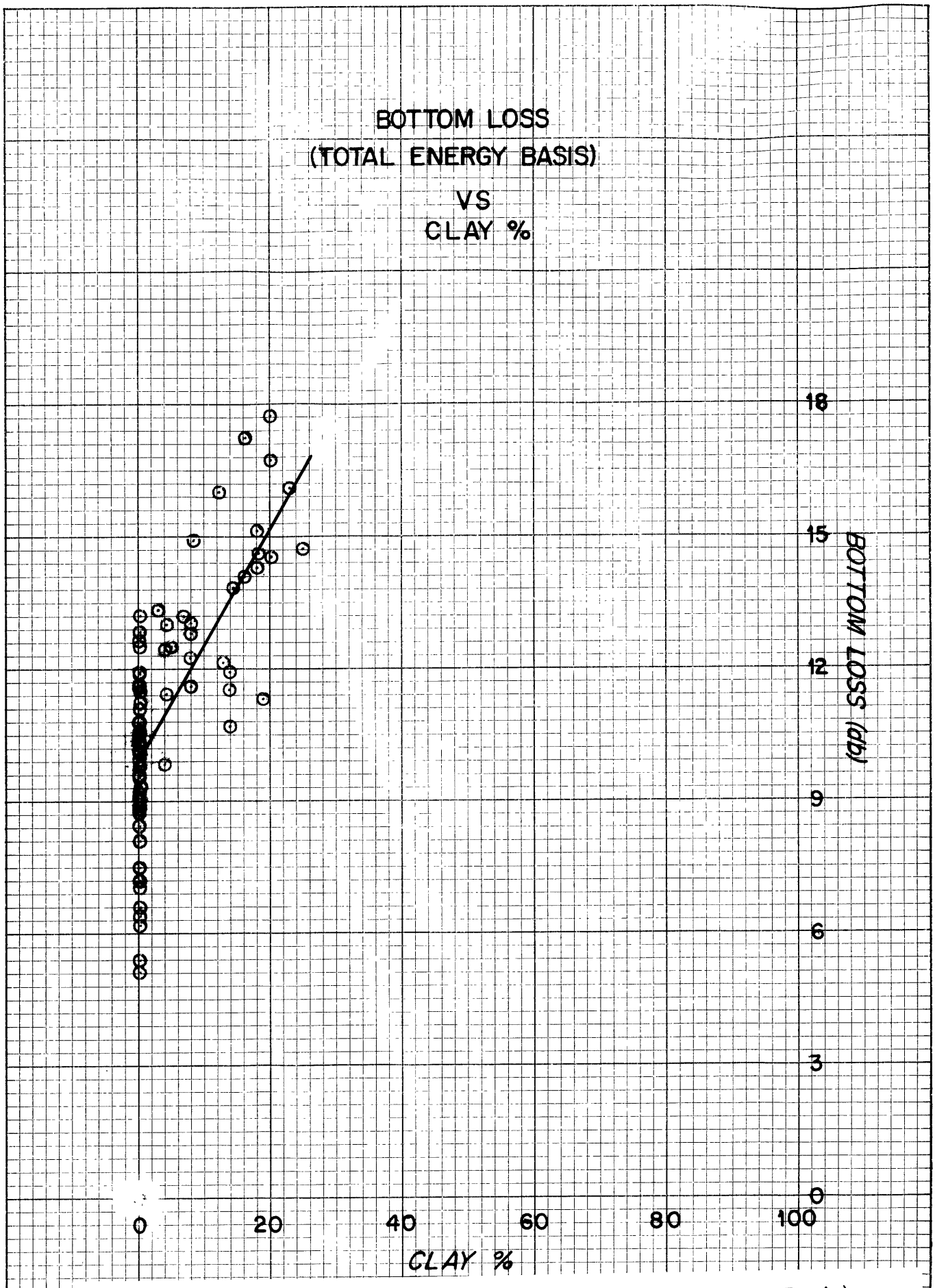

Figure 51. Scatter Diagram of Bottom Loss (Total Energy Basis) Versus Clay Percentage.

points have been plotted in the form of scatter diagrams in these figures along with the regression line for all the geological quantities except porosity. For this particular case the experimental points are plotted along with the theoretical curves of mass characteristics versus porosity, which were developed in Chapter II.

The regression line is the best-fitting line, chosen on a least squares basis, through the experimental data. The correlation coefficient is a measure of the degree to which the experimental data indicates that a linear relationship exists between the variables tested. The Z statistic is a normally distributed function of the correlation coefficient and is used to test its statistical significance. A correlation coefficient is considered significant (at the 95% level) when its absolute value is larger than two standard deviations of the Z statistic. The standard deviation of the Z statistic depends solely on the number of experimental points and is equal to . 117 for this investigation (76 points were used; the measurements at Station 23 seemed to be grossly in error and were not considered in the statistical analysis).

The magnitudes of the correlation coefficients presented in Table VII demonstrate that a significant correlation exists between bottom loss and all of the geological quantities that were tested. In particular, bottom loss is directly related to porosity and amount of

TABLE VII

STATISTICAL RELATIONSHIPS BETWEEN ACOUSTIC MEASUREMENTS AND SEDIMENT PROPERTIES

	Regression Line Slope	Correlation Coefficient	Z Statistic
	* Bottom Loss (db)	* Bottom Loss (db)	* Bottom Loss (db)
Porosity	.171 ± .039 db/% (.166 ± .034 db/%)	.706 (.745)	.878 ± .234 (.962 ± .234)
Grain Size	1.074 ± .292 db/phi unit (.961 ± .274 db/phi unit)	.646 (.627)	.768 ± .234 (.737 ± .234)
Sorting	1.054 ± .660 db/trask unit 1.258 ± .580 db/trask unit	.343 (.445)	.358 ± .234 (.478 ± .234)
Fine Material	.083 ± .015 db/% (.073 ± .014 db/%)	.786 (.752)	1.060 ± .234 (.977 ± .234)
Silt	.108 ± .020 db/% (.095 ± .020 db/%)	.782 (.742)	1.052 ± .234 (.954 ± .234)
Clay	.293 ± .060 db/% (.266 ± .056 db/%	.727 (.716)	.922 ± .234 (.898 ± .234)

* Measurements made on a total-energy basis are bracketed and those on a peak-pressure basis are not.

fine material, silt, and clay, and inversely related to median grain size (the phi unit is an inverse measure of the logarithm of grain size) and degree of size sorting (the Trask sorting coefficient is an inverse measure of sorting). The strength of the relationship appears greatest for amount of fine material, silt, and clay, slightly less for porosity, slightly less again for median grain size, and weakest for degree of size sorting. No significant difference was found between the acoustic measurement made on a peak-pressure basis and that made on a total-energy basis, with regard to the correlation observed between bottom loss and the various geological quantities tested.

These correlation coefficients only indicate the existence of a relationship between the acoustic and geological quantities; they do not imply any cause and effect. The relationships that do exist, however, may be explained by the causes and effects hypothesized in Chapter II. The relationship between bottom loss and porosity agrees quantitatively with that predicted on theoretical grounds. The slopes of the lines of best fit for the experimental points are . 171 and .166 db per percent porosity for bottom loss measured on a peak-pressure and total-energy basis, respectively; in this porosity range the theoretical curve of bottom loss versus porosity (Figures 40 and 41) is approximately linear; and posesses a slope of . 20 db per percent porosity. It is believed that much of the scatter of the

experimental points about the theoretical curve is due to positional error in sampling, and that the bottom loss versus porosity relationship would have shown the strongest correlation if the water-content measurements had been made on the original suite of sediment samples. The relationships found between bottom loss and all the sedimentological characteristics tested agree qualitatively with those qualitatively postulated on heuristic grounds.

The sediments are plotted on a three component textural diagram, and the values of bottom loss measured at the corresponding station sites are indicated by a system of color coding (Figures 52 and 53). Sand (gravel included), silt, and clay are used as the end members of the diagram and the regions that correspond to the sediment class categories defined by Shepard (Shepard, 1954) are delineated. This type of presentation facilitates comparison between the bottom loss measurements and both the sand-silt-clay ratios and the class names of the sediments.

The relative proportions of the end members present in the sediment are given by the positions of the points plotted in the diagram; where more than one sample has the same composition, the points are plotted on a horizontal line extending out of the diagram and the composition is given by the position of the rightmost point. Samples containing more than 20% gravel are noted by a black circle around the plotted point.

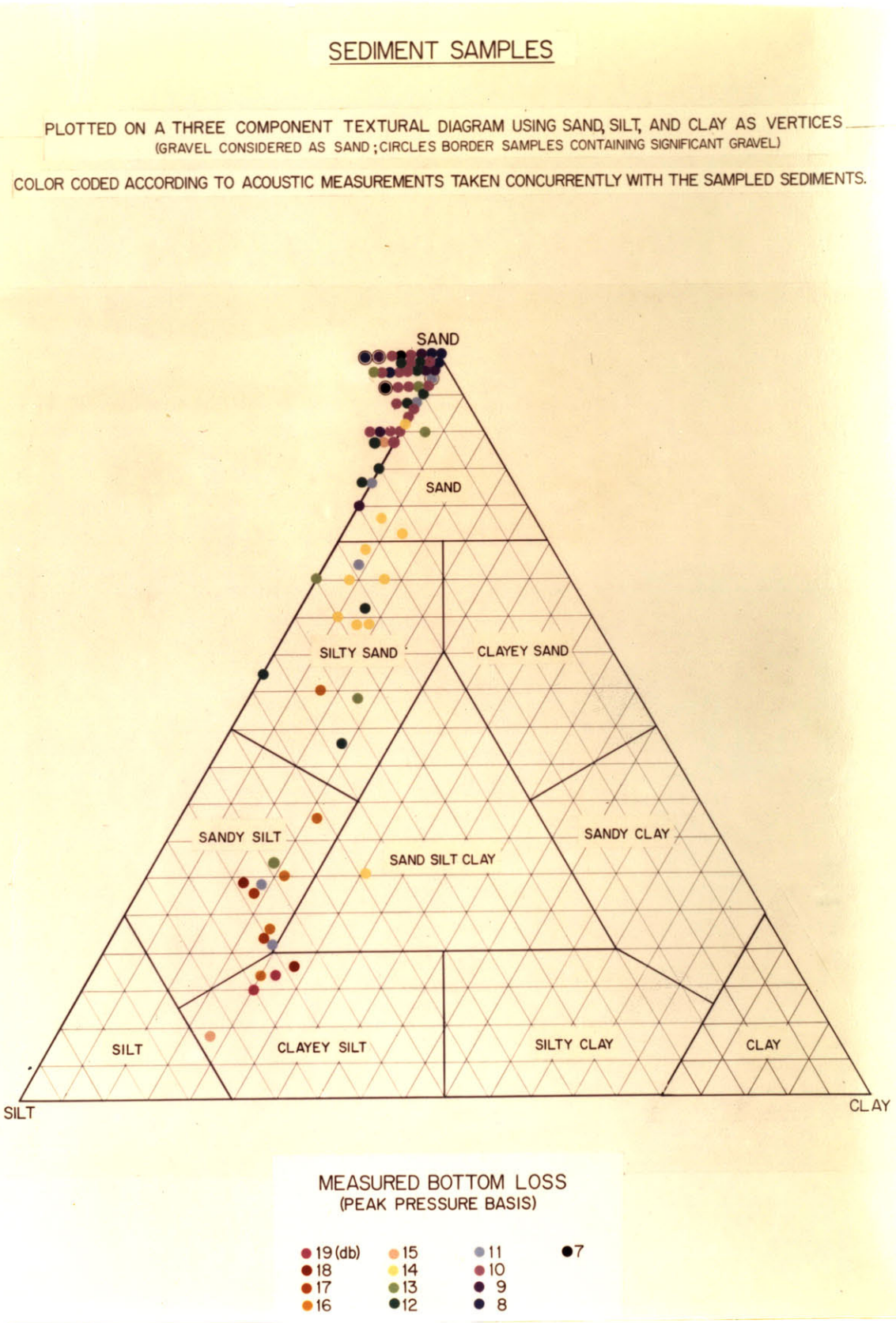

Figure 52. Bottom Loss Measurements (Peak Pressure Basis) at Sediment Stations Color Coded and Plotted on a Sand-Silt-Clay Diagram.

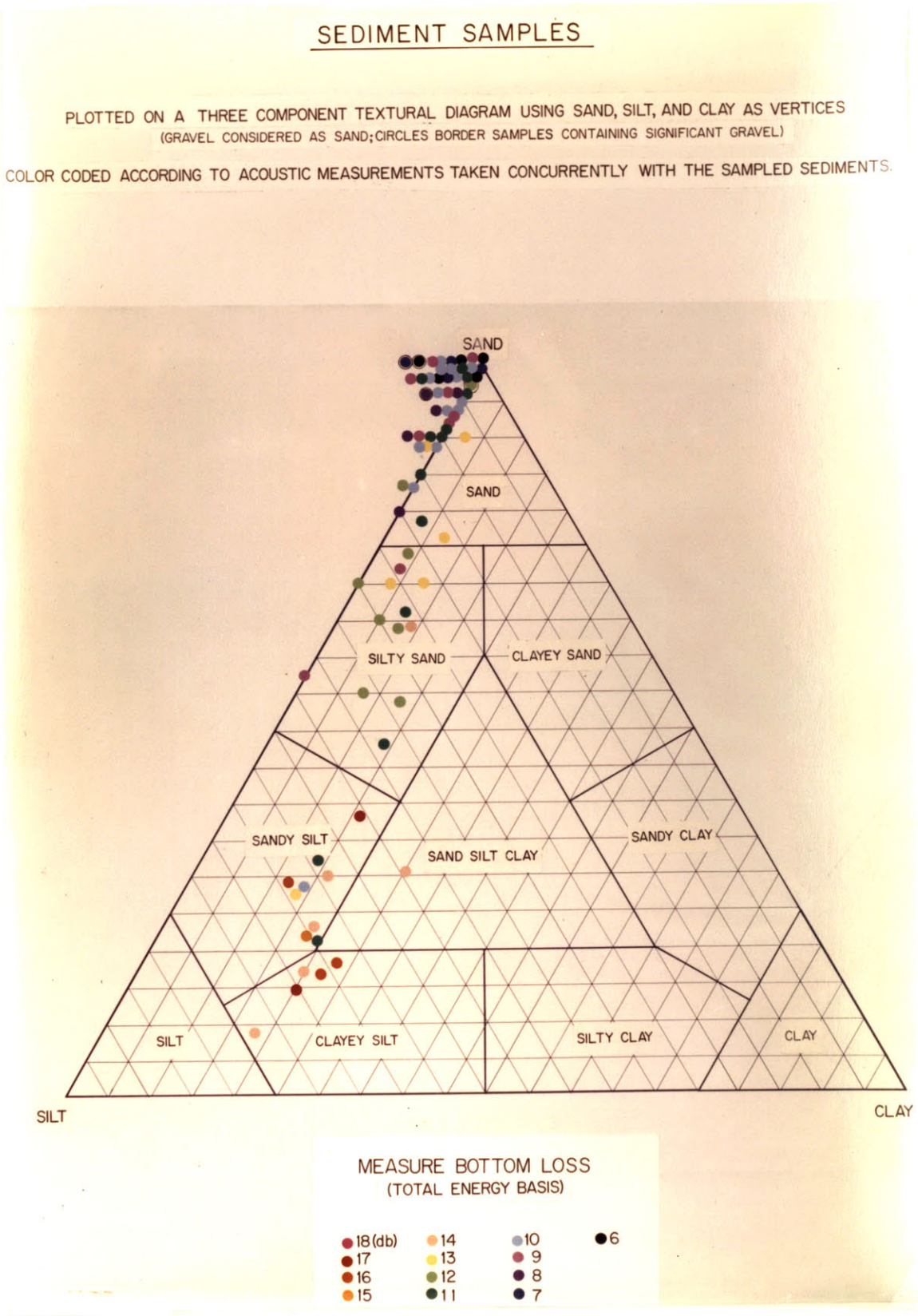

Figure 53. Bottom Loss Measurements (Total Energy Basis) at Sediment Stations Color Coded and Plotted on a Sand-Silt-Clay Diagram.

Bottom loss is displayed for measurements made on both a peak-pressure and total-energy basis according to a system in which the warmth of the color plotted represents the magnitude of the bottom loss. Each individual color represents a one decibel range of bottom loss. The absolute values of the colors are presented in the legends contained in the figures.

Inspection of figures 52 and 53 shows the correlation between acoustic bottom loss and sediment type. A visual traverse made from the sand vertex (100% sand) to the opposite side (100% fine material) shows an overall progression in the warmth of the colors plotted. Since the horizontal grid lines in the diagram represent loci of equal sand content, this traverse demonstrates the general tendency of bottom loss to increase as the percentage of fine material in the sediment increases. The cluster of cold, intermediate, and warm colors in the sand, silty sand, and both sandy silt and clayey silt zones, respectively, indicate that sand is a good reflector, silty sand is a moderate reflector and both sandy silt and clayey silt are poor reflectors. In particular, the average values of bottom loss for sand, silty sand, sandy silt and clayey silt are 10. 9 db, 13. 8 db, 15. 4 db, and 16. 0 db, respectively, when measured on a peak-pressure basis and 9. 8 db, 12. 2 db, 13. 8 db, and 15. 8 db, respectively, when measured on a total-energy basis.

Narragansett Bay Area

An investigation of the relationship between acoustic bottom loss and bottom sediment was made in the Narragansett Bay area. This area was selected because its geology had previously been studied and published (McMaster, 1960), and because of its proximity to the Woods Hole Oceanographic Institution. Approximately thirteen-thousand acoustic measurements were taken at different locations. Samples of sediment were taken at 32 different locations to check and supplement the published geological control.

The values of acoustic bottom loss, measured on both a peak-pressure and total-energy basis, have been color coded according to the system previously mentioned and plotted on charts of the area (Figures 54 and 55). The sites of the sediment stations are indicated by numerals and arrows, and the characteristics of the samples are listed in Tables III and IV. Transparent overlays showing the distribution of sediment types and showing the zonal distribution of sand content (after McMaster) are hinged to the edges of the figures, and may be flipped onto the chart to compare the quantities they represent with the measurements of acoustic bottom loss. The exactness of the boundaries of these distribution patterns must be viewed in the light of the sample spacing used by McMaster; this was a grid of one-half minute spacing within the Bay proper and one minute spacing off-shore.

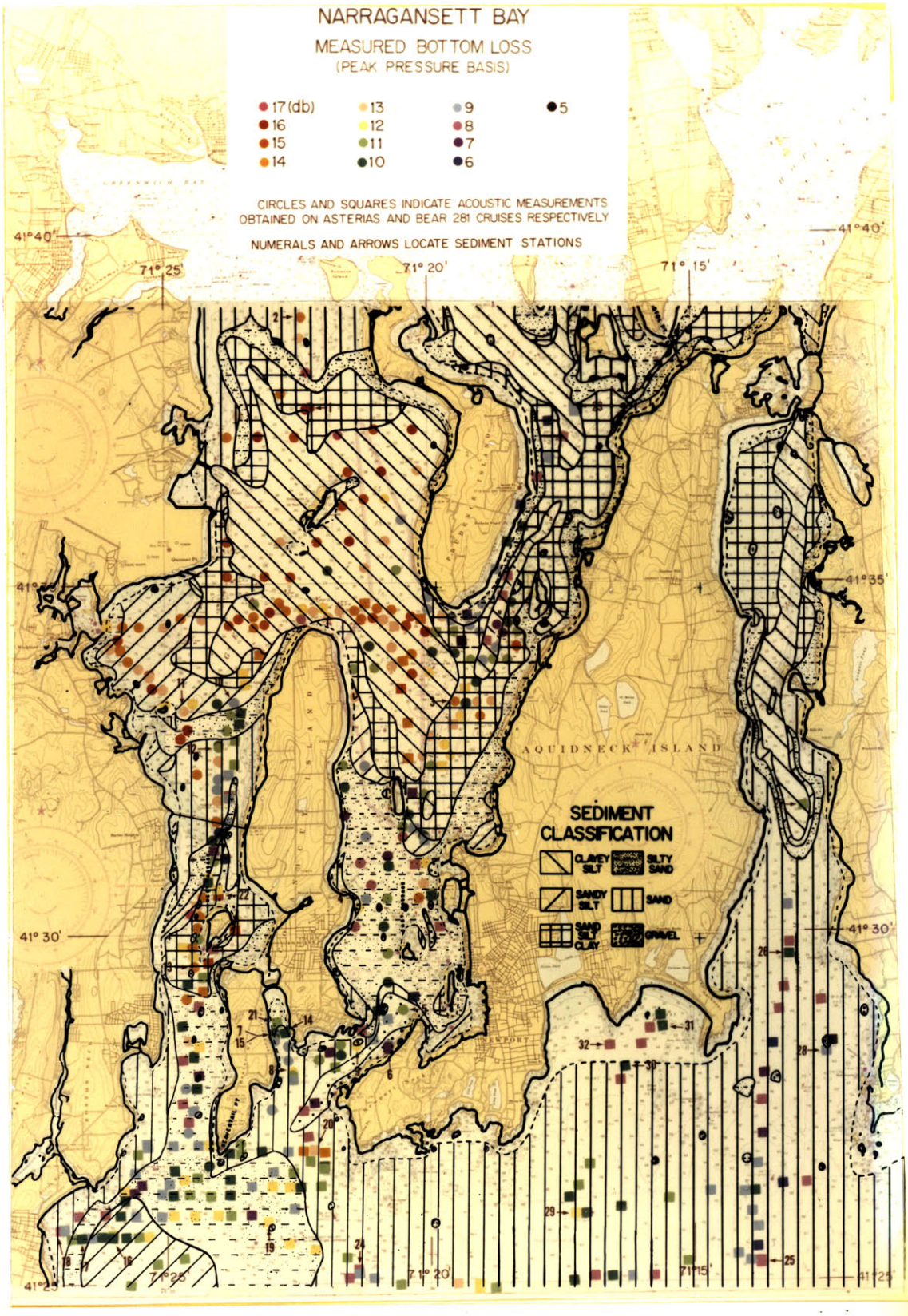

Figure 54. Bottom Loss Measurements (Peak Pressure Basis) Color Coded and Plotted on a Chart of Narragansett Bay.

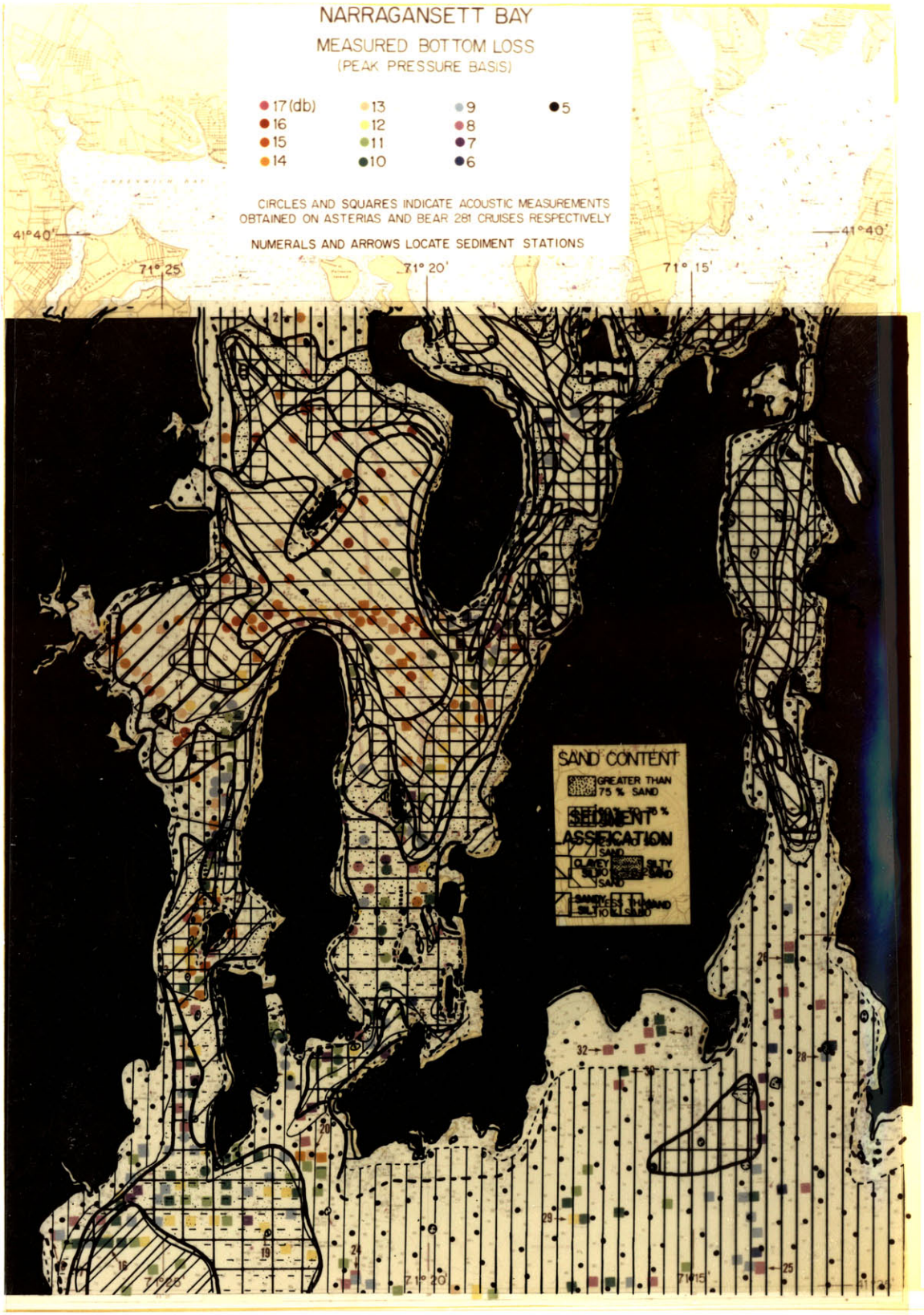

Figure 54. Bottom Loss Measurements (Peak Pressure Basis) Color Coded and Plotted on a Chart of Narragansett Bay.

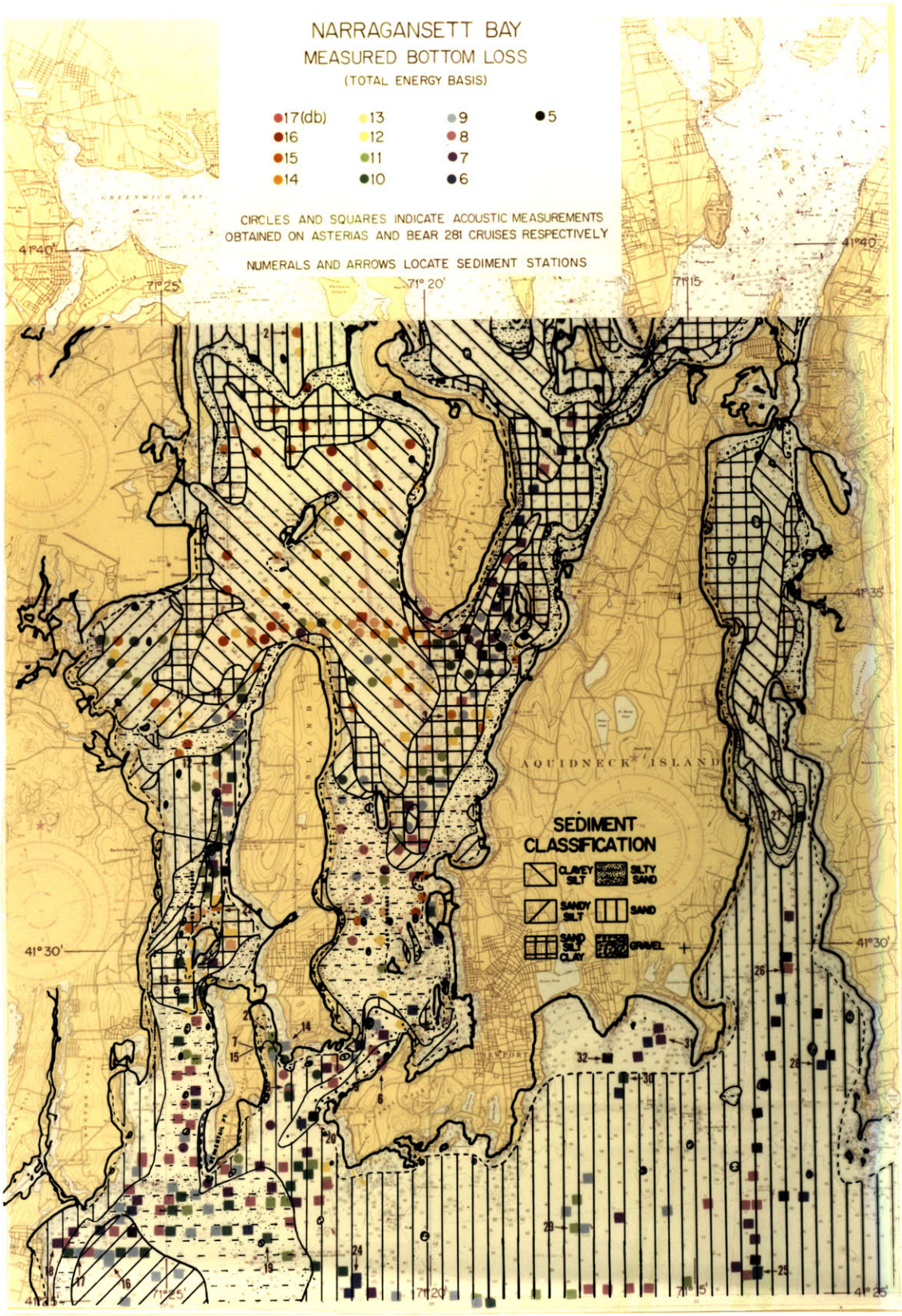

Figure 55. Bottom Loss Measurements (Total Energy Basis) Color Coded and Plotted on a Chart of Narragansett Bay.

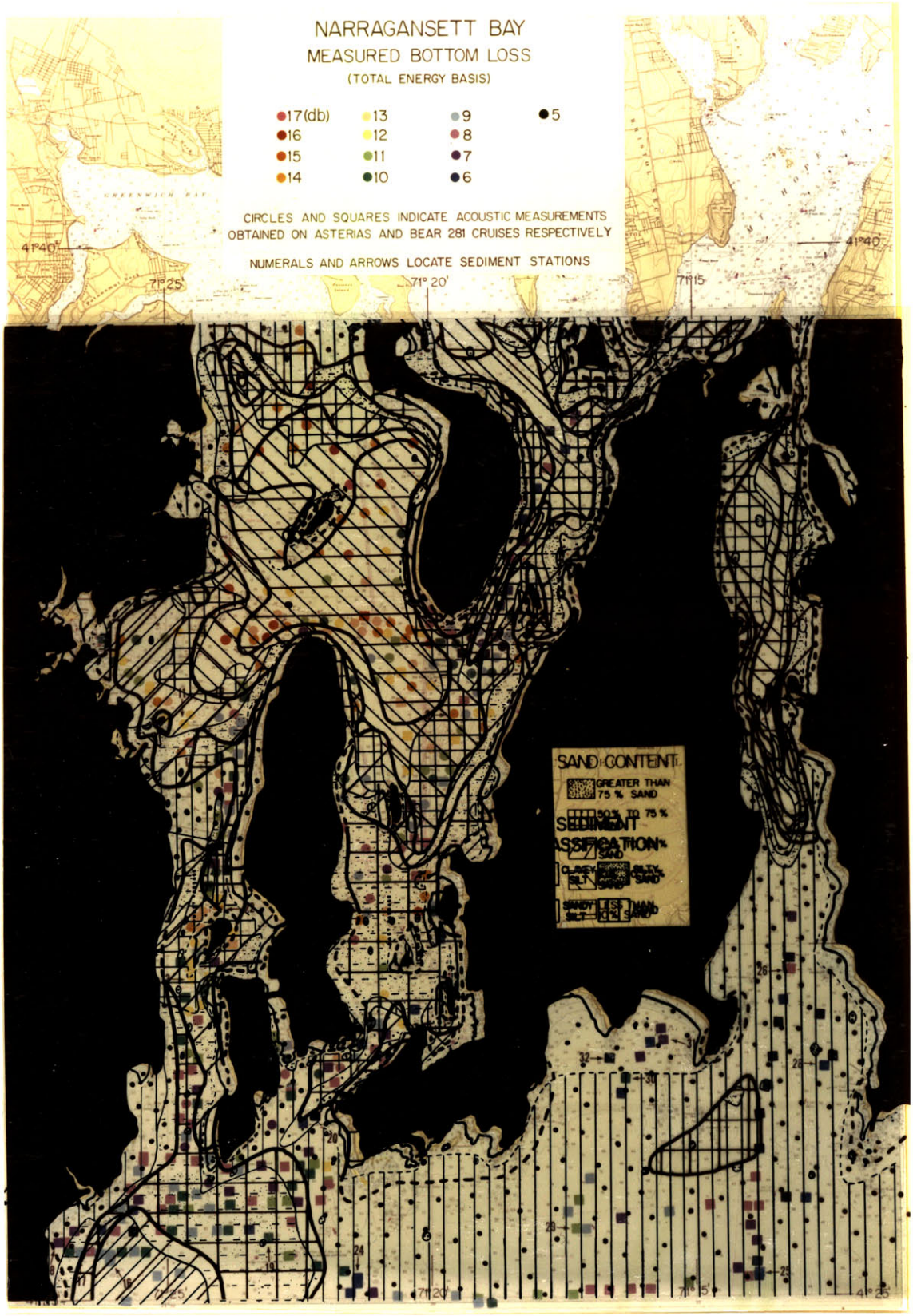

Figure 55. Bottom Loss Measurements (Total Energy Basis) Color Coded and Plotted on a Chart of Narragansett Bay.

Inspection of Figures 54 and 55 with both overlays flipped off of the chart shows that while the measurements of bottom loss made on an energy basis tend to be about 1 db lower than those made on a pressure basis, the general spatial distribution of the acoustic reflectivity of the region is the same for measurements made on either basis. The slight discrepancy in absolute value between the two types of acoustic measurements is ascribed to the reverberation component in the echo which is integrated along with the specular component when bottom loss is measured on a total-energy basis. Nevertheless, the equivalence of the patterns of relative reflectivities of this region, when measured on either basis, and the knowledge that the region encompasses a large variety of sediment types, leads to the conclusion that bottom loss measured on either basis is indicative of the same characteristic of the bottom sediment.

A comparison of the measurements of bottom loss and the sand content of the sediment is achieved by inspection of Figures 54 and 55 with the appropriate overlays flipped onto the charts. When this is done, it becomes apparent that generally the areas in which the sand content of the sediment is high (greater than 75 percent), moderate (between 50 and 75 percent) and low (less than 50 percent) respectively, exhibit high (cold colors), intermediate (intermediate colors) and low (warm colors) degrees of acoustic reflectivity.

In particular, good agreement is found for the extensive region of high-sand-content sediment south of Aquidneck Island extending into the mouths of East and Sakonnet Passages, the strip of high-sand-content sediment along the western border of the mouth of West Passage, the tongue of high-sand-content sediment extending almost across West Passage at its mid-point, the region of moderate-sand-content sediment in the middle and lower section of East Passage, the region of moderate-sand-content sediment south of Conanicut Island, the extensive region of low-sand-content in the upper bay extending down into the upper sections of both East and West Passages, and the region of low-sand-content sediment in the lower-middle section of West Passage. A lack of agreement is found for the small region of high and moderate-sand-content sediment in the topmost section of the upper bay, the region of low-sand-content sediment east of Prudence Island. This is believed to result from a disharmony between the sediments that exist in specific parts of these regions and those generally indicated on the overlay; the samples at Stations 2 (sand-silt-clay) and 16 (silty sand) are low and high-sand-content sediments, respectively, and the area south of Prudence Island has been and still is a dumping ground for dredged material (McMaster, 1960), (Captain Harold Payson, personal communication).

A comparison of the measurements of bottom loss and the type (class-name) of the sediment is achieved by inspection of figures 54 and 55 with the appropriate overlays flipped onto the charts. When this is done it becomes apparent that, in general, regions of sand or gravel exhibit a high degree of acoustic reflectivity (cold colors), regions of silty sand exhibit an intermediate degree of acoustic reflectivity (intermediate colors), and regions of sandy silt, clayey silt, or sand-silt-clay, exhibit a low degree of acoustic reflectivity (warm colors). This is to be expected in view of the relationship previously observed between bottom loss and sand content, since the class-name of a sediment is related to its sand content; sands contain more than 75% sand, silty sands usually contain between 50 and 75% sand, and sandy silts, clayey silts, and sand-silt-clays usually contain less than 50% sand.

The extent to which the measurements of bottom loss are related to the published geological control has been discussed in the above paragraphs. The results of this experiment indicate a definite correlation between the measurements of bottom loss and both the sand-content and class-name of the sediment. Bottom loss increases as the sand-content of a sediment decreases. Bottom loss also increases as the sediment type progresses from sand to silty sand to sandy silt, sand-silt-clay, or clayey silt.

Shallow Water Profiles

An investigation of the relationship between acoustic bottom loss and bottom sediment was made along two separate profiles on the continental shelf; one extending due south from Martha's Vineyard for a distance of 65 miles and the other extending south by east from Block Island for a distance of 58 miles. These particular profiles were selected because their geology had previously been studied and published (Stetson, 1938) and because of their proximity to the Woods Hole Oceanographic Institution. Approximately seven-thousand acoustic measurements were taken at 230 different locations. Samples of sediment were taken at 40 different locations to check and supplement the published geological control.

The values of acoustic bottom loss, measured on both a peak-pressure and total-energy basis, have been color coded according to the system previously described and plotted on charts of the area (Figures 56 and 57). The sites of the sediment stations are indicated by numerals and arrows and the characteristics of the samples are listed in Tables III and IV. Pictorial representations of the amounts of sand, silt, and clay in the sediment, based on the samples obtained during this investigation and those published by Stetson, are presented in conjunction with the acoustic measurements to facilitate comparison between them.

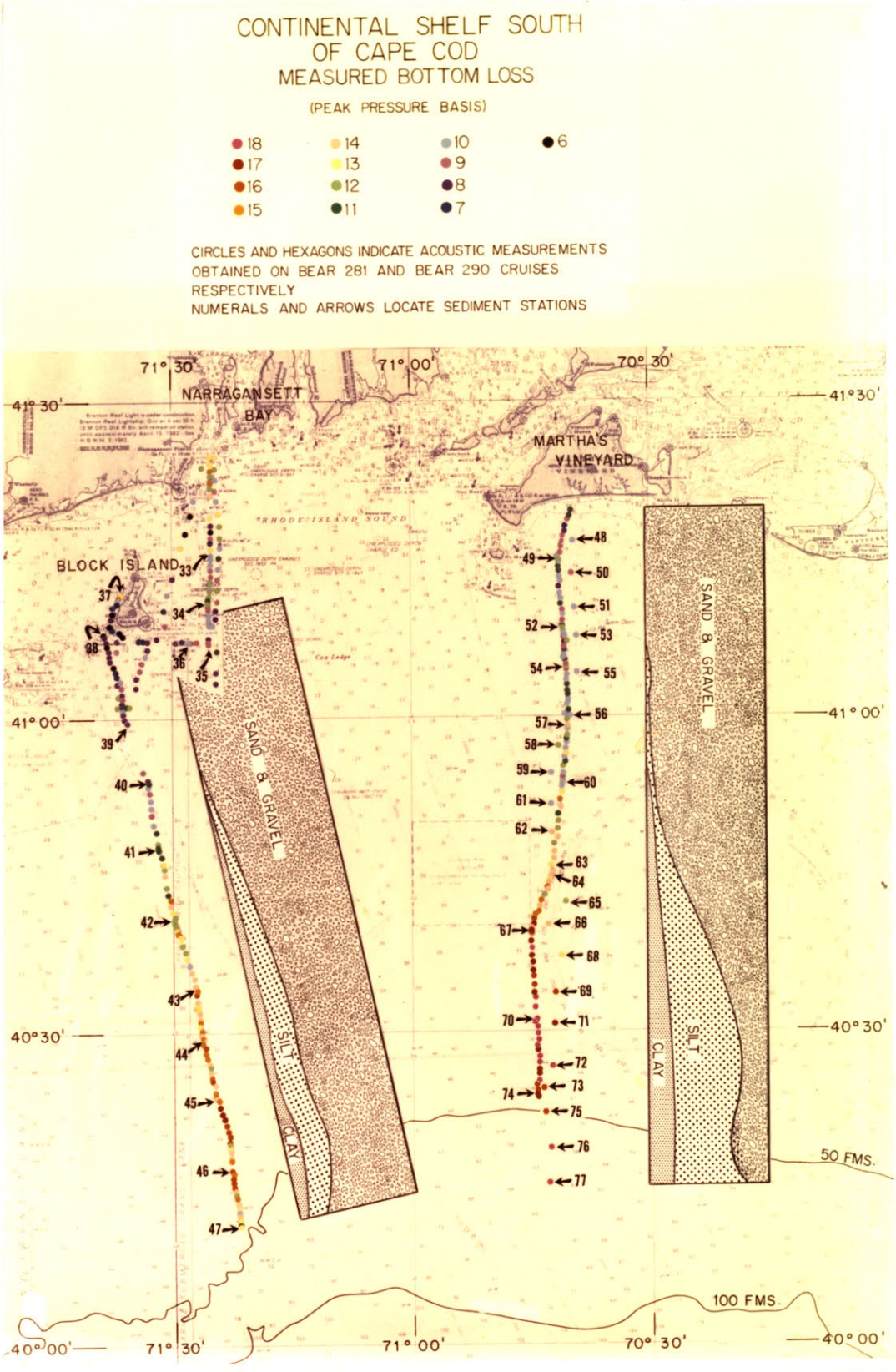

Figure 56. Bottom Loss Measurements (Peak Pressure Basis) Color Coded and Plotted on a Chart of the Continental Shelf South of Cape Cod.

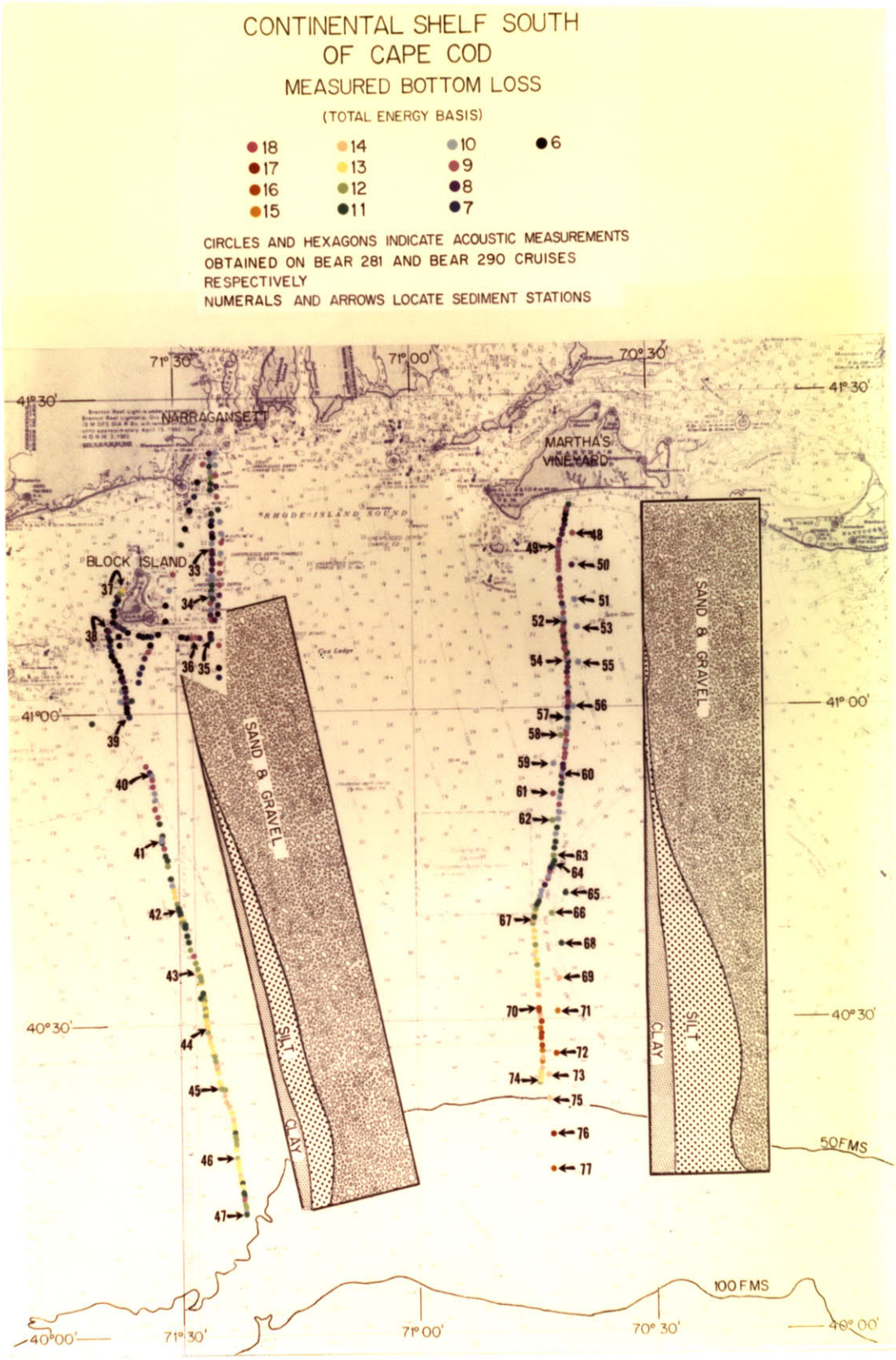

Figure 57. Bottom Loss Measurements (Total Energy Basis) Color Coded and Plotted on a Chart of the Continental Shelf South of Cape Cod.

Inspection of Figures 56 and 57 shows a decrease in acoustic reflectivity (increase in the warmth of color plotted) progressing seaward along both profiles, which is associated with a decrease in sediment sand content (increase in silt + clay). In particular, the Martha's Vineyard Profile is characterized by a long section of cold colors (good reflectors) abruptly followed by a short section of intermediate colors (moderate reflectors) abruptly followed by a long section of warm colors (poor reflectors), and the Block Island Profile is characterized by a short section of cold colors (good reflectors) gradually followed by a long section of predominately intermediate colors (moderate reflectors). These acoustic trends are representative of the geological control. Well sorted sands gravels are present at the inshore ends of the profiles and grade outward toward poorly sorted silts and clays; the zoning is abrupt and the content of fine material increases to about 80 % along the Martha's Vineyard Profile, whereas the zoning is blurred and the content of fine material increases to only about 60 % along the Block Island Profile (Stetson, 1938).

In addition, acoustic, mass, and grain-size characteristics are jointly displayed versus distance in miles along both the Martha's Vineyard (Figure 58) and Block Island (Figure 59) profiles. The top two curves represent acoustic measurements of bottom loss on a

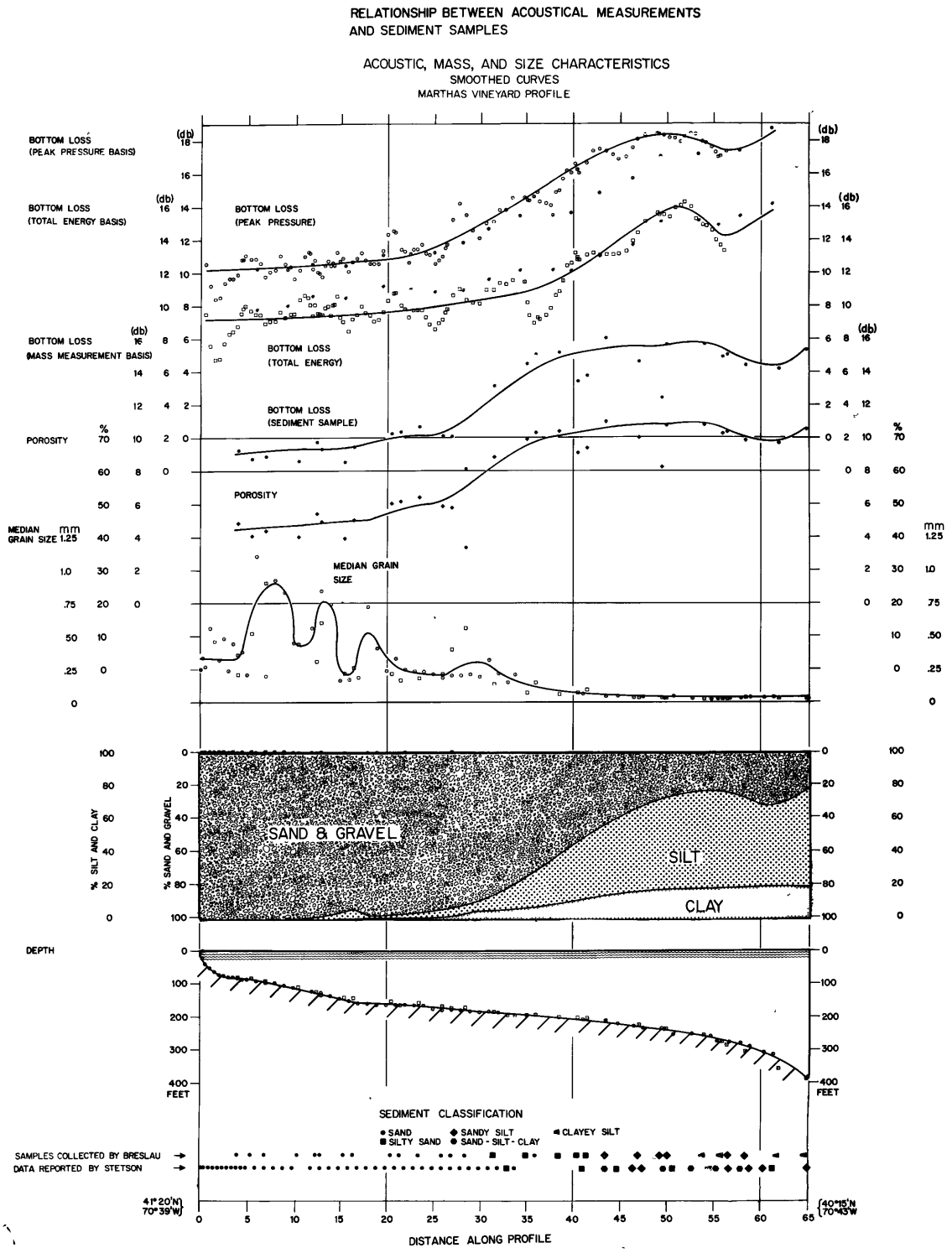

Figure 58. Acoustic, Mass, and Size Characteristics Plotted Versus Distance Along the Martha's Vineyard Profile.

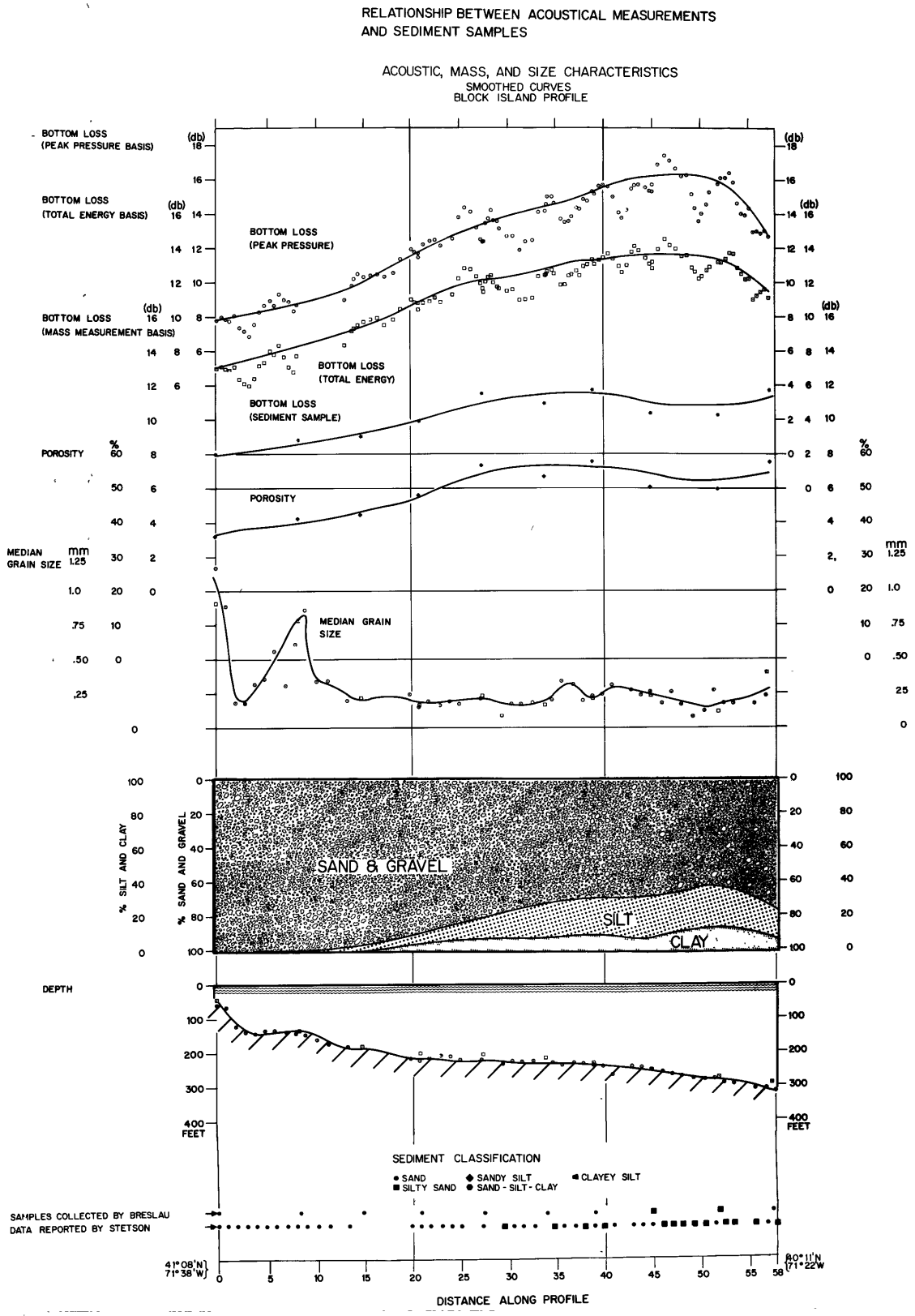

Figure 59. Acoustic, Mass, and Size Characteristics Plotted Versus Distance Along the Block Island Profile.

peak-pressure and total-energy basis, respectively (each point represents the running average of three measurements); the next two curves down represent bottom loss and porosity calculated from the measured water content of the samples; the next curve down represents the median grain size measured from the sediment samples; below this is a pictorial representation of the sand, silt, and clay fraction of the sediment; below this is a plot of the bathymetry based on water depths obtained in this investigation and published by Stetson; and lastly, the class-names of the sediments that were sampled along these profiles either during this investigation or by Stetson are indicated by symbols coded according to the accompanying legend. This type of presentation facilitates comparison between all of the qualities mentioned.

As noted previously the curves representing bottom loss, measured on either a peak-pressure or total-energy basis, versus distance in miles along profile, have a similar shape which indicates that both types of measurement sense the same characteristic of the bottom sediment. The measurements of bottom loss made on an energy basis tend to be about 1.5 db lower than those made on a pressure basis which is attributed to reverberation in the echo. The curves of bottom loss, calculated from the measured water content of the second set of sediment samples, versus distance along profile, have a shape that is similar to the cruves of directly

measured bottom loss versus distance along profile. This is considered significant evidence of a correlation between measured bottom loss and mass characteristic of the sediment. The absolute values of the computed bottom losses are slightly lower than the measured bottom losses but this is considered not significant in view of the experimental uncertainty in the absolute measurement of bottom loss. Finally, the similarity between the curves of computed bottom loss and measured porosity is noted. This is due to the approximately linear relationship between these qualities (Figure 3) over the range of porosities experienced in this investigation.

The curves of measured bottom loss versus distance in miles along profile are representative of the zoning of sediments parallel to the shore that was reported by Stetson; the zoning of sediments along the Block Island Profile is less distinct than along the Martha's Vineyard Profile. The bottom loss measurements best represent the percentage of fine material (silt + clay) in the sediment. This is explained by the association between porosity and percentage of fine material in the sediment that was hypothesized in Chapter II and is demonstrated here. While the bottom loss measurements are generally related to grain size, they are affected very little by the wide variations in the median grain size that occur in the northern

sections of the profiles. The reason for this is that the porosity of well-sorted pure sands, which are present there, is not strongly dependent on grain size.

The results of this experiment indicate a definite correlation between the acoustic measurements of bottom loss and the mass and grain-size characteristics of the sediment. Bottom loss increases as the porosity of the sediment increases. Bottom loss also increases as the percentage of silt + clay in the sediment increases (or as the sand-content of the sediment decreases) and as the sediment type progresses from sand to silty sand to sandy silt, sand-silt-clay, or clayey silt.

Deep Water Profiles

Long profiles of acoustic bottom loss were made during the early phase of this investigation to observe the range and variability of acoustic reflectivity present in the natural environment and to establish the repeatibility of this type of measurement. Two profiles (the "Bermuda" Profiles) were made along a track from Bermuda to Woods Hole and one profile (the "Puerto Rican" Profile) was made along a north-south track centered approximately west of Bermuda. The geological control over these profiles is not so good as that attained in the shallow-water investigations since the geology of the deep-water regions is not so well known and it was not

convenient to obtain sediment samples during the investigation. Nevertheless, since the profiles extend over various physiographic provinces of the ocean, it is at least possible to compare broadly the measurements of bottom loss on this basis.

Approximately six and a half-thousand acoustic measurements were taken at 340 different locations. The values of acoustic bottom loss, measured on both a peak-pressure and total-energy basis, have been color coded according to the system previously described and plotted (Figures 60 and 61) on physiographic charts (Heezen et al., 1959).

Inspection of Figures 60 and 61 shows that the outer continental shelf, the continental slope, and the Bermuda rise are poor reflectors and the continental rise and abyssal plain are good reflectors; the poorest reflectors are found on the Bermuda rise at a great distance from the continent and the best reflectors are found on the abyssal plain at the base of the continental rise. This pattern of acoustic reflectivity may broadly be explained by the type of sediment that is characteristic of these physiographic provinces in this region. The outer continental shelf is characterized by fine sediments with a narrow band of coarse sediment along the crest of the shelf break (Stetson, 1938). The continental slope receives fine material winnowed off the shelf (Stetson, 1949) (Uchupi, 1963). The sediments of the continental rise and abyssal plain are likely to be composed of turbidites (generally coarse material) that have originated on the

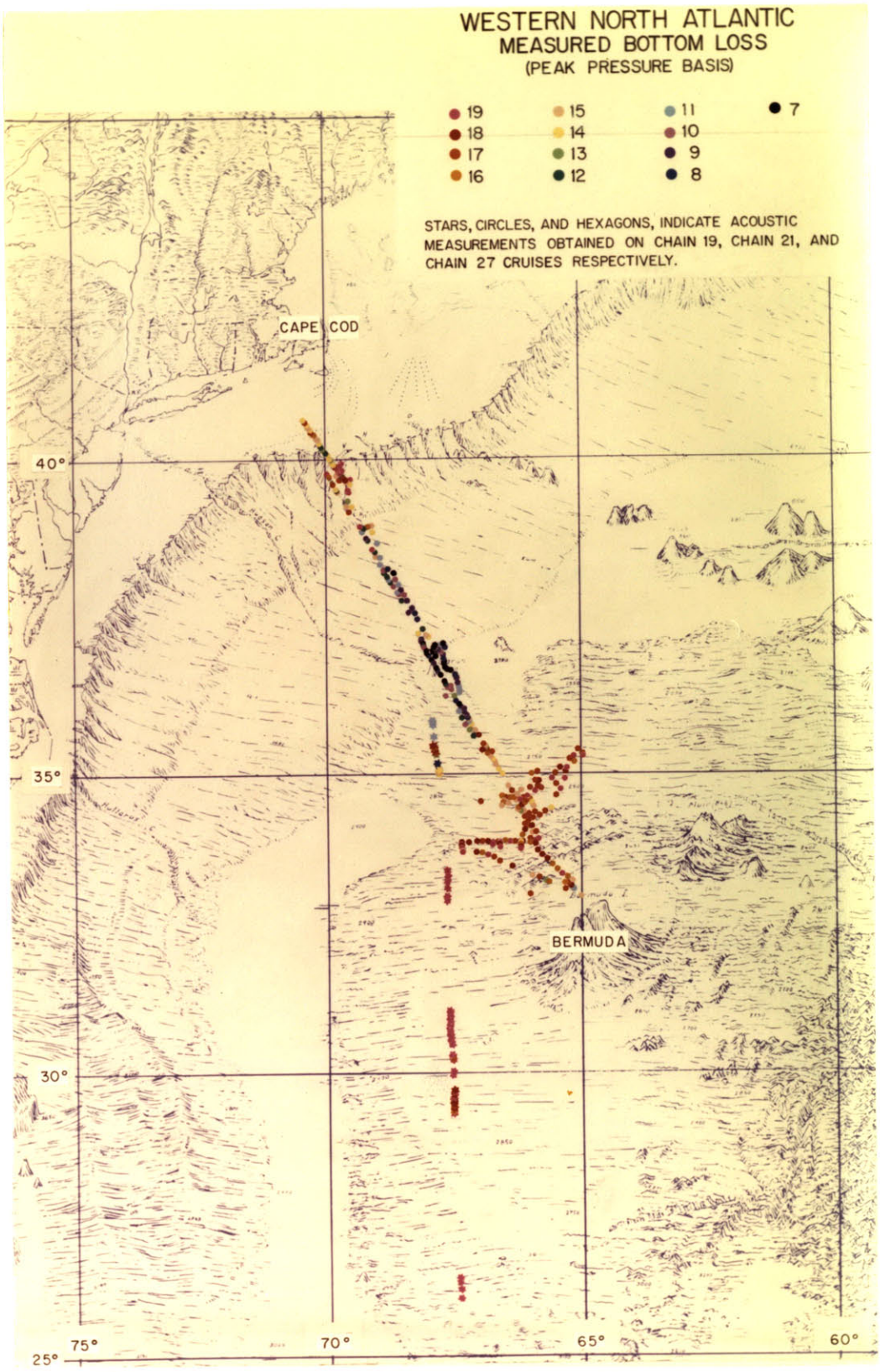

Figure 60. Bottom Loss Measurements (Peak Pressure Basis) Color Coded and Plotted on a Physiographic Map (After Heezen et al., 1959) of the Western North Atlantic.

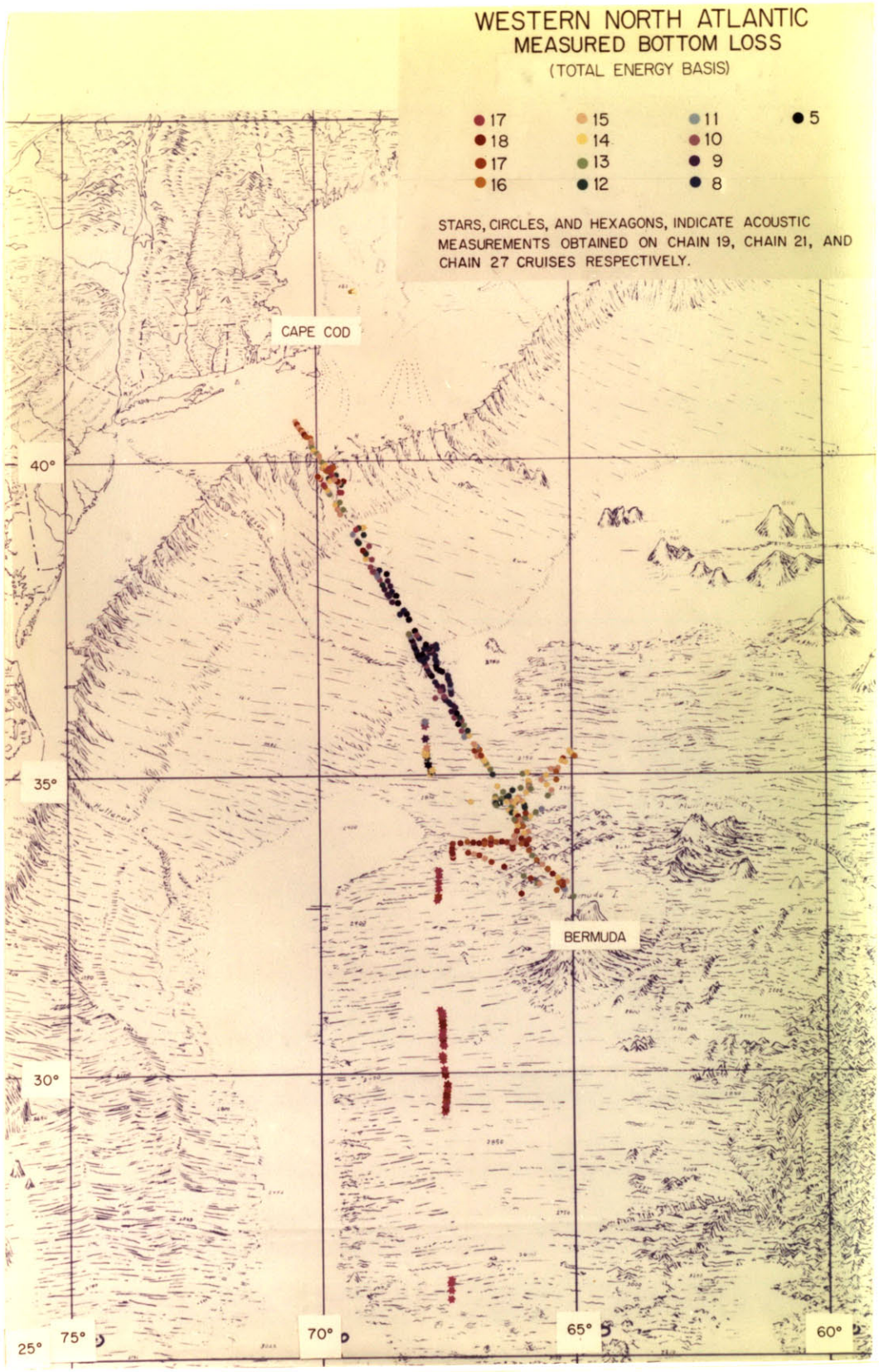

Figure 61. Bottom Loss Measurements (Total Energy Basis) Color Coded and Plotted on a Physiographic Map (After Heezen et al., 1959) of the Western North Atlantic.

continent and flowed down the various submarine canyons on the continental slope; Block Canyon, Atlantis Canyon, and Veatch Canyon are present in this area. The Hudson Canyon cuts across the continental slope and rise and empties into the abyssal plain near Caryn Seamount to form a large alluvial delta (Heezen et al., 1959). A large majority of the sediment cores taken on the continental rise and abyssal plain in this region (Ericson et al., 1961) contain sand and silt; those on the Bermuda Rise do not. This is because the deposition of turbidites is terminated by the topographic irregularities that skirt the edge of the Bermuda rise and only pelagic sedimentation containing generally fine material occurs on the Bermuda Rise.

Measurements of bottom loss on both a peak-pressure and total-energy basis, their standard deviations, and the bathymetry based on echo-soundings obtained during this investigation, are jointly displayed in Figures 62, 63, and 64 for measurements made on the "Puerto Rican" and "Bermuda" Profiles, respectively. The values of the acoustic measurements have been smoothed by taking the running average of three measurements. The measurements made on the "Bermuda" profiles have been plotted versus distance in miles along their common track, with Bermuda taken as its origin.

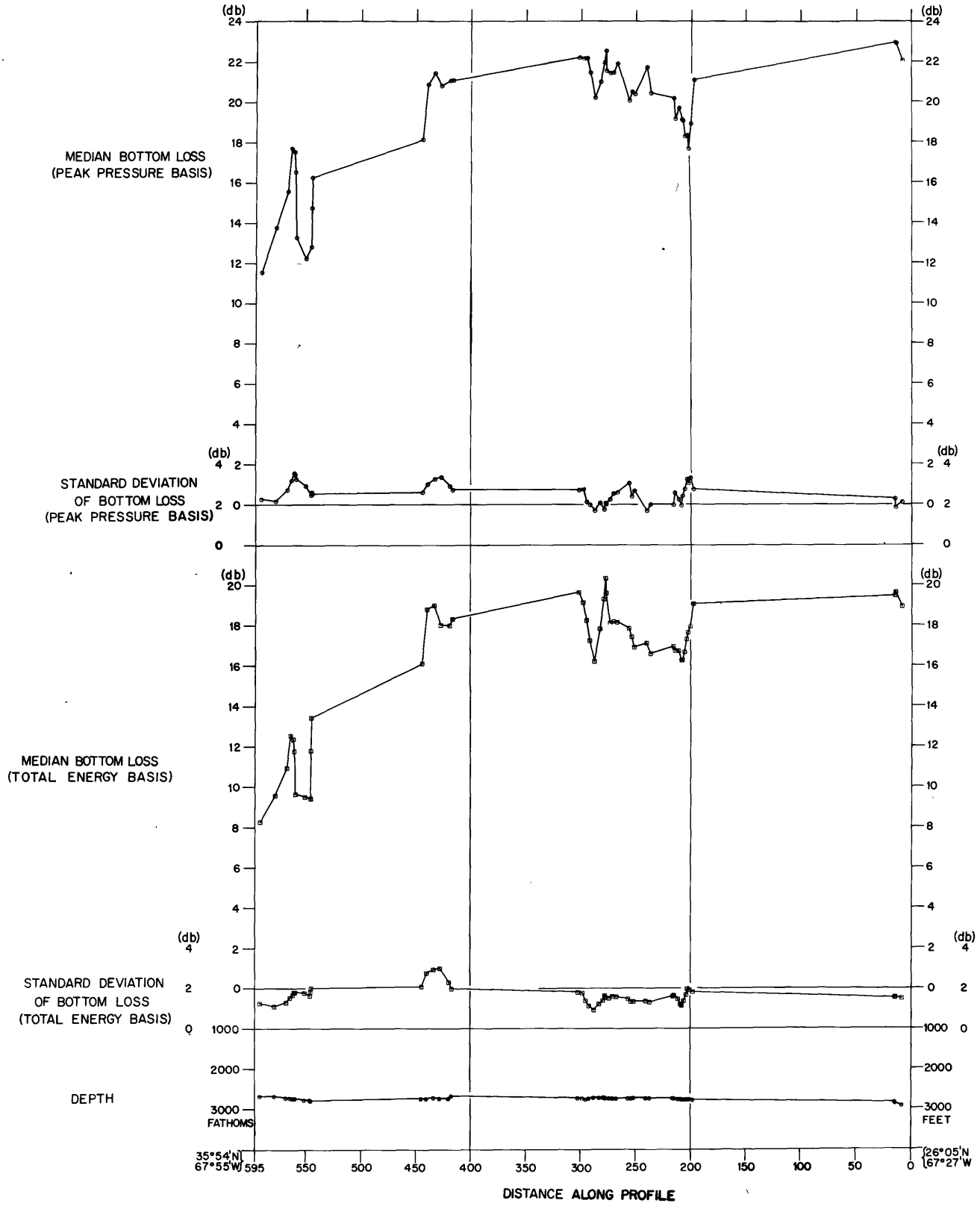

Figure 62. Bottom Loss Measurements (Running Average) Made During the CHAIN 19 Cruise Plotted Versus Distance Along the Puerto Rico Profile.

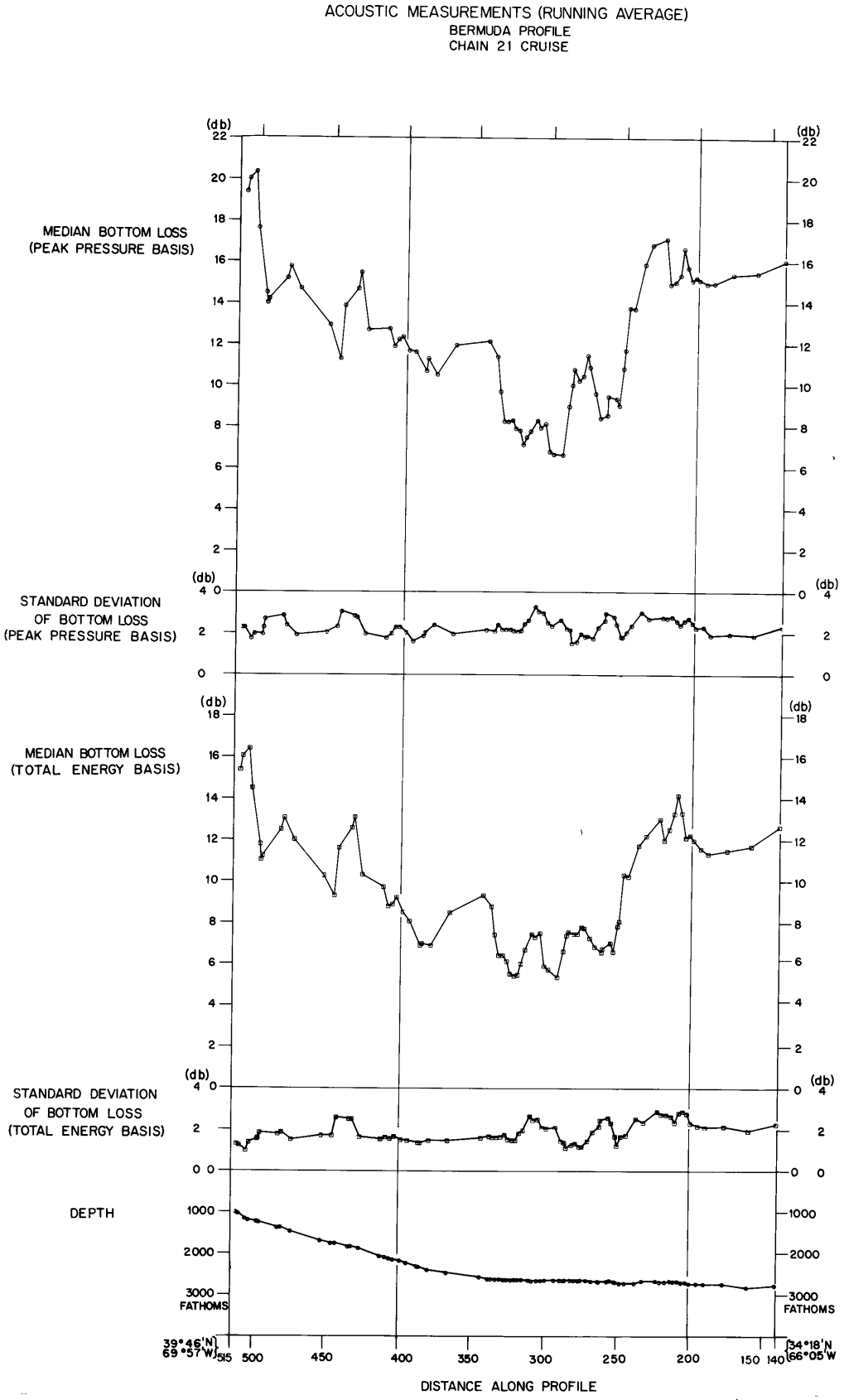

Figure 63. Bottom Loss Measurements (Running Average) Made During the CHAIN 21 Cruise Plotted Versus Distance Along the Bermuda Profile.

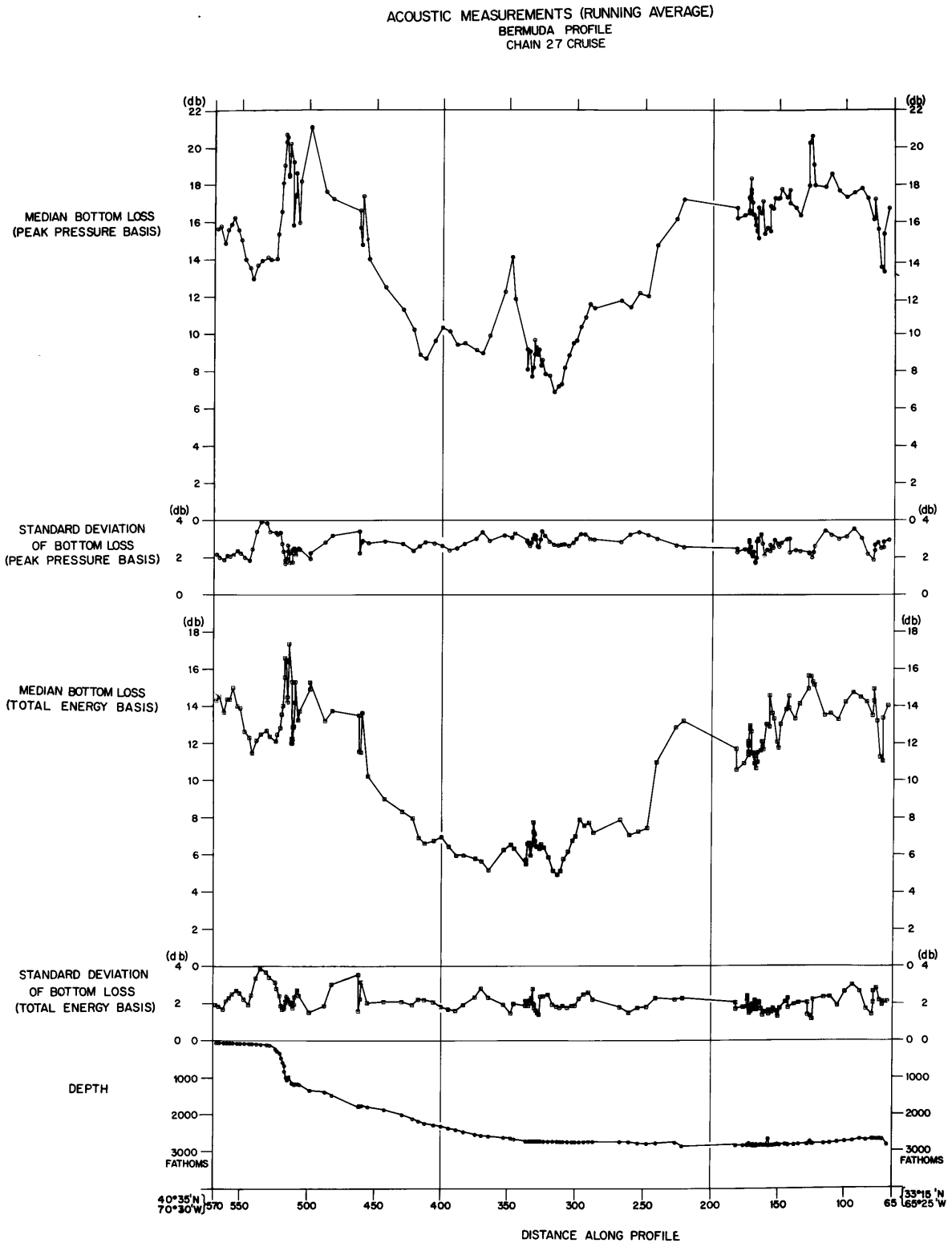

Figure 64. Bottom Loss Measurements (Running Average) Made During the CHAIN 27 Cruise Plotted Versus Distance Along the Bermuda Profile.

Inspection of Figures 62, 63, and 64 shows that the curves representing bottom loss, measured on either a peak-pressure or total-energy basis, versus distance along profile, have a similar shape which indicates that both types of measurement sense the same characteristic of the bottom sediment. The measurements of bottom loss made on an energy basis tend to be about 2 db lower than those made on a pressure basis which is attributed to reverberation in the echo. Inspection of Figures 63 and 64 shows that the curves of bottom loss versus distance along profile are similar for measurements made over the same section of the common track. This attests to the repeatibility of the bottom loss measurements since each of the Bermuda Profiles was obtained during a different cruise.

The results of this investigation are mainly contained in the presentation of measurements of bottom loss per se. along long profiles in the deep sea. It has been shown that these measurements are repeatible and that their values may broadly be explained in terms of the sediments characteristic of the physiographic provinces in this region.

CHAPTER X

CONCLUSION

Summary and Conclusions

1) Acoustic reflectivity of the sea floor is indicative of certain properties of the sediment, such as porosity, silt-clay percentage, and grain size, and also indicative of sediment type as defined by the Shepard (1954) system of nomenclature. While this sort of result is known from other work the present demonstration is valuable because of its detail and extent.

2) A practical technique was developed that could be used for routine acoustical surveying of sediments on the sea floor from a vessel underway. A highly automated system of data collection and analysis was developed, tested, and brought to a usable form. A present shortcoming is that oscilloscope photographs produced by the shipborne measurement system must be digitized by hand before being processed by the land-based digital computer.

3) An extensive investigation of acoustic reflectivity was made in shallow water and compared with the geological studies of other investigators. Acoustic reflectivity correlates well with the silt-clay percentage, grain size, and sediment type reported by Stetson (1938) along profiles on the continental shelf south of Cape

Cod, and with silt-clay percentage, and sediment type (grain size was not available) reported by McMaster (1960) in Narragansett Bay. Acoustic reflectivity correlates even better with the same properties of sediment samples taken during the present investigation in these areas.

4) The range and variability of acoustic reflectivity in deep water along long profiles was established. Two profiles were made along a track from Bermuda to Woods Hole and one profile was made along a north-south track centered approximately west of Bermuda. The results show that along these tracks the outer continental shelf, the continental slope, and the Bermuda rise are poor reflectors and that the continental rise and abyssal plain are good reflectors.

5) A shipborne instrument system to measure the peak pressure and integral of the squared pressure of a hydroacoustic transient was developed. This is of general utility in sound propagation studies.

Recommendations for Furture Work

1) Investigations should be made over all water-covered areas and especially the deep sea, to obtain more data on the relationship between acoustic reflectivity and properties of the

sediment as well as to map the sediment of the region per se. Data on the relationship between acoustic reflectivity and the very fine-grained sediments of the deep sea are particularly lacking. In addition, the advantage of acoustic surveying over sediment dredging is maximized in deep water due to the considerable time required to obtain a sample by the latter method.

2) Measurements of acoustic reflectivity should be taken in parallel with samples of sediment and in situ measurements of sound velocity and density of the sediment. Sound velocity and density, respectively, can be obtained by measurements of travel time and gamma ray absorption between probes inserted in the sediment.

3) The shipborne instrumentation system should be further refined to facilitate its use in routine surveying. The measurements should be recorded either directly in a machine-language form that is acceptable to a shore-based digital computer, or fed directly to a shipborne computer (digital computers are currently being used by oceanographers aboard ships).

4) The present system incorporated many pieces of standard laboratory equipment that were immediately available. Subsequent development could consolidate the system in a single console and drastically reduce its size.

ACKNOWLEDGMENTS

This work represents a joint effort between the Woods Hole Oceanographic Institution and the Massachusetts Institute of Technology. The author's personal support has come from NR 083-157, Contract Nonr 1841(74) with the Office of Naval Research and MIT. The IBM Computation Center at MIT donated time on the 7090 computer located there. Support for equipment, ship time, and computer time on the G. E. 225 computer at WHOI has come from contracts NObsr-72521 and NObsr-89464 with the Bureau of Ships and WHOI. The bulk of this work was actually performed while the author was located at WHOI.

The author extends his deep appreciation to Prof. J. B. Hersey for supervising this thesis and for making the experimental work possible through the facilities of the Geophysics Department at the Woods Hole Oceanographic Institution. Prof. Hersey first suggested, on the basis of his observations of the tonal characteristics of echo-sounding records, that an examination of the magnitudes of echoes from the sea floor would provide useful information about the nature of the sea floor. He has provided numerous valuable and stimulating discussions throughout the course of this thesis.

Many people contributed toward the design and construction of the electronic instrumentation. The author wishes to thank Mr. S. T. Knott, Mr. W. E. Witzell, Mr. W. Dow, Mr. L. Wilharm, and Mr. F. R. Hess for their aid with the acoustic reflectivity system; Dr. H. E. Edgerton and Mr. V. M. McRoberts for their aid with the precisely-timed submersible pinger, and Mr. D. M. Owen for his aid with the self-contained submersible tape recorder.

The success of the sea-going operations was made possible by the officers and crew of the research vessels CHAIN, BEAR, ASTERIAS, ATLANTIS, and CRAWFORD, and the scientific complement on the individual cruises. In particular, Captain H. Payson, Jr. performed the navigation, Mr. D. M. Owen took photographs of the sea floor with his camera, Mr. A. J. Nalwalk, and Mr. W. P. Horner dredged sediment, and Mr. J. E. Stiglitz operated the PGR, on many cruises. The author thanks all of them.

The acoustic data was reduced by Mrs. Fernande Breslau, my wife, who labored in my cause in numerous ways during the completion of this thesis. Needless to say, I am deeply grateful to her for her assistance.

The sediment samples were analyzed with the facilities of the Costal Studies Group at WHOI. Valuable advice and assistance

were proffered by Dr. J. M. Zeigler, Mr. W. D. Athearn, Mr. C. R. Hayes, Mrs. A. Biggs, and Dr. J. S. Schlee. The author appreciates their aid.

The author thanks Mrs. T. F. Webster for her assistance in debugging the computer programs.

This manuscript was written with the editorial assistance of Dr. R. H. Backus, and reviewed by Dr. J. B. Hersey, Dr. R. R. Shrock, and Dr. E. Mencher. The author wishes to thank all of them for their helpful suggestions and criticisms.

The author gratefully acknowledges the assistance of the Graphic Arts Group at WHOI under the direction of Mr. C. S. Innis. Miss C. M. Simons did most of the drafting and Mr. C. E. Spooner did most of the photography. The quality and quantity of the illustrations in this thesis attest to their efforts.

The typing of this manuscript was done by Miss S. S. Rhoads. Mrs. F. K. Mellor and Miss H. C. Hays assisted in the make-up and compilation. The author thanks all of them.

The author extends thanks to Dr. J. B. Hersey, Dr. E. E. Hays, Dr. A. D. Voorhis, and Mr. L. Baxter, II for their advice on hydroacoustics.

Dr. R. L. McMaster was very generous with his advice on the geology of Narragansett Bay and provided us with unpublished data that he obtained there. The author thanks him for this and for making the facilities of the Narragansett Marine Laboratory and the University of Rhode Island available to us during our investigation of Narragansett Bay. Dr. J. M. Zeigler, Dr. K. O. Emery, and Dr. E. Uchupi provided advice on the geology of the continental shelf and slope in this area.

The author gratefully acknowledges the financial support that he received while pursuing his doctoral studies, through assistantships with Dr. G. L. Clarke, Dr. H. E. Edgerton, and Dr. J. B. Hersey; and support received from the Earth Science Fellowship of the Standard Oil Company of California, and from an industrial scholarship with the firm of Edgerton, Germeshausen, and Grier, Inc.

The author extends very special thanks to Dr. H. E. Edgerton for the inspiration, help, and guidance that he has provided throughout the author's undergraduate and graduate years. Dr. Edgerton's "STROBE LAB" at MIT was the author's home-away-from-home during the period when the author was predominantly interested in electrical engineering. The author did his batchelor's and master's theses under Dr. Edgerton and has enjoyed his fellowship at MIT, out of MIT, and on many cruises.

BIBLIOGRAPHY

Atlantic Research Corp., 1963, Piezolectric Pressure Transducers, Alexandria, Virginia, 12 p.

Baxter, L., II, 1960, Development of Sound Analysis Equipment for Sonar Research, Pt. 2: Woods Hole Oceanographic Institution, Reference No. 60-25, 7 p.

Birch, F., Schairer, V. F., and Spicer, H. C., 1942, Handbook of Physical Constants: Geological Society of America Special Paper 36, 325 p.

Breslau, L. R., 1961, A Miniaturized Precision Time Source for Use in Self Contained Instruments: Woods Hole Oceanographic Institution, Reference No. 61-28, 8 p.

Breslau, L. R., Hersey, J. B., Edgerton, H. E., and Birch, F. S., 1962, A Precisely Timed Submersible Pinger for Tracking Instruments in the Sea: Deep Sea Research, V. 9, pp. 137-144.

Breslau, L. R., Zeigler, J. M., and Owen, D. M., 1962, A Self-Contained Portable Tape Recording System for Use by SCUBA Divers: Bulletin de l'Institut Oceanographique de Monaco, No. 1235, 4 p.

David Bogen Co., 1946, Instruction Book for Sonar Portable Testing Equipment - Navy Model OCP-1, New York, N. Y., 69 p.

Edgerton, H. E., and Cousteau, J. Y., 1959, Underwater Camera Positioning by Sonar: The Review of Scientific Instruments, V. 30, pp. 1125-1126.

Edo Corp., 1954, Instruction Book for Sonar Sounding Set AN/UQN-1C, College Point, N. Y., NAVSHIPS 92373(A), Department of the Navy, Bureau of Ships, 48 p.

E. G. & G., Inc., 1960, Instruction Manual for Types CA-8 and CA-9, Underwater Cameras, Boston, Massachusetts, 53 p.

E. G. & G., Inc., 1961, Instruction Manual for Types SP-8 and SP-9 Sonar Pingers, Boston, Massachusetts, 30 p.

Electronic Associates Inc., 1961, Operators Manual for Model 3033D DATAPLOTTER, Long Branch, New Jersey, 50 p.

Emery, K. O., 1960, The Sea off Southern California, A Modern Habitat of Petroleum: New York, London, John Wiley and Sons, Inc., 366 p.

Erath, R. L., 1959, Echo Soundings of the USCGC YAMACRAW Cruise in the Western Mediterranean Sea: Woods Hole Oceanographic Institution, Technical Memorandum 7-59, 22 p.

Ericson, D. B., Ewing, M., Wollin, G., and Heezen, B. C., 1961, Atlantic Deep-Sea Cores: Geological Society of America Bulletin, V. 72, p. 193-286.

Ewing, W. M., Jardetsky, W. S., Press, F., 1957, Elastic Waves in Layered Media: New York, Toronto, London, McGraw-Hill Book Co., Inc., 380 p.

Fairchild Camera and Instrument Corp., 1952, Instruction Manual for Oscilloscope Camera, Syosset, N. Y., U. S. Air Force Reference Number AN 10-IOEA-9, 32 p.

Frazer, H. J., 1935, Experimental Study of the Porosity and Permeability of Clastic Sediments: Journal of Geology, V. 43, pp. 910-1010.

General Electric Co., Inc., 1963, The GE-225 Information Processing System, Phoenix, Arizona, 86 p.

Gerber Scientific Instrument Co., Undated, Instruction Manual for Gerber Data Reduction System, Model GADRS-2, Hartford, Conn., 38 p.

Gifft, T. H., and Associates, Undated, The Precision Sonar Transceiver, Torrance, California, 23 p.

Graton, L. C., and Frazer, H. J., 1935, Systematic Packing of Spheres with Particular Relation to Porosity and Permeability: Journal of Geology, V. 43, pp. 785-909.

Hamilton, E. L., and Menard, H. W., 1956, Density and Porosity of Sea Floor Surface Sediments Off San Diego: The Bulletin of the American Association of Petroleum Geologists, V. 40, pp. 754-761.

Hamilton, E. L., Shumway, G., Menard, H. W. and Shipek, C. J., 1956, Acoustic and other Physical Properties of Shallow-Water Sediments off San Diego: Journal of the Acoustical Society of America, V. 28, pp. 1-15.

Heezen, B. C., Tharp, M., and Ewing, M., 1959, The Floors of the Oceans, Pt. 1, The North Atlantic: Geological Society of America Special Paper 65, 122 p.

Hewlett-Packard Co., 1961, Instruction Manual for the 560A Digital Printer, Palo Alto, California, 42 p.

Hewlett-Packard Co., 1961, Instruction Manual for the 405/CR Digital Voltmeter, Palo Alto, California, 39 p.

Hoel, P. G., 1962, Introduction to Mathematical Statistics: New York, John Wiley and Sons, Inc., 422 p.

Hoffman, J. H., and Wilkes, G. L., 1962, Bottom Acoustical Reflectivity and Penetration Studies: U. S. Navy Hydrographic Office, Informal Manuscript Report No. 0-43-62, 12 p.

Horton, J. W., 1959, Fundamentals of Sonar: Annapolis, Maryland, United States Naval Institute, 417 p.

Inman, D. L., 1952, Measures for Describing the Size Distribution of Sediments: Journal of Sedimentary Petrology, V. 22, pp. 125-145.

International Business Machines Corp., 1959, Reference Manual for the IBM 26 Printing Card Punch, White Plains, N. Y., 39 p.

International Business Machines Corp., 1959, Reference Manual for the Model 407 Accounting Machine, White Plains, N. Y., 223 p.

International Business Machines Corp., 1961, Reference Manual for the IBM 7090 Data Processing System, White Plains, N. Y., 140 p.

Jones, J. L., Leslie, C. B., and Barton, L. E., 1964, Acoustic Characteristics of Underwater Bottoms: The Journal of the Acoustical Society of America, V. 36, pp. 154-163.

Knott, S. T., 1962, Use of the Precision Graphic Recorder in Oceanography, p. 251-262 in Gaul, R. D., et al., Editor, Marine Sciences Instrumentation, V. 1: New York, Plenum Press, 354 p.

Knott, S. T. and Hersey, J. B., 1956, High Resolution Echo Sounding Techniques and Their Use in Bathymetry, Marine Geophysics and Biology: Deep Sea Research, V. 4, pp. 36-44.

Knott, S. T., and Witzell, W. E., 1960, Instruction Manual for Precision Graphic Recorder: Woods Hole Oceanographic Institution, Reference No. 60-38, 42 p.

Knott, S. T., and Witzell, W. E., 1960, A Light-Weight Towed Transducer Enclosure for Echo Sounding: Woods Hole Oceanographic Institution, Reference No. 61-40, 7 p.

Krumbein, W. C., and Pettijohn, F. J., 1938, Manual of Sedimentary Petrography: New York, Appleton-Century-Crofts, Inc., 549 p.

Krumbein, W. C., and Sloss, L. L., 1956, Stratigraphy and Sedimentation: San Francisco, W. H. Freeman and Co., 497 p.

Krynine, D. P., 1947, Soil Mechanics, Its Principles and Structural Applications: New York, London, McGraw Hill Book Co., Inc., 526 p.

Laughton, A. S., 1957, Sound Propagation in Compacted Ocean Sediments: Geophysics, V. 22, pp. 233-260.

Lieberman, L. N., 1948, Reflection of Sound from Coastal Sea Bottoms: The Journal of the Acoustical Society of America, V. 20, pp. 305-309.

Loring, D. H., 1962, Bottom Analysis of Sediments of the Gulf of St. Lawrence and the Atlantic Continental Shelf from Newfoundland to Georges Bank in Respect to Acoustical Reflection: Fisheries Research Board of Canada, No. 127, 28 p.

Lowry, H. R., 1960, General Electric Transistor Manual, Fifth Edition: Liverpool, N. Y., General Electric Co., 329 p.

Mackenzie, K. V., 1960, Reflection of Sound from Coastal Bottoms: The Journal of the Acoustical Society of America, V. 32, pp. 221-231.

McCracken, D. D., 1961, A Guide to Fortran Programming: New York, London, John Wiley and Sons, Inc., 88 p.

McKinney, C. M., and Anderson, C. D., 1964, Measurements of Backscattering of Sound from the Ocean Bottom: Journal of the Acoustical Society of America, V. 36, p. 158-163.

McMaster, R. L., 1960, Sediments of Narragansett Bay System and Rhode Island Sound, Rhode Island: Journal of Sedimentary Petrology, V. 30, pp. 249-274.

Nafe, J. E., and Drake, C. L., 1963, Physical Properties of Marine Sediments, p. 794-815, in Hill, M. N., Editor, The Sea, V. 3: New York, London, John Wiley and Sons, Inc., 963 p.

National Defense Research Committee, 1946, Physics of Sound in the Sea, Pt. 1, Transmission: Washington, D. C., U. S. Department of Commerce, Office of Technical Services, 244 p.

National Defense Research Committee, 1946, The Application of Oceanography to Subsurface Warfare: Washington, D. C. U. S. Department of Commerce, Office of Technical Services, 106 p.

Officer, C. B., 1958, Introduction to the Theory of Sound Transmission: New York, Toronto, London, McGraw-Hill Book Co., Inc., 284 p.

Owen, D. M., 1961, Underwater Photography and Self Contained Diving, p. 8-9, in Atlantic Oceanography conducted during period Jan. 1 - June 30, 1961: Woods Hole Oceanographic Institution, Reference No. 61-23, 31 p.

Payne, J. B., III, 1960, Voltage-Controlled Bootstrap Generator: Electronics, V. 33, N. 11, pp. 177-178.

Plumley, W. J., and Davis, D. H., 1956, Estimation of Recent Sediment Size Parameters from a Triangular Diagram: Journal of Sedimentary Petrology, V. 26, pp. 140-155.

Rayleigh, J. W. S., 1945, The Theory of Sound, V. 2: New York, N. Y., Dover Publications, 504 p.

Richards, A. F., Investigations of Deep-Sea Sediment Cores, Pt. 2, Mass Physical Properties: U. S. Navy Hydrographic Office, Technical Report TR-106, 146 p.

Sarmiento, R., and Kirby, R. A., 1962, Recent Sediments of Lake Maracaibo: Journal of Sedimentary Petrology, V. 32, pp. 698-724.

Sergeev, L. A., 1958, Ul'Trazvukovoe Ekholotirovanie olia Geofizicheskikh Tselei (Ultrasonic Echo Sounding for Geophysical Purposes): Prikladnaia Geofizika (Applied Geophysics), V. 20, pp. 141-154, Translation-115 of U. S. Naval Oceanographic Office, Translated by Slessers, M., 1963.

Shea, R. F., 1957, Transistor Circuit Engineering: New York, London, John Wiley and Sons Inc., 468 p.

Shepard, F. P., 1954, Nomenclature Based on Sand-Silt-Clay Ratios: Journal of Sedimentary Petrology, V. 24, pp. 151-158.

Shumway, G., 1960, Sound Speed and Absorption Studies of Marine Sediments by a Resonance Method, Pts. 1 and 2: Geophysics, V. 25, pp. 451-467, and 659-682.

Stetson, H. C., 1938, The Sediments of the Continental Shelf Off the Eastern Coast of the United States: Papers in Physical Oceanography and Meteorology, V. 5, N. 4, pp. 5-48.

Stetson, H. C., 1949, The Sediments and Stratigraphy of the East Coast Continental Margin: Georges Bank to Norfolk Canyon: Papers in Physical Oceanography and Meteorology, V. 11, N. 2, pp. 5-60.

Sutton, G. H., Berckhemer, H., and Nafe, J. E., 1957, Physical Analysis of Deep Sea Sediments: Geophysics, V. 22, pp. 779-812.

Taylor, D. W., 1948, Fundamentals of Soil Mechanics: New York, London, John Wiley and Sons, Inc., 700 p.

Terzaghi, K., and Peck, R. B., 1948, Soil Mechanics in Engineering Practice: New York, London, John Wiley and Sons Inc., 510 p.

Tektronix Inc., 1959, Instruction Manual for the Model 502 Dual Beam Oscilloscope, Portland, Oregon, 61 p.

Thamdrup, H. M., 1938, Der van Veen-Bodengreifer, Vergleich-Versuche über die Leistungsfähigkeit des van Veen-und des Petersen Bodengreifers: J. du Conseil, 13(2), pp. 206-212, (non vide).

Trask, P. D., 1932, Origin and Environments of Source Sediments of Petroleum: Houston, Texas, The Gulf Publishing Co., 310 p.

Uchupi, E., 1963, Sediments on the Continental Margin off Eastern United States: U. S. Geol. Survey Prof. Paper 475-C, pp. C132-C137.

Urick, R. J., 1947, A Sound Velocity Method for Determining the Compressibility of Finely Divided Substances: Journal of Applied Physics, V. 18, pp. 983-987.

Urick, R. J., 1954, The Backscattering of Sound from a Harbor Bottom: The Journal of the Acoustical Society of America, V. 26, pp. 231-235.

Urick, R. J., and Saling, D. S., 1962, Backscattering of Explosive Sound from the Deep Sea Bed: The Journal of the Acoustical Society of America, V. 34, pp. 1721-1724.

Underwater Sound Reference Laboratory, 1954, Calibration of OCP-1 Sonar Monitor, Orlando, Florida, 2 p.

Wentworth, C. K., 1922, A Scale of Grade and Class Terms for Clastic Sediments: Journal of Geology, V. 30, pp. 377-392.

Witzell, W. E., (In preparation), Sweep Synchronized Positionable Trigger and Supplementary Components: Woods Hole Oceanographic Institution.

Wood, A. B., 1941, A Textbook of Sound: London, G. Bell and Sons, 578 p.

Zeigler, J. M., Whitney, Jr., G. G., and Hayes, C. R., 1960, Woods Hole Rapid Sediment Analyzer: Journal of Sedimentary Petrology, V. 30, pp. 490-495.

BIOGRAPHICAL SKETCH

The author was born on January 9, 1935 in Brooklyn, New York and attended James Madison High School there. He entered M. I. T. in 1952 and started course work toward a degree in Electrical Engineering. His particular course option was a cooperative one with industry which involved on-the-job plant assignments with the General Electric Company and the American Gas and Electric Company.

One day he noticed an advertisement on the school board requesting applicants of an engineering background for a research voyage of the Lamont Geological Observatory. He applied, got the job, and spent the next four months aboard ship doing seismology in the North Atlantic and Mediterranean. He found that he enjoyed working in this type of environment and also concluded that the field of Oceanography offered a fertile area for research and the application of modern electronic techniques.

The author had come into contact with Dr. Harold E. Edgerton, one of the pioneers in underwater photography, through attending his course in Electronic Instrumentation. Their mutual interest in marine instrumentation led to the author writing his B. S. thesis in Electrical Engineering under Dr. Edgerton. A device called the "Bioluminescense Indicator" was developed which employed a photosensitive device in a towed "fish" to record the

presence of bioluminescent life at the ocean surface. The author obtained his S. B. in Electrical Engineering in 1957.

The author enrolled in the Department of Geology and Geophysics at M. I. T. in 1957. He received a research assistantship from the Woods Hole Oceanographic Institution to develop marine instrumentation for Dr. George L. Clarke, a marine biologist at Harvard University studying deep-sea bioluminescence. During the academic term he attended classes at M. I. T. and developed instrumentation in Dr. Edgerton's laboratory. During mid-term and summer vacations he worked at sea. A device called the "Luminescence Camera" was developed which employed a photosensitive device in a deep-sea camera to obtain photographs of the creatures responsible for the bioluminescence. This formed the subject of his combined S. B. -S. M. thesis, and he was graduated in 1959 with a S. B. and S. M. in Geophysics.

In the summer of 1959, Captain Cousteau, the Director of the Institut Oceanographique de Monaco, sailed the research vessel CALYPSO to the Mid-Atlantic Ridge to obtain deep-sea photographs of the crack in the sea floor. The author accompanied him and operated the deep-sea cameras. The author then returned to M. I. T. in the fall of 1959 and started a doctoral program in Oceanography. He was supported by the Earth Science Fellowship of the Standard Oil Company of California and a fellowship from Edgerton, Germeshausen & Grier, Inc.

In the summer of 1960 the author met Miss Fernande Portal of Boston, Massachusetts. They were married in the winter of 1961.

During the author's deep-water cruises he had made the acquaintance of Dr. J. B. Hersey, the Chairman of the Geophysics Department at the Woods Hole Oceanographic Institution. He invited the author to the Institution to do a Ph. D. thesis in underwater acoustics. From December 1960 until the present time, the author has been working on his Ph. D. thesis entitled "Geological Significance of Sound Reflection from the Sea Floor" under the supervision of Dr. Hersey.

The following is a list of the author's publications and speeches.

PUBLICATIONS

Lloyd R. Breslau

1958 Breslau, L. R. and H. E. Edgerton. The Luminescence Camera. J. Biol. Photographic Assoc., 264(2):49-58.

1959 Clarke, G. L. and L. R. Breslau. Measurements of Bioluminescence Off Monaco and Northern Corsica. Bull. de l'Institut Oceanographique #1147, WHOI Contr. No. 1043.

1960 Clarke, G. L. and L. R. Breslau. Studies of Luminescent Flashing in Phosphorescent Bay, Puerto Rico, and in the Gulf of Naples using a Portable Bathyphotometer. Bull. de l'Institut Oceanographique #1171, WHOI Contr. No. 1090.

1962 Breslau, L. R., J. M. Zeigler, and D. M. Owen. A Self-Contained Portable Tape Recording System for Use by SCUBA Divers. Bull. de l'Institut Oceanographique, No. 1235, WHOI Contr. No. 1282.

1962 Breslau, L. R., J. B. Hersey, H. E. Edgerton and F. S. Birch. A Precisely Timed Submersible Pinger for Tracking Instruments in the Sea. Deep-Sea Res., Vol. 9, No. 2, 137-144, WHOI Contr. No. 1269, 27 April 1962.

WHOI REFERENCE NUMBERS

Lloyd R. Breslau

1958 Breslau, L. R. and H. E. Edgerton. The Luminescence Camera. WHOI Ref. No. 58-14.

1959 Breslau, L. R. and H. E. Edgerton. The Interruption Camera. WHOI Ref. No. 59-27.

1959 Breslau, L. R. The Portable Bathyphotometer. WHOI Ref. No. 59-23.

1961 Breslau, L. R. A Miniaturized Precision Time Source for Use in Self-Contained Instruments. WHOI Ref. No. 61-28.

PHOTOGRAPHS PUBLISHED WITH CREDIT LINE

Lloyd R. Breslau

1957 Newsweek Science Section, October 7, 1957, Siphonophora Taken with Luminescence Camera.

1959 Scientific American, October, 1959. Four Photographs of Bioluminescent Creatures.

1961 Science, December 29, 1961, Front Cover, Photograph of Rare Bioluminescent Jellyfish.

SPEECHES

63rd Meeting of the Acoustical Society of America, May 26, 1962, Preliminary Investigation of Echo Strengths Received From the Sea Floor, L. R. Breslau, J. B. Hersey, and E. E. Hays.

44th Annual Meeting of the American Geophysical Union, April 18, 1963, Geological Exploration by Measuring the Total Energy in Bottom and Sub-bottom Seismic Echoes, L. R. Breslau and J. B. Hersey.

APPENDIX A

The System Synchronization and Control Unit

The System Synchronization and Control Unit (Figure 65) synchronizes and controls all the various components of the Acoustic Reflectivity System. It is contained in a single, completely transistorized chassis and is composed of four sections, a Main Synchronization Section, a Calibration Pulse Section, a Computer Freeze Section, and a Pulse Length Modulator Section.

The function of the Main Synchronization Section is to trigger the sweep of the information display oscilloscope, open and close the shutter of the oscilloscope camera, reset the Oceanographic Computer and initiate the operation of the Calibration Pulse and Computer Freeze Sections. In order to do all this it is necessary to convert the transient closure delivered by the Sweep Synchronized Positionable Trigger (mentioned in Chapter IV) into a relay closure of precise duration. The circuitry employed (Figure 66) consists of a conventional monostable multivibrator (Lowry, 1960), and a transistorized relay. The pair of 2N525 transistors (T2 and T3) are arranged in a flip-flop configuration through the use of the collector to base cross-coupling networks and the 2N1671B unijunction transistor (T1) provides the timing for monostable operation. T3 is conducting in the quiescent state.

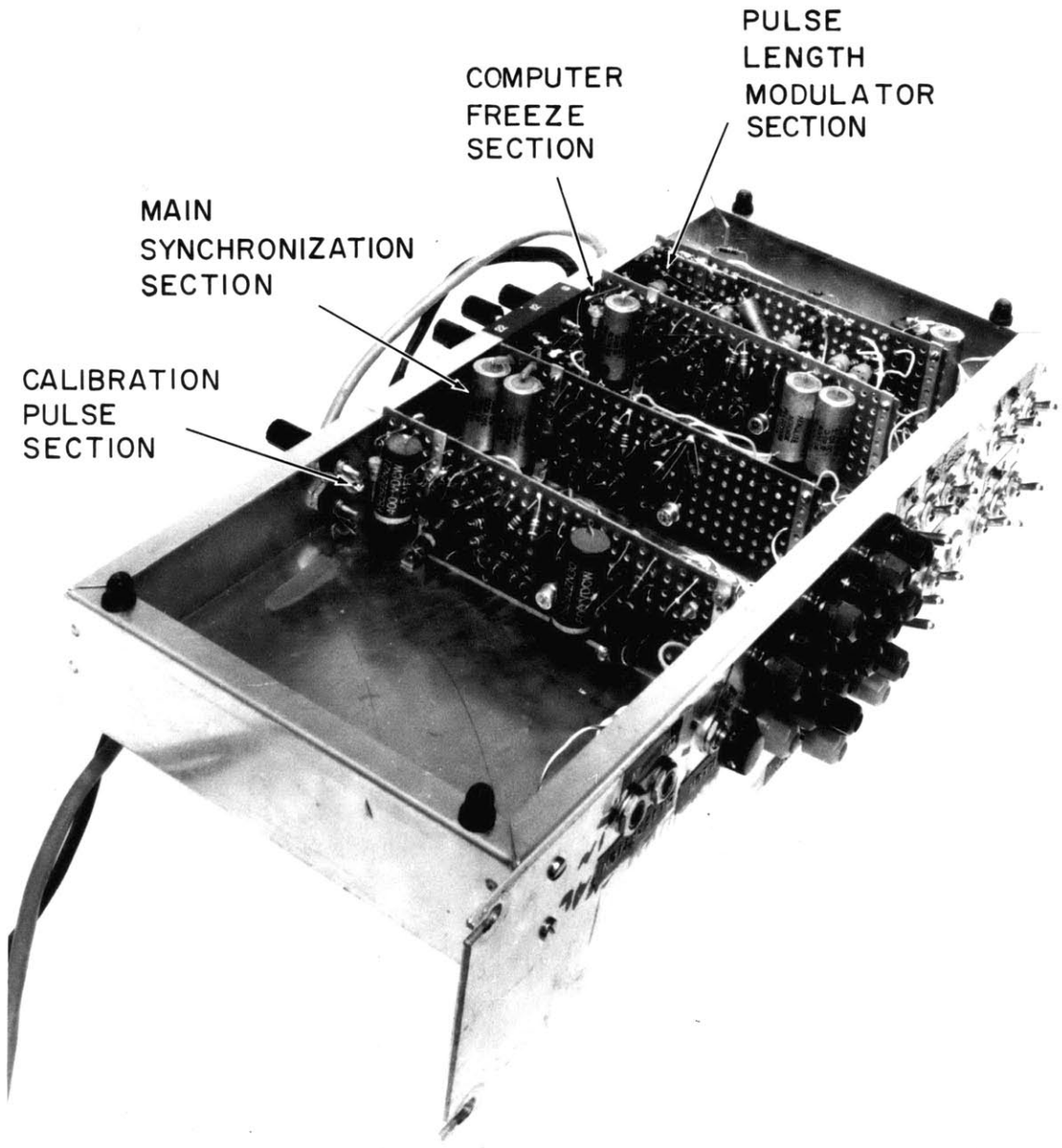

Figure 65. Photograph of the Electronic Circuitry of the System Synchronization and Control Unit of the Acoustic Reflectivity System.

SYSTEM SYNCHRONIZATION AND CONTROL UNIT

MAIN SYNCHRONIZATION SECTION

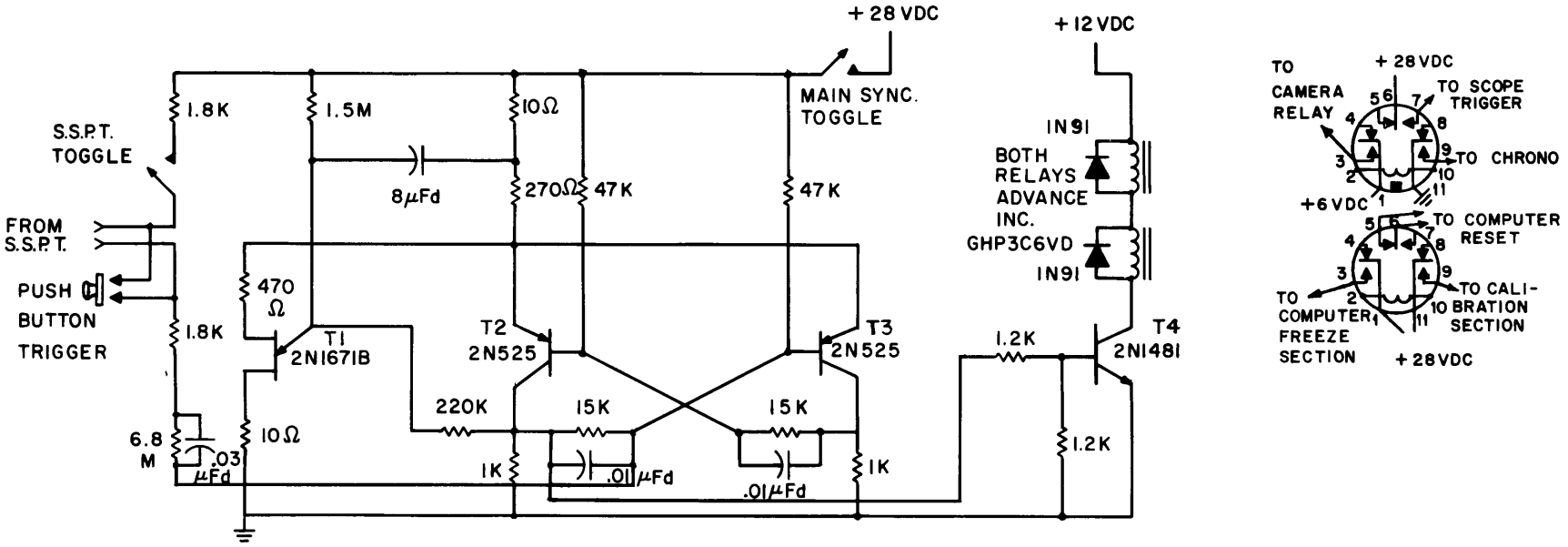

Figure 66. Schematic of the Main Synchronization Section of the System Synchronization and Control Unit.

When a transient closure from the Sweep Synchronized Positionable Trigger is received, a positive pulse is developed across the base of T3 which turns it off and consequently drives T2 into conduction. This causes a positive voltage to be applied to the base of the 2N1481 transistor (T4) which in turn energizes the relays. When T2 conducts, the timing capacitor (8 ufd) starts to discharge through the timing resistor (220 k) and after a definite interval the 2N1671B unijunction transistor fires and drives the base of T3 negative. This drives T3 into conduction which turns off T2 and deenergizes the relays to complete the cycle. The output is a relay closure which occurs when the transient closure is received from the Sweep Synchronized Positionable Trigger and lasts about 1. 8 seconds.

The function of the Calibration Pulse Section is to inject a 12 kcps pulse of precise duration into the transducer at the proper time for calibration purposes. In order to do this it is necessary to generate a relay closure of precise duration that is delayed a precise interval with respect to the synchronization from the Sweep Synchronized Positionable Trigger. The circuitry (Figure 67) consists of a time delay generator, a monostable multivibrator, and a transistorized relay. After this section is turned on through the output relay of the Main Synchronization Section, the 2N1671B unijunction transistor (T1) acting as a relaxation oscillator with a 50 millisecond time constant, delivers a series of positive pulses to

SYSTEM SYNCHRONIZATION AND CONTROL UNIT
CALIBRATION PULSE SECTION

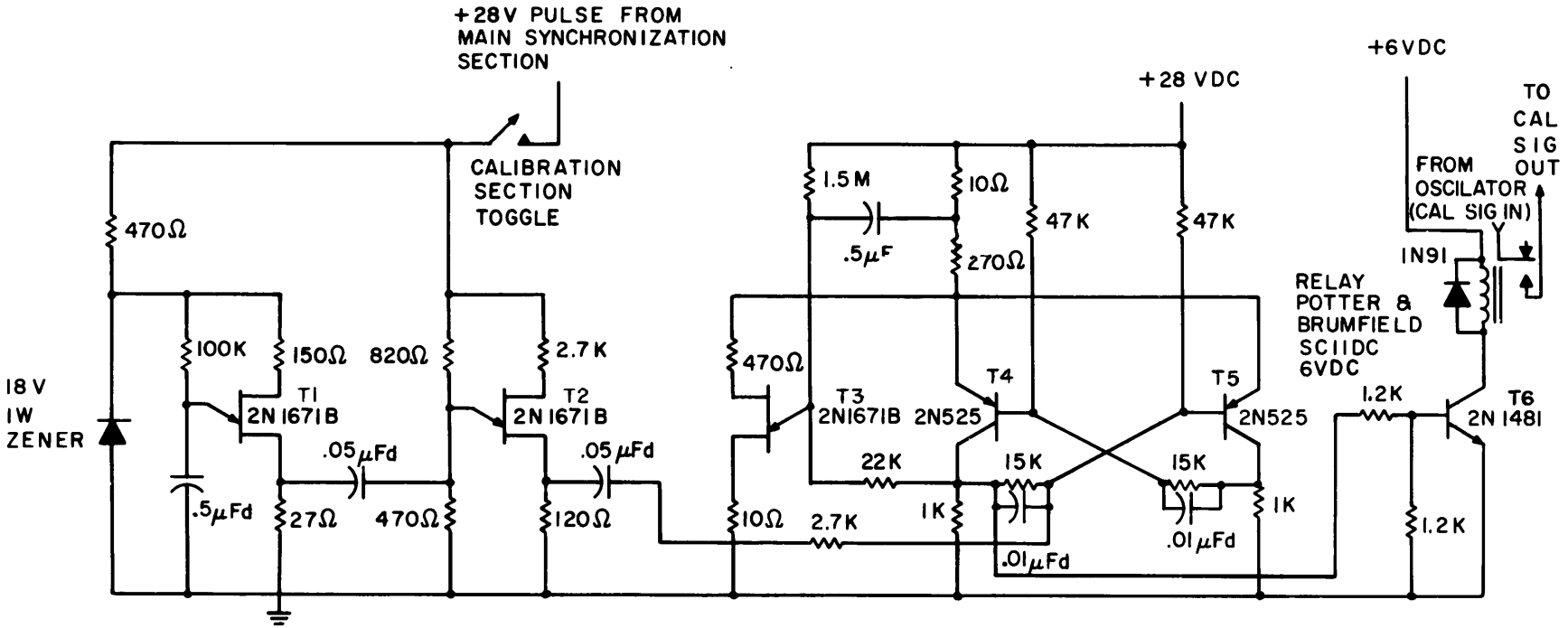

Figure 67. Schematic of the Calibration Pulse Section of the System Synchronization and Control Unit.

the emitter of the 2N1671B unijunction transistor (T2) in the following stage. Since T2 is biased to bistable operation, it acts as a single-pass gate and permits the first positive pulse to pass through it and trigger the following monostable multivibrator and associated transistorized relay. The monostable multibibrator and transistorized relay then goes through their cycle as previously described except that the time constant is 10 milliseconds. The output is a relay closure of 10 millisecond duration which occurs 50 milliseconds after the transient closure is received from the Sweep Synchronized Positionable Trigger.

The function of the Computer Freeze Section is to freeze the output of the Oceanographic Computer at the proper time and then trigger the digital voltmeter and Pulse Length Modulator Section, so that the computer output is recorded. In order to do this it is necessary to generate a relay closure of precise duration that is delayed a precise interval with respect to the synchronization from the Sweep Synchronized Positionable Trigger. The circuitry (Figure 68) is similar to that used in the Calibration Pulse Section except that the time constants are different and a single-pass gate is no longer necessary. The output is a relay closure of 1.2 second duration which occurs 400 milliseconds after the transient closure is received from the Sweep Synchronized Positionable Trigger.

SYSTEM SYNCHRONIZATION AND CONTROL UNIT
COMPUTER FREEZE SECTION

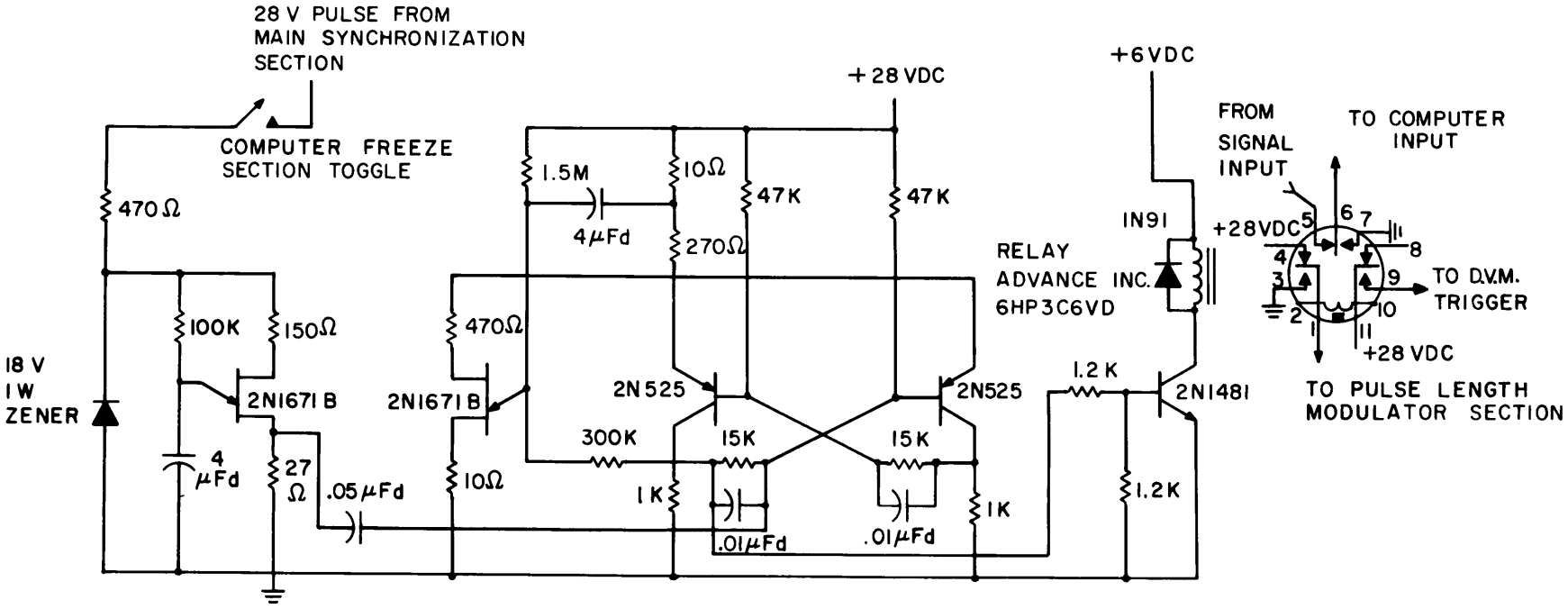

Figure 68. Schematic of the Computer Freeze Section of the System Synchronization and Control Unit.

The function of the Pulse Length Modulator is to generate a mark on the PGR of length proportional to the output of the Oceanographic Computer at a particular time. In order to do this it is necessary to generate a relay closure of duration proportional to the output voltage of the computer. The circuitry (Figure 69) consists of a flip-flop, a bootstrap sweep generator (Payne III, 1960), and a transistorized relay. The two left most 2N1672 transistors (T1 and T2) are arranged in a flip-flop configuration through the use of collector to base cross-coupling network and T2 is initially conducting. When a trigger is received from the Computer Freeze Section to initiate the pulse-length modulation process a negative pulse is applied to the base of T2 which turns the stage off. The accompanying rise in the collector voltage of this stage causes the diode D1 connected between it and the base of the following 2N1672 transistor (T3) to become back biased and thereby turns on the sweep circuit. This causes the voltage across the emitter resistor of T3, the sweep generator, to increase linearly with time until it reaches the value of modulating voltage that is developed at the output of the Oceanographic Computer; at this point the diode D2 between this emitter and the base of T2 becomes forward biased causing T2 to conduct, which completes the cycle. Therefore, the interval that T2 is non-conducting is proportional to the value of modulating voltage. Since the base of the 2N1310 transistor T4 in the

SYSTEM SYNCHRONIZATION AND CONTROL UNIT
PULSE LENGTH MODULATOR SECTION

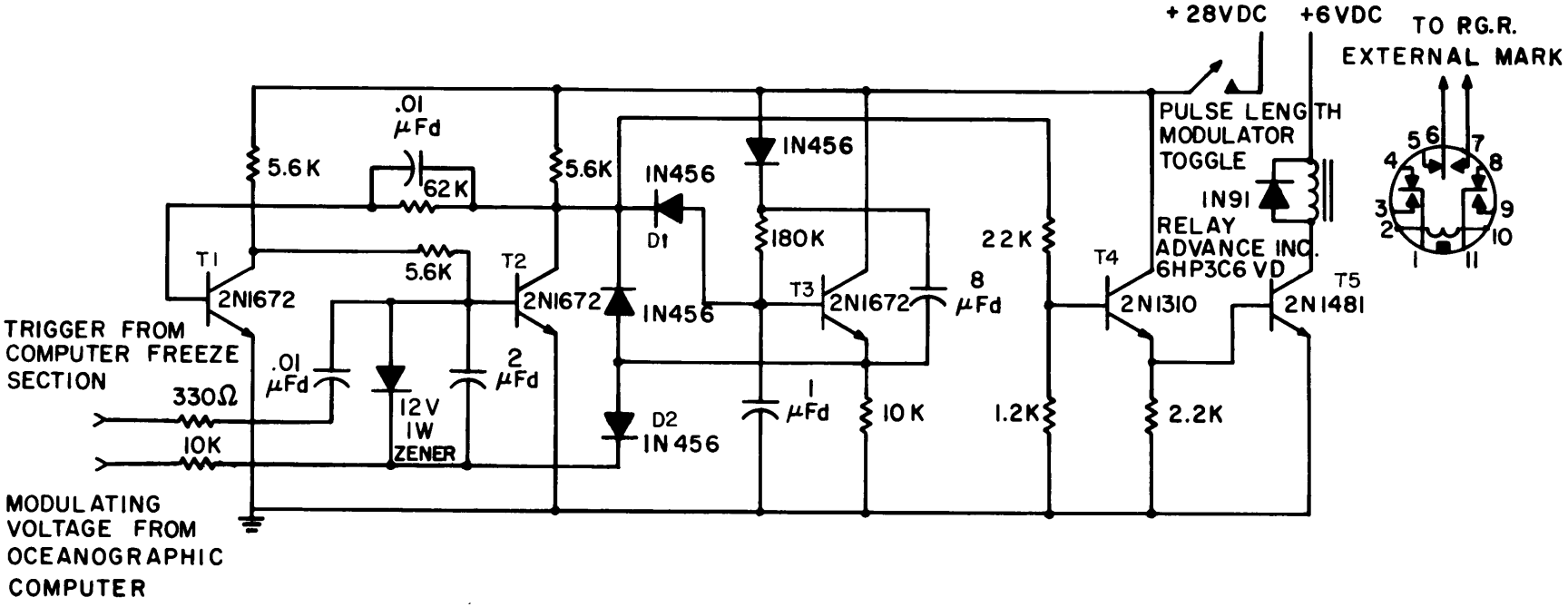

Figure 69. Schematic of the Pulse Width Modulator Section of the System Synchronization and Control Unit.

transistorized relay is connected to the collector of T2, the interval that the relay is energized is the same as the interval of non-conduction of T2, and a closure interval proportional to the modulating voltage is developed.

The Precisely-Timed Submersible Pinger

The Miniaturized Precision Time Source is composed of a 100-kcps oscillator, a buffer, and five frequency dividers (Figure 70). The output of the oscillator is buffered and successively divided to develop a synchronizing signal at precise one-second intervals.

The oscillator utilizes the standard transistorized Clapp configuration with a quartz crystal operating in its series resonant mode replacing the conventional series inductance-capacitance in the tank circuit (Shea, 1957). The output is a 100-kcps sinusoid, developed across the tank, and passed on to the buffer. The buffer is a single stage emitter follower which is biased to clip the negative-going portions of the input sinusoid and deliver 100-kcps positive pulses to the first frequency divider. The frequency divider utilizes a unijunction transistor as a synchronized relaxation oscillator. The synchronizing pulses delivered by the buffer are superimposed upon the voltage developed across the storage capacitor which is charged through the charging resistor. The time constant of the

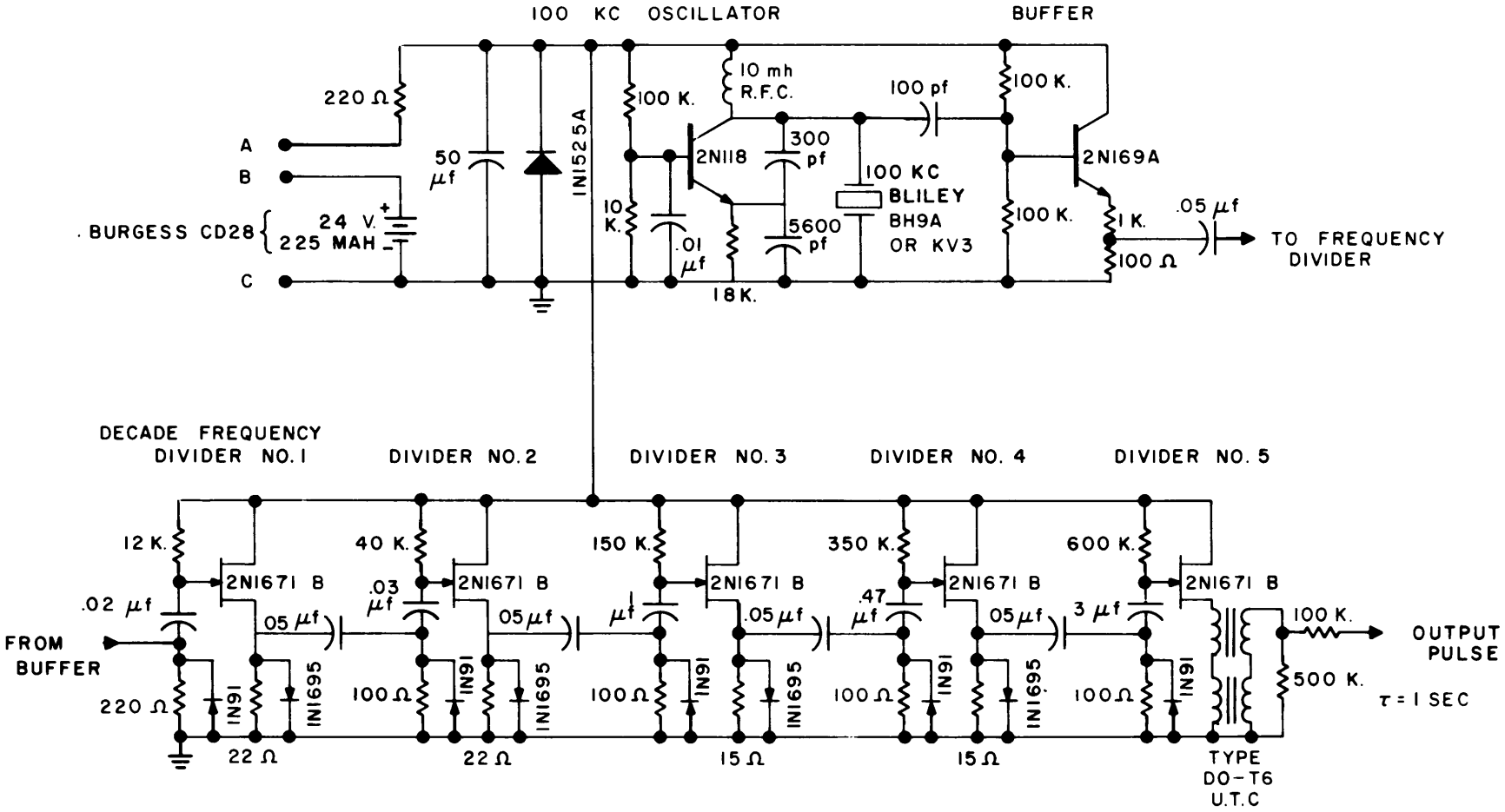

Figure 70. Schematic of the Miniaturized Precision Time Source.

circuit is set so that the tenth synchronization pulse causes the unijunction transistor to conduct and deliver a positive pulse to the next frequency divider. This is repeated by each of the remaining frequency dividers to achieve a total frequency division of 100,000. Therefore, the final output of the time source is a precise 1-cps.

The output of the time source is applied to a standard Edgerton pinger (E. G. & G. , Inc. , Model 220) (Figure 71) with the previously existing timing circuitry removed. This device consists of a driver, a pulse transformer, and a transducer. In the driver, a transistor oscillator, voltage doubler circuit, and capacitor discharge circuit transform the low voltage of the battery into a high voltage pulse which is applied to the primary of the pulse transformer. When this occurs, the tuned circuit, consisting of the secondary of the transformer and the transducer, oscillates at about twelve kilocycles for about half a millisecond thus generating a "ping". When the miniaturized precision time source is included, the pinger emits pings every second with a ping-to-ping jitter of less than one microsecond. The inaccuracy is less than two microseconds per degree centigrade as determined by the temperature coefficient of the quartz crystal employed in the miniaturized precision time source, which is operating at ambient temperature.

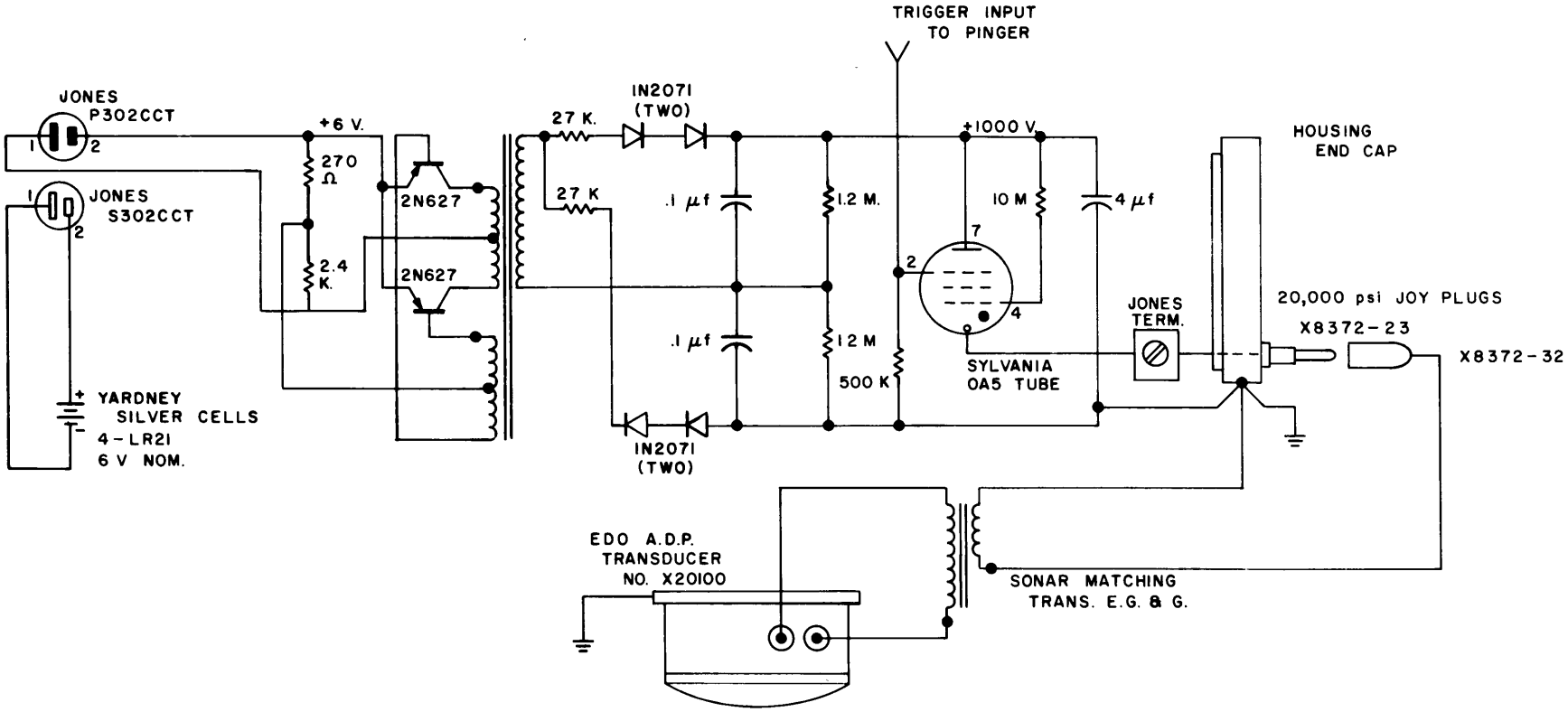

Figure 71. Schematic of a Standard (E.G. & G., Inc.) Submersible Pinger.

APPENDIX B

COMPUTER PROGRAM I

```
C       PROGRAM TO OBTAIN ACOUSTIC ECHO STRENGTH

        PRSLVLF(CALINJ,SIG,CAL)= -7.0 + 8.69 *LOGF(CALINJ * SIG/CAL)
        ENGLVLF(CALINJ,SIG,CAL)=-108.9 +4.34 *LOGF(CALINJ**2 * SIG/CAL)
      0 DIMENSION  NMFOTO(200), SIGPRS(200),  SIGENG(200)
        READ 12 , NSTART
   12   FORMAT ( I4 )
        NUMDTA = NSTART
    8   ISIZE = 0
   10   DO  6  K = 1 , 200
    3 0 READ 4 , NMFOTO(K) , CALPRS , MRKEND , SIGPRS(K) , CALENG
      1 , SIGENG(K) , CALINX , DEPTHX , LATX , LONGX
    4 0 FORMAT ( I5 , F5.0 , I1 , F4.0 , 2(F5.0) , F3.0 , 20X , A4 ,
      1 2(1XA6))
        IF ( MRKEND - 1 ) 11 ,7 , 5
    5   CALL  EXIT
   11   CALINJ = CALINX
        CLMDPR = CALPRS
        CLMDEG = CALENG
        DEPTH = DEPTHX
        LATITU = LATX
        LONGIT = LONGX
    6   ISIZE = ISIZE + 1
    7   IF ( ISIZE - 5) 8, 9, 9
    9   CONTINUE
        DIMENSION  N2FOTO(200)
        DO 15 NN = 1 , ISIZE
   15   N2FOTO(NN) = NMFOTO(NN)
```

```
      CALL MEDMAX  (  SIGPRS, NMFOTO, ISIZE, VALMED, VALMAX, MEDFOT  )
      NUMDYN = MEDFOT
      EKODYN = PRSLVLF  (CALINJ , VALMED , CLMDPR  )
      DYNMAX = PRSLVLF  (  CALINJ , VALMAX , CLMDPR  )
      CALL MEDMAX ( SIGENG, N2FOTO, ISIZE, VALMED, VALMAX, MEDFOT )
      NUMERG = MEDFOT
      FKOERG = ENGLVLF  (  CALINJ , VALMED , CLMDEG  )
      ERGMAX = ENGLVLF  (  CALINJ , VALMAX , CLMDEG  )
      DIMENSION PRSLV(200) , ENGLV(200)
      DO  20  N = 1,  ISIZE
      SIG = SIGPRS(N)
   20 PRSLV(N) = PRSLVLF ( CALINJ , SIG , CLMDPR )
      DEVDYN = STNDEV ( PRSLV , ISIZE , EKODYN )
      DO  30  M = 1 , ISIZE
      SIG = SIGENG(M)
   30 ENGLV(M) = ENGLVLF ( CALINJ , SIG , CLMDEG )
      DEVERG = STNDEV ( ENGLV , ISIZE , EKOERG )
      NUMDTA = NUMDTA + 1
     0 PUNCH 93 , NUMDTA , EKODYN , DEVDYN , NUMDYN , DYNMAX , ISIZE ,
     1 EKOERG , DEVERG , NUMERG , ERGMAX , DEPTH , LATITU , LONGIT
     0 PRINT 94 , NUMDTA , EKODYN , DEVDYN , NUMDYN , DYNMAX , ISIZE ,
     1 EKOERG , DEVERG , NUMERG , ERGMAX , DEPTH , LATITU , LONGIT
   93 0 FORMAT ( I3 , F6.1 , F4.1 , I6 , F6.1 , I4 , F7.1 , F4.1 ,
     1 I6 , F7.1 , 1XA4 , 2(1XA6) )
   94 0 FORMAT ( 1H0 , I3 , F6.1 , F4.1 , I6 , F6.1 , I4 , F7.1 , F4.1 ,
     1 I6 , F7.1 , 1XA4 , 2(1XA6) )
      GO  TO  8
      END
```

```
      SUBROUTINE MEDMAX ( VALUE, NMFOTO, ISIZE, VALMED, VALMAX, MEDFOT )
      DIMENSION VALUE (200) , NMFOTO (200)
      ISTOP = ISIZE - 1
      DO 55 I = 1 , ISTOP
      JJJ = I + 1
      DO  55 J = JJJ, ISIZE
      IF (VALUE (I) - VALUE (J) )  50 , 55 , 55
   50 VLTEMP = VALUE (I)
      VALUE (I) = VALUE (J)
      VALUE (J) = VLTEMP
      NMTEMP = NMFOTO (I)
      NMFOTO (I) = NMFOTO (J)
      NMFOTO (J) = NMTEMP
   55 CONTINUE
      VALMAX = VALUE (1)
      ITEST = ISIZE /2
      IMID = ITEST + 1
      MEDFOT = NMFOTO (IMID)
      IF (ITEST * 2 - ISIZE) 57, 59, 57
   57 VALMED = VALUE (IMID)
      RETURN
   59 VALMED = (VALUE (ITEST) + VALUE (IMID) ) / 2.0
      RETURN
      END
      FUNCTION  STNDEV  ( SETVAL , ISIZE , SETMDN )
      DIMENSION SETVAL (200)
      SUMSQ = 0
      DO 66 L = 1 , ISIZE
```

```
66   SUMSQ = SUMSQ + (SETVAL (L) - SETMDN) **2
     XSIZE = ISIZE
     STNDEV = SQRTF (SUMSQ / XSIZE )
     RETURN
     END
```

COMPUTER PROGRAM II

```
C       PROGRAM TO OBTAIN ACOUSTIC BOTTOM LOSS

  1   0 READ 2 , NUMDTA , MRKEND , EKODYN , DEVDYN , DYNMAX , ISIZE ,
      1 EKOERG , DEVERG , ERGMAX , DEPTH
  2   0 FORMAT ( I3 , I1 , F5.1 , F4.1 , 6X , F6.1 , I4 , F7.1 , F4.1 ,
      1 6X , F7.1 , 1X , F4.0 )
        IF ( MRKEND - 1 ) 7 , 5 , 6
  5     READ 3 , IPARAM , PRSREF , ENGREF , UNITS
  3     FORMAT ( I2 , 5X , F5.1 , 5X , F5.1 , 5X , F5.3 )
        GO TO 1
  6     CALL EXIT
  7     PATH = 2.0 * DEPTH * UNITS
        PROPLS = 8.69 * LOGF ( PATH ) + 1.2 * PATH / 1000.0
        BMLSPR = PRSREF - EKODYN - PROPLS
        BMLSEN = ENGREF - EKOERG - PROPLS
        PRLSMN = PRSREF - DYNMAX - PROPLS
        ENLSMN = ENGREF - ERGMAX - PROPLS
        SPRDPR = BMLSPR - PRLSMN
        SPRDEN = BMLSEN - ENLSMN
        VALDIF = BMLSPR - BMLSEN
        IDEPTH = DEPTH
      0 PUNCH 8 , NUMDTA , BMLSPR , DEVDYN , PRLSMN , IDEPTH , BMLSEN,
      1 DEVERG , ENLSMN , ISIZE , SPRDPR , SPRDEN , IPARAM , VALDIF
  8     FORMAT ( I3, 3(F5.1), I6, 3(F5.1), I5, 2(F5.1), I4, F5.1 )
      0 PRINT 9 , NUMDTA , BMLSPR , DEVDYN , PRLSMN , IDEPTH , BMLSEN,
      1 DEVERG , ENLSMN , ISIZE , SPRDPR , SPRDEN , IPARAM , VALDIF
  9     FORMAT ( 1H0, I3, 3(F5.1), I6, 3(F5.1), I5, 2(F5.1), I4, F5.1 )
        GO TO 1
        END
```

```
C     PROGRAM TO CLASSIFY SEDIMENTS AND COMPUTE
C           GRAIN SIZE CHARACTERISTICS

  01 0 READ 2,NUMBER, TYPE, MRKEND, DIST, DEPTH, Q3, XMED,
     1 Q1, GRAV, XSAND, SILT, XCLAY, COLL, NTYPE
  02   FORMAT [I2, A1, I1, F4.1, F6.1, 2[F7.3], F8.4, 5[F6.1], I1]
       IF [MRKEND-1] 4,3,4
  03   CALL EXIT
  04   PHIMED = -1.4 * LOGF [XMED]
       SORT = SQRTF [Q3/Q1]
       PHISRT = 1.44 * LOGF [SORT]
       IF [NTYPE -1] 75, 76, 75
 76    IDEPTH = DEPTH
       COARSE = XSAND + GRAV
       FINE = XCLAY + SILT + COLL
       IF [XSAND] 81, 80, 81
  80   XSAND = .001
  81   IF [SILT] 83, 82, 83
  82   SILT = .001
  83   IF [XCLAY] 85, 84, 85
 84    XCLAY = .001
  85   SAND = XSAND + GRAV
       CLAY = XCLAY + COLL
       IF [SAND-75.0] 5, 50, 50
  05   IF [SILT-75.0] 6, 51,51
  06   IF [CLAY -75.0] 99, 52, 52
 99    SANSIL = SAND/SILT
       CLYSND = CLAY/SAND
       SILCLY = SILT/CLAY
```

```
      IF [SAND-20.0] 7, 7, 10
07    IF [SANSIL-1.0] 8, 8, 53
 08   IF [SILCLY-1.0] 54, 9, 9
 09   IF [CLYSND-1.0] 56, 56, 55
10    IF [CLAY - 20.0] 11, 11 , 15
 11   IF [SANSIL-1.0] 56, 12, 12
 12   IF [SILCLY-1.0] 58, 58, 57
15    IF [SILT-20.0]  16, 16, 59
16    IF [ CLYSND - 1.0 ] 58 , 58 , 53
50    ICODE = 1
    0 PRINT 20 , NUMBER, TYPE, DIST, IDEPTH, ICODE, PHIMED, SORT,
    1 PHISRT, COARSE, FINE, SILT, CLAY
20  0 FORMAT [ 1H0, I2, A1, F6.1, I5, 13H SAND                    ,
    1 I2, F6.1, 2[F5.1], 4[F6.1] ]
    0 PUNCH 21 , NUMBER, TYPE, DIST, IDEPTH, ICODE, PHIMED, SORT,
    1 PHISRT, COARSE, FINE, SILT, CLAY
21  0 FORMAT [      I2, A1, F6.1, I5, 13H SAND                    ,
    1 I2, F6.1, 2[F5.1], 4[F6.1] ]
      GO TO 1
51    ICODE = 4
    0 PRINT 22 , NUMBER, TYPE, DIST, IDEPTH, ICODE, PHIMED, SORT,
    1 PHISRT, COARSE, FINE, SILT, CLAY
22  0 FORMAT [ 1H0, I2, A1, F6.1, I5, 13H SILT                    ,
    1 I2, F6.1, 2[F5.1], 4[F6.1] ]
    0 PUNCH 23 , NUMBER, TYPE, DIST, IDEPTH, ICODE, PHIMED, SORT,
    1 PHISRT, COARSE, FINE, SILT, CLAY
23  0 FORMAT [      I2, A1, F6.1, I5, 13H SILT                    ,
    1 I2, F6.1, 2[F5.1], 4[F6.1] ]
      GO TO 1
52    ICODE = 8
```

```
    0 PRINT 24 , NUMBER, TYPE, DIST, IDEPTH, ICODE, PHIMED, SORT,
    1 PHISRT, COARSE, FINE, SILT, CLAY
24  0 FORMAT [ 1H0, I2, A1, F6.1, I5, 13H CLAY                    ,
    1 I2, F6.1, 2[F5.1], 4[F6.1] ]
    0 PUNCH 25 , NUMBER, TYPE, DIST, IDEPTH, ICODE, PHIMED, SORT,
    1 PHISRT, COARSE, FINE, SILT, CLAY
25  0 FORMAT [      I2, A1, F6.1, I5, 13H CLAY                    ,
    1 I2, F6.1, 2[F5.1], 4[F6.1] ]
      GO TO 1
53    ICODE = 10
    0 PRINT 26 , NUMBER, TYPE, DIST, IDEPTH, ICODE, PHIMED, SORT,
    1 PHISRT, COARSE, FINE, SILT, CLAY
26  0 FORMAT [ 1H0, I2, A1, F6.1, I5, 13H SANDY CLAY              ,
    1 I2, F6.1, 2[F5.1], 4[F6.1] ]
    0 PUNCH 27 , NUMBER, TYPE, DIST, IDEPTH, ICODE, PHIMED, SORT,
    1 PHISRT, COARSE, FINE, SILT, CLAY
27  0 FORMAT [      I2, A1, F6.1, I5, 13H SANDY CLAY              ,
    1 I2, F6.1, 2[F5.1], 4[F6.1] ]
      GO TO 1
54    ICODE = 7
    0 PRINT 28 , NUMBER, TYPE, DIST, IDEPTH, ICODE, PHIMED, SORT,
    1 PHISRT, COARSE, FINE, SILT, CLAY
28  0 FORMAT [ 1H0, I2, A1, F6.1, I5, 13H SILTY CLAY              ,
    1 I2, F6.1, 2[F5.1], 4[F6.1] ]
    0 PUNCH 29 , NUMBER, TYPE, DIST, IDEPTH, ICODE, PHIMED, SORT,
    1 PHISRT, COARSE, FINE, SILT, CLAY
29  0 FORMAT [      I2, A1, F6.1, I5, 13H SILTY CLAY              ,
    1 I2, F6.1, 2[F5.1], 4[F6.1] ]
      GO TO 1
55    ICODE = 6
```

```
     0 PRINT 30 , NUMBER, TYPE, DIST, IDEPTH, ICODE, PHIMED, SORT,
     1 PHISRT, COARSE, FINE, SILT, CLAY
30   0 FORMAT [ 1H0, I2, A1, F6.1, I5, 13H CLAYEY SILT          ,
     1 I2, F6.1, 2[F5.1], 4[F6.1] ]
     0 PUNCH 31 , NUMBER, TYPE, DIST, IDEPTH, ICODE, PHIMED, SORT,
     1 PHISRT, COARSE, FINE, SILT, CLAY
31   0 FORMAT [      I2, A1, F6.1, I5, 13H CLAYEY SILT          ,
     1 I2, F6.1, 2[F5.1], 4[F6.1] ]
       GO TO 1
56     ICODE = 3
     0 PRINT 32 , NUMBER, TYPE, DIST, IDEPTH, ICODE, PHIMED, SORT,
     1 PHISRT, COARSE, FINE, SILT, CLAY
32   0 FORMAT [ 1H0, I2, A1, F6.1, I5, 13H SANDY SILT           ,
     1 I2, F6.1, 2[F5.1], 4[F6.1] ]
     0 PUNCH 33 , NUMBER, TYPE, DIST, IDEPTH, ICODE, PHIMED, SORT,
     1 PHISRT, COARSE, FINE, SILT, CLAY
33   0 FORMAT [      I2, A1, F6.1, I5, 13H SANDY SILT           ,
     1 I2, F6.1, 2[F5.1], 4[F6.1] ]
       GO TO 1
57     ICODE = 2
     0 PRINT 34 , NUMBER, TYPE, DIST, IDEPTH, ICODE, PHIMED, SORT,
     1 PHISRT, COARSE, FINE, SILT, CLAY
34   0 FORMAT [ 1H0, I2, A1, F6.1, I5, 13H SILTY SAND           ,
     1 I2, F6.1, 2[F5.1], 4[F6.1] ]
     0 PUNCH 35 , NUMBER, TYPE, DIST, IDEPTH, ICODE, PHIMED, SORT,
     1 PHISRT, COARSE, FINE, SILT, CLAY
35   0 FORMAT [      I2, A1, F6.1, I5, 13H SILTY SAND           ,
     1 I2, F6.1, 2[F5.1], 4[F6.1] ]
       GO TO 1
58     ICODE = 9
```

```
      0 PRINT 36 , NUMBER, TYPE, DIST, IDEPTH, ICODE, PHIMED, SORT,
      1 PHISRT, COARSE, FINE, SILT, CLAY
   36 0 FORMAT [ 1H0, I2, A1, F6.1, I5, 13H CLAYEY SAND          ,
      1 I2, F6.1, 2[F5.1], 4[F6.1] ]
      0 PUNCH 37 , NUMBER, TYPE, DIST, IDEPTH, ICODE, PHIMED, SORT,
      1 PHISRT, COARSE, FINE, SILT, CLAY
   37 0 FORMAT [       I2, A1, F6.1, I5, 13H CLAYEY SAND          ,
      1 I2, F6.1, 2[F5.1], 4[F6.1] ]
        GO TO 1
   59   ICODE = 5
      0 PRINT 38 , NUMBER, TYPE, DIST, IDEPTH, ICODE, PHIMED, SORT,
      1 PHISRT, COARSE, FINE, SILT, CLAY
   38 0 FORMAT [ 1H0, I2, A1, F6.1, I5, 13H SAN SIL CLY          ,
      1 I2, F6.1, 2[F5.1], 4[F6.1] ]
      0 PUNCH 39 , NUMBER, TYPE, DIST, IDEPTH, ICODE, PHIMED, SORT,
      1 PHISRT, COARSE, FINE, SILT, CLAY
   39 0 FORMAT [       I2, A1, F6.1, I5, 13H SAN SIL CLY          ,
      1 I2, F6.1, 2[F5.1], 4[F6.1] ]
        GO TO 1
        END
```

```
C       PROGRAM TO COMPUTE MASS CHARACTERISTICS OF OCEANIC SEDIMENTS

 1      READ 2, NUMBER, TYPE, MRKEND, XMED, Q3, Q1, WETSED, DRYSED
 2      FORMAT ( I2, A1, 1X, I1, 2(F6.0), 2(F7.0), F5.0)
        IF (MRKEND - 1) 4,3,4
 3      CALL EXIT
 4      WTRCON = (WETSED - DRYSED) / DRYSED
        POROUS = 2.67 * WTRCON / (2.67 * WTRCON + 1.0)
        DENSTY = 1.03 * POROUS + 2.75 * (1.0 - POROUS)
        COMPRS = (43.0 * POROUS + 2.0 * (1.0 - POROUS)) * 10.0 ** (-12)
        VELCTY = SQRTF (1.0 / (DENSTY * COMPRS)) * 10.0 ** (-5)
        XIMPED = DENSTY * VELCTY
        REFCOE = (XIMPED - 1.54) / (XIMPED + 1.54)
        BTMLOS = -8.69 * LOGF (REFCOE)
        VOIDSP = WTRCON * 2.67
        IF (XMED) 6,5,6
 5      PHIMED = 0.0
        SORT = 0.0
        PHISRT = 0.0
        GO TO 7
 6      PHIMED = -1.44 * LOGF (XMED)
        SORT = SQRTF (Q3 / Q1)
        PHISRT = 1.44 * LOGF (SORT)
 7    0 PUNCH 8, NUMBER, TYPE, XMED, PHIMED, SORT, PHISRT, WTRCON,
      1 VOIDSP, POROUS, DENSTY, VELCTY, XIMPED, REFCOE, BTMLOS
      0 PRINT 9, NUMBER, TYPE, XMED, PHIMED, SORT, PHISRT, WTRCON,
      1 VOIDSP, POROUS, DENSTY, VELCTY, XIMPED, REFCOE, BTMLOS
 8      FORMAT (   I2, A1, F6.3, 2(F5.1), F4.1, 3(F6.3), 4(F5.2), F5.1)
```

```
9     FORMAT(1H0, I2, A1, F6.3, 2(F5.1), F4.1, 3(F6.3), 4(F5.2), F5.1)
      GO TO 1
      END
```

COMPUTER PROGRAM V

```
C       PROGRAM TO PERFORM A CORRELATION AND REGRESSION ANALYSIS

        SUM X = 0
        SUM X X = 0
        SUM Y = 0
        SUM Y Y = 0
        SUM YX = 0
        NSIZE = 0
  1     READ 2, N, Y, X
  2     FORMAT [ I2, 30X, F8.1, F6.1 ]
        IF [ N ] 8, 10, 6
  6     NSIZE = NSIZE + 1
        SUM Y = SUM Y + Y
        SUM X = SUM X + X
        SUM YY = SUM YY +[Y * Y ]
        SUM X X = SUM X X + [ X * X ]
        SUM YX = SUM Y X + [ Y * X ]
        GO TO 1
 10     SIZE = NSIZE
        A = SUMYX - [SUMY * SUMX] / SIZE
        B = SUMXX - [SUMX * SUMX] / SIZE
        SLOPE = A/B
        YCEPT = [SUMY - SLOPE * SUMX] / SIZE
        C = SIZE * SUMYX -[SUMX * SUMY]
        D1 = SIZE * SUMXX - [SUMX * SUMX]
        D2 = SIZE * SUMYY - [SUMY * SUMY]
        D = SQRTF [ D1 * D2]
        CORE = C/D
        SYSY = SUM YY / SIZE - [ SUM Y * SUM Y / [ SIZE * SIZE ]  ]
```

COMPUTER PROGRAM V

```
      E = SYSY * ( 1.0 - (C * C) / (D * D)  )
      SYX = SQRTF ( E)
      FRAC = (1.0 + CORE) / (1.0 - CORE)
      Z = .5 * LOGF( FRAC)
      ZSTND = 1.0 / SQRTF (SIZE - 3.0)
      PRINT 70, N, NSIZE, ZSTND, YCEPT, SLOPE, CORE, Z, X
 70   FORMAT ( 1H0, I2, I3, 6F10.5 )
      PRINT 71, SUMY, SUMYY, SUMX, SUMXX, SUMYX
 71   FORMAT ( 1H0, 5F14.4 )

      PRINT 176, SYX
176   FORMAT ( 1H0, F10.5 )
  8   CALL EXIT
      END
```

APPENDIX C

TABLE VIII

ECHO STRENGTH MEASUREMENTS AT NORMAL INCIDENCE

TAG	P1	P2	P3	N	E1	E2	E3	DEPTH	LAT.	LONG.
				ECHO STRENGTH MESUREMENTS MADE ON CHAIN 19						
1	-9.6	2.6	-4.8	17	-90.4	1.6	-88.0	2830	26050N	67275W
2	-8.8	2.1	-4.9	14	-90.2	1.7	-87.2	2900	26140N	67280W
3	-8.7	1.7	-6.7	9	-88.7	1.2	-88.1	2850	26200N	67285W
4	-12.1	1.8	-8.0	14	-92.4	1.8	-89.4	2820	26205N	67285W
5	-7.8	3.4	-4.1	16	-88.6	1.6	-84.8	2760	29220N	67330W
6	-2.2	3.1	2.8	16	-86.6	2.0	-83.8	2740	29250N	67330W
7	-4.9	3.5	-1.0	7	-88.4	2.1	-85.2	2740	29270N	67325W
8	-3.9	2.6	1.1	9	-87.5	1.8	-83.8	2740	29280N	67325W
9	-4.2	3.7	-1.0	10	-85.6	1.1	-84.4	2740	29300N	67320W
10	-4.7	2.0	-1.7	7	-86.5	1.2	-84.5	2740	29320N	67320W
11	-6.2	1.6	-2.6	7	-86.2	1.1	-84.6	2730	29330N	67320W
12	-4.3	2.3	-1.6	9	-85.5	1.3	-83.3	2730	29355N	67325W
13	-6.3	2.9	-1.0	8	-87.8	2.0	-84.7	2720	29390N	67325W
14	-4.5	2.6	-1.1	19	-86.2	1.6	-85.2	2720	29400N	67330W
15	-7.3	0.5	-6.7	8	-86.0	1.2	-83.6	2720	30005N	67345W
16	-6.9	2.9	-0.3	7	-86.6	1.1	-84.2	2710	30040N	67345W
17	-8.3	1.7	-6.7	8	-87.7	1.8	-83.5	2710	30150N	67350W
18	-3.3	3.5	-1.5	11	-85.4	1.1	-83.4	2720	30175N	67350W
19	-7.4	2.0	-4.8	15	-88.2	1.1	-86.9	2720	30200N	67355W
20	-7.0	3.7	-3.1	9	-89.1	2.2	-87.0	2720	30305N	67360W
21	-8.8	2.1	-2.7	18	-86.2	1.4	-82.1	2710	30340N	67360W
22	-5.9	1.9	-3.3	9	-88.2	1.2	-86.2	2710	30370N	67360W
23	-6.9	2.8	-1.0	18	-88.8	1.9	-85.0	2710	30405N	67365W

TABLE VIII

ECHO STRENGTH MEASUREMENTS AT NORMAL INCIDENCE

TAG	P1	P2	P3	N	E1	E2	E3	DEPTH	LAT.	LONG.
24	-9.0	1.4	-6.8	12	-90.5	1.5	-89.3	2690	30410N	67365W
25	-8.8	2.1	-3.3	19	-90.3	1.5	-87.2	2700	30425N	67365W
26	-5.0	1.8	-1.8	14	-85.6	1.1	-84.6	2700	30460N	67370W
27	-6.2	2.4	-1.6	8	-86.2	1.0	-84.7	2700	30510N	67370W
28	-6.5	0.9	-5.6	7	-85.5	0.6	-84.6	2710	30550N	67370W
29	-9.1	2.7	-5.2	7	-89.0	1.8	-86.1	2740	30580N	67375W
30	-8.4	2.8	-3.3	10	-89.3	1.7	-86.2	2710	31010N	67380W
31	-6.5	2.8	-1.5	13	-88.2	1.8	-84.2	2710	31050N	67380W
32	-8.6	2.6	-3.7	8	-89.9	1.9	-86.1	2660	32585N	67400W
33	-5.0	2.8	-1.6	21	-85.4	2.2	-81.8	2720	33010N	67400W
34	-6.6	3.4	-0.7	8	-87.3	2.8	-83.5	2720	33090N	67400W
35	-8.1	3.9	-1.4	21	-90.3	3.9	-83.5	2700	33145N	67400W
36	-6.9	2.5	-2.2	6	-88.3	2.0	-84.7	2720	33210N	67395W
37	-4.9	2.6	0.6	14	-86.7	2.3	-83.2	2720	33255N	67395W
38	-0.4	2.7	5.0	14	-82.8	1.9	-78.8	2770	35045N	67490W
39	-1.7	2.3	2.7	14	-80.7	1.8	-78.4	2770	35050N	67490W
40	-0.6	2.9	6.0	15	-82.0	1.7	-78.1	2750	35055N	67490W
41	5.6	2.2	8.5	15	-75.5	1.4	-74.5	2750	35105N	67500W
42	0.5	3.7	8.1	14	-80.5	2.2	-76.2	2710	35190N	67510W
43	-3.4	3.9	4.2	7	-82.1	1.8	-78.8	2710	35200N	67510W
44	-3.9	2.9	2.5	7	-81.6	1.4	-79.2	2710	35210N	67515W
45	-2.4	3.9	7.5	14	-82.2	1.8	-76.8	2700	35235N	67520W
46	-3.8	2.8	0.7	14	-82.5	1.4	-79.5	2690	35270N	67525W
47	3.0	1.5	6.3	13	-76.3	0.7	-74.9	2660	35375N	67540W
48	3.4	2.2	7.6	14	-77.7	1.2	-76.2	2650	35505N	67545W

TABLE VIII

ECHO STRENGTH MEASUREMENTS AT NORMAL INCIDENCE

TAG	P1	P2	P3	N	E1	E2	E3	DEPTH	LAT.	LONG.
49	3.2	3.1	8.4	19	-78.3	1.9	-74.6	2650	35540N	67550W
					ECHO STRENGTH MESUREMENTS MADE ON CHAIN 21					
1	-3.6	2.7	0.2	5	-84.7	2.9	-81.3	2730	34175N	66050W
2	-0.6	2.5	3.3	20	-80.9	1.9	-79.3	2730	34185N	66065W
3	-2.1	1.9	1.7	20	-82.3	2.1	-80.3	2780	34355N	66175W
4	-1.6	1.4	1.7	14	-81.6	1.9	-77.3	2700	34500N	66270W
5	-0.1	2.7	3.7	12	-80.0	2.5	-78.1	2700	35015N	66345W
6	-0.2	1.7	2.0	8	-81.2	2.0	-79.5	2700	35060N	66375W
7	-1.5	2.6	4.7	16	-82.3	2.1	-77.5	2690	35105N	66410W
8	-0.3	2.6	2.6	13	-80.9	2.9	-78.6	2660	35125N	66425W
9	-0.2	2.4	3.3	15	-81.6	3.4	-78.1	2660	35150N	66445W
10	-0.6	3.3	8.0	13	-81.5	2.4	-75.6	2630	35175N	66465W
11	-2.0	2.2	3.0	11	-84.3	2.7	-78.6	2640	35200N	66480W
12	-2.7	1.8	0.5	16	-83.9	2.0	-80.8	2630	35220N	66500W
13	3.1	3.9	8.0	20	-79.0	3.3	-75.3	2650	35250N	66515W
14	-1.1	2.8	3.4	14	-82.1	2.9	-77.3	2650	35280N	66540W
15	-2.4	1.6	-0.6	5	-82.3	2.1	-80.5	2630	35305N	66560W
16	-3.3	4.0	2.4	9	-81.9	3.7	-79.2	2630	35390N	67015W
17	-0.5	2.6	5.0	12	-79.9	1.3	-77.2	2680	35435N	67050W
18	0.1	2.5	2.9	7	-81.3	2.6	-78.6	2680	35495N	67095W
19	2.7	2.1	6.4	12	-77.8	1.3	-75.5	2680	35525N	67120W
20	-0.4	1.6	2.7	14	-79.9	1.2	-77.8	2650	35550N	67135W
21	6.7	1.8	8.3	9	-74.2	1.2	-72.7	2630	35560N	67145W
22	5.8	2.2	9.0	14	-76.6	2.7	-73.7	2620	35585N	67160W

TABLE VIII

ECHO STRENGTH MEASUREMENTS AT NORMAL INCIDENCE

TAG	P1	P2	P3	N	E1	E2	E3	DEPTH	LAT.	LONG.
23	5.1	3.4	12.6	5	-76.1	3.1	-69.3	2640	36000N	67175W
24	5.6	2.9	11.9	11	-75.6	2.0	-71.6	2640	36050N	67180W
25	5.3	2.7	12.3	11	-75.9	2.3	-71.8	2640	36055N	67215W
26	7.9	2.3	12.1	12	-75.5	2.2	-71.3	2630	36095N	67245W
27	6.3	1.9	8.0	6	-76.2	1.2	-74.5	2610	36125N	67270W
28	1.9	1.1	3.1	7	-76.9	1.0	-76.5	2610	36160N	67290W
29	4.3	2.7	6.7	11	-76.8	1.4	-74.2	2610	36175N	67308W
30	4.6	1.8	7.8	15	-76.4	1.2	-74.1	2610	36200N	67325W
31	4.9	1.5	6.6	14	-75.8	1.5	-73.0	2610	36225N	67340W
32	4.9	1.5	6.8	8	-76.8	1.2	-75.0	2610	36255N	67365W
33	3.0	1.6	4.8	7	-76.7	0.7	-75.5	2610	36265N	67375W
34	7.2	3.5	12.9	11	-75.3	2.3	-70.5	2610	36285N	67395W
35	8.0	1.6	10.0	11	-74.5	1.4	-72.6	2610	36320N	67415W
36	10.0	2.9	14.9	8	-72.9	2.6	-69.1	2610	36375N	67455W
37	7.0	2.6	13.7	19	-76.5	2.2	-69.5	2620	36400N	67475W
38	7.5	2.1	11.5	11	-75.2	1.5	-72.7	2620	36425N	67495W
39	6.0	4.3	13.9	15	-77.7	3.8	-69.4	2620	36455N	67510W
40	7.6	2.8	11.5	14	-75.8	2.1	-71.8	2610	36475N	67530W
41	6.6	2.8	12.8	13	-75.5	2.1	-71.0	2600	36515N	67565W
42	7.8	2.3	10.5	10	-75.2	1.7	-72.3	2600	36540N	67580W
43	8.5	2.3	14.0	9	-73.7	1.7	-69.3	2600	36560N	67590W
44	7.7	1.8	11.4	16	-73.9	1.1	-71.8	2600	36580N	68010W
45	5.7	2.2	10.0	15	-75.1	1.7	-72.4	2600	37005N	68025W
46	8.2	2.4	12.3	11	-74.0	1.8	-70.8	2600	37025N	68030W
47	6.6	2.0	9.6	12	-75.6	1.8	-73.3	2590	37050N	68045W

TABLE VIII

ECHO STRENGTH MEASUREMENTS AT NORMAL INCIDENCE

TAG	P1	P2	P3	N	E1	E2	E3	DEPTH	LAT.	LONG.
48	6.0	2.2	9.9	14	-75.9	1.4	-73.5	2590	37075N	68055W
49	8.3	2.4	11.7	11	-73.8	1.7	-71.6	2580	37100N	68070W
50	2.3	2.7	9.3	11	-78.6	1.8	-74.3	2590	37120N	68080W
51	1.4	1.2	3.4	12	-79.6	1.6	-77.4	2540	37170N	68105W
52	7.2	2.6	9.9	11	-74.2	1.4	-71.8	2440	37370N	68215W
53	4.5	2.1	7.7	12	-74.5	1.4	-72.4	2380	37485N	68290W
54	7.5	2.5	10.9	13	-73.0	1.6	-70.0	2300	37540N	68325W
55	6.0	1.5	7.3	16	-73.4	1.1	-71.6	2290	37550N	68340W
56	7.9	1.6	10.2	11	-72.6	1.4	-69.8	2210	38015N	68400W
57	6.1	1.7	10.5	15	-75.1	1.9	-70.7	2160	38055N	68435W
58	7.4	2.8	12.6	6	-73.1	1.2	-71.0	2130	38095N	68460W
59	6.9	2.4	11.6	7	-73.8	1.9	-71.4	2100	38120N	68480W
60	7.3	1.7	10.6	8	-73.3	1.6	-70.7	2070	38145N	68500W
61	9.1	1.8	12.5	7	-72.1	1.4	-70.1	2050	38175N	68520W
62	6.5	1.8	10.3	13	-74.4	1.6	-71.8	1860	38300N	69005W
63	9.8	2.3	12.7	13	-72.7	1.9	-69.7	1820	38350N	69035W
64	2.9	4.2	11.3	20	-78.3	4.0	-70.7	1820	38365N	69045W
65	10.1	2.0	13.8	11	-71.7	1.6	-68.1	1740	38445N	69105W
66	13.0	2.9	15.8	12	-69.0	2.1	-66.0	1740	38470N	69120W
67	12.0	2.0	15.1	10	-70.0	1.4	-67.2	1680	38535N	69170W
68	8.0	1.2	10.3	12	-71.8	1.6	-69.2	1460	39115N	69310W
69	11.7	2.5	14.3	7	-70.2	1.5	-68.3	1360	39175N	69350W
70	12.1	3.4	19.0	11	-69.8	2.5	-64.2	1360	39195N	69370W
71	12.3	2.6	14.7	15	-67.6	1.3	-66.1	1240	39305N	69450W
72	16.3	2.0	18.1	11	-64.8	1.7	-62.9	1220	39315N	69460W

TABLE VIII

ECHO STRENGTH MEASUREMENTS AT NORMAL INCIDENCE

TAG	P1	P2	P3	N	E1	E2	E3	DEPTH	LAT.	LONG.
73	14.3	2.2	16.3	11	-67.6	1.8	-64.7	1220	39320N	69465W
74	11.2	1.6	14.5	14	-69.4	1.1	-67.9	1190	39370N	69500W
75	7.6	2.1	12.0	10	-72.3	1.2	-69.5	1150	39390N	69515W
76	8.7	1.5	11.2	12	-70.8	0.6	-69.6	1020	39430N	69550W
77	14.8	3.2	16.2	13	-65.7	1.9	-63.9	1000	39445N	69560W
78	11.6	2.1	15.0	16	-68.2	1.4	-66.2	1000	39460N	69570W
					ECHO STRENGTH MESUREMENTS MADE ON CHAIN 27					
1	-3.1	1.6	0.5	26	-81.3	1.7	-78.8	2720	33570N	65520W
2	-3.2	2.8	4.7	19	-79.8	0.7	-78.7	2610	33550N	65555W
3	1.7	2.4	3.6	23	-80.2	1.2	-78.8	2695	33531N	66000W
4	1.3	2.3	5.8	13	-82.0	1.8	-78.9	2700	33570N	66000W
5	0.7	3.3	2.5	16	-81.9	1.5	-79.2	2730	33035N	66006W
6	1.9	2.5	9.0	17	-80.4	2.0	-77.4	2725	34100N	66012W
7	1.0	2.4	4.2	15	-77.6	1.0	-76.2	2730	34155N	66026W
8	0.3	2.5	4.1	19	-81.9	1.4	-79.1	2745	34211N	66040W
9	2.5	2.1	7.2	19	-78.1	1.3	-75.9	2755	34230N	66070W
10	4.4	1.5	6.6	18	-76.8	0.8	-74.8	2745	34250N	66110W
11	2.2	2.3	4.4	8	-78.3	1.7	-75.8	2725	34270N	66140W
12	1.7	2.5	7.2	23	-77.3	1.6	-74.9	2720	34280N	66130W
13	-0.6	3.4	5.4	21	-77.9	1.8	-73.7	2710	34310N	66100W
14	1.5	1.9	5.7	34	-77.9	1.5	-74.5	2690	34330N	66060W
15	1.6	2.3	6.3	22	-78.3	1.4	-76.1	2665	34360N	66030W
16	2.2	2.2	6.4	22	-77.5	1.4	-74.7	2670	34360N	66010W

TABLE VIII

ECHO STRENGTH MEASUREMENTS AT NORMAL INCIDENCE

TAG	P1	P2	P3	N	E1	E2	E3	DEPTH	LAT.	LONG.
17	1.3	2.6	5.7	21	-78.1	2.3	-76.1	2695	34350N	66590W
18	3.2	2.7	8.7	19	-76.3	1.6	-74.8	2735	34320N	65580W
19	3.0	2.7	10.5	22	-76.6	1.6	-74.9	2745	34290N	65560W
20	2.1	3.4	10.6	21	-80.0	2.2	-75.3	2545	34230N	65540W
21	0.8	1.9	5.0	24	-77.8	1.0	-75.1	2700	34170N	66010W
22	-0.2	4.0	8.1	24	-80.6	3.2	-75.7	2700	34120N	66040W
23	1.6	1.8	3.9	19	-78.9	1.7	-76.9	2730	34060N	66060W
24	-0.6	3.2	7.7	22	-78.9	1.8	-73.8	2725	34010N	66090W
25	3.4	2.0	7.7	16	-78.8	1.7	-74.3	2715	33550N	66100W
26	1.4	2.8	5.9	13	-81.8	2.4	-77.2	2710	33550N	66110W
27	-0.5	2.7	3.5	14	-80.7	2.3	-78.5	2715	33550N	66110W
28	-1.0	3.4	3.3	17	-81.9	3.4	-77.6	2720	33550N	66120W
29	0.9	2.8	3.5	13	-80.7	1.3	-78.4	2705	33550N	66130W
30	-1.2	2.8	3.3	18	-81.7	2.5	-77.9	2710	33550N	66180W
31	2.0	2.7	6.5	18	-80.0	2.0	-76.7	2725	33550N	66240W
32	-1.3	3.7	8.1	29	-81.3	2.4	-75.9	2735	33550N	66300W
33	-0.8	3.4	7.5	26	-83.0	2.6	-76.8	2735	33550N	66370W
34	-1.6	4.1	7.2	34	-82.2	2.9	-76.2	2735	33550N	66370W
35	0.4	5.1	9.2	16	-80.3	3.8	-75.4	2740	33540N	66370W
36	-1.0	4.1	8.2	26	-80.5	2.7	-75.5	2735	33540N	66380W
37	-2.0	4.0	6.1	14	-81.2	2.9	-77.0	2750	33540N	66440W
38	-0.3	2.6	5.7	23	-82.1	2.3	-78.1	2755	33540N	66500W
39	0.2	2.2	3.9	20	-82.0	2.7	-78.8	2740	33550N	66570W
40	-0.1	3.0	6.2	22	-80.5	2.0	-77.6	2740	33550N	67030W
41	-0.6	2.8	5.5	30	-81.8	2.1	-77.6	2730	33540N	67120W

TABLE VIII

ECHO STRENGTH MEASUREMENTS AT NORMAL INCIDENCE

TAG	P1	P2	P3	N	E1	E2	E3	DEPTH	LAT.	LONG.
42	-0.2	2.7	3.8	26	-81.3	2.2	-78.0	2735	33540N	67210W
43	-2.5	3.3	5.5	10	-82.2	2.0	-77.9	2735	33540N	67210W
44	-0.7	2.2	1.7	13	-82.5	1.9	-79.1	2735	33540N	67220W
45	-1.4	4.2	5.7	12	-82.1	3.1	-77.8	2740	33530N	67220W
46	2.4	3.7	5.9	6	-79.4	3.0	-77.2	2730	33530N	67220W
47	-1.6	2.3	3.6	19	-82.0	1.8	-79.0	2735	33535N	67220W
48	0.1	2.0	3.4	11	-81.7	1.7	-79.1	2735	33445N	67040W
49	1.3	3.2	7.7	23	-79.7	2.2	-75.2	2730	33430N	66570W
50	-1.4	2.3	3.1	7	-81.1	1.5	-78.4	2730	33415N	66510W
51	0.9	3.5	7.2	12	-79.0	2.4	-76.0	2700	33390N	66440W
52	0.3	3.6	10.1	29	-81.2	2.6	-75.6	2730	33360N	66370W
53	0.3	2.7	5.4	28	-81.7	2.5	-77.4	2680	33300N	66220W
54	2.9	1.9	6.5	17	-76.3	1.0	-74.6	2650	33210N	65590W
55	3.2	3.0	9.1	13	-78.5	1.9	-75.1	2420	33180N	65500W
56	6.1	3.8	11.4	18	-76.0	1.9	-73.8	2605	33150N	65420W
57	2.2	3.2	7.3	12	-78.1	2.5	-74.3	2600	33140N	65400W
58	2.0	2.9	8.0	75	-79.1	3.0	-74.9	2550	33070N	65190W
59	4.6	2.6	10.7	52	-75.4	1.9	-71.4	2515	33000N	65010W
60	8.5	2.3	11.7	24	-73.6	1.4	-71.0	2550	33070N	65100W
61	8.1	8.4	12.6	47	-73.6	2.0	-70.2	2565	33090N	65110W
62	1.1	2.8	6.0	13	-80.0	3.2	-75.2	2570	33110N	65130W
63	2.3	3.2	8.0	67	-79.5	3.3	-75.6	2560	33130N	65140W
64	3.4	2.0	6.9	42	-78.7	1.5	-76.0	2555	33130N	65140W
65	4.2	1.9	8.8	17	-77.9	1.4	-74.4	2560	33140N	65120W
66	2.2	1.7	3.0	7	-77.5	1.4	-76.7	2600	33180N	65170W

TABLE VIII

ECHO STRENGTH MEASUREMENTS AT NORMAL INCIDENCE

TAG	P1	P2	P3	N	E1	E2	E3	DEPTH	LAT.	LONG.
67	-0.1	3.0	5.6	15	-81.0	2.4	-76.7	2565	33220N	65230W
68	2.1	4.4	11.6	32	-79.2	4.2	-73.4	2620	33270N	65290W
69	2.7	3.2	9.5	30	-78.5	2.4	-73.6	2630	33320N	65350W
70	-0.1	1.7	2.5	10	-80.1	1.3	-78.9	2655	33370N	65410W
71	0.5	4.1	10.2	7	-76.9	2.0	-72.5	2685	33420N	65470W
72	-0.5	3.8	8.3	14	-80.0	3.8	-73.7	2690	33460N	65520W
73	0.2	1.6	3.7	18	-81.8	1.6	-79.1	2690	33540N	65550W
74	2.8	2.9	9.7	109	-78.5	2.6	-74.0	2710	34030N	65570W
75	-0.2	2.5	4.7	17	-79.8	1.6	-76.5	2730	34100N	66000W
76	1.0	3.4	10.3	32	-77.0	1.9	-72.4	2730	34180N	65580W
77	1.0	2.9	6.8	21	-78.7	1.9	-74.7	2740	34200N	65500W
78	1.0	3.0	7.0	15	-77.0	1.9	-74.4	2740	34240N	65430W
79	3.6	2.1	6.8	15	-74.9	1.5	-73.2	2740	34270N	65360W
80	1.4	2.1	4.9	15	-76.7	1.3	-74.2	2655	34400N	65290W
81	-0.7	1.5	1.9	26	-78.1	1.1	-75.7	2625	34460N	65240W
82	-3.4	2.3	2.9	24	-79.5	1.3	-77.0	2580	34560N	65190W
83	0.9	2.6	8.0	36	-78.7	1.8	-74.0	2550	35040N	65180W
84	0.5	1.5	2.9	21	-78.0	1.4	-75.8	2555	35070N	65170W
85	2.6	2.5	6.9	18	-76.7	1.9	-72.3	2570	35130N	65080W
86	2.5	2.0	6.1	24	-76.3	1.4	-73.9	2475	35200N	64590W
87	-0.3	3.2	4.3	37	-78.9	3.7	-75.9	2580	35200N	64590W
88	2.0	2.1	5.7	18	-77.4	1.8	-74.3	2580	35240N	65030W
89	-0.8	2.5	3.5	12	-80.3	3.5	-76.9	2580	35170N	65090W
90	2.3	2.9	8.9	23	-76.9	2.1	-72.4	2560	35140N	65120W
91	0.5	2.2	4.2	17	-78.3	2.0	-74.7	2590	35060N	65240W

TABLE VIII

ECHO STRENGTH MEASUREMENTS AT NORMAL INCIDENCE

TAG	P1	P2	P3	N	E1	E2	E3	DEPTH	LAT.	LONG.
92	2.0	3.0	7.7	15	-77.3	1.9	-73.5	2610	35010N	65300W
93	-0.8	2.2	5.1	13	-78.6	1.3	-74.9	2615	34560N	65350W
94	1.2	2.4	4.3	9	-77.9	1.6	-75.7	2640	34510N	65300W
95	-1.4	1.5	1.9	6	-78.0	1.5	-77.7	2680	34470N	65490W
96	1.2	1.6	5.4	11	-77.1	1.1	-75.3	2675	34440N	65540W
97	1.0	2.7	4.7	14	-78.9	2.3	-76.4	2705	34040N	65530W
98	-1.3	2.2	3.5	9	-79.5	1.5	-77.7	2735	34370N	66030W
99	1.0	1.3	2.4	6	-78.2	1.0	-76.3	2740	34350N	66070W
100	-1.1	3.2	6.2	10	-78.9	2.0	-75.0	2735	34360N	66120W
101	1.9	2.9	5.6	13	-76.3	2.6	-73.0	2740	34370N	66180W
102	1.9	3.4	7.3	11	-77.6	2.3	-75.0	2730	34370N	66240W
103	0.5	2.5	4.7	6	-78.3	2.3	-76.3	2750	34370N	66300W
104	1.9	2.5	7.0	52	-77.4	2.1	-72.7	2750	34370N	66300W
105	2.8	2.4	5.7	16	-75.4	2.1	-73.0	2750	34340N	66315W
106	1.5	2.2	5.9	8	-76.7	2.1	-74.0	2765	34320N	66325W
107	2.3	3.6	8.8	7	-77.9	2.8	-73.4	2765	34310N	66330W
108	2.5	1.0	5.3	12	-76.9	1.4	-74.1	2760	34330N	66270W
109	0.9	3.0	7.1	18	-76.9	2.2	-73.9	2740	34450N	66220W
110	2.1	1.8	6.7	12	-76.2	1.1	-73.7	2745	34400N	66160W
111	2.7	2.0	5.4	13	-76.1	1.8	-73.3	2720	34450N	66110W
112	1.3	2.5	4.7	18	-77.3	2.0	-74.8	2680	34470N	66010W
113	1.3	1.7	5.9	25	-76.6	1.1	-73.4	2675	34490N	65520W
114	0.2	2.0	3.5	9	-77.8	1.2	-75.2	2655	34490N	65510W
115	-1.6	1.9	2.0	7	-78.2	1.5	-76.8	2630	34490N	65500W
116	0.5	2.0	4.3	25	-77.7	1.5	-74.1	2615	34530N	65510W

TABLE VIII

ECHO STRENGTH MEASUREMENTS AT NORMAL INCIDENCE

TAG	P1	P2	P3	N	E1	E2	E3	DEPTH	LAT.	LONG.
117	1.2	2.3	7.6	97	-77.0	1.8	-72.3	2615	34530N	65520W
118	1.4	2.1	4.1	12	-77.5	1.3	-75.3	2630	35020N	65520W
119	2.2	3.0	7.6	16	-76.1	3.0	-72.2	2625	35010N	65580W
120	0.2	2.4	6.6	26	-79.7	2.1	-75.0	2760	35210N	66480W
121	0.4	3.2	5.9	26	-80.6	2.9	-75.3	2640	35260N	66530W
122	6.3	2.3	9.8	19	-74.7	1.6	-71.8	2675	35390N	67050W
123	4.9	3.4	15.1	19	-73.5	2.3	-69.9	2690	35450N	67090W
124	8.3	3.8	17.4	18	-70.3	1.5	-68.4	2675	35510N	67130W
125	6.1	2.8	12.8	17	-73.8	1.5	-70.5	2640	35570N	67170W
126	7.6	3.0	15.5	53	-72.6	1.5	-70.0	2640	36030N	67210W
127	7.5	2.6	11.2	27	-72.4	2.4	-69.6	2635	36210N	67230W
128	7.4	3.2	13.3	32	-71.7	2.7	-67.3	2635	36240N	67230W
129	6.9	3.1	13.7	35	-74.2	2.6	-70.1	2640	36270N	67240W
130	9.6	3.4	14.9	39	-72.0	2.1	-68.6	2645	36300N	67250W
131	8.9	3.2	15.1	36	-72.8	2.0	-69.3	2645	36330N	67260W
132	9.0	2.3	15.4	32	-71.5	1.5	-68.4	2645	36350N	67260W
133	10.0	2.8	16.1	45	-71.3	2.1	-67.8	2640	36380N	67270W
134	11.0	2.7	16.9	37	-70.7	1.7	-66.7	2635	36410N	67330W
135	11.1	2.6	15.4	42	-70.4	1.8	-67.8	2635	36430N	67370W
136	12.7	2.7	18.4	37	-69.3	1.8	-66.0	2630	36450N	67400W
137	11.4	2.6	17.8	38	-70.1	1.9	-66.7	2630	36480N	67400W
138	12.0	2.7	16.9	33	-71.0	2.1	-67.3	2630	36510N	67400W
139	10.1	3.2	14.4	36	-71.5	3.4	-69.2	2630	36540N	67410W
140	9.8	3.5	14.8	26	-71.5	2.1	-69.1	2625	36570N	67410W
141	8.5	2.3	11.6	29	-72.1	1.9	-69.3	2625	36590N	67440W

TABLE VIII

ECHO STRENGTH MEASUREMENTS AT NORMAL INCIDENCE

TAG	P1	P2	P3	N	E1	E2	E3	DEPTH	LAT.	LONG.
142	10.7	3.7	17.7	38	-71.4	2.5	-68.7	2620	37000N	67470W
143	9.2	2.9	13.8	26	-73.2	2.5	-70.7	2615	37010N	67500W
144	9.0	3.2	14.1	34	-73.2	2.6	-70.0	2620	37010N	67450W
145	10.4	2.5	13.9	30	-71.5	2.2	-69.9	2625	37040N	67400W
146	8.0	3.0	13.3	23	-72.1	2.4	-68.4	2620	37050N	67450W
147	11.4	2.3	15.9	24	-71.1	1.0	-69.0	2615	37030N	67530W
148	11.2	1.8	15.0	19	-70.6	0.5	-69.7	2610	36580N	67580W
149	11.2	3.5	16.1	22	-71.5	1.6	-70.5	2615	36560N	67510W
150	9.9	2.9	13.9	19	-71.5	0.9	-70.6	2615	37000N	67480W
151	11.3	2.8	15.4	20	-70.9	1.4	-69.2	2620	37060N	67410W
152	12.1	3.5	15.3	18	-70.0	3.2	-66.3	2620	37020N	67500W
153	13.5	2.8	16.1	21	-68.8	2.6	-65.9	2610	37060N	67510W
154	5.2	3.1	10.1	12	-71.0	1.6	-68.8	2565	37140N	67590W
155	4.0	3.9	15.9	20	-72.7	1.7	-70.1	2530	37160N	68020W
156	7.4	2.1	9.6	5	-68.8	1.1	-67.4	2525	37210N	68050W
157	11.5	3.5	18.0	31	-69.4	3.0	-65.1	2490	37310N	68110W
158	11.5	3.0	18.0	26	-69.0	2.8	-65.3	2475	37360N	68140W
159	10.9	3.5	18.8	31	-69.6	2.5	-65.8	2440	37400N	68180W
160	11.8	2.4	18.0	22	-68.9	1.6	-65.0	2370	37480N	68240W
161	11.5	2.2	15.6	47	-68.5	1.6	-65.9	2320	37530N	68270W
162	12.4	2.8	19.9	21	-68.4	1.6	-64.0	2280	37580N	68310W
163	10.8	2.1	13.9	25	-69.1	1.8	-66.4	2225	38030N	68340W
164	12.1	2.9	19.2	23	-68.8	2.0	-64.5	2195	38080N	68360W
165	15.9	3.2	19.9	31	-66.4	2.4	-63.9	2150	38140N	68380W
166	15.1	2.3	19.3	20	-67.3	2.1	-64.3	2090	38180N	68460W

TABLE VIII

ECHO STRENGTH MEASUREMENTS AT NORMAL INCIDENCE

TAG	P1	P2	P3	N	E1	E2	E3	DEPTH	LAT.	LONG.
167	13.0	2.2	16.9	22	-68.2	2.1	-66.2	2020	38220N	68550W
168	13.9	2.5	19.6	27	-67.4	1.5	-64.5	1920	38290N	68540W
169	14.7	3.4	20.9	23	-65.6	2.6	-62.1	1790	38410N	68580W
170	12.3	2.6	16.1	31	-67.4	2.1	-64.3	1720	38520N	69030W
171	11.7	2.2	16.9	18	-68.7	1.3	-65.4	1680	38580N	69050W
172	10.6	1.8	17.3	33	-68.7	1.3	-64.9	1700	38570N	69090W
173	15.4	4.3	23.1	21	-66.9	4.0	-59.2	1680	38560N	69130W
174	3.5	2.5	7.1	39	-75.6	4.0	-71.9	1725	38580N	69170W
175	16.0	3.3	23.5	34	-65.1	2.5	-59.6	1400	39160N	69280W
176	17.3	3.6	24.0	55	-63.8	2.4	-58.5	1320	39210N	69320W
177	7.1	1.4	9.7	19	-69.3	0.6	-68.4	1285	39310N	69320W
178	6.8	1.6	11.4	71	-70.1	1.5	-67.7	1285	39310N	69320W
179	16.2	2.3	20.7	59	-62.2	1.8	-58.3	1080	39430N	69410W
180	19.4	2.9	24.2	39	-59.9	2.6	-55.8	1030	39460N	69420W
181	21.5	3.5	23.7	24	-60.2	2.2	-57.2	1100	39420N	69370W
182	11.4	1.6	15.3	17	-66.9	1.2	-63.7	1140	39410N	69290W
183	19.6	2.7	23.8	47	-60.4	2.4	-55.5	1120	39380N	69310W
184	15.5	2.9	22.9	21	-66.1	3.3	-58.5	1105	39390N	69320W
185	13.0	1.8	17.6	16	-69.0	2.4	-65.4	1110	39410N	69350W
186	14.6	1.4	17.7	21	-65.8	2.1	-63.1	1070	39430N	69370W
187	11.4	1.4	14.6	19	-69.9	1.9	-67.2	910	39450N	69390W
188	12.8	2.3	19.6	29	-68.8	2.1	-63.3	930	39450N	69390W
189	14.0	2.7	21.5	14	-64.7	2.4	-60.0	950	39460N	69400W
190	13.3	1.3	16.5	20	-67.8	1.7	-65.0	920	39470N	69410W
191	14.4	1.7	18.1	19	-65.4	2.1	-61.3	760	39480N	69420W

TABLE VIII

ECHO STRENGTH MEASUREMENTS AT NORMAL INCIDENCE

TAG	P1	P2	P3	N	E1	E2	E3	DEPTH	LAT.	LONG.
192	18.9	1.9	23.7	19	-59.6	1.6	-58.6	615	39480N	69420W
193	21.3	1.9	25.1	19	-58.0	1.4	-55.5	530	39490N	69430W
194	25.2	3.1	31.4	21	-53.8	2.0	-50.1	410	39500N	69440W
195	29.7	3.1	35.8	27	-50.2	2.2	-45.3	290	39510N	69450W
196	34.5	3.7	42.0	32	-47.1	2.9	-41.4	230	39530N	69470W
197	37.7	2.8	40.9	21	-44.0	3.2	-41.7	170	39540N	69480W
198	40.0	3.4	44.9	38	-42.7	3.2	-38.0	80	39580N	69510W
199	38.5	3.8	45.2	109	-44.0	3.7	-36.9	80	40000N	69530W
200	39.0	4.2	45.4	123	-43.4	4.0	-37.1	75	40040N	69560W
201	43.0	3.6	46.7	40	-39.5	3.7	-35.9	60	40070N	69590W
202	42.7	2.2	46.3	27	-39.6	2.2	-36.6	55	40100N	70020W
203	44.0	1.4	45.3	14	-38.6	1.3	-37.2	55	40120N	70040W
204	42.8	1.8	45.3	14	-40.4	2.2	-37.0	50	40150N	70060W
205	43.1	2.7	46.8	19	-38.8	3.1	-36.4	45	40180N	70080W
206	42.7	2.1	46.9	19	-40.5	2.3	-35.6	45	40200N	70100W
207	43.1	2.2	46.7	19	-38.8	2.6	-34.7	40	40230N	70130W
208	43.2	2.0	47.5	20	-39.7	2.5	-34.8	35	40250N	70150W
209	45.9	1.9	47.8	18	-36.6	1.7	-34.9	35	40270N	70170W
210	46.5	2.3	49.4	20	-36.3	2.1	-34.2	30	40290N	70190W
211	46.9	1.3	48.8	19	-36.0	1.2	-34.2	30	40320N	70210W
212	44.7	2.3	48.8	19	-37.6	2.2	-33.6	30	40340N	70230W
213	46.9	2.8	49.6	18	-35.7	2.4	-33.3	30	40360N	70250W
	ECHO STRENGTH MESUREMENTS MADE ON ASTERIAS									
1	63.8	3.1	70.7	20	-23.7	3.0	-16.6	23	41344N	71238W

TABLE VIII

ECHO STRENGTH MEASUREMENTS AT NORMAL INCIDENCE

TAG	P1	P2	P3	N	E1	E2	E3	DEPTH	LAT.	LONG.
2	63.4	3.1	68.2	26	-24.5	2.7	-19.7	26	41344N	71233W
3	63.0	3.2	67.0	21	-25.2	2.9	-20.0	24	41344N	71231W
4	71.7	2.2	75.8	22	-14.9	2.5	-11.5	21	41345N	71224W
5	61.6	2.6	64.9	24	-26.5	2.3	-23.4	39	41345N	71219W
6	61.9	2.3	65.7	22	-25.1	2.4	-21.0	30	41345N	71210W
7	62.3	2.7	68.2	23	-24.8	2.7	-19.3	28	41345N	71203W
8	62.6	2.8	69.2	24	-25.5	3.0	-18.4	33	41345N	71197W
9	64.2	3.5	68.9	22	-23.8	3.4	-19.9	45	41345N	71191W
10	65.6	2.3	70.5	23	-21.4	2.7	-17.1	35	41344N	71185W
11	65.3	2.7	70.0	23	-22.9	3.2	-17.0	36	41347N	71184W
12	59.6	2.7	66.9	24	-27.9	2.8	-20.7	80	41347N	71190W
13	70.0	2.3	74.4	22	-17.0	2.6	-12.0	21	41345N	71196W
14	76.7	2.3	78.8	22	-9.8	2.8	-7.8	10	41348N	71200W
15	62.8	3.4	69.6	38	-25.2	3.0	-17.9	40	41352N	71206W
16	64.0	2.7	67.4	26	-23.9	2.4	-20.0	28	41352N	71212W
17	69.2	3.5	74.1	25	-19.3	3.4	-13.3	21	41352N	71219W
18	64.6	3.1	70.7	25	-20.8	2.7	-14.3	22	41351N	71226W
19	64.3	2.9	67.6	22	-21.4	2.2	-18.1	23	41351N	71231W
20	62.6	2.8	67.2	22	-25.5	2.3	-21.3	26	41351N	71238W
21	62.5	2.9	66.4	24	-25.0	2.7	-20.0	26	41356N	71238W
22	65.3	3.7	72.1	23	-22.2	3.9	-15.0	24	41356N	71228W
23	64.1	2.7	68.1	25	-22.8	2.6	-18.6	22	41356N	71221W
24	62.7	3.3	70.3	21	-24.0	3.1	-16.1	23	41356N	71215W
25	64.9	3.6	72.1	25	-22.4	3.6	-14.8	27	41356N	71208W
26	66.0	2.4	69.6	23	-22.1	2.2	-17.7	34	41359N	71205W

TABLE VIII

ECHO STRENGTH MEASUREMENTS AT NORMAL INCIDENCE

TAG	P1	P2	P3	N	E1	E2	E3	DEPTH	LAT.	LONG.
27	63.8	2.4	68.8	21	-24.3	2.5	-19.6	32	41362N	71208W
28	62.3	2.4	65.9	25	-24.1	2.9	-21.1	26	41362N	71212W
29	62.8	3.2	68.8	25	-24.5	2.9	-18.7	26	41361N	71216W
30	60.0	3.3	68.1	21	-29.4	3.2	-20.5	35	41366N	71215W
31	63.0	3.0	67.6	24	-23.9	2.4	-19.9	23	41366N	71209W
32	64.8	2.3	69.7	21	-22.9	2.7	-17.7	27	41366N	71202W
33	64.4	3.3	69.8	26	-22.7	2.8	-17.9	20	41372N	71203W
34	64.9	2.2	69.4	25	-22.4	2.4	-17.6	21	41372N	71210W
35	62.7	2.7	66.3	22	-24.0	2.4	-20.0	21	41371N	71217W
36	64.9	2.5	68.7	27	-22.1	2.1	-18.0	20	41371N	71225W
37	63.0	2.4	67.6	22	-23.6	2.4	-19.6	23	41371N	71232W
38	66.3	1.9	70.4	22	-21.0	2.1	-17.0	19	41371N	71238W
39	72.6	3.2	76.7	25	-15.9	3.4	-10.6	11	41374N	71236W
40	65.4	2.9	70.3	21	-22.4	2.8	-17.4	21	41377N	71228W
41	64.5	1.6	67.8	14	-22.6	2.0	-20.0	20	41375N	71223W
42	64.0	3.1	70.4	34	-24.6	2.8	-17.9	20	41375N	71223W
43	64.1	3.2	68.3	23	-23.2	2.9	-19.2	18	41380N	71223W
44	70.0	1.9	72.4	19	-17.5	2.5	-14.2	15	41385N	71224W
45	63.7	3.6	70.0	51	-24.7	3.6	-17.6	27	41388N	71224W
46	71.0	2.2	73.2	11	-15.5	2.3	-13.0	14	41344N	71261W
47	69.4	3.5	73.6	18	-17.9	2.9	-13.7	13	41344N	71258W
48	69.4	3.9	75.1	25	-15.2	3.8	-10.3	14	41344N	71255W
49	75.7	2.9	78.6	26	-10.1	2.6	-7.4	7	41344N	71250W
50	66.2	2.8	69.9	21	-19.8	2.8	-16.7	19	41345N	71247W
51	66.4	3.6	74.5	26	-20.1	3.2	-12.5	22	41345N	71243W

TABLE VIII

ECHO STRENGTH MEASUREMENTS AT NORMAL INCIDENCE

TAG	P1	P2	P3	N	E1	E2	E3	DEPTH	LAT.	LONG.
52	63.5	2.7	67.8	23	-22.2	1.8	-19.0	25	41345N	71236W
53	63.6	3.2	69.1	22	-23.3	3.1	-18.3	25	41345N	71233W
54	62.9	2.6	69.4	27	-24.8	2.4	-18.2	24	41346N	71230W
55	65.4	2.8	71.0	27	-22.2	2.6	-16.7	22	41346N	71227W
56	62.3	1.9	64.9	12	-24.9	1.7	-23.9	35	41346N	71222W
57	64.7	3.6	69.8	23	-22.7	3.4	-17.6	27	41346N	71217W
58	63.6	3.0	69.3	21	-23.8	2.8	-17.7	28	41346N	71214W
59	62.7	1.8	67.1	21	-23.7	1.7	-20.1	28	41346N	71210W
60	62.6	2.9	68.1	28	-24.9	2.8	-18.8	30	41346N	71207W
61	68.0	2.7	71.3	21	-19.4	2.6	-15.8	29	41346N	71200W
62	68.5	2.5	71.6	21	-19.0	2.7	-16.0	28	41345N	71196W
63	63.5	3.0	67.9	22	-22.9	3.5	-18.7	50	41344N	71192W
64	63.3	2.6	68.1	25	-24.5	2.6	-19.1	63	41344N	71187W
65	67.4	3.4	72.9	34	-21.1	3.5	-14.7	23	41343N	71183W
66	63.0	2.8	69.1	20	-23.5	2.5	-18.1	24	41341N	71183W
67	60.1	2.1	64.3	20	-26.1	1.5	-22.8	55	41339N	71185W
68	59.5	2.6	63.9	23	-27.4	2.4	-22.8	57	41339N	71188W
69	57.3	3.4	64.0	22	-29.6	3.0	-24.1	80	41339N	71192W
70	61.0	2.9	63.7	30	-27.1	2.5	-23.7	55	41340N	71195W
71	67.4	3.5	76.3	22	-19.7	3.2	-10.3	27	41340N	71199W
72	62.8	2.3	65.8	25	-24.6	2.1	-21.7	30	41340N	71203W
73	62.7	2.6	67.4	24	-23.4	2.7	-20.7	32	41341N	71207W
74	63.4	1.8	66.9	27	-23.5	1.5	-20.3	43	41341N	71211W
75	62.2	2.6	67.2	22	-24.7	2.3	-20.1	42	41338N	71214W
76	62.8	2.8	66.5	32	-24.6	2.2	-21.3	39	41338N	71210W

TABLE VIII

ECHO STRENGTH MEASUREMENTS AT NORMAL INCIDENCE

TAG	P1	P2	P3	N	E1	E2	E3	DEPTH	LAT.	LONG.
77	62.4	2.8	67.5	23	-24.7	2.1	-20.5	36	41338N	71207W
78	60.7	1.9	64.2	17	-26.2	1.7	-23.6	34	41337N	71203W
79	66.4	3.6	72.5	21	-21.6	4.0	-14.4	24	41337N	71200W
80	57.5	2.2	61.8	106	-30.3	2.3	-26.0	51	41333N	71195W
81	55.2	2.3	60.3	23	-31.7	2.5	-27.0	75	41333N	71191W
82	59.9	2.8	65.4	29	-27.4	2.4	-22.0	45	41333N	71188W
83	59.0	1.8	63.1	25	-28.5	2.0	-24.0	45	41331N	71190W
84	58.9	2.3	62.8	24	-28.6	2.2	-24.0	50	41328N	71200W
85	58.1	2.3	62.4	25	-28.4	2.2	-24.5	60	41325N	71196W
86	57.6	2.4	63.0	23	-28.7	2.3	-24.3	60	41325N	71201W
87	61.8	2.6	65.8	32	-26.0	2.2	-21.9	60	41324N	71212W
88	61.9	2.7	67.5	24	-25.6	2.7	-20.6	48	41324N	71216W
89	61.7	2.3	65.1	24	-25.5	2.1	-23.3	55	41321N	71216W
90	64.4	2.7	69.0	22	-23.7	3.0	-18.8	52	41317N	71216W
91	59.4	3.3	64.8	36	-27.8	2.9	-23.1	76	41314N	71212W
92	58.3	2.8	62.4	25	-29.3	2.2	-25.3	97	41314N	71205W
93	55.3	2.4	60.5	11	-31.0	2.0	-28.0	105	41314N	71201W
94	58.8	4.0	66.3	9	-29.4	4.4	-21.0	49	41307N	71201W
95	58.7	2.9	63.8	77	-28.8	2.6	-23.6	83	41305N	71212W
96	56.5	2.8	63.1	22	-31.0	2.3	-25.4	117	41307N	71211W
97	58.4	2.2	61.9	34	-29.4	1.8	-25.8	101	41311N	71208W
98	55.1	3.1	62.1	52	-32.0	2.8	-24.9	95	41315N	71205W
99	54.3	3.5	61.4	30	-32.8	3.3	-25.8	120	41317N	71204W
100	55.9	2.2	60.1	23	-30.9	2.1	-26.2	95	41320N	71201W
101	57.4	2.9	62.4	36	-28.7	2.7	-24.2	72	41324N	71199W

TABLE VIII

ECHO STRENGTH MEASUREMENTS AT NORMAL INCIDENCE

TAG	P1	P2	P3	N	E1	E2	E3	DEPTH	LAT.	LONG.
102	57.2	2.7	62.2	39	-29.9	2.5	-24.1	71	41327N	71197W
103	56.0	1.7	58.5	22	-30.7	2.0	-27.4	80	41331N	71194W
104	57.7	3.9	62.1	28	-30.0	3.0	-25.4	86	41333N	71193W
105	57.5	3.3	63.8	24	-29.7	2.9	-23.6	84	41336N	71191W
106	59.8	3.1	63.6	24	-27.6	2.9	-23.1	69	41339N	71189W
107	61.7	2.1	63.9	17	-25.8	2.1	-23.1	59	41341N	71187W
108	62.3	2.3	66.6	28	-24.0	2.7	-17.6	70	41343N	71186W
109	61.1	2.0	64.9	22	-24.2	2.2	-19.4	60	41343N	71190W
110	64.1	2.9	68.0	22	-22.8	2.9	-19.3	35	41343N	71195W
111	62.3	3.1	68.6	20	-24.5	2.7	-18.8	25	41343N	71200W
112	63.0	1.9	68.6	34	-24.3	2.1	-18.9	26	41344N	71204W
113	64.3	2.2	69.0	29	-22.4	2.3	-18.8	27	41345N	71209W
114	63.6	2.6	69.3	21	-23.9	2.6	-17.5	27	41345N	71213W
115	63.6	2.4	66.8	20	-22.6	2.4	-20.2	34	41346N	71220W
116	63.3	2.7	65.4	19	-23.3	2.4	-20.8	33	41346N	71223W
117	61.5	2.4	66.8	21	-25.1	1.9	-19.9	33	41347N	71228W
118	68.3	2.9	71.8	23	-19.4	2.5	-16.2	22	41347N	71233W
119	60.6	3.3	67.1	44	-28.5	2.5	-22.3	42	41334N	71214W
120	59.8	2.9	64.2	24	-29.8	2.7	-25.2	85	41310N	71213W
121	55.5	2.9	62.0	27	-33.9	2.5	-27.8	106	41310N	71208W
122	58.9	3.5	66.3	25	-30.9	3.3	-23.1	56	41310N	71201W
123	62.3	3.2	68.3	25	-27.0	3.2	-21.0	31	41305N	71202W
124	56.6	2.7	62.9	39	-32.9	2.7	-25.8	82	41305N	71208W
125	55.1	2.8	59.3	26	-34.3	2.6	-29.3	85	41304N	71213W
126	62.7	2.2	67.1	24	-25.2	2.5	-20.6	57	41301N	71214W

TABLE VIII

ECHO STRENGTH MEASUREMENTS AT NORMAL INCIDENCE

TAG	P1	P2	P3	N	E1	E2	E3	DEPTH	LAT.	LONG.
127	53.5	2.6	58.8	26	-35.9	1.7	-32.1	126	41301N	71209W
128	53.5	2.5	57.7	25	-34.7	2.5	-31.6	122	41297N	71208W
129	54.1	2.5	58.5	24	-35.9	2.3	-31.8	123	41293N	71208W
130	57.0	3.0	61.7	54	-32.7	2.5	-27.2	84	41289N	71205W
131	63.5	2.7	68.5	107	-24.5	2.5	-20.1	48	41284N	71208W
132	64.8	2.3	69.8	105	-24.3	2.3	-18.7	50	41284N	71208W
133	65.1	2.0	69.7	106	-23.6	2.0	-19.6	48	41284N	71208W
134	56.0	3.2	63.0	44	-33.5	3.5	-25.8	87	41284N	71217W
135	61.8	2.0	65.2	27	-27.8	1.9	-25.0	60	41284N	71227W
136	66.9	1.3	69.6	100	-22.8	1.5	-20.2	30	41286N	71229W
137	67.5	1.7	70.8	118	-22.9	1.7	-19.0	28	41286N	71229W
138	65.6	1.9	69.5	51	-21.6	2.3	-17.3	29	41286N	71229W
140	60.6	3.3	65.3	27	-29.1	2.1	-24.9	70	41282N	71227W
141	56.2	2.7	60.5	21	-33.1	2.2	-29.6	110	41275N	71230W
142	58.1	2.4	63.0	28	-32.5	2.5	-27.4	70	41270N	71236W
143	65.5	3.3	70.8	22	-23.1	2.6	-18.1	35	41267N	71242W
144	62.9	1.2	65.2	21	-26.4	1.2	-24.0	51	41272N	71246W
145	64.2	1.8	67.6	22	-25.6	1.5	-22.8	42	41278N	71246W
146	59.9	3.3	67.3	21	-28.5	2.7	-21.9	43	41285N	71246W
147	59.3	3.1	67.2	18	-29.0	2.4	-22.8	41	41291N	71246W
148	59.5	2.3	64.6	20	-28.5	2.3	-23.8	40	41298N	71245W
149	61.1	2.7	66.9	28	-27.6	2.8	-22.8	26	41303N	71245W
150	60.4	2.6	64.2	25	-29.6	2.4	-25.5	47	41311N	71243W
151	63.8	3.3	71.5	23	-24.2	1.8	-19.4	25	41316N	71240W
152	60.7	3.1	66.5	23	-26.5	2.2	-22.6	36	41323N	71244W

TABLE VIII

ECHO STRENGTH MEASUREMENTS AT NORMAL INCIDENCE

TAG	P1	P2	P3	N	E1	E2	E3	DEPTH	LAT.	LONG.
153	63.7	2.0	65.0	16	-26.4	1.9	-24.8	24	41328N	71247W
154	63.9	3.1	68.1	20	-24.9	2.7	-20.0	21	41335N	71252W
155	69.5	2.3	73.2	20	-18.1	2.1	-14.7	13	41339N	71257W
156	71.6	3.3	74.9	25	-16.5	2.8	-12.8	12	41341N	71260W
157	69.4	3.6	75.0	22	-18.9	3.8	-12.5	12	41342N	71259W
158	66.9	3.7	70.9	23	-21.4	3.1	-17.7	17	41337N	71253W
159	61.8	2.8	65.5	22	-28.4	2.2	-23.7	26	41329N	71246W
160	67.0	1.5	69.5	98	-23.4	1.5	-20.7	28	41286N	71229W
161	67.4	2.1	70.9	103	-23.5	2.1	-19.9	29	41286N	71229W
162	52.9	2.6	56.7	9	-34.3	2.5	-33.2	98	41280N	71226W
163	54.2	2.9	59.6	108	-34.6	2.5	-28.3	98	41280N	71226W
164	55.2	2.8	61.1	101	-33.8	2.2	-28.3	99	41280N	71226W
165	56.8	3.7	60.2	23	-33.5	3.6	-29.5	85	41282N	71221W
166	55.1	2.8	58.9	22	-34.5	2.6	-31.0	115	41283N	71217W
167	54.3	2.9	60.6	102	-34.4	2.2	-28.5	100	41284N	71214W
168	72.9	2.3	77.9	23	-15.2	2.4	-9.6	11	41344N	71261W
169	70.4	2.6	75.5	25	-18.5	4.3	-5.9	12	41341N	71259W
170	70.3	2.6	75.8	23	-18.3	2.6	-11.7	13	41338N	71255W
171	68.9	2.8	72.8	21	-20.8	2.7	-16.2	16	41337N	71253W
172	65.2	2.8	68.4	15	-25.0	2.4	-22.3	24	41335N	71251W
173	66.6	1.9	68.6	9	-24.1	2.1	-21.3	24	41333N	71250W
174	65.8	3.6	67.3	9	-24.5	3.3	-22.4	25	41333N	71245W
175	66.2	1.7	69.3	21	-24.0	1.8	-21.5	31	41333N	71240W
176	67.2	1.9	70.6	101	-22.9	1.9	-18.9	32	41333N	71237W
177	63.5	2.1	68.7	98	-26.8	2.9	-10.8	31	41332N	71246W

TABLE VIII

ECHO STRENGTH MEASUREMENTS AT NORMAL INCIDENCE

TAG	P1	P2	P3	N	E1	E2	E3	DEPTH	LAT.	LONG.
178	64.4	2.3	67.3	18	-24.6	2.1	-22.3	34	41331N	71237W
179	66.9	4.0	71.6	31	-23.5	3.5	-18.2	25	41329N	71238W
180	64.4	3.0	69.0	30	-26.4	3.4	-14.1	38	41327N	71240W
181	63.3	2.2	68.4	96	-26.5	2.1	-20.7	38	41327N	71240W
182	63.7	2.6	68.1	23	-27.2	2.5	-22.5	31	41325N	71240W
183	67.5	3.7	70.6	20	-21.7	2.4	-18.7	30	41322N	71240W
184	65.6	2.4	69.1	35	-24.8	2.2	-21.1	36	41321N	71240W
185	66.3	1.9	69.2	20	-22.7	1.9	-18.5	21	41319N	71240W
186	71.7	4.5	76.3	24	-17.4	2.8	-12.6	25	41315N	71240W
187	61.3	3.4	67.7	21	-28.4	2.5	-21.9	52	41313N	71241W
188	61.5	2.4	66.3	28	-27.9	3.3	-23.5	47	41311N	71241W
189	59.4	2.6	65.3	24	-30.5	2.3	-24.9	53	41308N	71242W
190	61.9	3.7	68.5	26	-28.1	3.6	-21.1	33	41305N	71243W
191	60.7	2.7	66.0	30	-28.6	2.1	-23.4	36	41303N	71244W
192	64.0	3.4	72.2	22	-25.5	3.0	-17.9	26	41301N	71244W
193	67.1	1.8	71.2	26	-21.7	2.4	-17.1	26	41299N	71244W
194	61.2	2.7	65.9	22	-29.7	2.6	-24.1	42	41297N	71245W
195	59.4	2.2	64.4	102	-29.6	2.0	-24.6	43	41296N	71245W

ECHO STRENGTH MESUREMENTS MADE ON BEAR 281

1	60.8	3.1	68.2	62	-27.2	2.9	-20.6	65	41264N	71221W
2	59.3	2.4	62.7	25	-28.6	2.9	-25.9	82	41264N	71225W
3	58.2	3.0	66.0	24	-31.5	3.1	-22.2	79	41264N	71230W
4	61.2	2.6	65.7	24	-28.6	2.7	-24.7	77	41264N	71234W
5	59.9	3.0	65.2	25	-30.4	4.4	-24.6	79	41263N	71238W

TABLE VIII

ECHO STRENGTH MEASUREMENTS AT NORMAL INCIDENCE

TAG	P1	P2	P3	N	E1	E2	E3	DEPTH	LAT.	LONG.
6	59.8	2.4	64.6	24	-29.9	1.9	-24.1	76	41263N	71242W
7	60.8	3.1	64.1	24	-30.3	2.9	-26.5	67	41263N	71246W
8	63.4	2.4	66.0	24	-26.1	3.0	-22.4	59	41263N	71251W
9	66.1	2.4	69.6	25	-23.5	2.8	-18.1	56	41263N	71256W
10	63.3	2.5	67.6	47	-26.7	1.9	-22.2	56	41262N	71258W
11	66.8	2.3	71.2	71	-24.2	2.1	-18.8	51	41264N	71255W
12	63.8	2.0	67.3	25	-26.3	1.5	-23.2	57	41264N	71250W
13	60.9	3.4	66.5	24	-28.5	2.0	-24.1	64	41265N	71244W
14	60.3	2.8	64.8	29	-27.6	1.7	-25.2	74	41265N	71238W
15	60.8	3.1	66.4	26	-28.1	1.8	-23.2	79	41266N	71230W
16	58.1	3.5	66.8	24	-31.8	3.0	-24.7	90	41266N	71226W
17	59.3	2.8	67.8	76	-28.8	1.7	-21.7	82	41267N	71220W
18	58.5	3.1	64.6	60	-31.9	2.1	-26.5	80	41267N	71220W
19	69.9	1.6	72.8	126	-19.9	1.5	-17.5	26	41286N	71228W
20	71.0	1.9	73.2	94	-21.5	1.5	-17.7	25	41286N	71229W
21	58.9	4.6	65.6	51	-30.1	3.5	-20.5	60	41269N	71220W
22	57.4	2.9	63.2	29	-31.0	1.9	-27.4	78	41269N	71224W
23	59.0	2.4	64.0	23	-30.1	1.6	-25.9	95	41269N	71227W
24	57.3	3.1	63.0	26	-31.3	1.9	-26.1	113	41269N	71232W
25	59.6	3.3	66.5	21	-30.0	2.8	-23.9	76	41269N	71236W
26	61.8	2.2	66.1	50	-27.5	2.0	-23.5	66	41269N	71238W
27	61.0	2.5	66.7	49	-27.6	1.8	-24.3	59	41270N	71242W
28	64.7	3.2	67.2	23	-25.2	2.3	-22.8	53	41270N	71244W
29	65.6	2.7	67.7	24	-24.5	1.8	-22.0	46	41270N	71249W
30	67.9	2.7	70.2	24	-22.0	2.6	-19.1	35	41270N	71254W

TABLE VIII

ECHO STRENGTH MEASUREMENTS AT NORMAL INCIDENCE

TAG	P1	P2	P3	N	E1	E2	E3	DEPTH	LAT.	LONG.
31	67.2	2.9	70.7	48	-22.6	2.5	-18.4	38	41270N	71254W
32	64.6	2.9	70.4	26	-24.8	2.4	-20.0	43	41269N	71255W
33	66.3	1.4	69.4	24	-23.8	1.3	-21.0	45	41266N	71256W
34	62.0	1.9	65.1	24	-25.8	1.3	-24.1	51	41263N	71258W
35	62.9	2.4	67.2	21	-26.2	1.6	-22.9	57	41260N	71259W
36	60.6	2.5	65.9	29	-27.5	1.6	-24.3	61	41257N	71261W
37	61.3	6.0	65.8	49	-27.8	2.2	-23.8	60	41257N	71261W
38	62.1	4.9	65.8	98	-27.8	3.0	-24.3	60	41257N	71261W
39	57.3	4.1	65.8	23	-31.2	2.7	-24.6	58	41257N	71261W
40	66.1	5.7	70.9	47	-24.0	3.5	-18.9	41	41257N	71266W
41	69.4	2.4	73.4	25	-20.0	2.1	-16.5	33	41260N	71267W
42	67.6	1.2	69.9	20	-21.3	1.0	-19.5	44	41260N	71262W
43	63.5	2.8	74.0	24	-23.4	2.1	-15.3	62	41260N	71256W
44	62.0	2.5	67.3	23	-27.7	1.9	-22.6	68	41260N	71251W
45	58.5	2.5	63.4	23	-29.2	1.7	-25.9	75	41260N	71245W
46	58.4	2.9	63.7	34	-29.7	2.2	-25.4	79	41260N	71240W
47	58.6	3.3	64.1	48	-30.8	2.7	-25.6	79	41260N	71238W
48	63.2	2.8	67.4	24	-26.2	2.9	-21.2	75	41260N	71234W
49	58.7	4.4	65.2	69	-29.9	2.7	-24.4	74	41259N	71231W
50	58.4	3.7	66.5	17	-31.4	3.0	-23.8	78	41264N	71226W
51	58.4	2.6	65.0	25	-30.9	1.8	-25.5	81	41268N	71223W
52	57.7	4.4	64.0	98	-32.0	2.8	-25.6	76	41269N	71222W
53	58.0	2.9	63.7	26	-31.3	2.6	-24.7	131	41275N	71224W
54	61.5	2.7	64.5	9	-28.1	3.1	-24.2	61	41280N	71226W
55	65.5	2.1	68.5	23	-24.2	1.7	-21.8	46	41280N	71226W

TABLE VIII

ECHO STRENGTH MEASUREMENTS AT NORMAL INCIDENCE

TAG	P1	P2	P3	N	E1	E2	E3	DEPTH	LAT.	LONG.
56	69.9	2.7	73.4	166	-20.9	2.0	-16.9	23	41287N	71229W
57	61.6	2.9	66.3	24	-29.3	2.4	-23.8	90	41283N	71219W
58	56.7	2.1	59.9	24	-32.3	1.3	-29.9	145	41286N	71213W
59	56.2	2.4	59.0	25	-34.1	2.5	-29.8	126	41289N	71210W
60	64.0	3.5	71.2	24	-24.6	2.3	-18.6	44	41306N	71200W
61	62.8	2.7	67.0	24	-28.0	2.5	-22.3	72	41310N	71202W
62	58.5	2.8	63.0	25	-31.1	2.5	-25.8	100	41315N	71203W
63	63.2	1.5	65.8	23	-27.2	1.3	-25.1	75	41320N	71203W
64	61.8	2.1	66.6	24	-26.5	1.5	-23.7	40	41325N	71204W
65	62.7	2.0	67.1	24	-26.2	1.8	-22.8	38	41330N	71204W
66	62.7	2.1	68.0	24	-26.4	1.7	-22.4	34	41335N	71205W
67	64.9	2.4	69.5	24	-24.0	1.9	-19.9	30	41339N	71205W
68	66.1	2.3	72.2	25	-22.7	1.7	-17.6	27	41344N	71206W
69	66.4	2.5	72.7	25	-25.6	1.4	-23.2	24	41347N	71212W
70	66.7	2.7	70.2	28	-23.1	2.4	-20.2	30	41337N	71235W
71	66.6	2.6	71.4	27	-23.4	2.3	-19.3	36	41330N	71236W
72	63.1	3.0	68.5	26	-26.2	2.2	-21.4	61	41323N	71238W
73	63.4	2.2	68.3	25	-27.8	2.4	-22.1	65	41320N	71238W
74	64.8	2.1	69.1	29	-26.2	2.2	-21.5	66	41312N	71241W
75	64.3	3.7	69.7	27	-26.8	3.0	-21.2	50	41308N	71242W
76	66.5	2.9	70.2	26	-24.6	2.9	-19.8	26	41304N	71244W
77	63.2	2.7	68.6	26	-25.6	2.3	-21.5	43	41298N	71246W
78	67.4	1.8	70.2	24	-23.6	1.9	-20.6	33	41293N	71246W
79	66.6	2.6	69.2	25	-24.3	2.4	-19.9	38	41287N	71247W
80	68.2	2.6	69.9	25	-22.6	2.6	-20.7	40	41282N	71247W

TABLE VIII

ECHO STRENGTH MEASUREMENTS AT NORMAL INCIDENCE

TAG	P1	P2	P3	N	E1	E2	E3	DEPTH	LAT.	LONG.
81	66.7	2.4	70.2	25	-24.5	2.2	-20.2	48	41276N	71247W
82	60.4	3.0	65.4	23	-28.7	2.3	-24.5	63	41265N	71247W
83	58.9	2.2	62.2	25	-30.5	1.6	-27.4	82	41254N	71247W
84	55.6	2.5	59.8	24	-32.8	2.2	-28.7	94	41246N	71247W
85	56.1	2.1	59.0	24	-32.5	1.8	-30.2	100	41235N	71247W
86	57.9	2.1	60.6	24	-31.9	1.9	-29.0	102	41225N	71247W
87	58.3	2.4	61.4	24	-31.2	1.7	-27.4	103	41215N	71247W
88	57.6	2.5	60.9	24	-32.5	1.9	-29.1	102	41204N	71245W
89	54.9	2.6	62.9	23	-33.9	2.1	-27.3	104	41192N	71243W
90	55.6	3.1	60.6	24	-33.5	2.2	-29.5	107	41181N	71241W
91	54.8	2.5	59.6	37	-34.1	2.0	-29.6	109	41170N	71241W
92	55.9	2.2	59.3	24	-33.8	1.5	-30.7	120	41161N	71241W
93	56.4	2.5	60.7	24	-33.9	2.5	-29.5	113	41151N	71242W
94	56.7	2.8	60.5	26	-33.0	2.5	-29.4	112	41141N	71242W
95	57.6	2.0	60.6	23	-33.2	1.8	-29.6	116	41131N	71243W
96	55.4	2.3	59.5	21	-33.2	2.3	-30.2	111	41121N	71243W
97	57.4	2.6	61.9	28	-32.4	2.5	-27.4	116	41110N	71244W
98	59.7	2.4	63.4	19	-29.8	2.3	-27.2	100	41101N	71246W
99	59.0	2.6	64.1	22	-30.0	2.4	-25.7	115	41093N	71247W
100	55.7	3.2	59.3	7	-33.8	1.7	-30.4	120	41062N	71245W
101	58.1	2.1	62.5	14	-31.5	1.8	-27.9	127	41042N	71246W
102	57.3	2.2	62.6	24	-33.1	2.1	-27.7	139	41032N	71246W
103	66.2	2.6	71.0	44	-22.8	2.1	-17.8	38	41082N	71371W
104	63.4	2.4	68.0	24	-25.2	1.4	-21.4	67	41073N	71371W
105	58.5	2.8	63.7	45	-28.2	1.3	-25.0	100	41064N	71370W

TABLE VIII

ECHO STRENGTH MEASUREMENTS AT NORMAL INCIDENCE

TAG	P1	P2	P3	N	E1	E2	E3	DEPTH	LAT.	LONG.
106	55.8	3.9	61.0	49	-33.0	2.5	-28.3	128	41032N	71368W
107	54.7	3.2	62.9	31	-34.3	2.3	-27.9	122	41020N	71368W
108	54.3	3.0	59.6	30	-35.3	2.2	-30.0	128	41010N	71369W
109	54.7	3.9	60.0	34	-35.0	2.8	-29.2	126	41010N	71364W
110	56.4	2.6	62.2	29	-33.4	2.3	-27.4	111	41010N	71358W
111	55.2	4.4	62.7	28	-34.6	3.4	-28.3	108	41011N	71356W
112	58.1	2.1	61.4	30	-31.4	1.7	-27.8	119	41029N	71346W
113	58.7	2.4	62.8	24	-31.2	1.9	-26.9	115	41037N	71344W
114	57.8	2.2	61.3	23	-31.4	1.9	-27.9	117	41044N	71341W
115	58.5	3.8	62.4	24	-31.5	2.3	-28.5	105	41052N	71338W
116	62.9	2.3	65.0	22	-26.9	2.1	-23.2	59	41058N	71334W
117	65.9	2.5	69.8	24	-22.2	1.8	-17.7	50	41064N	71330W
118	64.4	2.6	68.2	24	-22.7	1.6	-19.7	61	41075N	71320W
119	63.1	2.8	67.1	23	-24.5	2.1	-21.0	66	41087N	71310W
120	61.7	2.8	65.9	20	-25.2	1.7	-21.9	90	41102N	71311W
121	57.5	2.4	61.3	24	-33.1	1.6	-30.0	105	41117N	71306W
122	59.5	3.2	63.7	27	-31.8	2.4	-27.2	100	41132N	71301W
123	53.1	2.0	56.9	28	-35.5	1.6	-33.2	120	41161N	71290W
124	67.2	2.3	71.3	23	-23.1	2.4	-17.8	56	41176N	71284W
125	68.5	2.6	72.6	25	-21.3	2.1	-16.5	50	41192N	71278W
126	62.5	3.4	70.1	24	-25.4	2.0	-20.3	63	41206N	71273W
127	68.2	1.9	71.6	24	-21.5	1.9	-18.3	56	41220N	71268W
128	57.4	2.3	61.6	35	-30.5	1.9	-27.8	83	41236N	71262W
129	59.2	2.0	63.7	24	-29.2	1.6	-25.4	76	41250N	71257W
130	63.6	2.3	67.1	24	-26.5	2.2	-22.1	50	41263N	71249W

TABLE VIII

ECHO STRENGTH MEASUREMENTS AT NORMAL INCIDENCE

TAG	P1	P2	P3	N	E1	E2	E3	DEPTH	LAT.	LONG.
131	66.1	1.6	69.3	24	-24.4	1.6	-21.0	50	41275N	71245W
132	68.5	1.5	70.5	24	-22.0	1.8	-19.1	42	41280N	71244W
133	63.2	2.8	70.0	24	-26.7	2.5	-19.9	44	41284N	71244W
134	71.7	1.0	72.4	23	-19.7	2.2	-16.1	27	41290N	71244W
135	64.3	3.2	70.0	24	-25.8	2.6	-20.6	42	41294N	71243W
136	67.7	3.1	70.2	23	-22.6	3.0	-18.4	41	41298N	71241W
137	63.0	2.4	66.0	24	-27.5	1.5	-24.9	41	41302N	71237W
138	64.4	2.7	70.0	99	-25.9	1.9	-21.3	28	41306N	71240W
139	64.6	2.3	68.1	24	-25.6	1.8	-22.3	36	41306N	71240W
140	62.9	3.0	66.8	24	-27.0	2.3	-23.1	86	41311N	71239W
141	62.9	2.8	70.3	24	-27.5	2.5	-20.3	62	41316N	71239W
142	62.8	2.4	68.2	24	-26.9	2.2	-22.4	65	41320N	71238W
143	66.2	3.4	70.4	24	-24.2	3.0	-18.7	36	41324N	71237W
144	64.6	1.9	68.6	24	-24.5	1.7	-21.1	43	41328N	71237W
145	66.9	3.8	72.0	24	-22.9	2.8	-17.9	35	41332N	71236W
146	66.7	2.7	71.3	24	-22.5	2.2	-18.6	30	41336N	71235W
147	65.9	3.3	72.7	23	-25.0	2.1	-20.4	27	41340N	71232W
148	64.7	2.7	70.4	48	-24.1	2.1	-19.3	28	41345N	71202W
149	67.9	3.1	72.6	25	-22.6	2.6	-18.3	29	41343N	71199W
150	68.2	2.1	72.1	26	-22.0	1.9	-18.0	56	41342N	71194W
151	65.7	2.4	71.3	24	-22.1	1.8	-18.2	65	41345N	71192W
152	63.2	2.2	67.8	30	-26.0	2.0	-21.3	64	41352N	71187W
153	61.0	2.3	66.6	30	-27.2	1.7	-24.0	69	41356N	71185W
154	67.3	2.1	70.7	30	-22.8	2.0	-19.0	52	41361N	71182W
155	62.2	2.7	67.5	24	-26.4	2.2	-21.3	77	41365N	71179W

TABLE VIII

ECHO STRENGTH MEASUREMENTS AT NORMAL INCIDENCE

TAG	P1	P2	P3	N	E1	E2	E3	DEPTH	LAT.	LONG.
156	63.9	2.7	68.9	23	-26.2	2.1	-21.3	58	41368N	71177W
157	64.8	2.3	69.2	24	-24.5	1.9	-20.8	60	41371N	71174W
158	69.1	2.0	70.9	31	-20.6	2.1	-16.8	32	41375N	71172W
159	64.8	2.5	70.2	100	-24.3	2.2	-19.2	50	41375N	71172W
160	65.5	1.5	69.0	22	-24.2	1.5	-20.9	65	41373N	71177W
161	60.3	2.7	66.9	16	-28.3	1.9	-23.2	80	41358N	71182W
162	60.3	2.8	67.5	26	-28.6	2.0	-21.7	93	41351N	71185W
163	62.2	2.7	65.9	22	-26.3	2.0	-22.3	78	41348N	71186W
164	60.5	1.8	63.0	26	-28.2	1.5	-26.3	98	41342N	71189W
165	58.4	2.1	62.6	21	-29.0	1.2	-27.4	79	41335N	71193W
166	58.0	2.8	63.1	10	-31.2	2.2	-27.1	68	41330N	71195W
167	59.3	2.2	62.9	8	-29.3	1.8	-26.4	71	41324N	71198W
168	58.9	2.3	62.2	18	-31.0	1.5	-27.0	100	41314N	71201W
169	66.9	2.7	70.7	23	-24.0	2.9	-17.8	35	41306N	71200W
170	66.2	2.2	70.5	23	-22.3	2.2	-17.3	47	41301N	71198W
171	71.0	2.5	73.4	36	-19.2	2.8	-15.1	34	41291N	71203W
172	54.9	2.8	60.7	28	-33.9	2.3	-29.3	151	41288N	71208W
173	57.2	2.5	60.7	26	-32.8	1.9	-29.5	128	41285N	71211W
174	55.2	2.8	61.2	32	-33.5	2.0	-29.0	127	41281N	71218W
175	58.7	3.2	62.6	27	-31.1	2.6	-27.1	136	41276N	71222W
176	61.8	2.7	64.9	35	-28.7	2.6	-25.5	85	41271N	71223W
177	60.8	2.8	64.0	24	-29.2	2.0	-26.9	80	41261N	71226W
178	57.2	2.9	61.9	31	-32.0	2.7	-26.9	83	41256N	71227W
179	58.1	3.3	64.5	34	-31.0	2.8	-24.8	82	41255N	71222W
180	60.0	3.3	66.2	25	-30.3	3.4	-22.6	73	41254N	71216W

TABLE VIII

ECHO STRENGTH MEASUREMENTS AT NORMAL INCIDENCE

TAG	P1	P2	P3	N	E1	E2	E3	DEPTH	LAT.	LONG.
181	64.0	2.3	65.9	27	-25.3	2.0	-22.5	64	41252N	71214W
182	64.1	2.7	70.0	99	-24.9	2.4	-19.7	65	41252N	71214W
183	61.4	3.1	67.2	49	-26.9	2.2	-21.4	80	41252N	71214W
184	62.0	2.9	67.2	42	-27.0	2.4	-22.2	84	41251N	71215W
185	60.6	3.1	65.0	27	-28.1	2.4	-24.5	81	41251N	71211W
186	58.3	3.1	64.0	26	-30.4	1.8	-25.9	87	41250N	71206W
187	55.4	2.9	61.8	66	-31.5	1.8	-27.2	97	41250N	71195W
188	56.6	3.0	61.1	22	-31.0	1.7	-27.8	93	41249N	71191W
189	56.6	2.9	61.5	31	-32.8	2.2	-28.6	92	41249N	71191W
190	58.3	3.2	62.8	14	-31.7	2.2	-28.0	90	41249N	71188W
191	53.7	11.1	62.3	5	-32.3	2.8	-27.3	87	41250N	71180W
192	59.6	2.6	61.4	8	-31.8	4.0	-28.2	82	41250N	71173W
193	61.5	2.6	63.0	20	-28.7	2.4	-26.5	80	41251N	71169W
194	59.5	2.5	63.9	21	-29.1	2.1	-25.2	80	41251N	71166W
195	61.2	2.2	64.8	26	-29.2	2.3	-25.2	78	41251N	71162W
196	62.0	2.2	65.2	25	-28.6	2.2	-24.3	76	41251N	71158W
197	59.3	2.4	64.1	22	-30.9	2.4	-26.6	74	41252N	71151W
198	61.7	2.3	67.1	24	-26.6	1.9	-21.7	72	41254N	71142W
199	62.3	2.5	67.6	34	-27.4	2.2	-21.8	68	41253N	71139W
200	63.0	2.7	68.2	107	-25.5	2.2	-20.2	68	41253N	71138W
201	62.7	2.1	66.7	99	-26.1	1.9	-21.8	70	41253N	71138W
202	64.7	2.6	69.2	24	-22.7	2.0	-19.0	71	41255N	71138W
203	61.9	2.7	67.6	24	-26.8	2.3	-21.5	71	41258N	71138W
204	61.9	3.1	68.7	24	-27.0	2.7	-21.3	68	41260N	71139W
205	61.7	2.9	65.1	23	-27.2	2.3	-24.2	65	41263N	71139W

TABLE VIII

ECHO STRENGTH MEASUREMENTS AT NORMAL INCIDENCE

TAG	P1	P2	P3	N	E1	E2	E3	DEPTH	LAT.	LONG.
206	62.7	2.7	69.4	24	-26.8	2.8	-20.0	63	41267N	71138W
207	65.5	3.4	71.3	25	-22.3	3.0	-17.2	57	41271N	71137W
208	65.5	2.9	70.5	24	-22.2	2.6	-17.4	56	41276N	71137W
209	66.8	2.2	71.8	24	-21.9	2.4	-16.5	54	41280N	71136W
210	67.9	2.6	71.5	24	-21.0	2.6	-16.3	50	41284N	71135W
211	67.4	2.8	71.7	24	-21.2	2.6	-17.0	44	41289N	71134W
212	68.1	2.4	70.9	24	-20.0	2.3	-17.5	38	41292N	71133W
213	67.7	2.1	71.5	98	-20.9	2.1	-16.4	33	41297N	71132W
214	69.8	1.5	72.2	24	-18.1	2.0	-14.2	32	41298N	71132W
215	70.9	1.1	73.5	24	-18.0	1.3	-15.5	26	41304N	71132W
216	69.5	2.4	72.6	98	-21.1	2.7	-14.4	25	41318N	71129W
217	68.6	2.3	72.7	24	-19.5	2.1	-14.3	39	41290N	71126W
218	69.6	2.7	72.3	20	-18.3	2.5	-15.6	45	41284N	71124W
219	66.0	2.2	70.1	95	-22.3	2.0	-17.6	46	41283N	71125W
220	64.1	2.4	67.2	25	-24.4	2.3	-20.8	62	41264N	71129W
221	65.4	2.8	69.7	24	-24.0	2.9	-18.7	66	41264N	41133W
222	62.6	2.7	68.5	24	-27.5	2.5	-21.5	66	41263N	71140W
223	62.4	2.5	66.2	24	-27.8	2.0	-23.5	69	41263N	71147W
224	60.1	2.5	63.1	24	-28.7	1.9	-26.1	70	41262N	71155W
225	60.9	2.8	65.6	24	-27.5	2.1	-22.4	73	41261N	71164W
226	60.6	2.5	64.5	23	-28.8	1.9	-26.3	74	41260N	71171W
227	58.3	3.1	66.1	98	-31.8	2.7	-23.0	77	41260N	71172W
228	60.1	2.5	64.1	15	-29.6	2.3	-25.9	78	41262N	71174W
229	59.2	2.8	64.6	19	-30.9	2.8	-25.3	74	41264N	71172W
230	60.1	3.9	67.8	21	-29.1	3.1	-22.6	74	41267N	71170W

TABLE VIII

ECHO STRENGTH MEASUREMENTS AT NORMAL INCIDENCE

TAG	P1	P2	P3	N	E1	E2	E3	DEPTH	LAT.	LONG.
231	65.8	2.2	70.2	25	-23.1	1.9	-19.6	54	41279N	71164W
232	64.0	2.3	69.1	94	-26.7	2.3	-20.8	50	41281N	71163W
233	66.5	1.5	68.6	35	-23.4	1.4	-21.4	49	41284N	71160W
234	67.8	3.8	71.5	24	-21.2	3.3	-16.2	42	41286N	71158W
235	68.5	1.4	71.2	24	-19.2	1.5	-17.0	30	41288N	71156W
236	68.2	1.9	72.2	95	-19.1	1.7	-15.2	30	41287N	71156W
237	67.8	2.4	71.2	99	-19.6	2.0	-16.2	40	41284N	71166W
238	63.0	3.1	69.5	23	-26.7	3.2	-19.0	33	41301N	71237W
239	58.7	2.8	63.6	25	-30.0	1.9	-25.4	55	41296N	71242W
240	61.6	2.6	64.6	24	-27.0	2.0	-24.8	41	41292N	71243W
241	65.4	2.0	67.6	24	-23.9	1.8	-21.5	44	41283N	71245W
242	64.8	1.8	68.4	23	-25.2	2.0	-21.4	42	41278N	71245W
243	64.7	1.5	67.8	27	-25.4	1.5	-21.6	50	41273N	71246W
244	62.6	2.3	64.3	25	-27.7	1.6	-25.0	60	41266N	71248W
245	59.0	2.4	63.9	28	-29.7	1.7	-26.2	70	41260N	71249W
246	59.8	2.6	64.4	24	-29.5	1.9	-24.9	68	41257N	71254W
247	62.5	2.7	64.3	24	-27.3	2.2	-24.5	57	41257N	71262W
248	66.1	1.5	69.2	26	-23.8	1.7	-20.1	44	41257N	71264W
249	64.8	2.5	68.8	100	-25.2	2.3	-20.4	43	41257N	71267W
250	70.4	2.5	76.5	97	-18.9	1.8	-14.6	30	41258N	71270W
251	69.1	2.4	73.0	100	-21.1	2.3	-16.5	32	41258N	71269W
252	61.4	2.9	65.4	25	-29.1	1.8	-25.4	64	41257N	71258W
253	60.7	2.5	64.5	23	-28.7	1.6	-25.5	69	41257N	71255W
254	58.6	3.5	65.4	26	-30.2	2.6	-24.1	79	41253N	71252W
255	56.1	2.1	60.8	25	-32.3	1.6	-28.7	87	41246N	71253W

TABLE VIII

ECHO STRENGTH MEASUREMENTS AT NORMAL INCIDENCE

TAG	P1	P2	P3	N	E1	E2	E3	DEPTH	LAT.	LONG.
256	56.2	2.4	62.4	24	-32.2	1.7	-27.3	92	41240N	71253W
257	54.0	2.3	61.2	24	-33.7	1.8	-28.2	93	41234N	71253W
258	56.0	2.2	61.5	38	-32.7	1.6	-29.7	95	41228N	71253W
259	53.5	2.0	58.8	40	-34.3	1.5	-30.4	98	41222N	71253W
260	55.7	2.2	58.8	24	-33.5	1.3	-31.4	99	41217N	71253W
261	54.3	2.4	59.6	24	-33.7	1.5	-30.7	98	41211N	71253W
262	55.7	3.1	61.3	6	-33.5	2.2	-28.5	92	41189N	71253W
263	61.8	2.7	65.2	23	-27.7	2.6	-24.0	81	41182N	71252W
264	64.2	2.3	68.1	26	-25.5	2.1	-21.7	79	41177N	71252W
265	60.4	2.6	63.0	31	-28.9	1.5	-26.8	83	41170N	71252W
266	61.7	2.3	65.1	26	-28.3	2.1	-25.4	91	41167N	71252W
267	53.4	2.6	60.1	25	-34.4	2.1	-29.9	120	41161N	71252W
268	56.7	3.8	64.2	95	-32.9	2.7	-26.1	120	41154N	71252W
269	57.2	1.6	60.8	40	-31.6	1.4	-29.1	110	41150N	71252W
270	57.2	2.2	62.0	24	-31.5	1.9	-27.6	112	41145N	71253W
271	58.6	2.7	62.8	20	-31.6	2.2	-27.5	110	41140N	71253W
272	58.7	3.5	64.6	23	-31.4	2.6	-25.1	109	41134N	71253W
273	55.1	2.9	61.2	35	-34.2	2.1	-29.6	115	41129N	71254W
274	56.3	3.0	61.9	33	-34.2	2.4	-29.0	118	41124N	71254W
275	54.4	3.1	59.8	24	-35.7	2.4	-30.9	125	41120N	71254W
276	53.7	2.9	59.3	34	-36.5	2.5	-30.5	130	41115N	71255W
277	54.7	2.6	57.6	20	-35.6	2.0	-32.9	131	41111N	71255W
278	53.6	2.8	61.0	120	-36.4	2.2	-29.3	131	41108N	71255W
279	57.0	3.2	59.7	24	-33.2	2.4	-30.7	126	41108N	71255W
280	56.7	2.5	60.6	25	-34.1	2.1	-30.4	126	41103N	71255W

TABLE VIII

ECHO STRENGTH MEASUREMENTS AT NORMAL INCIDENCE

TAG	P1	P2	P3	N	E1	E2	E3	DEPTH	LAT.	LONG.
281	56.7	3.2	60.9	29	-34.1	2.9	-29.3	111	41097N	71255W
282	58.4	2.4	62.7	26	-31.0	2.1	-28.1	96	41092N	71255W
283	57.7	2.8	63.8	31	-32.3	2.5	-26.0	104	41087N	71255W
284	57.8	3.2	64.2	24	-31.1	2.4	-25.5	104	41088N	71253W
285	60.7	3.0	66.1	26	-28.9	2.4	-23.4	97	41073N	71255W
286	58.8	3.1	65.7	109	-29.8	2.5	-23.2	101	41070N	71256W
287	59.1	2.9	65.9	24	-30.9	3.0	-23.1	98	41071N	71255W
288	59.7	2.3	65.1	25	-30.3	2.1	-24.9	90	41071N	71271W
289	60.3	2.3	62.6	24	-30.0	2.2	-27.2	82	41071N	71276W
290	60.1	4.2	64.7	101	-30.3	3.2	-25.1	82	41071N	71279W
291	60.3	2.3	64.8	24	-29.7	2.5	-23.8	81	41071N	71282W
292	62.1	2.6	66.4	27	-27.1	2.2	-23.2	79	41071N	71285W
293	59.4	2.7	63.6	33	-29.3	2.3	-24.3	86	41071N	71290W
294	61.8	2.2	67.0	33	-27.4	1.9	-23.4	85	41071N	71294W
295	62.3	2.0	66.0	24	-26.8	1.9	-23.7	74	41072N	71331W
296	64.3	2.5	68.7	23	-24.5	2.4	-20.7	65	41072N	71336W
297	63.7	2.5	69.4	27	-25.4	2.3	-19.6	73	41073N	71341W
298	65.5	2.8	69.4	27	-23.9	2.3	-20.8	73	41074N	71347W
299	67.2	2.7	70.4	24	-23.1	2.8	-19.3	68	41077N	71361W
300	67.1	2.4	70.1	24	-24.0	2.1	-19.9	53	41080N	71367W
301	70.4	2.2	73.3	26	-21.0	2.2	-17.4	36	41083N	71374W
302	70.3	2.4	74.4	29	-20.7	3.0	-14.7	37	41087N	71378W
303	70.7	1.9	73.8	25	-18.8	2.5	-13.6	31	41094N	71377W
304	69.4	2.5	72.5	24	-19.3	2.2	-16.8	49	41099N	71376W
305	65.3	2.7	70.3	25	-25.3	2.5	-20.1	58	41104N	71374W

TABLE VIII

ECHO STRENGTH MEASUREMENTS AT NORMAL INCIDENCE

TAG	P1	P2	P3	N	E1	E2	E3	DEPTH	LAT.	LONG.
306	66.6	2.2	71.0	24	-23.2	2.4	-19.0	55	41107N	71371W
307	60.5	2.7	65.7	26	-28.0	1.2	-25.5	72	41112N	71370W
308	53.8	2.7	59.7	27	-34.0	2.7	-29.3	88	41114N	71368W
309	58.0	2.6	62.7	100	-33.1	2.2	-27.7	74	41116N	71365W
310	69.5	2.7	75.1	112	-20.7	2.6	-14.0	44	41078N	71386W
311	66.7	2.7	71.7	23	-23.4	2.5	-18.8	44	41077N	71385W
312	66.7	2.7	72.6	24	-23.3	2.9	-17.2	47	41072N	71383W
313	66.4	2.8	69.7	24	-23.5	2.1	-20.2	58	41000J	71382W
314	62.8	1.4	65.2	23	-27.3	1.1	-25.0	73	41064N	71381W
315	61.4	2.9	67.7	24	-28.8	2.5	-23.4	90	41059N	71380W
316	60.2	2.5	64.2	21	-29.2	1.9	-25.1	103	41054N	71379W
317	61.4	1.6	63.8	39	-28.7	1.4	-25.6	110	410001	71374W
318	59.5	2.1	63.0	27	-30.6	1.5	-26.9	119	410001	71371W
319	59.3	2.6	62.2	25	-30.6	1.3	-28.6	126	4103 N	71368W
320	58.0	3.0	65.4	24	-31.3	1.9	1.3	129	41034N	71366W
321	56.6	3.9	63.4	23	-33.6	3.6	-24.9	130	41029N	71364W
322	57.8	1.7	60.3	24	-31.4	2.1	-27.5	130	41023N	71364W
323	57.4	2.9	63.0	28	-33.0	2.5	-27.4	126	41019N	71363W
324	58.2	3.1	62.9	27	-32.4	2.5	-27.5	122	41014N	71363W
325	56.2	2.8	64.9	24	-32.6	2.8	-24.4	122	41009N	71362W
326	58.5	2.9	62.8	25	-30.7	2.7	-27.1	125	41004N	71362W
327	58.0	1.6	62.4	26	-31.3	1.9	-27.4	131	40599N	71361W
328	57.1	3.2	61.9	45	-32.5	2.6	-27.4	133	40596N	71357W
329	54.2	2.3	57.8	29	-36.6	1.9	-32.6	176	40548N	71339W
330	54.5	1.6	57.5	31	-35.9	1.7	-33.2	178	40540N	71332W

TABLE VIII

ECHO STRENGTH MEASUREMENTS AT NORMAL INCIDENCE

TAG	P1	P2	P3	N	E1	E2	E3	DEPTH	LAT.	LONG.
331	51.9	2.7	58.4	96	-37.7	1.9	-31.3	180	40538N	71330W
332	52.5	2.1	57.5	35	-37.5	1.9	-34.1	185	40534N	71330W
333	53.3	2.3	57.3	31	-36.9	1.7	-34.0	186	40528N	71329W
334	52.2	2.0	56.2	30	-38.6	1.8	-34.4	188	40521N	71328W
335	51.9	2.4	55.3	26	-38.2	1.9	-34.5	190	40514N	71328W
336	52.8	2.9	56.0	26	-37.4	2.0	-35.2	192	40507N	71327W
337	52.2	1.9	55.9	32	-37.8	1.6	-34.7	200	40498N	71324W
338	50.5	2.4	53.7	21	-39.9	1.4	-37.1	204	40491N	71322W
339	49.8	2.4	53.5	26	-39.8	1.9	-36.2	204	40480N	71319W
340	50.5	2.1	53.2	26	-39.4	1.9	-36.5	200	40477N	71318W
341	51.2	3.5	54.9	37	-39.1	2.4	-35.3	200	40473N	71318W
342	50.2	2.0	54.4	32	-39.6	1.6	-36.9	200	40473N	71318W
343	51.3	2.1	53.8	19	-38.2	2.0	-35.9	200	40468N	71315W
344	48.7	3.4	55.6	15	-40.6	2.9	-34.5	202	40461N	71314W
345	49.4	2.3	53.6	20	-39.9	1.9	-35.7	204	40456N	71312W
346	50.9	2.1	54.8	23	-39.2	1.7	-34.6	206	40450N	71311W
347	49.2	2.4	53.4	19	-40.2	2.0	-36.5	210	40438N	71308W
348	47.6	2.2	51.0	24	-41.8	1.6	-38.5	212	40432N	71306W
349	46.7	1.9	48.9	21	-42.5	1.6	-40.6	212	40426N	71304W
350	47.5	2.5	50.7	21	-42.0	1.8	-39.8	210	40420N	71303W
351	48.8	1.8	51.2	16	-41.2	1.5	-38.8	208	40414N	71301W
352	50.0	2.3	51.9	21	-40.7	1.9	-38.3	206	40410N	71299W
353	50.0	3.5	55.4	37	-40.3	2.7	-34.8	204	40408N	71299W
354	49.4	2.5	52.8	25	-40.1	2.2	-37.0	202	40407N	71300W
355	50.1	2.3	53.5	31	-39.9	2.0	-36.0	201	40405N	71299W

TABLE VIII

ECHO STRENGTH MEASUREMENTS AT NORMAL INCIDENCE

TAG	P1	P2	P3	N	E1	E2	E3	DEPTH	LAT.	LONG.
356	46.9	2.9	51.9	22	-42.1	2.4	-37.6	202	40402N	71297W
357	48.5	1.9	52.0	29	-41.0	1.9	-37.6	203	40399N	71296W
358	48.5	3.2	52.6	23	-40.3	2.6	-37.8	204	40397N	71294W
359	48.7	3.6	53.6	25	-40.8	2.7	-36.5	205	40393N	71293W
360	48.5	2.8	51.9	23	-40.5	2.3	-37.5	207	40391N	71292W
361	49.6	2.6	54.8	30	-40.1	2.1	-35.5	208	40383N	71289W
362	49.9	2.2	52.9	24	-40.5	2.1	-37.1	208	40377N	71286W
363	48.1	2.9	54.1	25	-41.2	2.7	-36.5	209	40370N	71284W
364	51.9	2.5	54.7	25	-38.4	2.3	-35.6	210	40364N	71281W
365	47.9	2.7	50.6	25	-41.1	2.1	-38.9	211	40357N	71278W
366	47.8	2.4	51.8	33	-41.5	2.2	-37.5	212	40351N	71275W
367	46.8	3.2	49.9	52	-42.4	2.1	-38.3	215	40344N	71273W
368	47.5	2.8	52.7	58	-41.4	1.9	-36.6	215	40343N	71273W
369	46.4	1.9	50.9	25	-41.9	1.7	-39.3	217	40342N	71272W
370	45.3	2.9	50.4	27	-43.1	2.0	-38.6	220	40337N	71272W
371	47.4	2.3	49.5	39	-41.8	1.6	-39.0	220	40333N	71272W
372	47.5	1.8	51.7	28	-41.2	1.5	-38.2	220	40328N	71270W
373	48.1	2.3	51.2	26	-41.2	1.9	-38.9	221	40324N	71270W
374	47.8	2.5	52.6	25	-41.9	2.0	-37.9	220	40320N	71269W
375	47.3	3.1	54.0	24	-42.8	2.6	-36.4	221	40317N	71269W
376	47.2	3.1	52.4	25	-41.5	2.5	-37.4	222	40312N	71268W
377	46.3	2.6	52.0	25	-42.6	1.9	-37.3	224	40309N	71267W
378	47.6	3.2	52.2	25	-41.9	2.5	-38.0	225	40305N	71267W
379	45.4	2.8	51.1	25	-43.2	2.0	-39.3	227	40301N	71266W
380	46.5	2.4	50.2	25	-43.1	1.7	-39.5	229	40296N	71266W

TABLE VIII

ECHO STRENGTH MEASUREMENTS AT NORMAL INCIDENCE

TAG	P1	P2	P3	N	E1	E2	E3	DEPTH	LAT.	LONG.
381	45.6	4.5	51.3	96	-43.0	2.2	-38.6	230	40294N	71265W
382	45.8	2.5	50.1	38	-42.4	2.0	-39.6	230	40289N	71264W
383	45.0	2.2	49.4	28	-43.9	1.4	-40.8	230	40285N	71262W
384	45.4	2.4	48.8	28	-43.5	1.9	-40.1	231	40280N	71261W
385	46.0	2.2	51.0	29	-43.2	1.6	-39.4	232	40275N	71259W
386	46.8	3.5	52.7	37	-43.1	2.6	-37.0	234	40269N	71257W
387	48.0	2.6	53.7	23	-42.2	2.2	-36.6	235	40266N	71256W
388	46.7	2.7	53.1	40	-42.4	2.1	-37.2	238	40261N	71254W
389	45.0	2.4	48.7	21	-44.6	1.5	-41.2	240	40256N	71253W
390	44.1	3.3	51.0	27	-44.8	2.4	-39.0	242	40253N	71252W
391	45.8	2.7	49.1	20	-43.8	1.9	-40.9	245	40249N	71250W
392	44.6	2.0	48.8	29	-44.0	1.3	-41.1	248	40242N	71249W
393	44.5	1.9	48.0	23	-43.7	1.5	-40.3	250	40238N	71248W
394	46.2	3.2	51.6	50	-42.9	2.1	-38.2	250	40235N	71246W
395	44.6	3.2	49.4	55	-43.4	1.8	-40.6	250	40235N	71245W
396	43.1	1.7	46.7	25	-44.8	1.5	-41.6	250	40229N	71243W
397	42.7	2.3	47.1	25	-45.3	1.4	-41.9	252	40222N	71240W
398	42.9	2.2	48.9	25	-45.3	1.5	-41.2	254	40217N	71238W
399	43.9	1.8	47.6	25	-43.8	1.2	-41.6	256	40211N	71235W
400	43.8	2.3	48.4	25	-45.0	1.9	-40.6	260	40205N	71233W
401	44.0	2.0	47.2	25	-44.2	1.4	-40.9	260	40200N	71231W
402	43.5	2.0	47.2	25	-44.2	1.7	-42.4	260	40195N	71231W
403	47.4	3.0	53.1	25	-42.6	2.4	-37.1	258	40192N	71230W
404	46.4	2.2	50.5	25	-43.5	1.8	-39.0	260	40188N	71230W
405	45.7	2.3	50.6	25	-43.1	1.8	-38.6	263	40185N	71230W

TABLE VIII

ECHO STRENGTH MEASUREMENTS AT NORMAL INCIDENCE

TAG	P1	P2	P3	N	E1	E2	E3	DEPTH	LAT.	LONG.
406	45.5	2.3	49.6	25	-43.5	1.7	-40.4	267	40180N	71229W
407	44.5	2.1	48.0	25	-44.8	1.4	-41.5	270	40177N	71229W
408	43.3	3.1	48.7	80	-44.1	1.6	-40.1	272	40168N	71228W
409	43.8	1.9	49.7	25	-44.5	1.3	-39.5	273	40165N	71227W
410	43.3	2.4	48.2	25	-44.7	1.5	-41.6	273	40160N	71227W
411	43.3	2.5	47.8	25	-45.0	1.6	-41.8	274	40156N	71226W
412	42.7	2.1	46.6	25	-45.7	1.2	-42.6	276	40152N	71225W
413	45.0	2.7	49.6	25	-44.5	1.8	-39.9	278	40148N	71224W
414	46.8	2.6	49.7	25	-42.7	2.1	-39.9	280	40144N	71223W
415	44.3	2.8	50.5	25	-45.0	1.7	-39.2	282	40140N	71222W
416	45.0	2.3	49.0	25	-43.6	1.8	-40.2	284	40136N	71221W
417	45.4	2.8	50.5	25	-43.1	2.2	-39.2	283	40132N	71220W
418	48.6	2.9	52.7	35	-41.2	2.2	-37.4	283	40128N	71220W
419	44.8	3.0	50.7	22	-44.5	2.5	-38.9	282	40124N	71219W
420	45.6	3.3	51.8	23	-43.8	2.4	-38.8	288	40120N	71218W
421	47.9	3.6	53.7	26	-41.9	2.8	-36.4	287	40116N	71217W
422	45.7	4.5	53.5	43	-43.0	2.4	-36.6	289	40116N	71217W
423	41.5	2.4	47.0	32	-44.3	0.9	-41.2	285	40238N	70445W
424	41.6	2.5	45.8	44	-45.5	2.1	-41.1	285	40238N	70445W
425	42.4	1.6	45.1	25	-45.3	1.5	-42.1	280	40242N	70445W
426	42.7	1.5	45.1	25	-44.9	1.6	-41.7	275	40247N	70444W
427	41.3	1.4	45.3	25	-46.1	1.6	-41.9	270	40251N	70442W
428	41.9	2.2	46.6	24	-46.6	2.1	-41.3	267	40257N	71441W
429	42.3	1.7	45.4	25	-45.3	1.8	-41.8	263	40261N	70441W
430	41.4	1.7	45.7	25	-46.0	1.7	-42.1	260	40268N	70441W

TABLE VIII

ECHO STRENGTH MEASUREMENTS AT NORMAL INCIDENCE

TAG	P1	P2	P3	N	E1	E2	E3	DEPTH	LAT.	LONG.
431	41.0	2.6	47.6	25	-47.2	2.1	-41.2	256	40273N	70442W
432	42.5	2.5	46.9	24	-47.2	2.7	-41.6	253	40280N	70443W
433	42.3	2.5	47.5	24	-46.5	2.4	-41.3	250	40284N	70443W
434	42.5	2.2	49.1	24	-46.1	2.1	-39.9	245	40290N	70443W
435	42.1	2.6	47.8	15	-46.3	2.5	-41.0	242	40296N	70443W
436	42.6	2.4	50.8	25	-44.4	2.2	-38.1	240	40302N	70444W
437	42.3	3.0	48.8	27	-46.4	2.8	-39.9	237	40307N	70446W
438	42.2	2.8	49.2	88	-46.0	2.4	-39.8	234	40309N	70446W
439	42.9	2.5	49.8	25	-44.5	2.2	-38.5	230	40322N	70446W
440	42.9	1.6	45.9	25	-44.2	1.6	-41.6	228	40330N	70446W
441	43.4	1.9	47.0	25	-43.5	1.3	-41.2	224	40335N	70447W
442	44.7	1.9	47.4	25	-42.9	1.8	-40.0	222	40342N	70448W
443	44.7	1.8	49.4	25	-42.2	1.4	-39.3	220	40350N	70448W
444	43.8	2.3	50.3	25	-43.0	2.1	-36.6	217	40356N	70449W
445	44.2	2.3	48.9	25	-42.4	1.5	-39.5	212	40363N	70449W
446	44.4	2.6	50.6	25	-41.9	2.4	-36.3	211	40370N	70450W
447	43.7	2.3	51.3	25	-42.7	1.8	-37.5	210	40377N	70451W
448	45.0	2.1	48.2	25	-42.3	1.9	-38.4	206	40384N	70451W
449	47.3	2.2	49.9	25	-40.9	1.6	-38.3	202	40392N	70452W
450	46.1	2.8	52.5	49	-41.2	2.5	-36.2	202	40394N	70452W
451	44.3	3.5	51.6	54	-42.9	2.6	-39.0	202	40394N	70452W
452	47.4	2.3	50.8	30	-40.3	1.9	-36.1	201	40396N	70451W
453	45.1	2.2	49.8	33	-42.5	2.1	-37.3	202	40400N	70448W
454	46.0	2.1	50.2	24	-40.8	1.8	-38.1	203	40405N	70446W
455	46.8	2.3	51.0	25	-39.9	1.9	-36.2	201	40409N	70444W

TABLE VIII

ECHO STRENGTH MEASUREMENTS AT NORMAL INCIDENCE

TAG	P1	P2	P3	N	E1	E2	E3	DEPTH	LAT.	LONG.
456	46.9	2.7	53.4	25	-39.6	2.2	-35.9	200	40413N	70441W
457	48.3	1.7	50.7	25	-38.8	1.6	-36.8	200	40417N	70440W
458	47.0	2.4	51.2	25	-39.2	1.7	-35.5	200	40422N	70438W
459	49.5	2.8	52.5	24	-37.1	2.3	-33.8	199	40427N	70434W
460	47.8	2.3	51.8	23	-37.5	1.9	-32.9	198	40434N	70431W
461	46.9	2.0	50.4	24	-38.4	2.7	-32.8	197	40436N	70430W
462	47.9	3.0	54.6	22	-37.4	2.3	-32.0	195	40440N	70428W
463	49.0	2.5	54.2	29	-36.1	2.5	-32.8	193	40445N	70426W
464	47.8	4.0	54.3	101	-39.6	2.6	-35.0	191	40447N	70424W
465	47.9	2.1	53.2	23	-39.6	1.9	-35.4	191	40450N	70423W
466	48.7	2.9	52.2	21	-39.7	1.8	-36.4	190	40463N	70421W
467	48.0	3.0	54.8	25	-39.8	2.2	-34.3	190	40470N	70421W
468	50.3	3.5	54.2	29	-38.6	2.5	-35.0	188	40477N	70420W
469	48.8	2.5	52.8	26	-39.9	1.8	-36.4	187	40483N	70418W
470	50.6	2.9	54.7	29	-38.0	2.0	-35.3	182	40491N	70417W
471	50.8	2.9	55.5	27	-38.5	2.1	-33.1	182	40498N	70416W
472	51.9	2.7	55.9	23	-36.9	2.4	-32.9	181	40505N	70415W
473	49.2	2.7	54.9	32	-38.3	2.1	-34.4	180	40512N	70413W
474	48.0	2.6	52.7	22	-38.9	1.7	-36.4	180	40519N	70413W
475	50.0	2.3	55.4	23	-38.7	2.0	-33.2	177	40526N	70412W
476	52.7	2.2	58.0	43	-36.7	2.3	-28.3	173	40532N	70411W
477	53.0	4.1	61.1	104	-35.8	3.1	-30.0	170	40534N	70411W
478	51.4	2.0	56.2	27	-37.4	2.0	-32.9	161	40537N	70410W
479	54.9	1.8	57.6	24	-34.6	1.9	-31.4	160	40541N	70409W
480	54.3	2.9	58.4	24	-34.5	2.7	-30.7	158	40545N	70409W

TABLE VIII

ECHO STRENGTH MEASUREMENTS AT NORMAL INCIDENCE

TAG	P1	P2	P3	N	E1	E2	E3	DEPTH	LAT.	LONG.
481	52.4	2.9	58.2	19	-36.0	2.6	-31.4	156	40551N	70408W
482	53.2	2.2	57.4	24	-35.6	1.9	-31.5	158	40555N	70407W
483	53.9	2.5	57.9	19	-35.9	2.1	-32.4	160	40559N	70407W
484	50.3	3.3	56.8	24	-37.8	2.4	-32.5	166	40564N	70406W
485	53.9	2.4	59.4	27	-36.0	2.0	-32.5	164	40568N	70405W
486	53.8	1.9	56.7	20	-35.9	1.9	-33.1	161	40573N	70405W
487	53.2	1.8	56.8	24	-35.9	1.9	-32.4	158	40577N	70404W
488	52.2	1.4	54.6	22	-37.2	1.3	-34.9	155	40581N	70403W
489	53.9	2.1	56.3	24	-36.2	2.0	-33.3	153	40587N	70402W
490	49.9	3.7	56.4	95	-38.3	2.7	-32.6	162	40589N	70403W
491	51.7	3.3	58.3	24	-37.1	2.9	-30.9	158	40595N	70403W
492	54.6	2.4	57.9	24	-34.9	2.0	-31.6	154	41000N	70403W
493	53.6	2.9	58.3	24	-35.6	2.3	-30.6	151	41005N	70403W
494	54.8	2.7	58.4	24	-35.0	2.4	-30.6	145	41010N	70403W
495	54.9	2.7	58.3	24	-34.3	2.6	-30.4	146	41014N	70403W
496	53.9	1.9	58.2	24	-36.3	1.7	-31.7	145	41019N	70403W
497	54.1	2.8	59.5	24	-35.5	2.8	-29.6	146	41023N	70404W
498	53.7	2.5	58.0	24	-35.4	2.0	-32.2	144	41028N	70404W
499	55.2	2.3	59.5	24	-34.4	2.4	-29.6	142	41033N	70404W
500	55.0	2.2	58.1	23	-34.4	2.1	-31.4	141	41037N	70404W
501	55.8	3.0	61.5	24	-32.9	2.8	-27.4	140	41043N	70404W
502	52.8	6.3	60.3	91	-36.2	3.5	-29.5	139	41046N	70405W
503	55.7	3.0	61.4	26	-35.1	2.9	-28.7	140	41049N	70405W
504	54.1	2.4	57.4	17	-36.7	2.1	-33.0	139	41052N	70405W
505	55.4	2.7	61.3	24	-34.5	2.7	-28.7	139	41054N	70407W

TABLE VIII

ECHO STRENGTH MEASUREMENTS AT NORMAL INCIDENCE

TAG	P1	P2	P3	N	E1	E2	E3	DEPTH	LAT.	LONG.
506	55.1	3.4	59.7	25	-34.9	3.2	-31.4	139	41056N	70407W
507	54.9	3.0	60.4	24	-34.7	3.1	-29.5	138	41059N	70407W
508	54.5	3.5	61.9	24	-36.3	3.2	-28.7	137	41062N	70407W
509	56.2	3.3	63.9	26	-34.3	3.1	-26.2	136	41065N	70407W
510	57.2	3.8	61.1	25	-33.2	3.4	-29.2	136	41068N	70407W
511	53.6	3.4	60.0	25	-36.7	3.0	-31.2	138	41070N	70407W
512	56.1	1.7	59.0	25	-34.3	1.9	-31.1	134	41073N	70408W
513	55.3	1.7	58.2	22	-34.5	2.1	-28.7	132	41075N	70408W
514	56.0	3.9	62.4	18	-33.8	3.4	-28.0	128	41078N	70408W
515	53.9	4.2	61.0	66	-35.7	3.8	-14.6	122	41080N	70408W
516	56.1	3.0	62.5	8	-34.7	3.0	-28.8	117	41084N	70409W
517	58.0	2.8	61.2	9	-33.4	2.6	-29.3	114	41089N	70409W
518	57.2	3.1	63.6	11	-33.9	2.9	-27.4	112	41095N	70409W
519	58.3	3.0	64.0	22	-31.4	2.6	-26.5	107	41099N	70410W
520	56.7	1.8	60.1	22	-32.4	2.0	-28.6	101	41105N	70411W
521	57.7	2.9	64.9	20	-32.2	2.6	-25.5	100	41110N	70411W
522	58.3	2.2	64.0	23	-31.0	1.8	-26.0	92	41115N	70412W
523	60.8	2.5	65.8	25	-29.3	2.6	-23.8	87	41121N	70413W
524	59.2	2.2	62.9	24	-31.0	2.1	-26.6	87	41126N	70412W
525	59.7	3.2	65.5	27	-30.1	3.1	-24.8	86	41131N	70413W
526	58.3	4.2	65.1	31	-30.9	3.0	-24.0	87	41136N	70414W
527	58.5	3.1	64.6	27	-31.0	2.7	-25.8	86	41141N	70414W
528	60.0	2.7	63.0	27	-30.5	2.6	-27.0	84	41147N	70415W
529	58.1	4.6	65.8	100	-31.3	3.6	-23.8	82	41149N	70415W
530	59.6	2.4	66.5	27	-30.1	2.4	-22.8	83	41151N	70414W

TABLE VIII

ECHO STRENGTH MEASUREMENTS AT NORMAL INCIDENCE

TAG	P1	P2	P3	N	E1	E2	E3	DEPTH	LAT.	LONG.
531	60.3	3.0	65.5	27	-29.3	2.9	-23.4	82	41155N	70412W
532	61.1	3.1	66.9	24	-28.8	2.8	-22.2	80	41160N	70411W
533	60.9	3.1	67.2	33	-28.6	2.9	-22.3	77	41164N	70408W
534	61.4	3.5	68.0	36	-27.7	3.1	-20.7	72	41169N	70408W
535	63.3	3.1	68.1	24	-25.7	3.0	-21.5	69	41174N	70405W
536	64.9	3.1	69.7	28	-24.4	3.2	-19.1	66	41179N	70404W
537	63.4	2.4	67.1	28	-25.9	2.3	-22.0	59	41184N	70402W
538	63.7	3.0	68.6	24	-25.4	2.8	-21.4	49	41189N	70400W
539	66.0	2.3	70.5	27	-25.1	2.4	-19.6	37	41193N	70398W

ECHO STRENGTH MESUREMENTS MADE ON BEAR 290

1	68.5	2.0	71.7	46	-18.2	2.2	-15.7	62	41165N	70394W
2	68.3	2.2	72.2	49	-19.0	2.1	-17.8	72	41134N	70396W
3	65.3	2.9	70.4	49	-22.7	3.2	-18.0	90	41102N	70395W
4	63.4	3.1	69.4	49	-24.3	3.1	-19.2	114	41075N	70390W
5	62.6	3.1	66.7	50	-25.4	2.8	-22.1	122	41040N	70390W
6	62.4	3.1	67.7	49	-25.6	2.9	-22.3	132	41000N	70400W
7	59.9	3.8	66.2	48	-28.1	3.1	-22.8	136	40571N	70414W
8	60.7	2.5	66.6	49	-26.4	2.1	-22.8	147	40545N	70424W
9	61.0	3.1	67.9	99	-26.2	2.5	-22.2	150	40515N	70425W
10	56.3	3.0	63.0	50	-30.2	2.3	-26.4	164	40488N	70425W
11	56.6	2.2	62.1	50	-29.8	1.9	-26.5	174	40455N	70425W
12	57.0	2.3	61.5	49	-29.6	1.8	-26.4	180	40420N	70408W
13	55.4	2.6	60.7	49	-31.1	1.9	-27.2	182	40400N	70428W
14	55.3	2.8	62.7	49	-30.5	2.0	-26.5	192	40370N	70415W

TABLE VIII

ECHO STRENGTH MEASUREMENTS AT NORMAL INCIDENCE

TAG	P1	P2	P3	N	E1	E2	E3	DEPTH	LAT.	LONG.
15	52.2	2.3	57.0	50	-33.4	1.5	-30.5	204	40335N	70420W
16	51.0	2.5	57.4	50	-34.8	2.0	-30.8	216	40305N	70422W
17	49.4	3.0	57.3	50	-36.5	2.1	-30.1	236	40265N	70425W
18	49.9	2.4	55.1	50	-35.6	1.4	-33.8	255	40244N	70435W
19	49.4	2.4	54.9	50	-36.2	1.6	-33.5	285	40221N	70435W
20	45.0	3.4	51.5	50	-41.3	2.1	-37.7	336	40187N	70428W
21	42.6	2.0	47.1	53	-41.1	1.9	-37.7	366	40154N	70430W

TABLE IX

GRAIN SIZE MEASUREMENTS OF SEDIMENT SAMPLES

TAG	DEPTH	Q3	MEDIAN	Q1	GRAV.	SAND	SILT	CLAY
1	20	0.230	0.026	0.0072	0.	38.0	46.0	16.0
2	27	0.082	0.018	0.0040	0.	30.0	44.0	25.0
3	51	0.450	0.094	0.0420	17.0	47.0	28.0	8.0
4	83	0.560	0.410	0.2100	0.	87.0	13.0	0.
5	84	5.100	1.200	0.3600	42.0	55.0	3.0	0.
6	50	22.000	4.800	0.7300	60.0	36.0	4.0	0.
7	30	0.110	0.094	0.0820	0.	90.0	10.0	0.
8	98	0.180	0.140	0.1100	0.	88.0	12.0	0.
9	100	0.190	0.086	0.0150	0.	57.0	43.0	0.
10	32	0.130	0.100	0.0700	0.	80.0	20.0	0.
11	31	0.140	0.098	0.0500	0.	70.0	30.0	0.
12	38	0.250	0.180	0.1000	0.	83.0	17.0	0.
13	43	0.400	0.190	0.0300	0.	65.0	30.0	5.0
14	26	0.120	0.090	0.0800	0.	92.0	8.0	0.
15	25	0.110	0.100	0.0960	0.	90.0	10.0	0.
16	60	0.120	0.090	0.0550	0.	72.0	24.0	4.0
17	41	0.130	0.100	0.0850	0.	90.0	10.0	0.
18	30	0.160	0.140	0.1100	0.	99.9	1.0	0.
19	74	0.430	0.280	0.1600	0.	95.0	5.0	0.
20	76	0.110	0.096	0.0900	0.	96.0	4.0	0.
21	23	0.038	0.014	0.0049	0.	21.0	60.0	19.0
22	28	0.028	0.014	0.0056	0.	9.0	73.0	18.0
23	50	0.055	0.019	0.0068	0.	24.0	60.0	16.0
24	65	3.600	1.400	0.7000	38.0	62.0	0.	0.
25	68	0.230	0.200	0.1800	0.	99.9	0.1	0.
26	33	0.210	0.170	0.1300	0.	96.0	4.0	0.

TABLE IX

GRAIN SIZE MEASUREMENTS OF SEDIMENT SAMPLES

TAG	DEPTH	Q3	MEDIAN	Q1	GRAV.	SAND	SILT	CLAY
27	25	0.086	0.024	0.0088	0.	29.0	57.0	14.0
28	46	0.230	0.190	0.1500	0.	98.0	2.0	0.
29	77	0.220	0.200	0.1800	0.	98.0	2.0	0.
30	50	0.300	0.190	0.1300	0.	98.0	2.0	0.
31	30	0.190	0.120	0.0980	0.	98.0	2.0	0.
32	40	0.250	0.170	0.1200	0.	98.0	2.0	0.
33	120	0.340	0.180	0.0940	0.	90.0	10.0	0.
34	131	0.190	0.100	0.0400	0.	66.0	26.0	8.0
35	101	24.000	9.100	3.4000	82.0	18.0	0.	0.
36	82	0.220	0.200	0.1900	0.	99.9	0.1	0.
37	74	0.130	0.110	0.0920	0.	90.0	7.0	3.0
38	44	1.200	0.910	0.7200	8.0	92.0	0.	0.
39	133	0.860	0.780	0.6200	0.	99.9	0.1	0.
40	180	0.250	0.210	0.1600	0.	98.0	2.0	0.
41	200	0.210	0.160	0.1200	0.	94.0	6.0	0.
42	204	0.330	0.230	0.1400	0.	85.0	15.0	0.
43	215	0.300	0.160	0.0630	0.	76.0	17.0	7.0
44	230	0.300	0.210	0.1400	0.	88.0	12.0	0.
45	250	0.400	0.230	0.0600	0.	74.0	22.0	4.0
46	272	0.220	0.090	0.0230	0.	55.0	37.0	8.0
47	289	0.460	0.410	0.3500	0.	98.0	2.0	0.
48	80	0.270	0.210	0.1800	0.	96.0	4.0	0.
49	82	0.960	0.520	0.3500	6.0	94.0	0.	0.
50	90	1.200	0.900	0.5000	0.	99.9	0.1	0.
51	108	0.530	0.430	0.3500	0.	99.0	1.0	0.
52	122	0.840	0.300	0.1800	14.0	85.0	1.0	0.

TABLE IX

GRAIN SIZE MEASUREMENTS OF SEDIMENT SAMPLES

TAG	DEPTH	Q3	MEDIAN	Q1	GRAV.	SAND	SILT	CLAY
53	132	0.640	0.600	0.4900	0.	99.0	1.0	0.
54	139	0.240	0.210	0.1900	0.	99.0	1.0	0.
55	140	0.420	0.260	0.1800	0.	94.0	6.0	0.
56	150	0.290	0.210	0.1700	0.	96.0	4.0	0.
57	162	0.220	0.160	0.1200	0.	91.0	9.0	0.
58	154	0.240	0.180	0.1100	0.	83.0	17.0	0.
59	165	0.400	0.210	0.1100	0.	88.0	12.0	0.
60	170	0.480	0.400	0.3600	0.	99.9	0.1	0.
61	168	0.760	0.560	0.4300	0.	98.0	2.0	0.
62	182	0.380	0.130	0.0470	0.	70.0	22.0	8.0
63	192	0.150	0.068	0.0210	0.	54.0	33.0	13.0
64	191	0.260	0.150	0.0700	0.	78.0	18.0	4.0
65	198	0.170	0.056	0.0150	0.	48.0	38.0	14.0
66	200	0.120	0.072	0.0560	0.	70.0	26.0	4.0
67	202	0.180	0.096	0.0330	0.	64.0	28.0	8.0
68	210	0.072	0.043	0.0170	0.	32.0	54.0	14.0
69	222	0.062	0.032	0.0110	0.	23.0	59.0	18.0
70	234	0.075	0.035	0.0130	0.	30.0	58.8	12.0
71	234	0.066	0.032	0.0100	0.	22.0	60.0	18.0
72	254	0.052	0.024	0.0060	0.	18.0	59.0	23.0
73	273	0.052	0.028	0.0078	0.	17.0	63.0	20.0
74	285	0.070	0.028	0.0100	0.	28.0	58.0	14.0
75	303	0.072	0.037	0.0130	0.	30.0	54.0	16.0
76	354	0.049	0.029	0.0084	0.	15.0	65.0	20.0
77	384	0.052	0.027	0.0086	0.	17.0	63.0	20.0

TABLE X

WATER CONTENT MEASUREMENTS ON SEDIMENT SAMPLES

TAG	WET WEIGHT	DRY WEIGHT
1	238.9	136.9
2	209.2	103.1
3	205.0	101.4
4	249.0	167.8
5	217.5	126.7
6	247.4	174.5
7	248.3	166.9
8	222.1	140.2
9	271.1	205.2
10	238.7	160.5
11	213.9	123.5
12	218.5	125.8
13	231.9	144.7
14	238.5	157.8
15	248.3	166.9
16	237.6	160.7
17	267.6	199.5
18	270.7	210.0
19	132.9	105.0
20	247.9	169.3
21	244.0	167.4
22	199.3	101.5
23	185.6	66.7
24	274.7	223.8
25	284.0	235.6
26	271.0	210.2

TABLE X

WATER CONTENT MEASUREMENTS ON SEDIMENT SAMPLES

TAG	WET WEIGHT	DRY WEIGHT
27	222.0	133.5
28	260.3	201.6
29	272.2	213.5
30	276.8	220.7
31	292.9	236.4
32	262.3	202.6
33	298.0	254.1
34	238.7	166.9
35	275.6	222.4
36	266.4	214.4
37	209.8	147.2
38	270.7	223.5
39	271.6	215.4
40	272.7	214.2
41	264.7	196.8
42	230.6	155.1
43	251.9	176.8
44	232.3	154.0
45	246.8	179.6
46	257.5	188.4
47	244.9	162.5
48	266.1	205.0
49	254.3	203.3
50	244.0	192.1
51	266.2	213.2
52	265.5	199.0

TABLE X

WATER CONTENT MEASUREMENTS ON SEDIMENT SAMPLES

TAG	WET WEIGHT	DRY WEIGHT
53	265.6	204.5
54	280.9	226.1
55	279.4	213.3
56	254.8	184.9
57	257.2	185.5
58	253.7	180.4
59	252.3	185.4
60	239.3	176.6
61	280.3	230.5
62	196.2	117.2
63	186.7	100.6
64	206.1	106.0
65	171.5	87.5
66	211.0	123.9
67	211.8	120.2
68	193.6	91.4
69	204.6	109.6
70	154.1	97.3
71	200.6	97.7
72	195.1	95.0
73	190.7	99.3
74	202.9	103.8
75	199.7	108.6
76	203.6	112.7
77	195.7	97.9

APPENDIX D

SEDIMENT SAMPLES
PARTICLE SIZE DISTRIBUTION

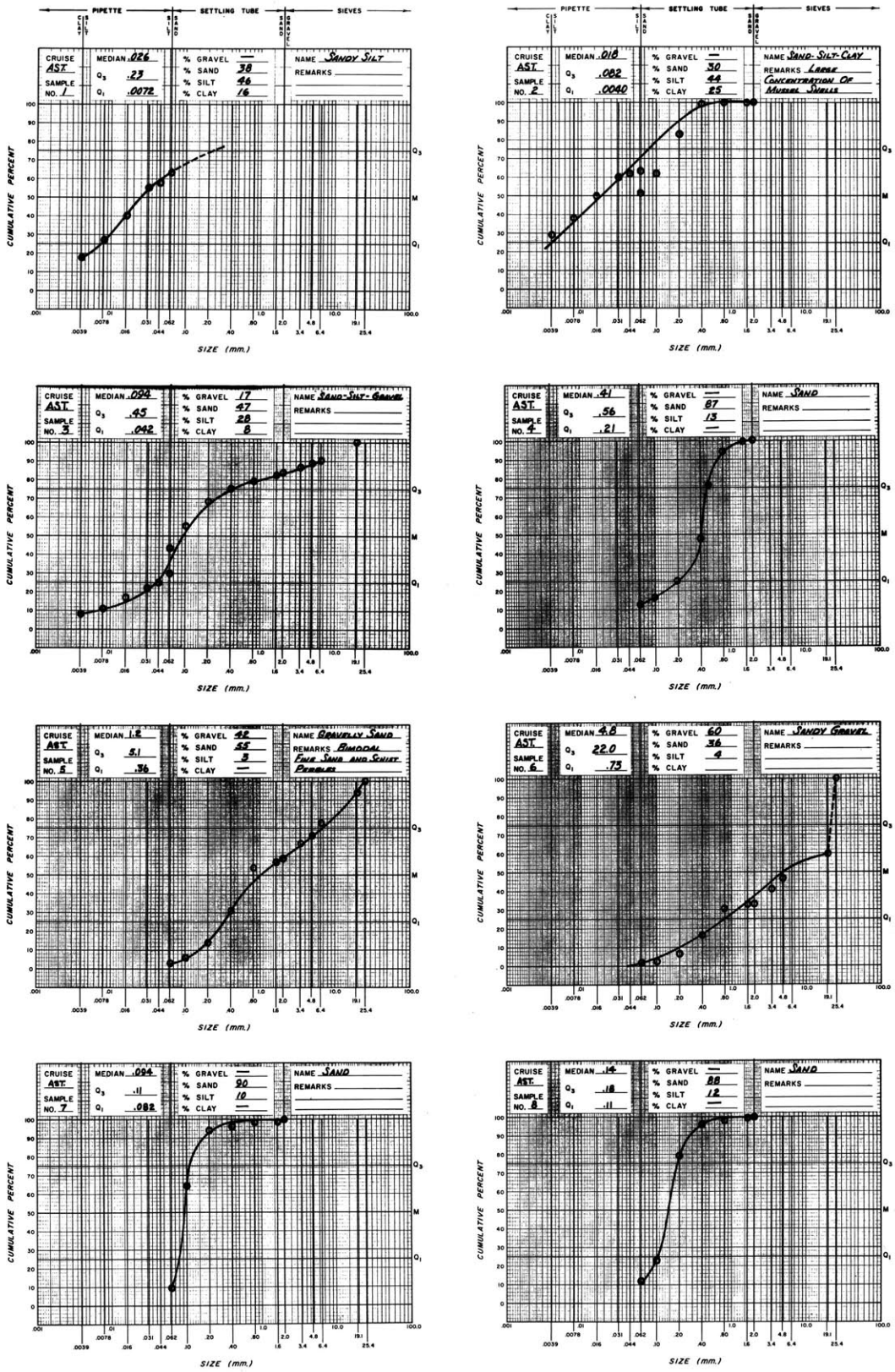

Figure 72. Cumulative Size Distribution Curves for Sediment Samples 1-8.

SEDIMENT SAMPLES
PARTICLE SIZE DISTRIBUTION

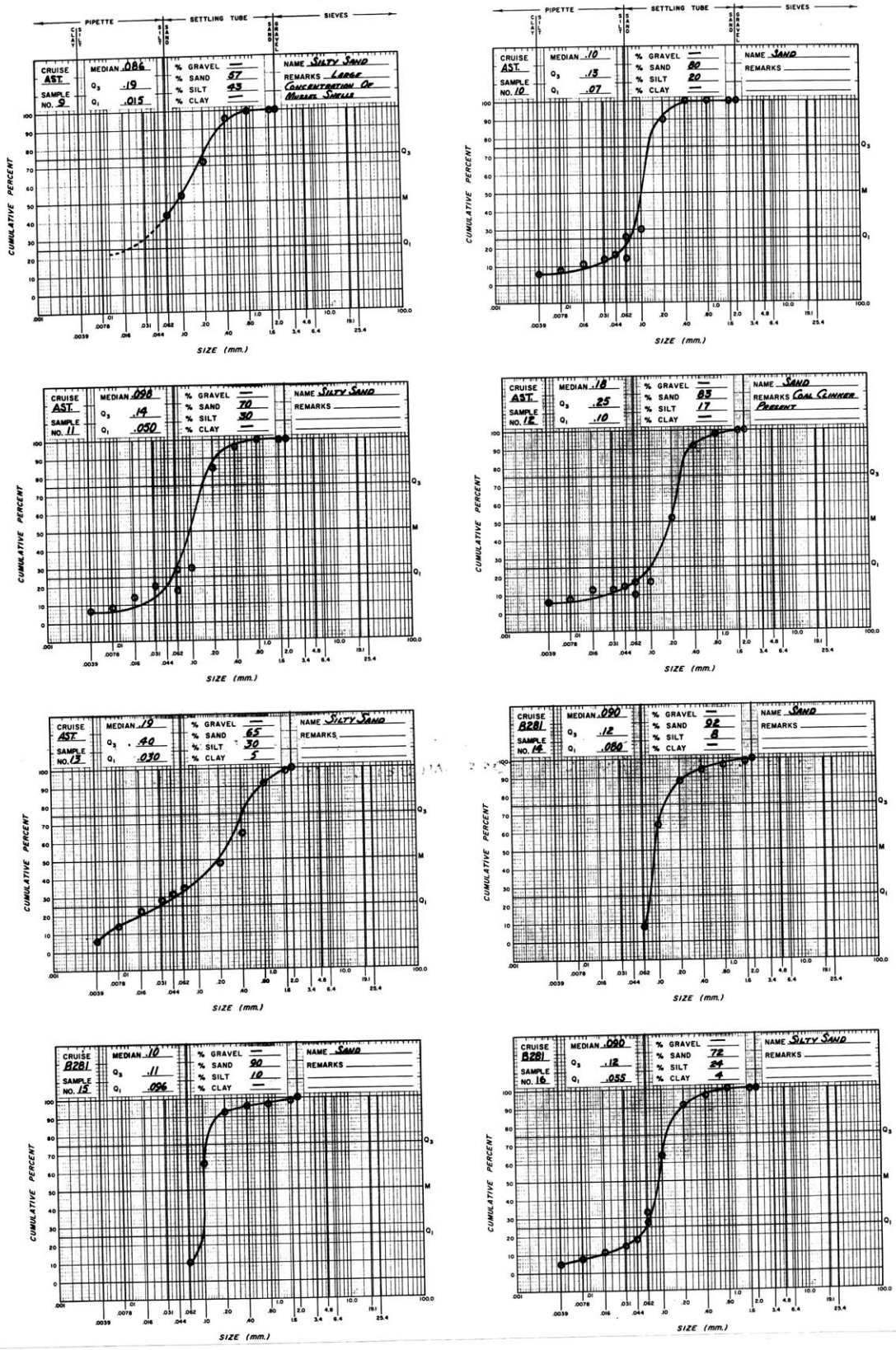

Figure 73. Cumulative Size Distribution Curves for Sediment Samples 9-16.

SEDIMENT SAMPLES
PARTICLE SIZE DISTRIBUTION

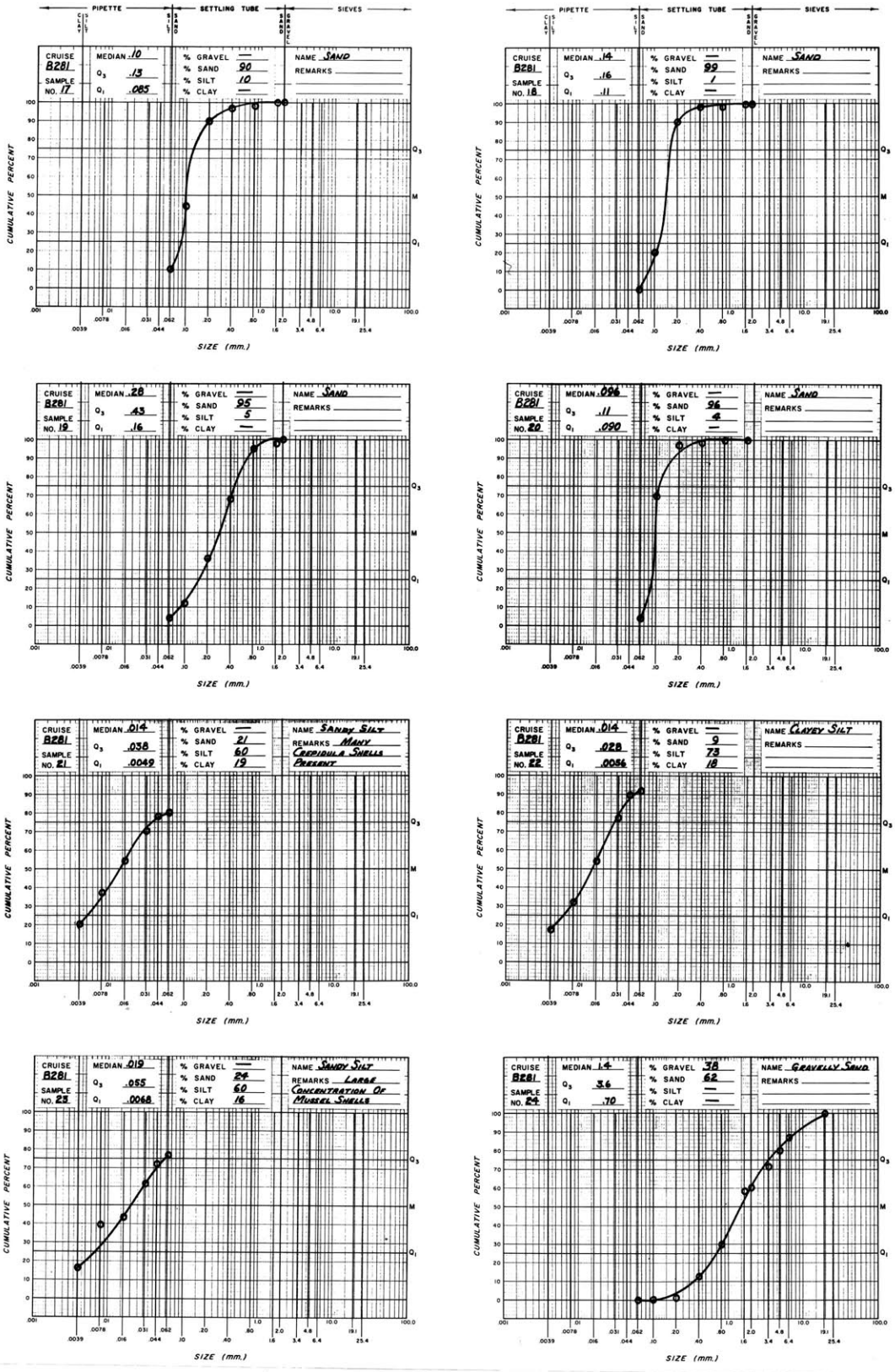

Figure 74. Cumulative Size Distribution Curves for Sediment Samples 17-24.

SEDIMENT SAMPLES
PARTICLE SIZE DISTRIBUTION

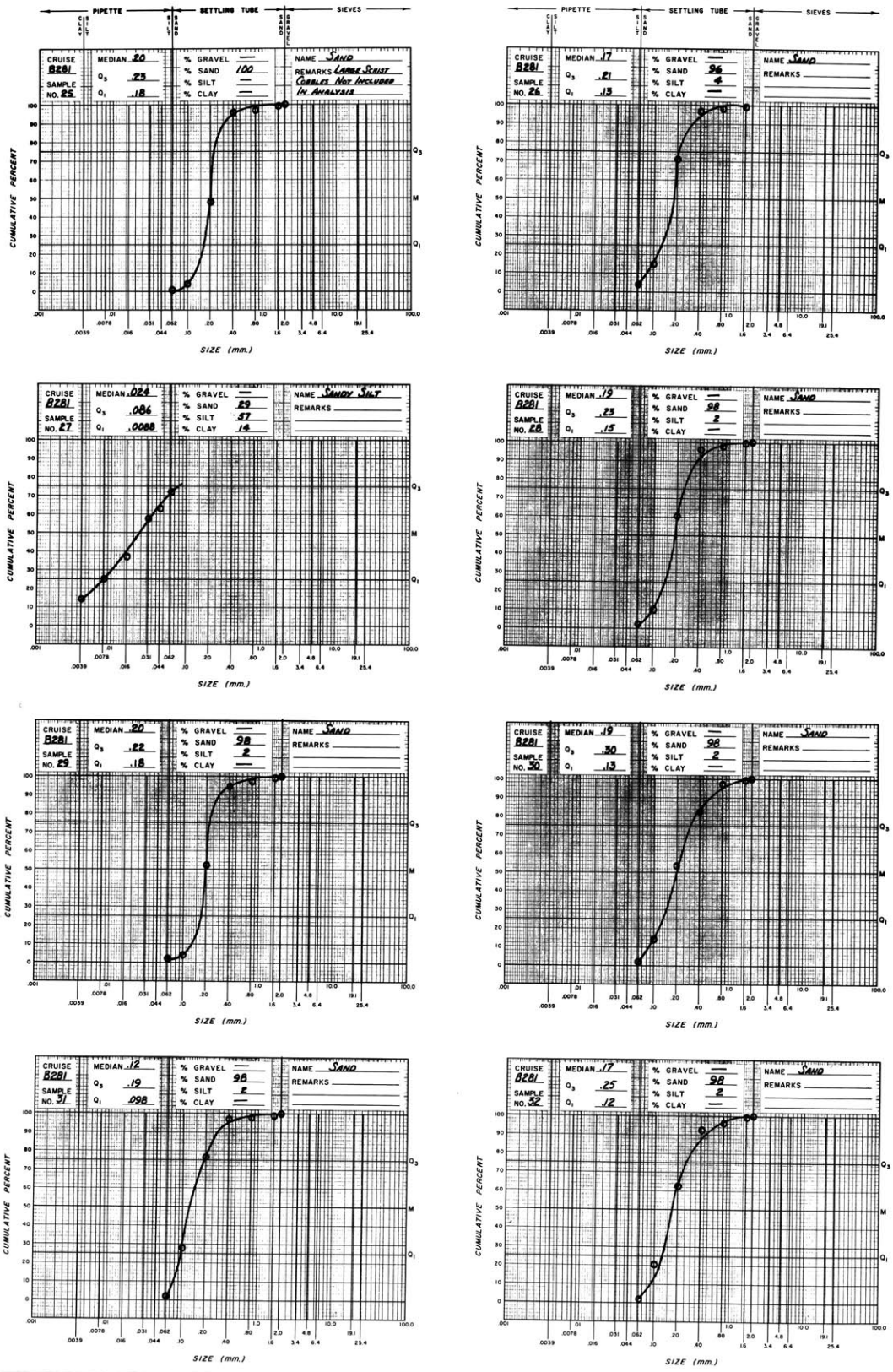

Figure 75. Cumulative Size Distribution Curves for Sediment Samples 25-32.

SEDIMENT SAMPLES
PARTICLE SIZE DISTRIBUTION

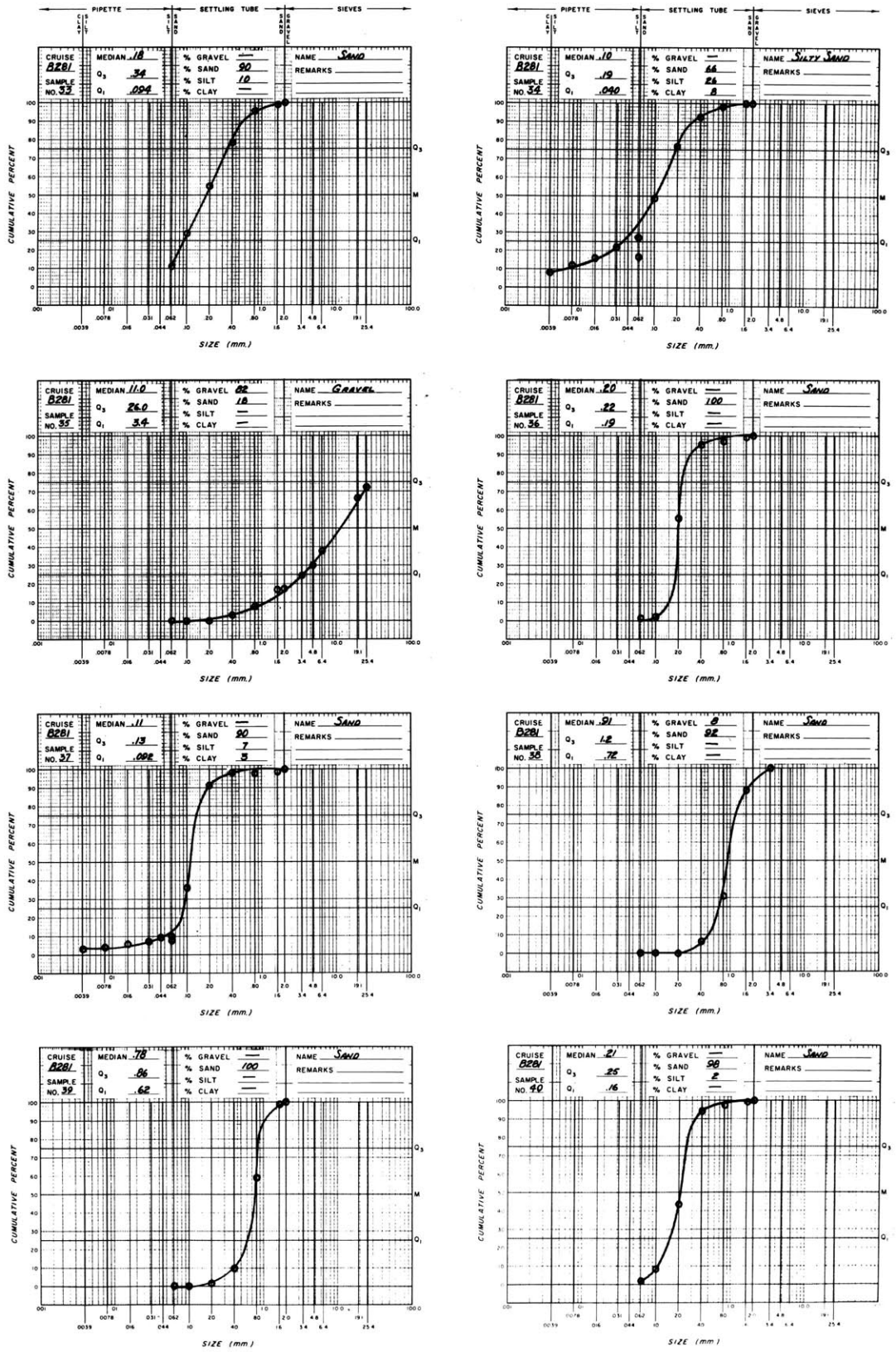

Figure 76. Cumulative Size Distribution Curves for Sediment Samples 33-40.

SEDIMENT SAMPLES
PARTICLE SIZE DISTRIBUTION

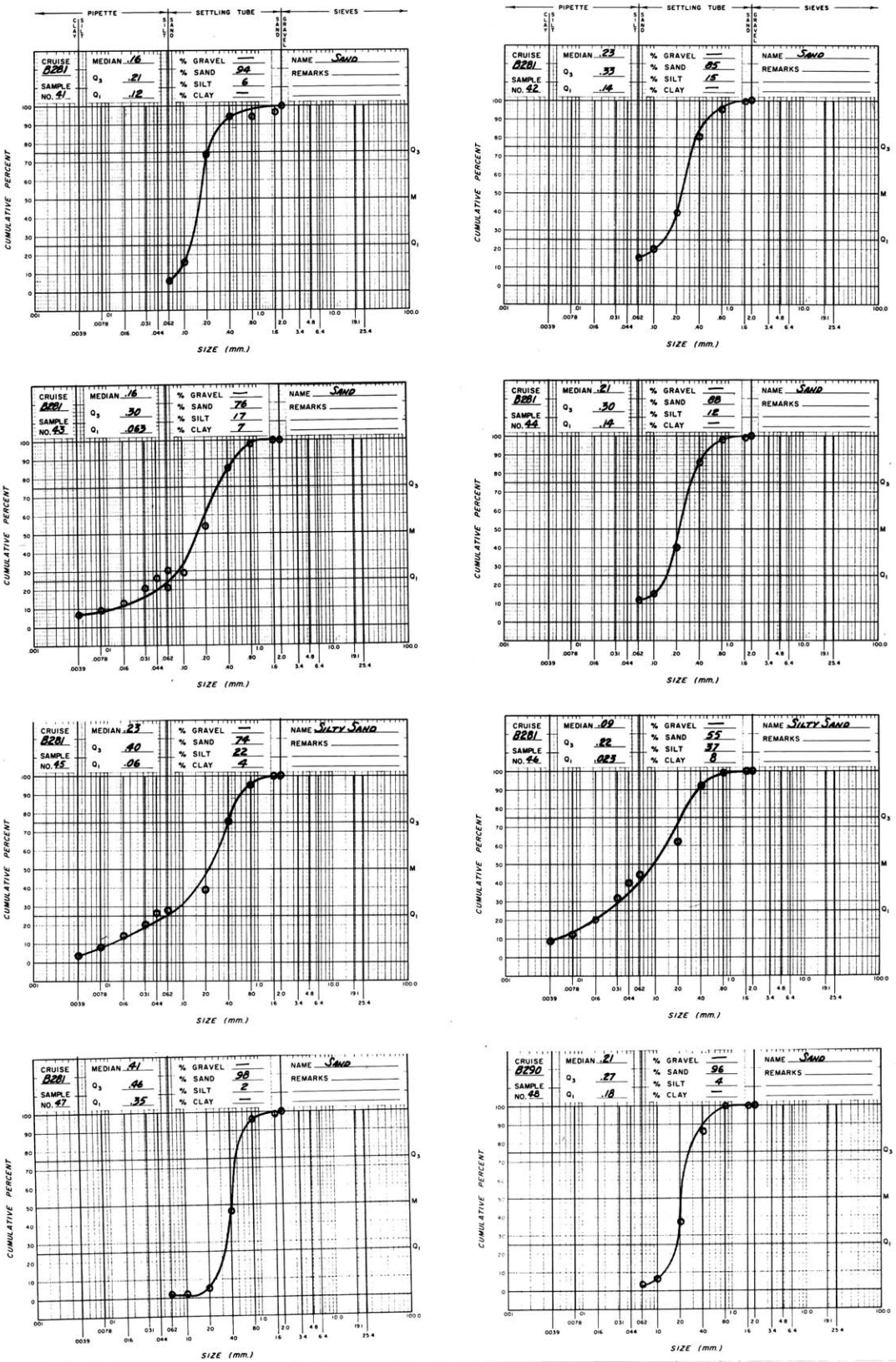

Figure 77. Cumulative Size Distribution Curves for Sediment Samples 41-48.

SEDIMENT SAMPLES
PARTICLE SIZE DISTRIBUTION

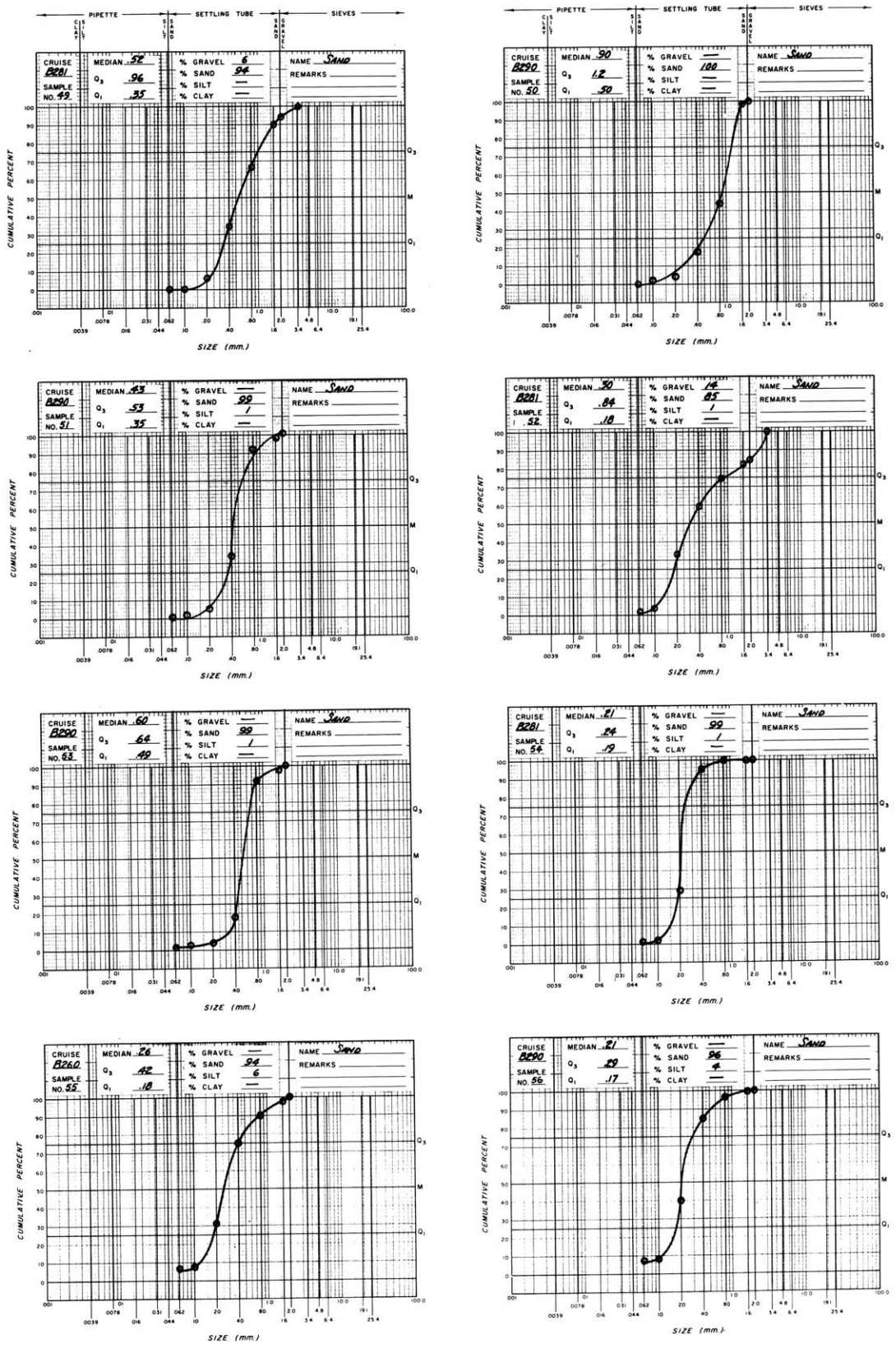

Figure 78. Cumulative Size Distribution Curves for Sediment Samples 49-56.

SEDIMENT SAMPLES
PARTICLE SIZE DISTRIBUTION

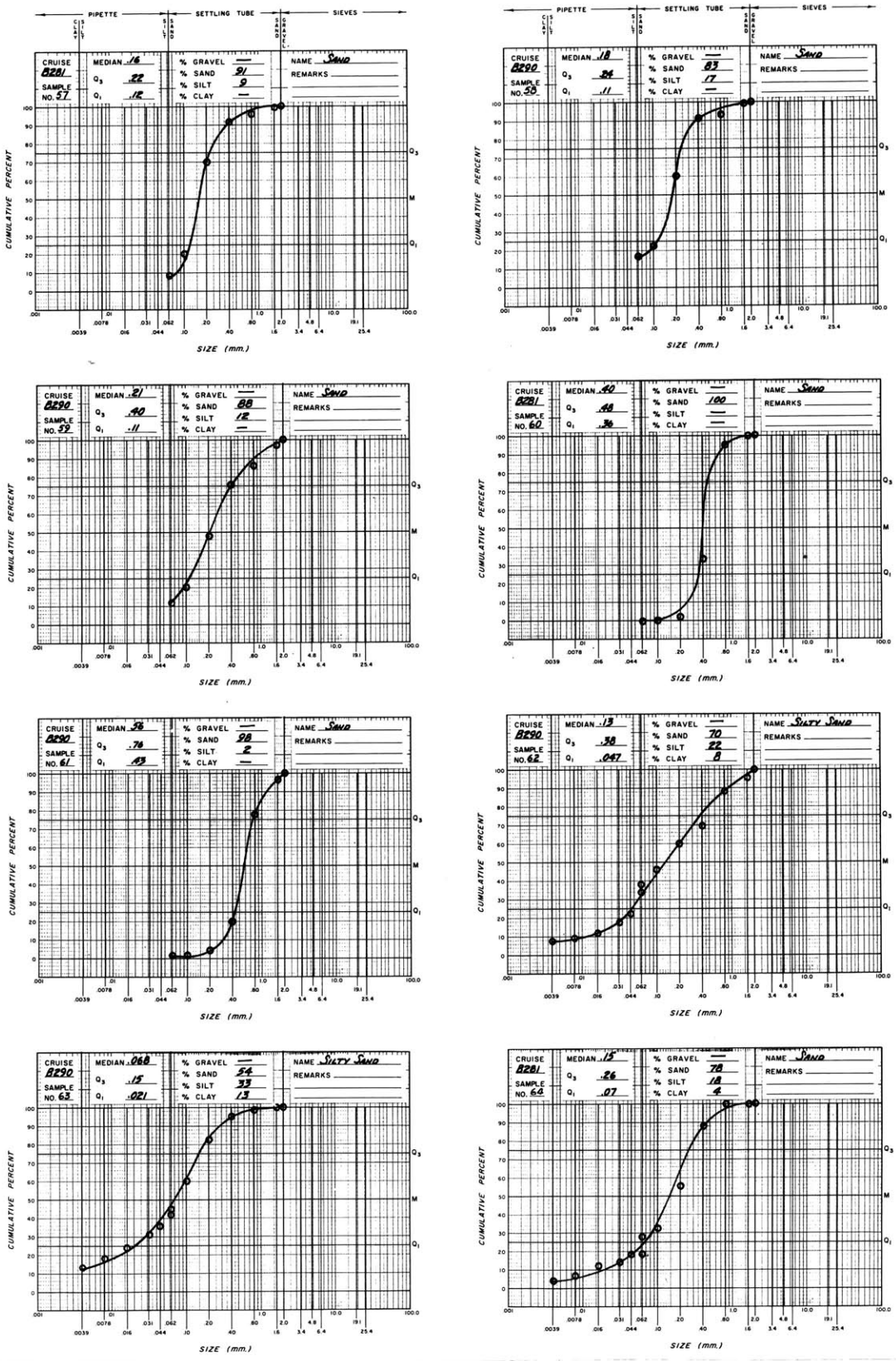

Figure 79. Cumulative Size Distribution Curves for Sediment Samples 57-64.

SEDIMENT SAMPLES
PARTICLE SIZE DISTRIBUTION

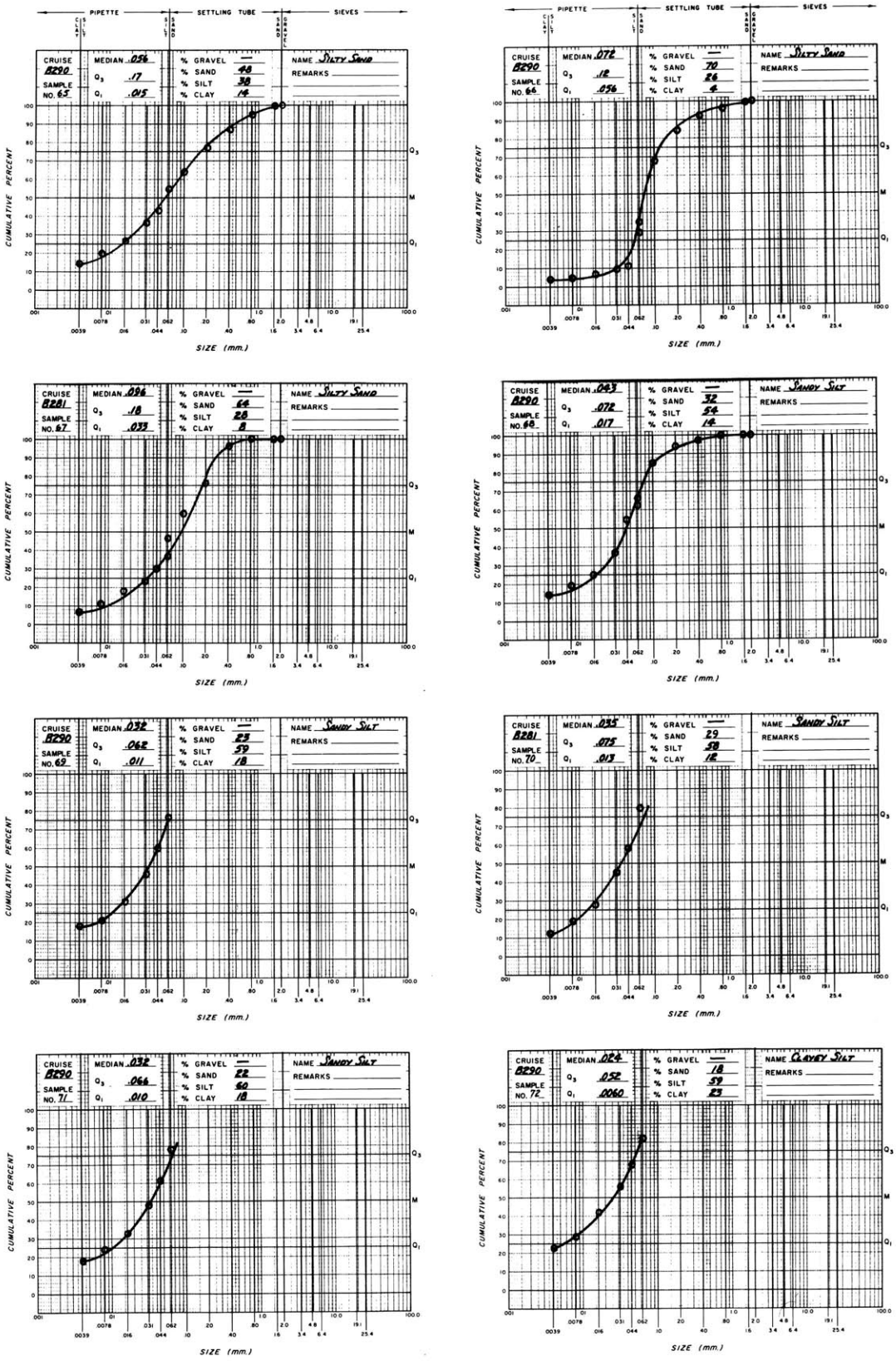

Figure 80. Cumulative Size Distribution Curves for Sediment Samples 65-72.

SEDIMENT SAMPLES
PARTICLE SIZE DISTRIBUTION

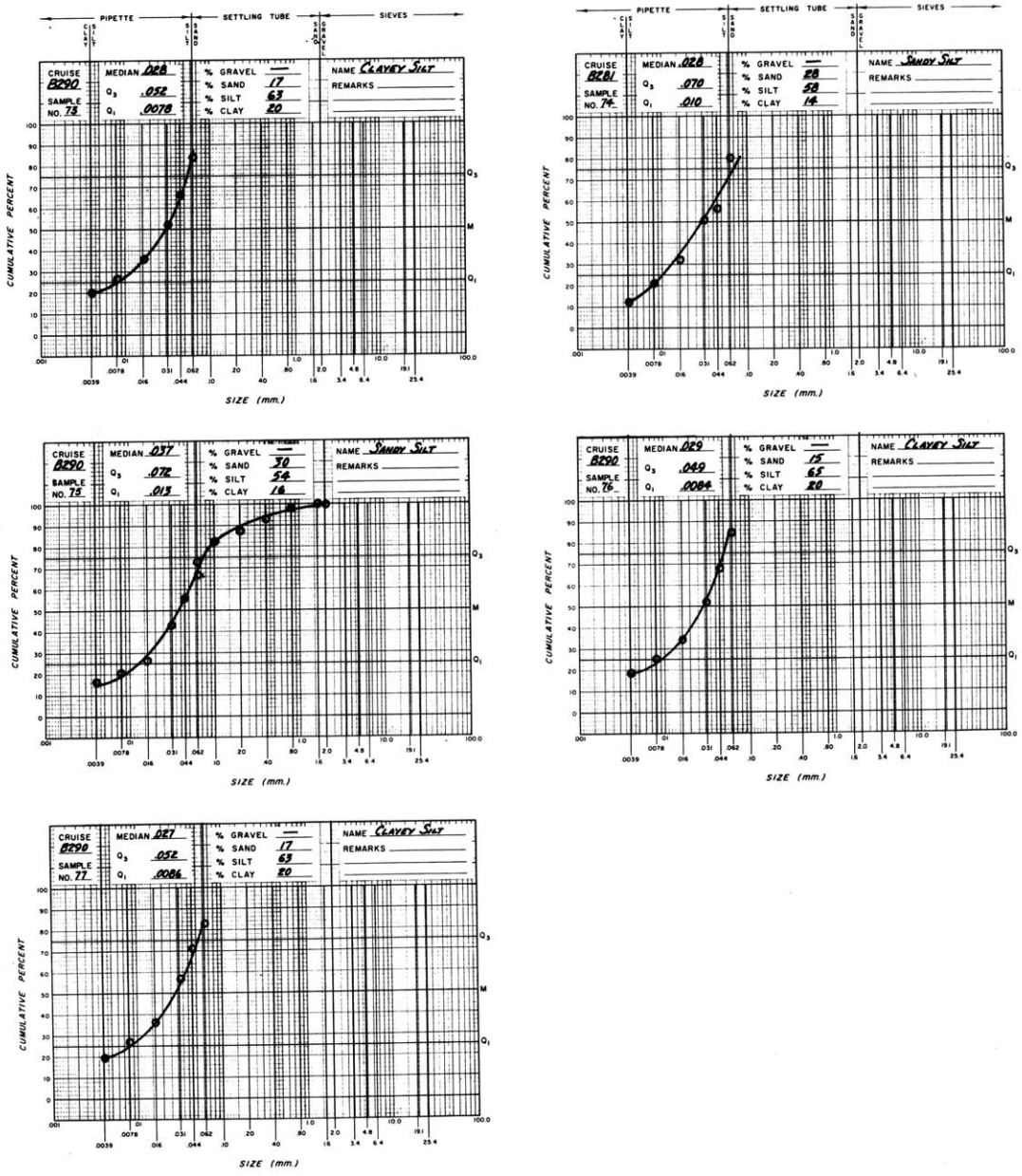

Figure 81. Cumulative Size Distribution Curves for Sediment Samples 73-77.